

---

SYSTEMATIC REVISION OF THE SAND SCORPIONS,  
GENUS *BUTHACUS* BIRULA, 1908  
(BUTHIDAE C.L. KOCH, 1837) OF THE LEVANT,  
WITH REDESCRIPTION OF  
*BUTHACUS ARENICOLA* (SIMON, 1885)  
FROM ALGERIA AND TUNISIA

---

SHLOMO CAIN, ERAN GEFEN, AND LORENZO PRENDINI



BULLETIN OF THE AMERICAN MUSEUM OF NATURAL HISTORY

SYSTEMATIC REVISION OF THE SAND  
SCORPIONS, GENUS *BUTHACUS* BIRULA, 1908  
(*BUTHIDAE* C.L. KOCH, 1837) OF THE LEVANT,  
WITH REDESCRIPTION OF  
*BUTHACUS ARENICOLA* (SIMON, 1885)  
FROM ALGERIA AND TUNISIA

SHLOMO CAIN

*Department of Evolutionary and Environmental Biology*  
*Faculty of Natural Sciences*  
*University of Haifa, Israel*

ERAN GEFEN

*Department of Biology and Environment*  
*Faculty of Natural Sciences*  
*University of Haifa – Oranim, Israel*

LORENZO PRENDINI

*Scorpion Systematics Research Group*  
*Division of Invertebrate Zoology*  
*American Museum of Natural History*

BULLETIN OF THE AMERICAN MUSEUM OF NATURAL HISTORY

Number 450, 134 pp., 53 figures, 13 tables

Issued April 27, 2021

## CONTENTS

Abstract .....	3
Introduction .....	3
Taxonomic history .....	4
Material and methods .....	15
Results .....	19
Systematics .....	21
Family Buthidae C.L. Koch, 1837 .....	21
<i>Buthacus</i> Birula, 1908 .....	21
Key to the species of <i>Buthacus</i> occurring in the Levant .....	24
<i>Buthacus amitaii</i> , sp. nov. .....	25
<i>Buthacus arava</i> , sp. nov. .....	31
<i>Buthacus arenicola</i> (Simon, 1885) .....	45
<i>Buthacus leptochelys</i> (Ehrenberg, 1829) .....	68
<i>Buthacus levyi</i> , sp. nov. .....	80
<i>Buthacus nitzani</i> Levy et al., 1973, stat. nov. .....	85
<i>Buthacus tadmorensis</i> (Simon, 1892), stat. rev. .....	95
<i>Buthacus yotvatensis</i> Levy et al., 1973, stat. rev. .....	107
Acknowledgments .....	107
References .....	119
Appendix 1. Currently recognized species, subspecies and synonyms of sand scorpions, genus <i>Buthacus</i> Birula, 1908 (Buthidae C.L. Koch, 1837), and species, previously assigned to <i>Buthacus</i> , currently accommodated in other genera .....	127
Appendix 2. Tissue samples and GenBank accession codes for DNA sequences used for phylogenetic analysis of sand scorpions, genus <i>Buthacus</i> Birula, 1908 (Buthidae C.L. Koch, 1837) .....	128
Appendix 3. Qualitative morphological characters and character states used for phylogenetic analysis of the sand scorpions, genus <i>Buthacus</i> Birula, 1908 (Buthidae C.L. Koch, 1837) of the Levant .....	132
Appendix 4. Ratios and counts used for nonmetric multidimensional scaling and as quantitative morphological characters in phylogenetic analysis of the sand scorpions, genus <i>Buthacus</i> Birula, 1908 (Buthidae C.L. Koch, 1837) of the Levant .....	133

## ABSTRACT

Scorpions of the genus *Buthacus* Birula, 1908 (Buthidae C.L. Koch, 1837), commonly known as “sand scorpions,” are widespread in the sandy deserts of the Palearctic, from West Africa to India. Although many new species of *Buthacus* were described in recent years, no modern revision exists for the genus and the limits of many infrageneric taxa remain unclear. The present contribution addresses the species of *Buthacus* recorded from the Levant, defined here as the region of the Middle East including Syria, Lebanon, Jordan, Israel, the Palestinian territories, and the Sinai Peninsula (Egypt). Prior to this study, five species and subspecies, including several synonyms, were recognized from the region. Based on extensive new collections, a reassessment of the morphology (including multivariate statistical analysis), and a phylogenetic analysis of morphological and DNA sequence data, published elsewhere, seven species of *Buthacus* are now recognized from the Levant, raising the number of species in the genus to 30. Three new species are described: *Buthacus amitaii*, sp. nov., endemic to Israel; *Buthacus arava*, sp. nov., endemic to Israel and Jordan; and *Buthacus levyi*, sp. nov., endemic to Egypt, Israel, and perhaps Libya. *Buthacus arenicola* (Simon, 1885) is redescribed and restricted to northeastern Algeria and central Tunisia, and *Buthacus leptochelys* (Ehrenberg, 1829) redescribed and restricted to Egypt, Sudan, and perhaps Libya. *Buthacus armasi* Lourenço, 2013, stat. rev., from southern Algeria, and *Buthacus spatzi* (Birula, 1911), stat. rev., from southern Tunisia and western Libya, are revalidated, and *Buthacus fuscata* Pallary, 1929, stat. nov. et stat. rev., from southern Algeria, revalidated and elevated to the rank of species. *Buthacus nitzani* Levy et al., 1973, stat. nov., currently restricted to Israel but probably present in the Sinai Peninsula (Egypt), is elevated to the rank of species. *Buthacus tadmorensis* (Simon, 1892), stat. rev., recorded from Iran, Iraq, Jordan, Syria, and Turkey, and *Buthacus yotvatensis* Levy et al., 1973, stat. rev., endemic to Israel and Jordan, are redescribed and revalidated. Three new synonyms are presented: *Androctonus (Leiurus) macrocentrus* Ehrenberg, 1828 = *Buthacus leptochelys* (Ehrenberg, 1829), syn. nov.; *Buthus pietschmanni* Penther, 1912 = *Buthacus tadmorensis* (Simon, 1892), syn. nov.; *Buthacus granosus* Borelli, 1929 = *Buthacus leptochelys* (Ehrenberg, 1829), syn. nov. *Buthacus arenicola* and the seven species of *Buthacus* occurring in the Levant are diagnosed and illustrated to modern standards, with updated distribution maps. A list of the currently recognized species of *Buthacus*, and a key to identification of the species occurring in the Levant are also presented.

## INTRODUCTION

Scorpions of the genus *Buthacus* Birula, 1908 (Buthidae C.L. Koch, 1837), commonly known as “sand scorpions,” are widespread in the sandy deserts of the Palearctic region, from the Atlantic coast of West Africa across the Sahara, and throughout the Middle East to India (Vachon, 1952; Levy et al., 1973; Levy and Amitai, 1980; Fet and Lowe, 2000; Lourenço, 2004a; Lourenço and Qi, 2006a; Yağmur et al., 2008; Zambre and Lourenço, 2010; table 1). All species of the genus inhabit sandy substrates (fig. 1; Navidpour et al., 2008, 2013; Shehab et al., 2011). However, the stability of the substrate, a function of its hardness, texture, and the density of rock and vegetation

varies, from shifting sand dunes, through semi-consolidated dunes, flats, or dry watercourses, to consolidated sand, gravel, and loess plains. The suite of ultrapsammophilous to semipsammophilous adaptations these scorpions possess for locomotion and burrowing on sandy substrata include elongation of the legs, especially legs III and IV, dorsoventral compression of the basitarsi of legs I–III, rows of elongated macrosetae (“sand combs”) along the retrolateral margins of the tibae and the pro- and retrolateral margins of the basitarsi of legs I–III, elongated macrosetae on the lateral and ventral surfaces of the telotarsi, and elongated unguis, often unequal in length on the telotarsi of legs I and II (Prendini, 2001). Additionally, many species exhibit loss or reduc-

tion of granulation and carination on the tegument, and pale coloration, often associated with a loss or reduction of infuscation (figs 2, 3).

Although many new species of *Buthacus* were described in recent years, no modern revision exists for the genus, and the limits of many infragenetic taxa, based on singletons, often female or sexually immature, remain unclear. The present contribution addresses the species of *Buthacus* recorded from the Levant, defined here as the region of the Middle East including Syria, Lebanon, Jordan, Israel, the Palestinian territories and the Sinai Peninsula (Egypt). The scorpion fauna of this region, particularly Israel, the Palestinian territories, and the Sinai Peninsula, was well studied by Gershom Levy and Pinchas Amitai in the 1970s, culminating in the contributions of Levy et al. (1973) and Levy and Amitai (1980). Various updates were provided subsequently (Vachon and Kinzelbach, 1987; El-Hennawy, 1987, 1992; Amr et al., 1988, 2015; Amr and El-Oran, 1994; Kabakibi et al., 1999; Kovařík, 2001, 2005; Kovařík and Whitman, 2004; Lourenço, 2006; Shehab et al., 2011; Amr, 2015; Saleh et al., 2017; Badry et al., 2018; Lowe et al., 2019; Amr et al., 2021). Prior to the present study, five infragenetic taxa of *Buthacus*, including several synonyms, were recognized from the Levant: *Buthacus arenicola* (Simon, 1885); *Buthacus leptochelys* (Ehrenberg, 1829); *Buthacus leptochelys nitzani* Levy et al., 1973; *Buthacus macrocentrus* (Ehrenberg, 1828); and *Buthacus yotvatensis* Levy et al., 1973.

Based on new collections, a reassessment of the morphology (including multivariate statistical analysis), and a phylogenetic analysis of morphological and DNA sequence data from two nuclear and three mitochondrial gene loci, published elsewhere (Cain et al., in press), seven species of *Buthacus* are now recognized from the region (figs. 4–7, 9, 10), raising the number of species in the genus to 30 (appendix 1). Three new species are described: *Buthacus amitaii*, sp. nov., endemic to Israel; *Buthacus arava*, sp. nov., endemic to Israel and Jordan; and *Buthacus levyi*, sp. nov., endemic

to Egypt, Israel, and perhaps Libya. *Buthacus arenicola* (Simon, 1885) is redescribed and restricted to northeastern Algeria and central Tunisia, and *Buthacus leptochelys* (Ehrenberg, 1829) redescribed and restricted to Egypt, Sudan, and perhaps Libya. *Buthacus armasi* Lourenço, 2013, stat. rev., from southern Algeria, and *Buthacus spatzi* (Birula, 1911), stat. rev., from southern Tunisia and western Libya, are revalidated, and *Buthacus fuscata* Pallary, 1929, stat. nov. et stat. rev., from southern Algeria, revalidated and elevated to the rank of species. *Buthacus nitzani* Levy et al., 1973, stat. nov., currently restricted to Israel but probably present in the Sinai Peninsula (Egypt), is elevated to the rank of species. *Buthacus tadmicensis* (Simon, 1892), stat. rev., recorded from Iran, Iraq, Jordan, Syria, and Turkey, and *Buthacus yotvatensis* Levy et al., 1973, stat. rev., endemic to Israel and Jordan, are redescribed and revalidated. Three new synonyms are presented: *Androctonus (Leiurus) macrocentrus* Ehrenberg, 1828 = *Buthacus leptochelys* (Ehrenberg, 1829), syn. nov.; *Buthus pietschmanni* Penther, 1912 = *Buthacus tadmicensis* (Simon, 1892), syn. nov.; *Buthacus granosus* Borelli, 1929 = *Buthacus leptochelys* (Ehrenberg, 1829), syn. nov. *Buthacus arenicola* and the seven species of *Buthacus* occurring in the Levant are diagnosed and illustrated to modern standards, with updated distribution maps (figs 4–10). A list of the currently recognized species of *Buthacus*, and a key to identification of the species occurring in the Levant are also presented.

## TAXONOMIC HISTORY

The first five species to be accommodated within *Buthacus* were originally assigned to other genera. Three of these, including the eventual type species of the genus, were described from Egypt and the Sinai Peninsula: *Androctonus (Leiurus) leptochelys* Ehrenberg, 1829; *Androctonus (Leiurus) macrocentrus* Ehrenberg, 1828; *Androctonus (Leiurus) thebanus* Ehrenberg, 1828. The

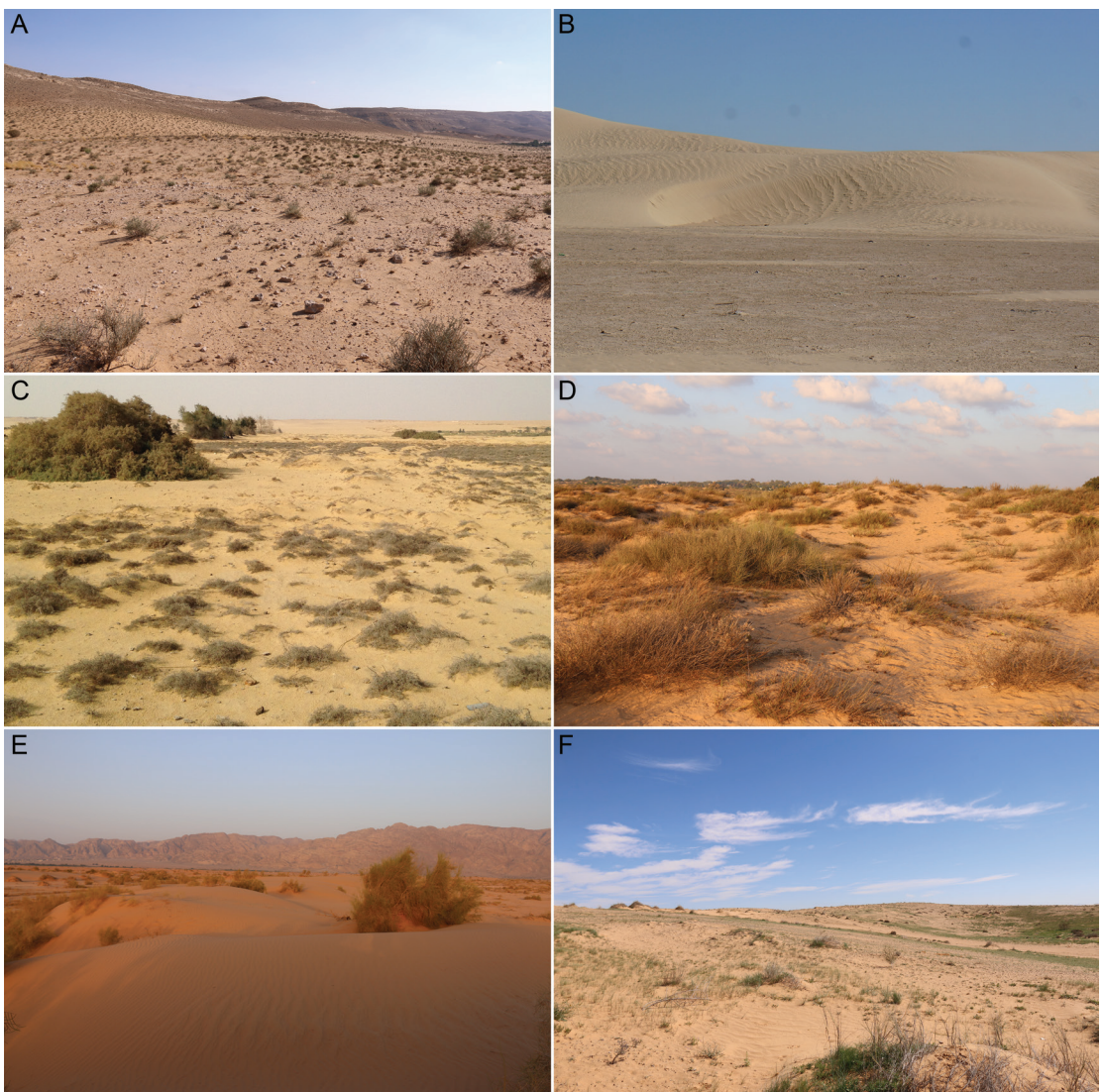


FIGURE 1. *Buthacus* Birula, 1908, representative habitats. A. Mamshit [Kurnub], Israel, habitat of *Buthacus amitaii*, sp. nov. B. Naftah to Ong Jmal, Tunisia, habitat of *Buthacus arenicola* (Simon, 1885). C. Faiyim Oasis, Egypt, habitat of *Buthacus leptochelys* (Ehrenberg, 1829). D. Ashdod Nizzanim Nature Reserve, Israel, habitat of *Buthacus nitzani* Levy et al., 1973, stat. nov. E. Yotvata, Israel, habitat of *Buthacus arava*, sp. nov., and *Buthacus yotvatensis* Levy et al., 1973, stat. rev. F. Be'er Milka, Israel, Holot Haluza sand dunes, Israel, habitat of *Buthacus levyi*, sp. nov., and *B. nitzani*.

fourth, *Buthus arenicola* Simon, 1885, was described from Tunisia and the fifth, *Buthus tadmurensis* Simon, 1892, from Syria.

Kraepelin (1891) regarded the three species from Egypt and the Sinai Peninsula as a single species, *Buthus leptochelys* (Ehrenberg, 1829),

and incorrectly treated *A. (L.) macrocentrus* and *A. (L.) thebanus* as junior synonyms, despite their nomenclatural priority (*B. leptochelys* subsequently won widespread acceptance, however, achieving the status of nomen protectum; ICZN, 1999; Kovařík, 2005). Pocock (1895) synony-

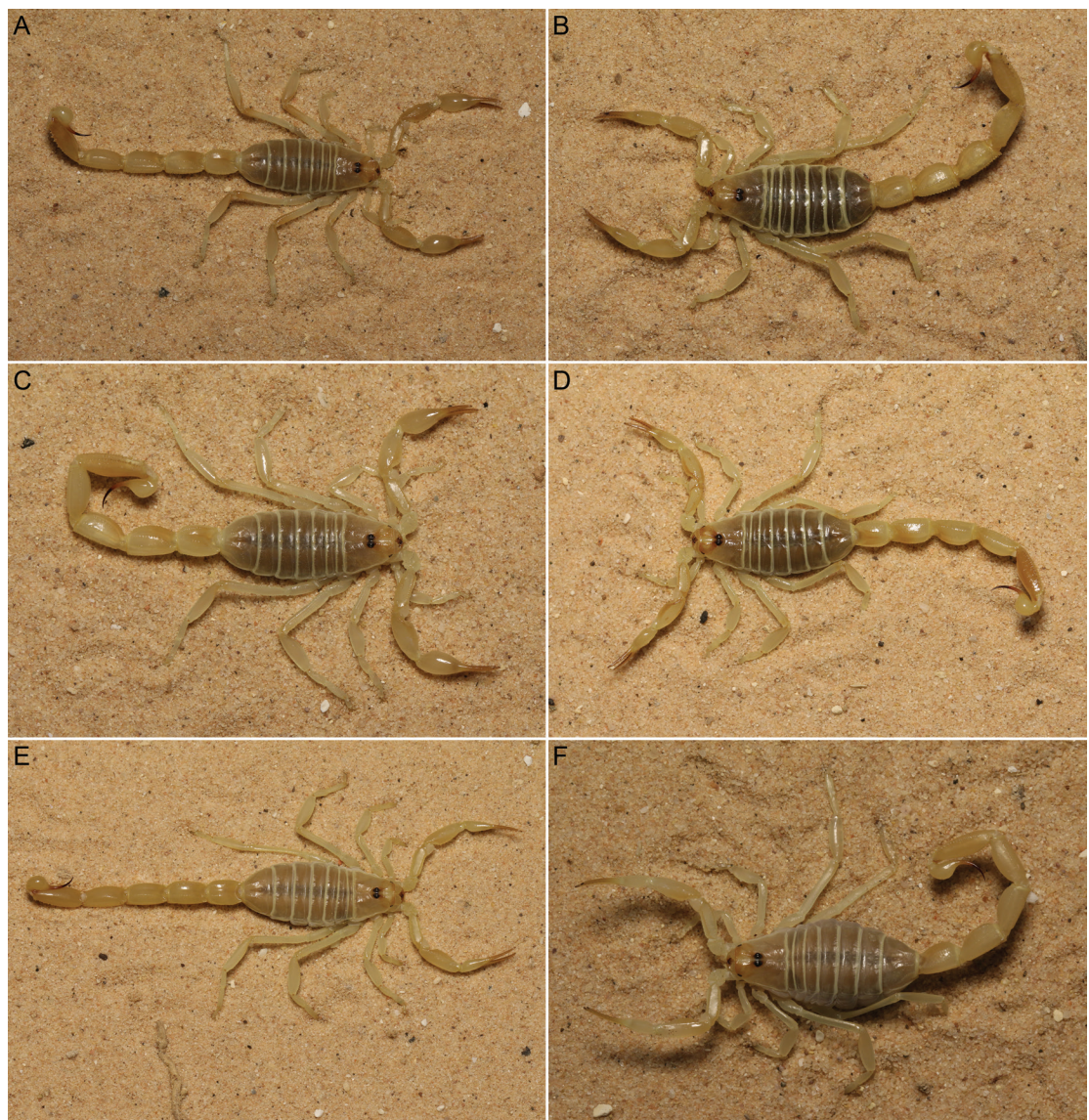


FIGURE 2. *Buthacus* Birula, 1908, habitus in life. A, B. *Buthacus amitaii*, sp. nov., ♂ (A), ♀ (B). C, D. *Buthacus nitzani* Levy et al., 1973, stat. nov., ♂ (C), ♀ (D). E, F. *Buthacus levyi*, sp. nov., ♂ (E), ♀ (F).

mized *B. arenicola* with *B. leptochelys*, an opinion accepted by Kraepelin (1899), who also synonymized *B. tadmorensis* with *B. leptochelys* (Kovařík, 2005). Birula (1908) revalidated *B. arenicola* and *B. tadmorensis*, however, and created *Buthacus* as a subgenus of *Buthus* Leach, 1815, with *B. leptochelys* as the type species, to accommodate them. Although Birula (1911, 1917) continued to

regard *Buthacus* as a subgenus of *Buthus*, Simon (1910) elevated *Buthacus* to the rank of genus, a decision followed by subsequent workers.

The first revisions and keys for *Buthacus* were presented for the species of North and West Africa by Vachon (1949a, 1952, 1958) and for the species of the Levant by Levy and Amitai (1980), by which time, another 11 infrageneric taxa had

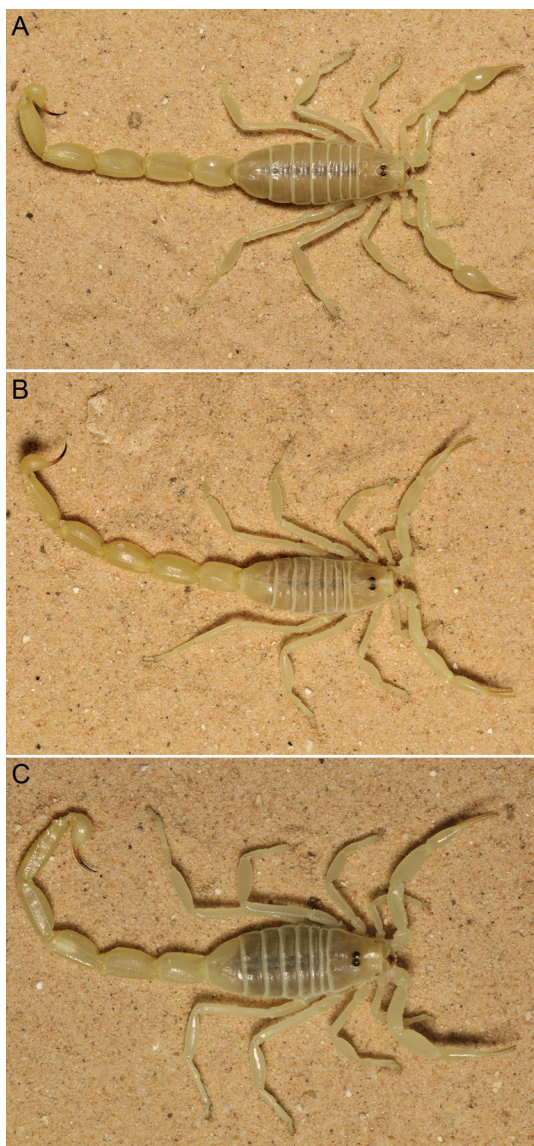


FIGURE 3. *Buthacus* Birula, 1908, habitus in life. A. *Buthacus arava*, sp. nov., ♂. B, C. *Buthacus yotvatensis* Levy et al., 1973, stat. rev., ♂ (B), ♀ (C).

been added to the genus (Birula, 1911, 1917; Penther, 1912; Borelli, 1929; Pallary, 1934; Werner, 1936a; Vachon, 1948, 1949a, 1952, 1953; Levy et al., 1973). Several of these, e.g., *B. tadmorensis*, *Buthus pietschmanni* Penther, 1912, and *Buthacus arenicola fuscata* Pallary, 1934, were subsequently synonymized (Levy et al., 1973;

Pérez, 1974; El-Hennawy, 1992), such that eight species and four subspecies were listed by Fet and Lowe (2000). The validity of various species, e.g., *B. macrocentrus*, *B. tadmorensis*, and *B. yotvatensis*, continues to be debated, however (Levy et al., 1973; Levy and Amitai, 1980; Kinzelbach, 1985; Fet and Lowe, 2000; Kovářík, 2005, 2018; Lourenço, 2006; Lourenço and Qi, 2006a; Lourenço and Leguin, 2009; Kovářík et al., 2016).

There is some agreement regarding the recognition of two species groups within *Buthacus*. Vachon (1952: 191) first suggested that *B. arenicola* and *B. leptochelys* could each represent a complex of several species. Levy et al. (1973) and Levy and Amitai (1980) divided the genus into two groups based on the dentition of the movable fingers of the pedipalp chela, species of the *B. leptochelys* group bearing a complete, or almost complete, series of retrolateral accessory denticles, compared with species of the *B. arenicola* group, in which all or most of the retrolateral accessory denticles are absent. However, the reliability of finger dentition as a diagnostic character in *Buthacus* has since been questioned. For example, Lourenço (2006: 60) observed significant variation in the character within the *B. arenicola* and *B. leptochelys* groups, leading to the conclusion that “even if the two groups can be substantiated, the association of a given species to one or the other of them may pose some difficult problems.” Despite these concerns, retrolateral accessory denticles on the pedipalp chela fingers remain in widespread use as diagnostic characters in *Buthacus* (Kovářík, 2005; Lourenço, 2006; Zambre and Lourenço, 2010; Lourenço and Sadine, 2015; Kovářík et al., 2016; Kovářík, 2018; Alqahtani and Badry, 2020).

The limits of *Buthacus* with respect to several other psammophilous Palearctic buthid genera, e.g., *Buthiscus* Birula, 1905, *Liobuthus* Birula, 1898, *Pectinibuthus* Fet, 1984, *Plesiobuthus* Pocock, 1900, and *Vachoniulus* Levy et al., 1973, also remains unclear (Kovářík et al., 2013, 2016; Kovářík, 2018; Lowe et al., 2019; Alqahtani and Badry, 2020). For example, Kovářík et al. (2016: 2) suggested, without presenting any phylogenetic evidence, that *Buthacus* might be a paraphyletic

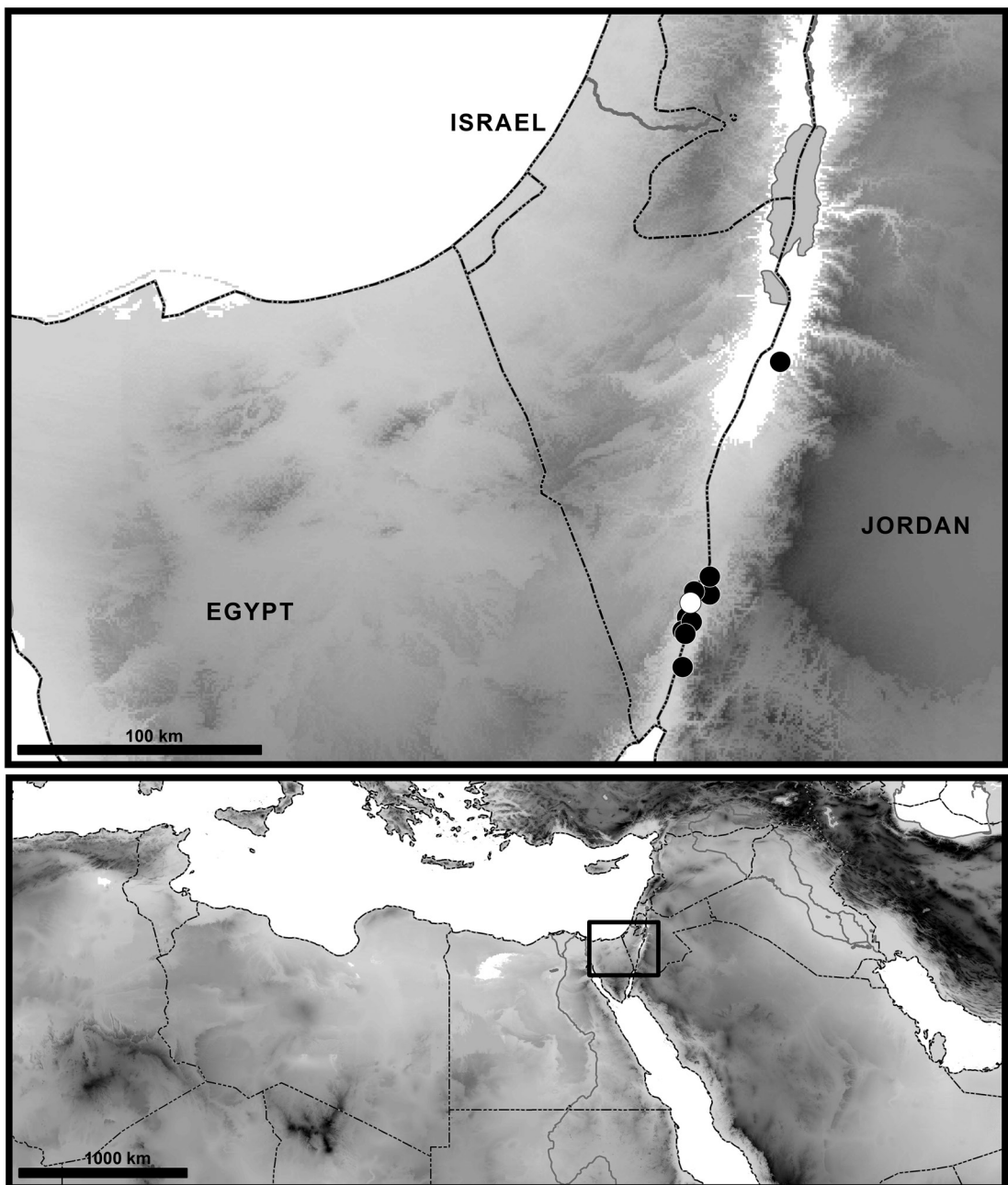


FIGURE 4. Map of southwestern Levant, plotting known locality records for *Buthacus arava*, sp. nov. in Israel and Jordan, based on material examined for the present study. White symbol denotes type locality.

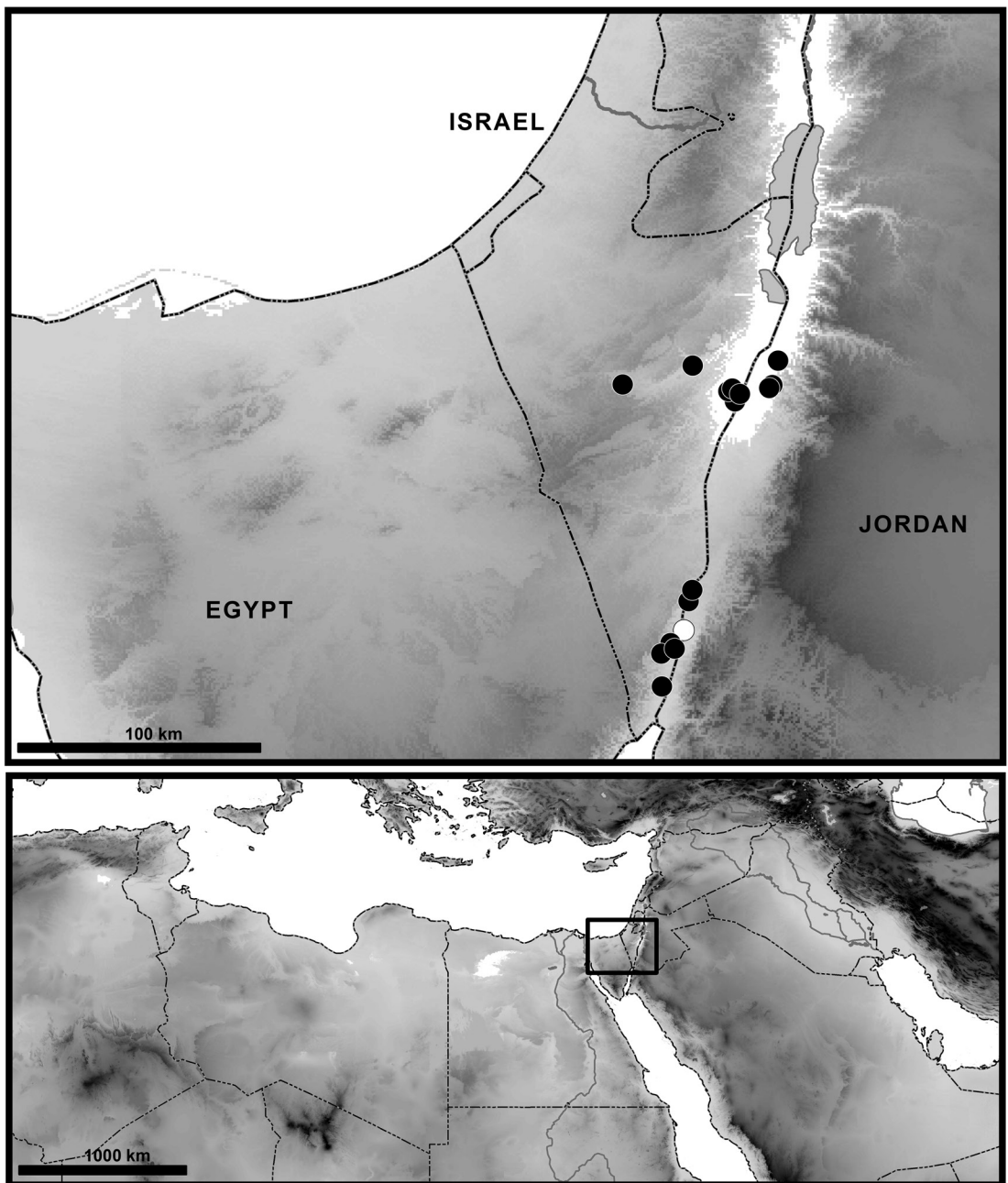


FIGURE 5. Map of southwestern Levant, plotting known locality records for *Buthacus yotvatensis* Levy et al., 1973, stat. rev., in Israel and Jordan, based on material examined for the present study and the literature. White symbol denotes type locality.

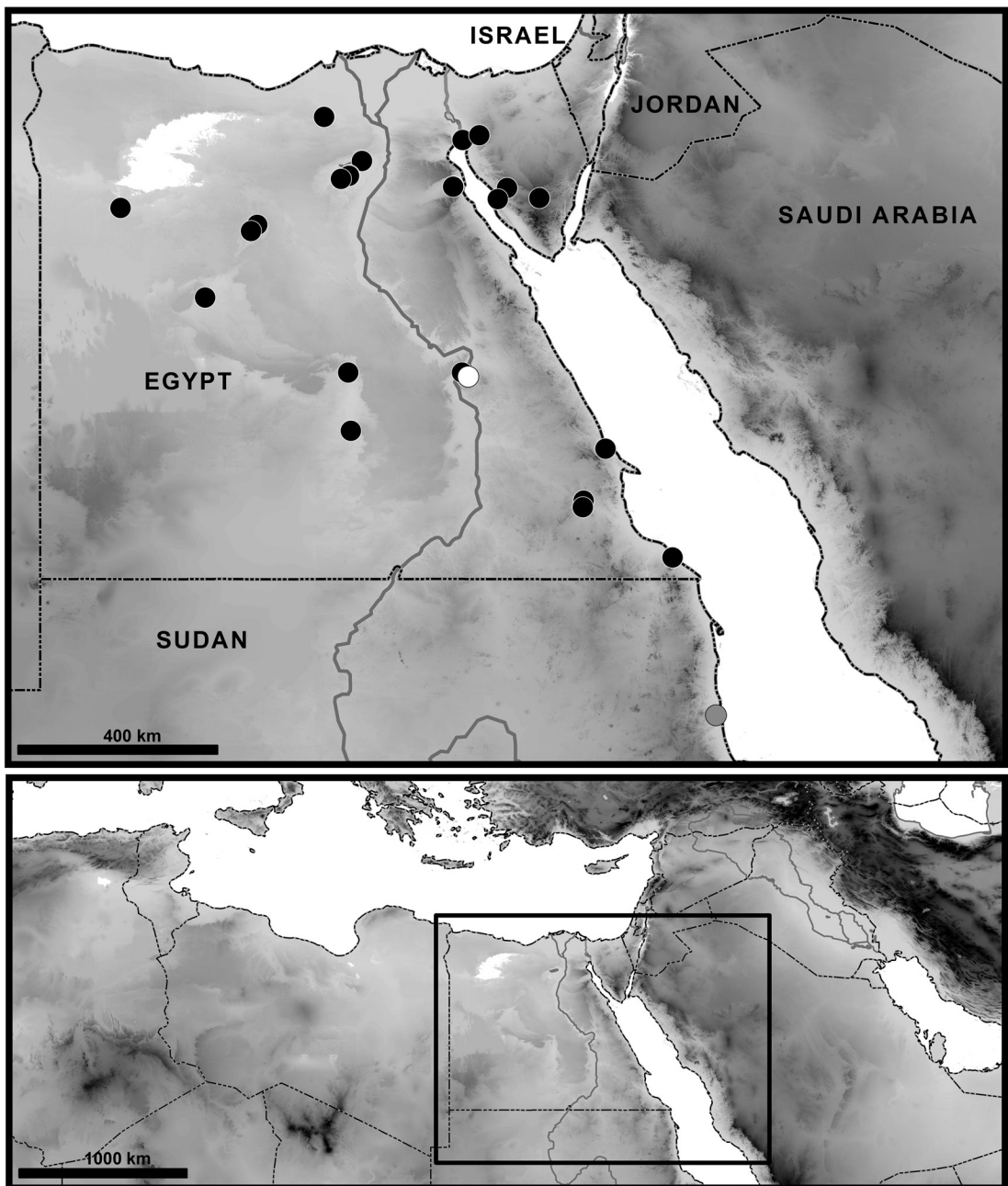
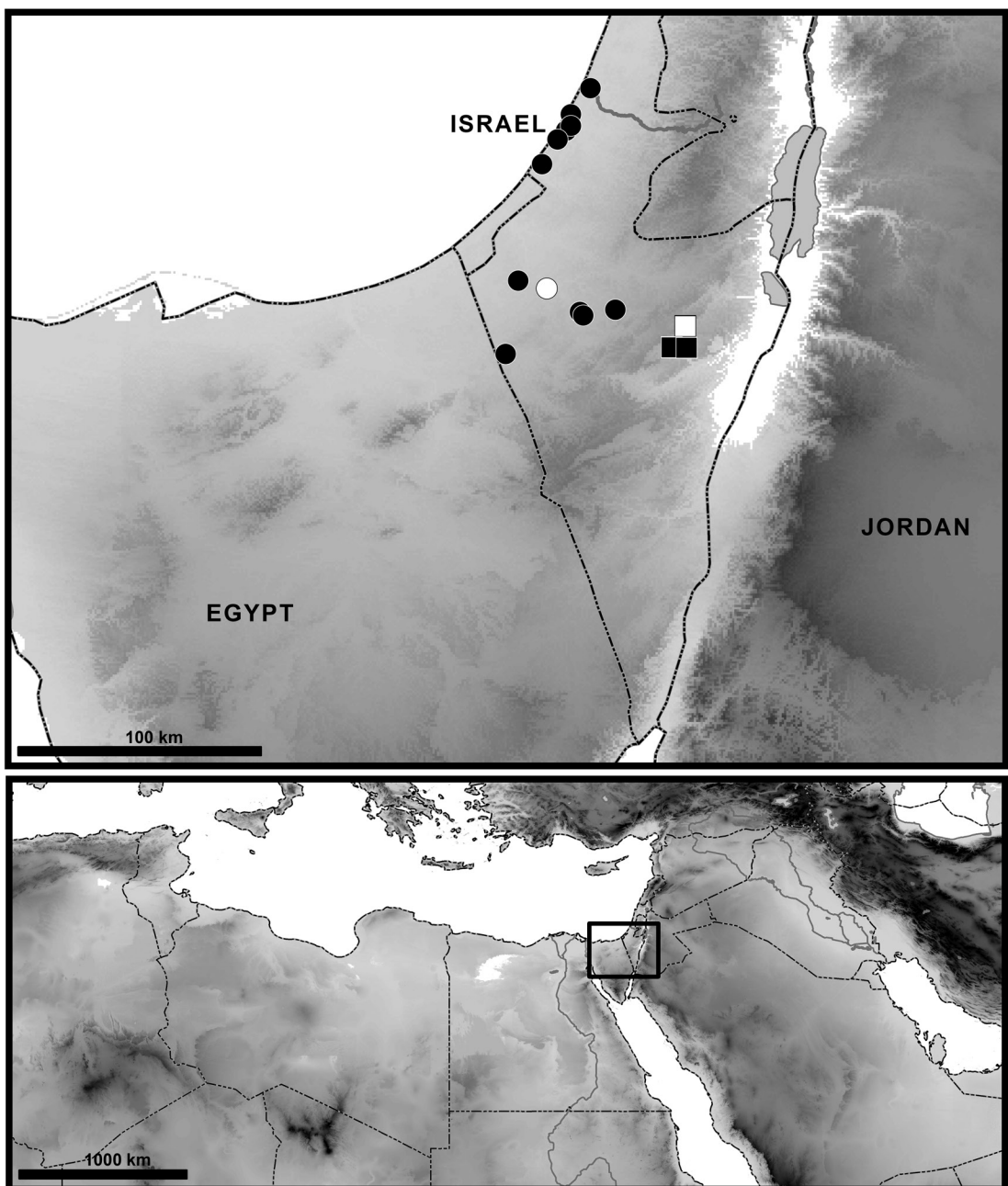


FIGURE 6. Map of southwestern Levant, plotting known locality records for *Buthacus leptochelys* (Ehrenberg, 1829) in Egypt and Israel, based on material examined for the present study and the literature. Pale gray symbol denotes type locality of the junior synonym, *Androctonus (Leiurus) thebanus* Ehrenberg, 1828 whereas dark gray symbol denotes type locality of the junior synonym, *Buthacus granosus* Borelli, 1929.



[FIGURE 7. Map of southwestern Levant, plotting known locality records for *Buthacus amitaii*, sp. nov. (squares), and *Buthacus nitzani* Levy et al., 1973, stat. nov. (circles), based on material examined for the present study and the literature. White symbols denote type localities.]

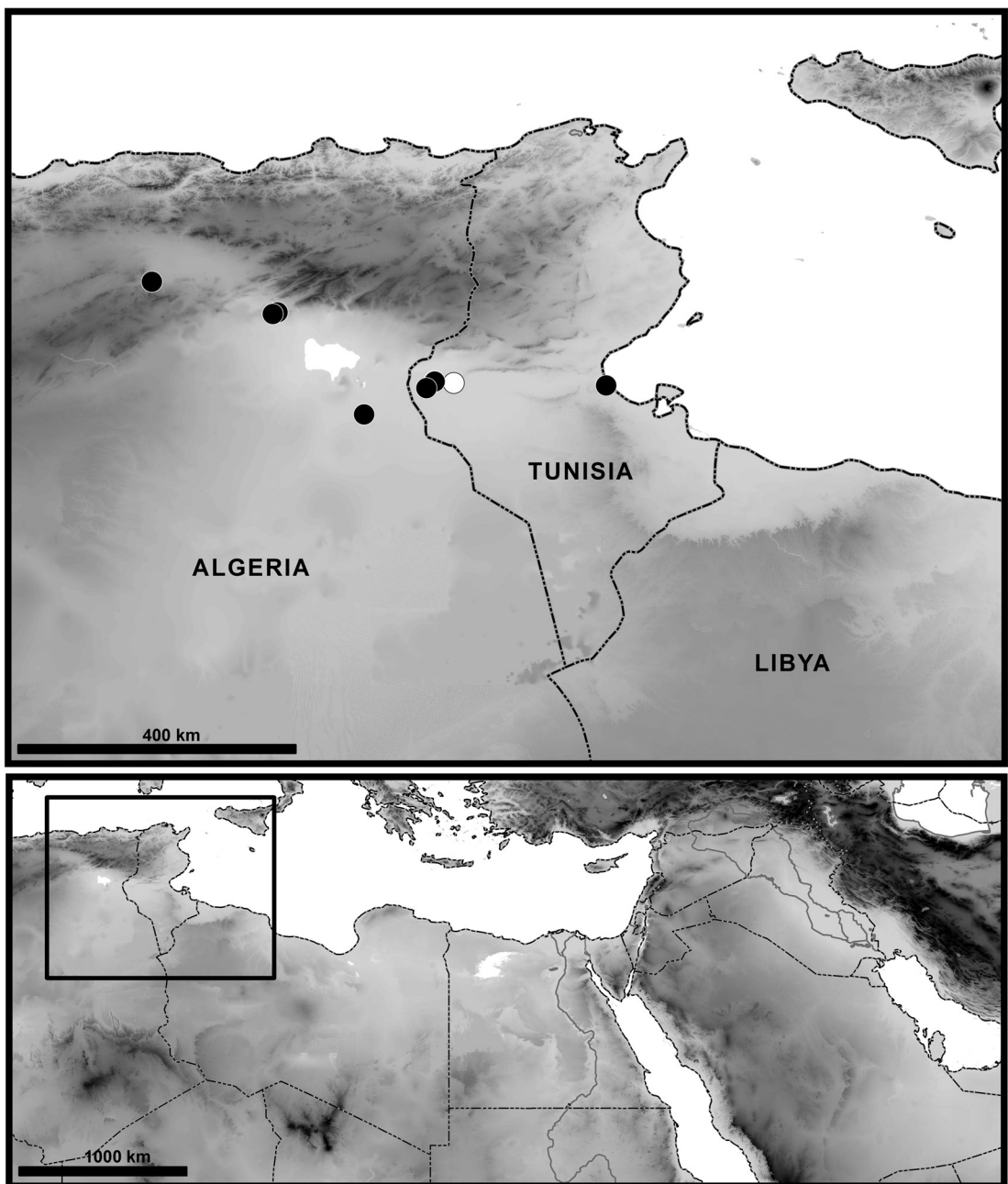


FIGURE 8. Map of the Maghreb, plotting known locality records for *Buthacus arenicola* (Simon, 1885) in Algeria and Tunisia, based on material examined for the present study and the literature. White symbol denotes locality of lectotype.

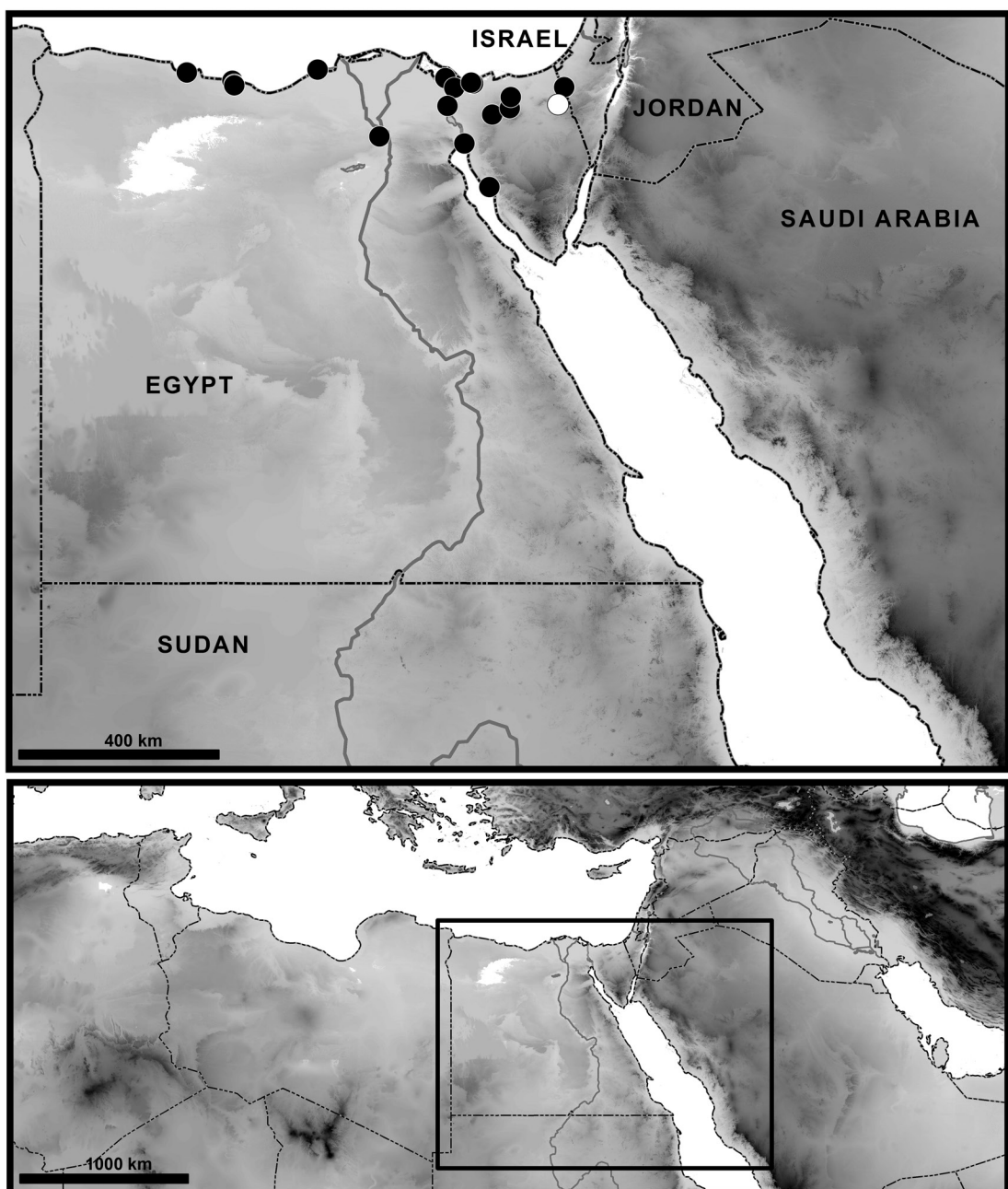


FIGURE 9. Map of southwestern Levant, plotting known locality records for *Buthacus levyi*, sp. nov. in Egypt and Israel, based on material examined for the present study and the literature. White symbol denotes type locality.

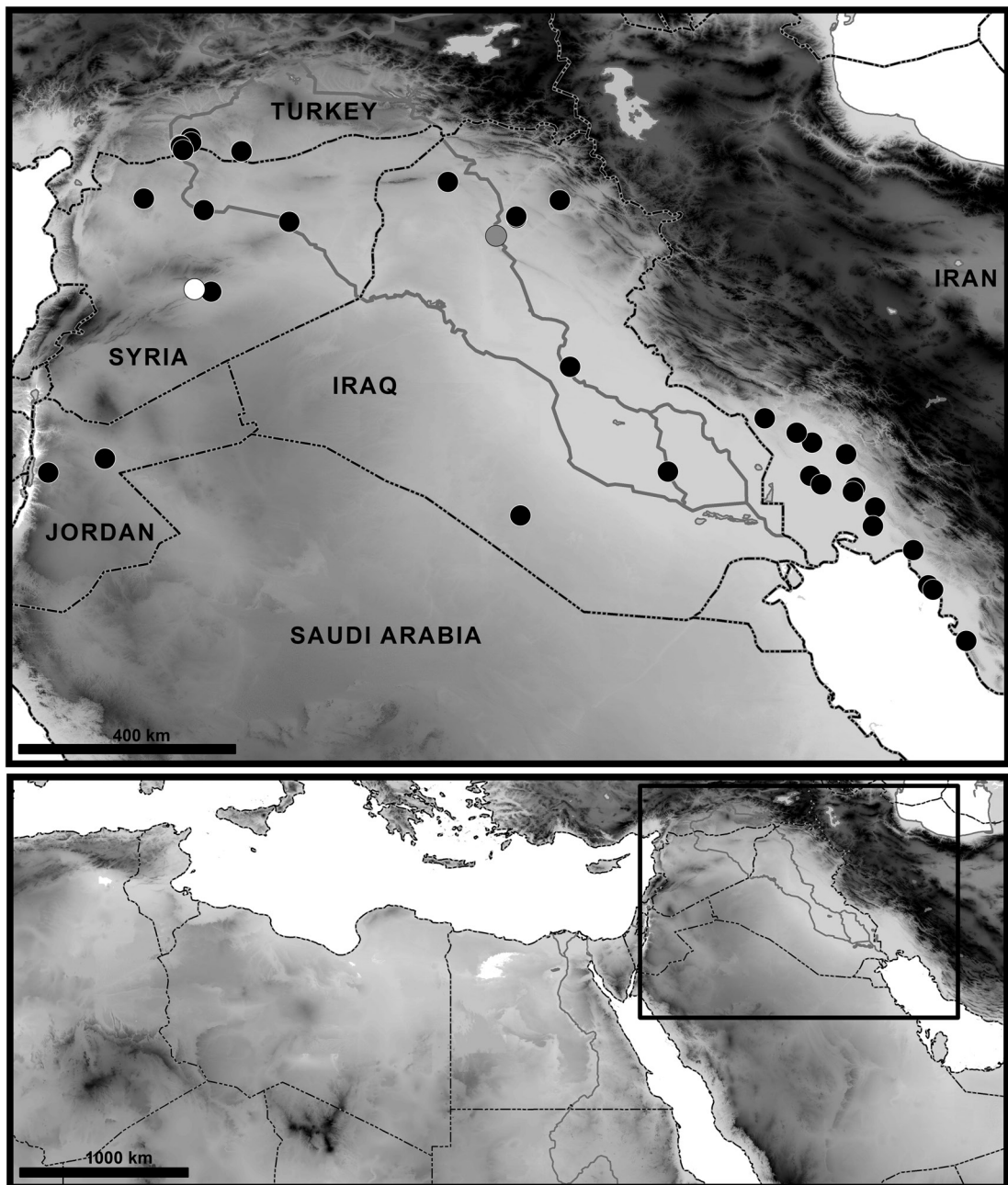


FIGURE 10. Map of the Fertile Crescent, plotting known locality records for *Buthacus tadmorensis* (Simon, 1892), stat. rev., in Iran, Iraq, Jordan, Syria and Turkey, based on material examined for the present study and the literature. White symbol denotes type locality whereas gray symbol denotes type locality of the junior synonym, *Buthus pietschmanni* Penther, 1912.

assemblage because many of the putative diagnostic characters for the genus appear to be plesiomorphic. On the other hand, a phylogenetic analysis based on 16S rDNA sequences for seven *Buthacus* terminals representing three ingroup exemplar species, and five outgroup taxa, by Alqahtani and Badry (2020), recovered the monophyly of *Buthacus*. These findings raise questions about the validity of genera, i.e., *Gint* Kovařík et al., 2013, and *Trypanothacus* Lowe et al., 2019, described in the absence of phylogenetic analyses, to which species previously assigned to *Buthacus*, i.e., *Buthacus calviceps* (Pocock, 1900) and *Buthacus buettikeri* Hendrixson, 2006, were transferred, respectively (appendix 1).

## MATERIAL AND METHODS

**FIELDWORK AND MATERIAL:** Scorpions were collected by actively searching on warm, dark nights, around the new moon, using ultraviolet (UV) light detection (Stahnke, 1972) with portable UV-LED lamps. Most of the material was preserved in 80% ethanol for morphological study, with some specimens preserved in 96% ethanol for DNA isolation.

Material is deposited in the following collections: American Museum of Natural History, New York (AMNH), including tissue samples stored in the Ambrose Monell Cryocollection (AMCC); National Natural History Collections, the Hebrew University of Jerusalem (HUJ); Jordan University of Science and Technology (JUST), Amman; Museum National d'Histoire Naturelle, Paris (MNHN); Naturhistorisches Museum Wien (NHMW), Austria; Steinhardt Museum of Natural History (SMNH), Tel Aviv University, Israel; University of Tunisia, el Manar (UTM); Museum für Naturkunde (ZMB), Berlin, Germany; Zoologisches Museum, Universität Hamburg (ZMH), Germany.

**GEOREFERENCING AND MAPPING:** Localities of field-collected material were georeferenced in the field with a portable GPS (Garmin eTrex® 10). All records of sufficient accuracy were isolated from the material examined and published

literature, e.g., Penther (1912), Levy et al. (1973), Levy and Amitai (1980), Kovařík (2005), Lourenço (2006), Navidpour et al. (2008), Yağmur et al. (2008), and Badry (2018), to create a point-locality geographical dataset for mapping distributional ranges. Records for which georeferences were not provided were retroactively georeferenced using Google Maps, version 10.31.1, or Google Earth, version 7.3. Distribution maps were produced using ArcGIS, version 10.2 (Environmental Systems Research Institute, Redlands, California), by superimposing point-locality records and political boundaries on the GTOPO30 global digital elevation model (<https://lta.cr.usgs.gov/GTOPO30>).

**DNA SEQUENCING:** Two loci in the nuclear genome, the internal transcribed spacer 2 (ITS2) and 28S rDNA (28S), and three loci in the mitochondrial genome, cytochrome c oxidase subunit I (COI), 16S rDNA (16S), and 12S rDNA (12S), were Sanger dideoxy sequenced using an ABI Prism 3730 XL DNA Sequencer (Perkin-Elmer, Melville, NY) at the AMNH Sackler Institute of Comparative Genomics and a 3130 DNA Sequencer at the Institute of Evolution, University of Haifa – Oranim. Double-stranded sequences were edited and contiged into consensus sequences using Sequencher ver. 5.4.6 (Gene Codes Corporation, Ann Arbor, MI) and MEGA6 (Tamura et al., 2013), and deposited in GenBank (<https://www.ncbi.nlm.nih.gov/genbank>; appendix 2). Sequence length of the 28S locus varied from 186–510 base-pairs (bp) with an average of 474 bp, the ITS2 from 318–541 bp with an average of 438 bp, the 12S from 246–281 bp with an average of 274 bp, the 16S from 238–270 bp with an average of 266 bp, and the COI from 261–616 bp with an average of 600 bp.

**SEQUENCE ALIGNMENT AND STATISTICS:** Sequences were aligned using MAFFT v. 7.402 (Katoh and Standley, 2013) on the CIPRES Science Gateway v. 3.3 (<https://www.phylo.org>; Miller et al., 2010). The COI and ITS2 loci were aligned using the G-INS-i alignment strategy, whereas the ribosomal 12S, 16S, and 28S loci were aligned using the Q-INS-i strategy, which

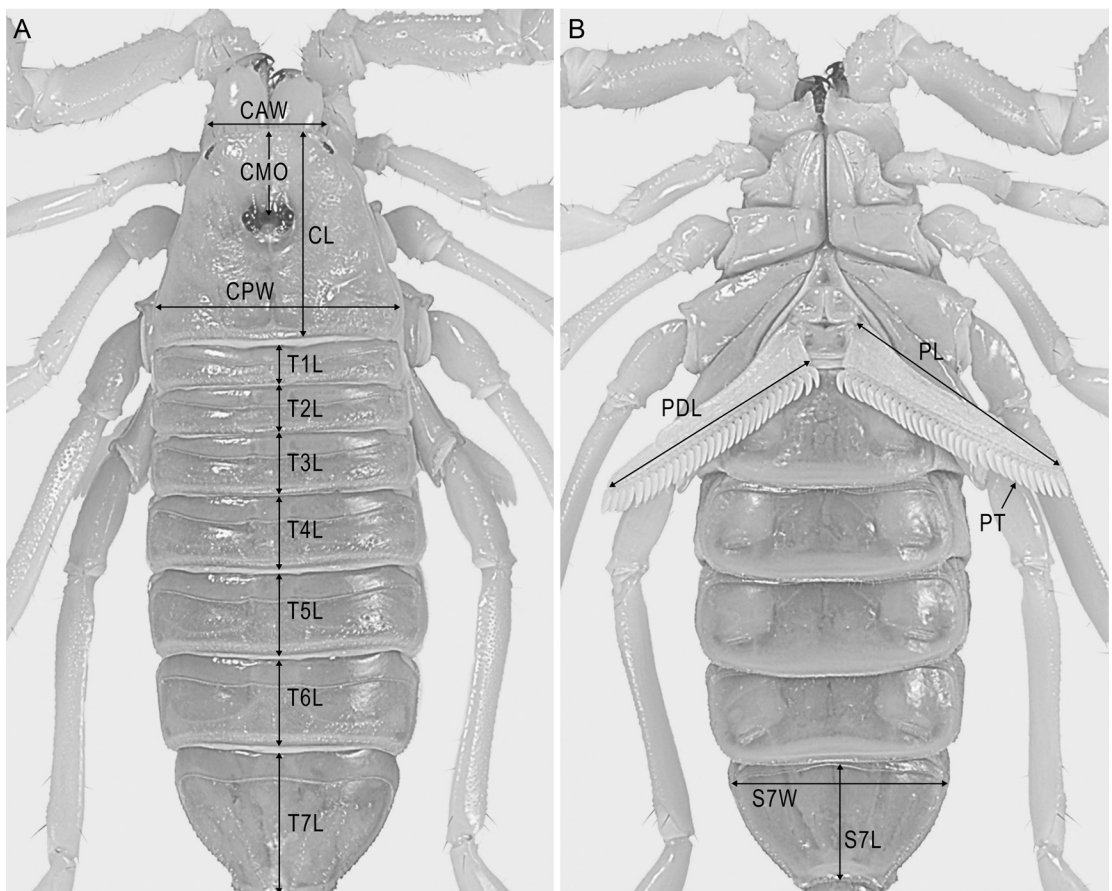


FIGURE 11. *Buthacus nitzani* Levy et al., 1973, stat. nov., ♂ (HUJ INV SC 3227), partial habitus, dorsal (A) and (B) ventral aspects, illustrating standard measurements and counts. Abbreviations: CAW, carapace anterior width; CL, carapace length; CMO, carapace median ocelli distance from anterior margin; CPW, carapace posterior width; S7L, sternite VII length; S7W, sternite VII width; T1L, tergite I length; T2L, tergite II length; T3L, tergite III length; T4L, tergite IV length; T5L, tergite V length; T6L, tergite VI length; T7L, tergite VII length; PDL, pecten length along dentate margin; PL, pecten total length; PT, pectinal tooth count.

considers the RNA secondary structure. The aligned sequences were then concatenated to create a multilocus dataset with a total length of 2218 bp. Average percent GC content and the number of variable and parsimony-informative sites was calculated for each locus.

The aligned nuclear 28S locus contained 3% of the variable sites, whereas the nuclear ITS and mitochondrial 12S, 16S and COI loci respectively contained 31%, 36%, 34%, and 26% of the variable sites. The 28S, ITS, 12S, 16S, and COI loci respectively contained 2%, 11%, 28%, 28%, and

21% of the parsimony-informative sites. The concatenated alignment contained 24% variable sites and 16% parsimony-informative sites.

**PHYLOGENETIC ANALYSIS:** The multilocus molecular dataset was analyzed separately and simultaneously with 22 qualitative (appendix 3) and 48 quantitative morphological characters (appendix 4) using parsimony in TNT v. 1 (<https://cladistics.org/tnt>; Goloboff et al., 2008), Bayesian inference (BI) in MrBayes v. 3.2.7a (Ronquist and Huelsenbeck, 2003), and maximum likelihood (ML) in RAxML v. 8.2.12 (Stamatakis, 2006, 2014)

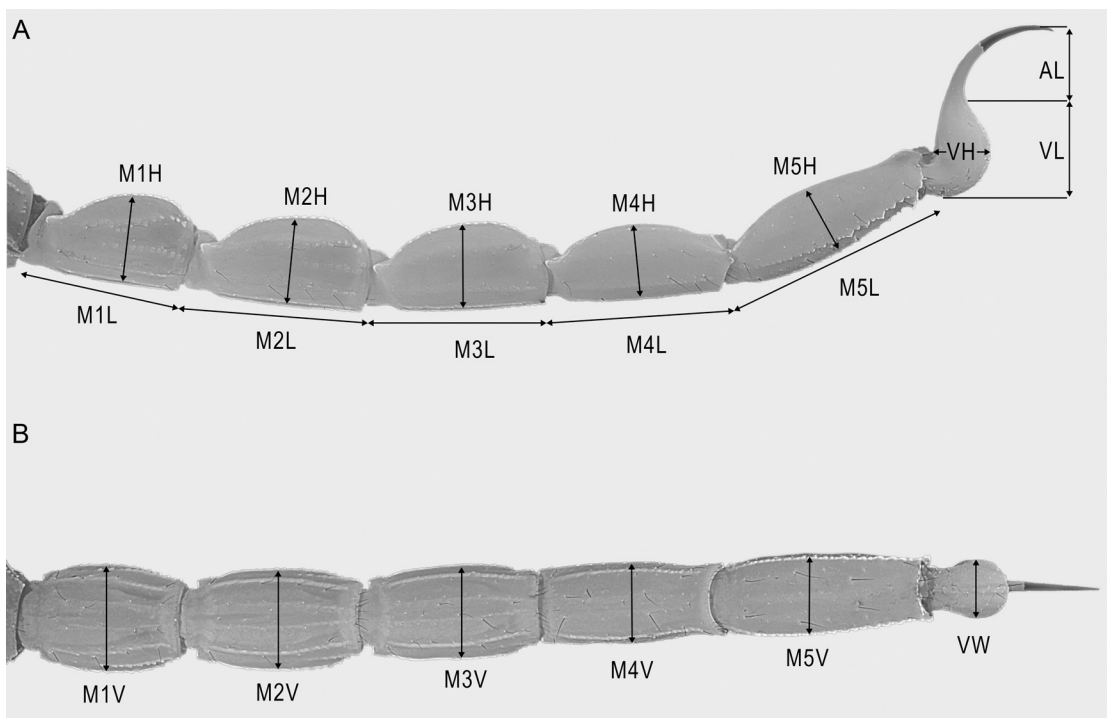


FIGURE 12. *Buthacus* Birula, 1908, metasomal segments I–V and telson, A, lateral and B, ventral aspects, illustrating standard measurements and counts. A. *Buthacus nitzani* Levy et al., 1973, stat. nov., ♀ (HUJ INV SC 3226). B. *Buthacus yotvatensis* Levy et al., 1973, stat. rev., ♀ (HUJ INV SC 3318). Abbreviations: AL, telson aculeus length; M1H, metasomal segment I height; M1L, metasomal segment I length; M1W, metasomal segment I width; M2H, metasomal segment II height; M2L, metasomal segment II length; M2W, metasomal segment II width; M3H, metasomal segment III height; M3L, metasomal segment III length; M3W, metasomal segment III width; M4H, metasomal segment IV height; M4L, metasomal segment IV length; M4W, metasomal segment IV width; M5H, metasomal segment V height; M5L, metasomal segment V length; M5W, metasomal segment V width; VH, telson vesicle height; VL, telson vesicle length; VW, telson vesicle width.

on CIPRES. The dataset was partitioned by loci and a multigamma model applied to the five molecular partitions, whereas the Mk model (Lewis, 2001) was applied to the morphological partition in the BI and ML analyses. Five qualitative morphological characters (1, 3–5 and 12) were deactivated in the analyses with quantitative characters. A rapid bootstrap analysis was used to search for the best scoring ML tree and nodal support evaluated using rapid bootstrapping with 1000 iterations. Nodal support for the BI tree was evaluated using posterior probabilities. A more detailed explanation of the phylogenetic analyses is presented by Cain et al. (in press).

**MICROSCOPY, IMAGING, AND MORPHOLOGY:** Morphological examination of specimens was conducted using a Nikon SMZ 745 or 1500 stereomicroscope. Photomicrographs were taken under visible and UV light using a Microptics ML-1000 digital imaging system with a Nikon D300 DSLR camera. Multiple image layers were stacked using Helicon Focus 6 (<https://www.heliconsoft.com>) and edited using Adobe Photoshop CS5.

The sex and life stage of specimens were determined by pectinal tooth counts, the presence or absence of genital papillae, and secondary sexual characters. Specimens were

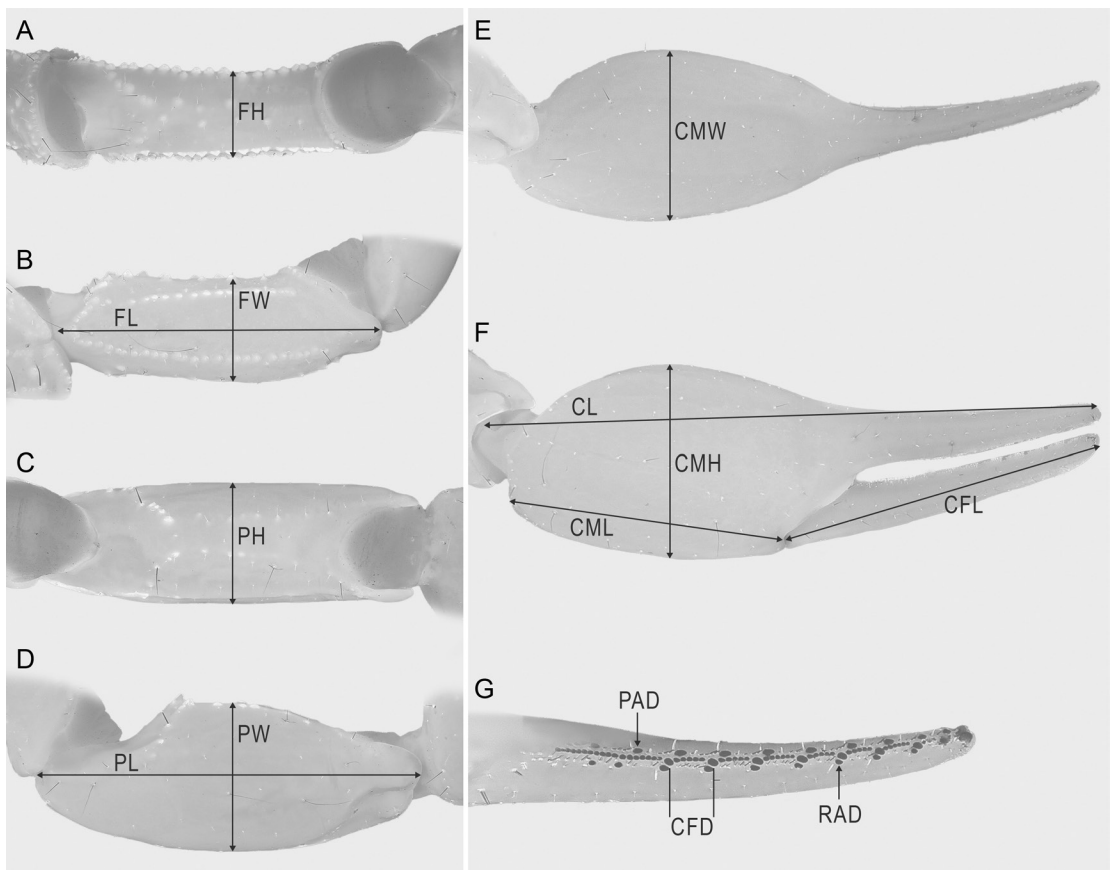


FIGURE 13. *Butaculus nitzani* Levy et al., 1973, stat. nov., ♂ (HUJ INV SC 3227), pedipalp femur (A, B), patella (C, D), chela (E, F) and movable finger (G), prolateral (A, C), dorsal (B, D, E, G) and retro-lateral (F) aspects, illustrating standard measurements and counts. Abbreviations: CFD, pedipalp chela fingers median denticle subrows count (left/right); CFL, pedipalp chela movable finger length; CMH, pedipalp chela manus height; CML, pedipalp chela manus length along retroventral carina; CMW, pedipalp chela manus width; CL, pedipalp chela total length including fixed finger; FH, pedipalp femur height; FL, pedipalp femur length; FW, pedipalp femur width; PAD, pedipalp chela fingers prolateral accessory denticle count; PH, pedipalp patella height; PL, pedipalp patella length; PW, pedipalp patella width; RAD, pedipalp chela fingers retro-lateral accessory denticle count.

sorted according to the species identification key of Levy and Amitai (1980). Morphological terminology follows recent publications by the last author, e.g., González-Santillán and Prendini (2013), Tahir et al. (2014) and Esposito et al. (2016). Forty-nine measurements (mm) and seven counts (figs. 11–13), following Tahir et al. (2014), were recorded for 79 specimens using Mitutoyo® digital calipers or a stereomicroscope. Morphometric ratios, expressed as

means, are provided separately for adult males and females.

**MULTIVARIATE STATISTICAL ANALYSIS:** Non-metric multidimensional scaling (NMDS) (fig. 15) and permutational multivariate analysis of variance (ADONIS) were conducted on 24 ratios and counts, each sex analyzed separately (appendix 4), using the programs “vegan” (Oksanen et al., 2007) and “ggplot2” (Wickham, 2009) in R version 3.1.2 (R Core Team, 2013).

## RESULTS

Phylogenetic analysis of the five gene loci (two from the nuclear genome, and three from the mitochondrial genome), 18 qualitative, and 48 quantitative morphological characters (fig. 14, Cain et al., in press), and multivariate analysis of the morphometric data (NMDS and ADONIS, fig. 15) both supported the recognition of three new species, raising the number of *Buthacus* species occurring in the Levant, to seven. The most informative morphological characters for species diagnosis were the carapace dimensions, chela shape, relative proportions of the metasomal segments, proportions of the telson vesicle and aculeus, pectinal tooth counts, pilosity/density of macrosetae on the metasoma and telson, and macrosulpture of the metasomal carinae.

Reflecting the sexual dimorphism evident among species of *Buthacus*, the morphology of the adult males was found to be more divergent than that of the adult female and immature stages in each species. This is evident, for example, in the NMDS plot, in which the males formed several distinct clusters (fig. 15A), compared with the females, which were more evenly distributed (fig. 15B). Five groups were identified in the male plot (fig. 15A). Three species occurring in the Jordan Valley and to the east, and in the Arabian Peninsula and the Middle East, *B. arava*, *B. tadmorensis*, and *B. yotvatensis*, were well separated from one another, and from the two other groups, comprising *B. arenicola* and related species, and *B. leptochelys* and related species, all of which occur to the west of the Jordan Valley, in the Sinai Peninsula and Africa. A similar pattern, although less pronounced, was observed in the female plot (fig. 15B).

The identification of two main groups of species, to the east and west of the Jordan Valley, by the multivariate analyses was supported by the phylogenetic analyses, which recovered two main clades, an African clade, comprising *Buthacus* species occurring to the west of the Jordan Valley, i.e., *B. arenicola*, *B. leptochelys* and related species (fig. 14), and an Asian clade, comprising

species occurring in the Jordan Valley and to the east, i.e., *B. arava* and *B. yotvatensis* (fig. 14). These two clades may be separated by a number of morphological characters, e.g., the telson ventral surface, which is smooth and glabrous in the African clade but granular in the Asian clade, and the presence of a gap between the pedipalp chela fingers, proximally, when closed in the African clade and absent in the Asian clade. A similar finding was recently obtained by Alqahtani and Badry (2020), based on an analysis of mitochondrial 16S rDNA sequences for seven *Buthacus* terminals representing three ingroup exemplar species, and five outgroup taxa.

The identification of two groups of species to the west of the Jordan Valley, in Africa and the Sinai Peninsula, by the multivariate analyses (fig. 15) was again supported by the phylogenetic analyses (fig. 14), which recovered two subclades in the African clade, one comprising material formerly assigned to *B. leptochelys*, the other comprising material formerly assigned to *B. arenicola*. This finding, also recovered in the study of Alqahtani and Badry (2020), reflects the opinions of previous authors (Vachon, 1952; Levy et al., 1973; Levy and Amitai, 1980) who divided the species of *Buthacus* into two groups, the *B. arenicola* group and the *B. leptochelys* group, based on the dentition of the pedipalp chela movable finger.

The subclade of material formerly assigned to *B. leptochelys* also comprised two subclades in the phylogenetic analyses (fig. 14). The first of these comprised material from the northeastern Negev Desert, Israel, described below as a new species, *B. amitaii*, whereas the second comprised material assigned to *B. leptochelys* and *B. nitzani*. Although *B. leptochelys* and *B. nitzani* were very closely related in the phylogenetic analysis (fig. 14), the two species were clearly separated by the multivariate analyses (fig. 15), especially the female plot, with a larger female sample size (fig. 15B), and confirmed by a between-species ADONIS test ( $r^2 = 0.83$ ;  $Pr = 0.003$ ). The diagnostic characters separating *B. amitaii*, *B. leptochelys*, and *B.*

*nitzani* include the proportions of the male pedipalp chela (manus width:length and height:length), retrolateral accessory denticles on the pedipalp chela movable finger, pectinal tooth counts, proportions of the metasomal segments (width:length ratios), macrosculpture of the metasomal carinae and intercarinal surfaces (median lateral carinae of segments I–III, ventrosubmedian and ventrolateral carinae of segments II and III, ventral intercarinal surfaces and posterior processes on the ventrolateral carinae of segment V), and shape of the telson vesicle.

Within the subclade comprising material formerly assigned to *B. arenicola*, material conspecific with *B. arenicola* from the vicinity of the type locality in Tunisia, was well separated from material originating in Israel and Egypt in the phylogenetic analyses (fig. 14). Although only two adult males of *B. arenicola* from Tunisia were available for inclusion in the multivariate morphometric analyses (fig. 15), a marked separation from the material originating from Israel and Egypt was identified by a between-species ADONIS test for the males ( $r^2 = 0.36$ ,  $Pr = 0.043$ ). Based on these results, material from Israel and Egypt, until recently assigned to *B. arenicola*, is described below as a new species, *B. levyi*. The two species may be separated by several diagnostic characters, including the proportions of the pedipalp chela (manus and movable finger), proportions of the metasomal segments (width:length ratios of the metasomal segments), and the development of the dorsolateral carinae on metasomal segment IV (well developed in *B. arenicola* but obsolete to absent in *B. levyi*).

Among the species of the Asian clade, occurring in the Jordan Valley and to the east, *B. arava* and *B. yotvatensis* were well separated in the phylogenetic analyses (fig. 14) and by a between-species ADONIS test for the males ( $r^2 = 0.8$ ;  $Pr = 0.001$ ). *Buthacus arava* and *B. yotvatensis* also separated clearly from *B. tadmorensis* in the NMDS plot (fig. 15). Numerous diagnos-

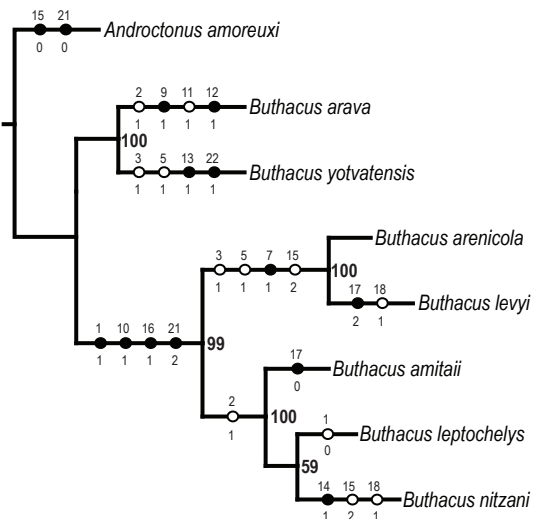


FIGURE 14. Phylogeny of *Buthacus* Birula, 1908, species, obtained by simultaneous phylogenetic analysis of 22 morphological characters and 2205 bp of DNA sequence from three mitochondrial (12S rDNA, 16S rDNA, and COI) and two nuclear (28S rDNA and ITS2) genes, for 104 samples (Cain et al., in press). Maximum likelihood tree with unambiguous morphological synapomorphies optimized. Black circles indicate uniquely derived apomorphic states, white circles parallel derivations of apomorphic states. Numbers above circles indicate characters, numbers below indicate states (appendix 3). Bootstrap support values are indicated at nodes.

tic characters separate the three species, including chela proportions, especially in the adult male (the chela manus is short and broad in *B. arava*, but long and narrow in *B. tadmorensis* and *B. yotvatensis*), pectinal tooth counts (much lower counts in *B. arava* than in *B. tadmorensis* and *B. yotvatensis*), pilosity/density of macrosetae on the metasoma and telson (sparsely setose in *B. arava*, but densely setose in *B. tadmorensis* and *B. yotvatensis*), and the macrosculpture of the ventral carinae of the metasoma (ventrosubmedian and ventrolateral carinae of metasomal segments II and III, and ventrolateral carinae of V, weakly developed, posterior processes slightly enlarged and spiniform in *B. arava* and *B. yotvatensis* but well developed, greatly enlarged, and lobate in *B. tadmorensis*).

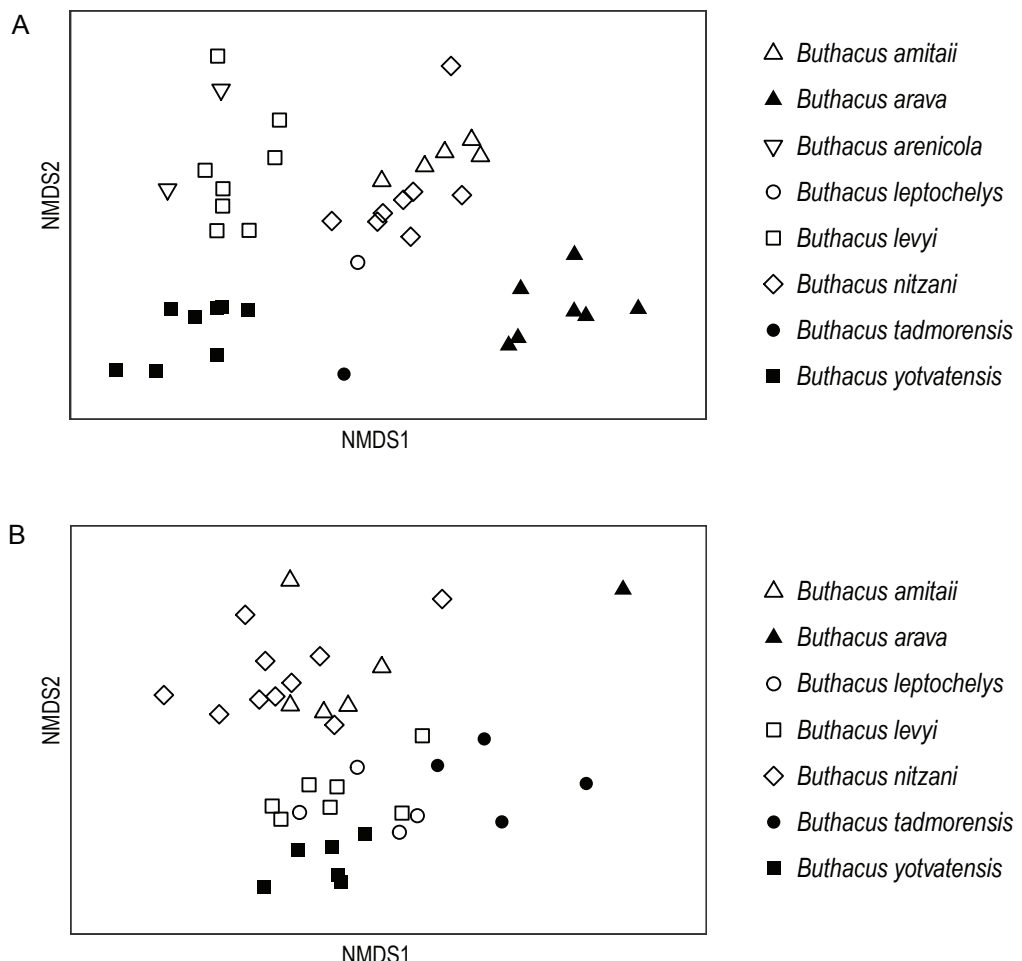


FIGURE 15. Nonmetric multidimensional scaling (NMDS) plots for **A**, male and **B**, female *Buthacus* Birula, 1908, based on 24 morphometric ratios and counts, for 79 adults (each symbol represents an individual): *Buthacus amitaii*, sp. nov. (white triangles); *Buthacus arava*, sp. nov. (black triangles); *Buthacus arenicola* (Simon, 1885) (white inverted triangles); *Buthacus leptochelys* (Ehrenberg, 1829) (white circles); *Buthacus levyi*, sp. nov. (white squares); *Buthacus nitzani* Levy et al., 1973, stat. nov. (white diamonds); *Buthacus tadmorensis* (Simon, 1892), stat. rev. (black circles); *Buthacus yotvatensis* Levy et al., 1973, stat. rev. (black squares).

#### SYSTEMATICS

FAMILY BUTHIDAE C.L. KOCH, 1837

Subfamily Buthinae C.L. Koch, 1837

*Buthacus* Birula, 1908

*Butthus* (*Buthacus*) Birula, 1908: 139, 140; type

species by original designation

*Androctonus* (*Leiurus*) *leptochelys*

Ehrenberg, 1829 [= *Buthacus leptochelys* (Ehrenberg, 1829)].

*Buthacus*: Simon, 1910: 74; Werner, 1934: 269; Kästner, 1941: 231; Vachon, 1948: 473–475, figs 229–232; Vachon, 1952: 178–180, figs. 229–232, 578; Bürgerl, 1964: 57; Stahnke, 1972: 131; Lamoral and Reynders, 1975: 499; Vachon, 1979: 44; Levy and Amitai, 1980: 75, 76; Francke, 1985: 6, 15; Sissom,

- 1990: 101; El-Hennawy, 1992: 97, 101, 112–114; Nenilin and Fet, 1992: 15–17; Amr and El-Oran, 1994: 186–187, 189; Kovařík, 1995: 19; 1997a: 49; 1997b: 179; Braunwalder and Fet, 1998: 32–34; Fet et al., 1998: 615, 616; Kabakibi et al., 1999: 82, 88; Fet and Lowe, 2000: 81–86; ICZN, 2000: 7; Lourenço, 2001: 255–268, figs. 23, table 1; Kovařík, 2001: 80; Crucitti and Vignoli, 2002: 438–443, figs. 3–5, 16; Kovařík, 2002: 5; Fet et al., 2003: 1–6, 10, fig. 1, table 1; Kovařík, 2003: 135, 137, 155, table 1; Lourenço, 2003: 877, 880, fig. 10; Soleglad and Fet, 2003a: 5, 26, table 2; 2003b: 7, 13, 88, 149, 151, 152, figs. B-1, B-2, table 9; Kovařík and Whitman, 2004: 106; Lourenço, 2004a: 205–209, figs. 1–6; 2004b: 226–230, figs. 1–16, table 1; Kovařík, 2005: 1–10, figs. 1–8, table 1; Prendini and Wheeler, 2005: 481, table 10; Hendrixson, 2006: 33, 36, 46–56, 59, 91, 99, 100, 109, figs. 4–7, plates 3–5, table 1; Lourenço, 2006: 59–69, figs. 1–43, table 1; Lourenço and Qi, 2006a: 161–164, figs. 1–16, table 1; 2006b: 301–306; Dupré, 2007: 3, 4, 12, 16; Yağmur et al., 2008: 13–17, figs. 2, 4; Navidpour et al., 2008: 1–9, 28, 30, 35, figs. 3, 4, 6, 12, 56–59; Zourgui et al., 2008: 81, 84, 85, 89, fig. 4, plate 5, 7, table 2; Al-Asmari et al., 2009a: 612, 613, 617–619, 621, 622, 624, 626, figs. 8, 9, 12F, G, tables 1, 2; 2009b: 96, 100, 102, 104, 106, fig. 6K, L, tables 5–7; Lourenço and Leguin, 2009: 103–107, figs. 1–12, table 1; Zarei et al., 2009: 46–49, 51, fig. 2; Zambre and Lourenço, 2010: 115–118, figs. 1–10, table 1; Mirshamsi et al., 2011: 17, 24, 26, fig. 1a, table 1; Shehab et al., 2011: 333–340, figs. 2E, 3–5, tables 1, 2; Lourenço et al., 2012: 307, 309, 313–316, 336, 337, figs. 12–23, 89, 90; Al-Asmari et al., 2013: 2, 5–16, figs. 6–10, 12–13, table 1; Kovařík et al., 2013: 1, 3, 4, 18, figs. 6; Lourenço, 2013: 89–97, figs. 1–14, table 1; Navidpour et al., 2013: 1, 3–5, 21, figs. 2, 4; Amr, 2015: 182–185, 192, 197, 198, figs. 1, 2C, table 3; Caliskan, 2015: 327–332, 336, 337, 343, figs. 1, 3, 5B; Lourenço and Sadine, 2015: 55–59, figs. 1–18; table 1; Navidpour, 2015: 10, 11, table 1; Amr et al., 2015: 30–33, 1C, D; Kovařík et al., 2016: 1–17, figs. 1–63, table 1; Lourenço et al., 2016: 2–10, figs. 1, 4–16; Lourenço et al., 2017a: 31–40, figs. 1, 2, 5–17; 2017b: 18–28, figs. 1, 5–16, tables 1, 2; Saleh et al., 2017: 9, 13, table 2; Sharifinia et al., 2017: 232–236, table 2; Badry et al., 2018: 77, 83; Dehghani and Kassiri, 2018: S881, table 2; Kovařík, 2018: 1–3, 6–10, figs. 10–14, 19–22; Sadine et al., 2018: 51, 53–57, figs. 3C, D, 4, table 1; Al-Khazali and Yağmur, 2019: 85–87, fig. 2C; Alqahtani et al., 2019: 19, 21–25, fig. 2C; Bousmaha et al., 2019: 141–145, figs. 2, 3, table 1; Francke, 2019: 6, 20, 37; Koç et al., 2019: 108–112, figs. 1, 5–7, table 1; Lowe et al., 2019: 1–5, 11, 15, 22, 24, 25, 28, figs. 45, 46, 78–81; Alqahtani and Badry, 2020: 178–183, figs. 1, 3, tables 1, 2; Hussen and Ahmed, 2020: 6711–6713, 6715, 6716, 6718, 6719, 6722, 6723, figs. 1, 7, tables 1, 2; Obuid-Allah et al., 2020: 227, 229–237, figs. 2G, H, 3D, tables 1, 3–6; Alqahtani and Badry, 2021: 3, 4, 7, 12, fig. 4, table 1; Amr et al., 2021: 84–90, 95, 97, fig. 3A, B, tables 1–5, 9–11, 17; Mansouri et al., 2021: 763, 765, 767, table 2; Said et al., 2021: 17, 18, 20, 21, 25, 26, fig. 4, table 1.

**DIAGNOSIS:** The genus *Buthacus* is most similar morphologically to other psammophilous buthid genera from the Palearctic deserts, notably *Buthiscus*, *Liobuthus*, *Pectinibuthus*, *Plesiobuthus*, *Trypanothacus*, and *Vachoniolus*, from which it differs as follows. Tibial spurs are present on legs III and IV in *Buthacus* and *Trypanothacus*, but may be reduced or absent on leg III; present only on leg IV in *Buthiscus*; and absent in *Liobuthus*, *Pectinibuthus*, *Plesiobuthus*, and *Vachoniolus* (Sissom, 1990; Levy et al., 1973; Fet et al., 2001; Lowe, 2010; Kovařík et al., 2016). The pedipalp chela movable finger bears 9–12 subrows of median denticles in

*Buthacus*, compared with 7 in *Liobuthus*, 7–9 in *Trypanothacus*, 9 in *Vachoniolus*, 10 in *Pectinibuthus*, and 12 in *Plesiobuthus* (Sissom, 1990; Levy et al., 1973; Fet et al., 2001; Lowe, 2010; Kovařík et al., 2016). The telson vesicle is pyriform, with a long, curved aculeus in *Buthacus*, whereas the vesicle is more bulbous, with a shorter aculeus in *Trypanothacus* (Lowe et al., 2019).

**DISTRIBUTION:** The species of *Buthacus* are widespread in the sandy deserts of the Palearctic region, occurring from the Atlantic coast of West Africa across the Sahara and the Sahel, and throughout the Middle East to India. In Africa, the genus has been recorded from the following countries and territories: Algeria, Chad, Egypt, Libya, Mauritania, Morocco, Niger, Nigeria, Senegal, Sudan, Tunisia, and Western Sahara. The presence of *Buthacus* in Burkina Faso, Eritrea, and Mali, while presently unconfirmed, seems likely. In Asia, the genus has been recorded from the following countries: Afghanistan, Bahrain, India, Iran, Iraq, Israel, Jordan, Kuwait, Lebanon, Oman, Pakistan, Qatar, Saudi Arabia, Syria, Turkey, the United Arab Emirates. *Buthacus* probably also occurs in Yemen and the Gaza Strip.

**ECOLOGY:** All species of *Buthacus* inhabit sandy substrates (fig. 1). However, the stability of the substrate, a function of its hardness, texture, and the density of rock and vegetation vary, from shifting sand dunes, through semiconsolidated dunes, flats, or dry watercourses, to consolidated sand, gravel, and loess plains. Closely related species may inhabit substrata of very different hardness and texture. For example, *B. arava*, sp. nov., inhabits semiconsolidated to shifting sand dunes, whereas the closely related *B. tadmorensis* inhabits loose to hard, compacted sandy plains and wadis, often with stones. The suite of ultrapsammophilous to semipsammophilous adaptations these scorpions possess for locomotion and burrowing on sandy substrata include elongation of the legs, especially legs III and IV, dorsoventral compression of the basitarsi of legs I–III, rows of elongated macrosetae (“sand combs”) along the retrolateral margins of the tibae and the pro- and retrolateral margins of the basitarsi of legs I–III, elongated macrosetae on the lateral and ven-

tral surfaces of the telotarsi, and elongated ungues, often unequal in length on legs I and II (Prendini, 2001). Additionally, many species exhibit loss or reduction of granulation and carination on the tegument, and pale coloration, often associated with a loss or reduction of infuscation.

**INCLUDED SPECIES:** The genus *Buthacus* currently includes 30 species and one subspecies: *Buthacus agarwali* Zambre and Lourenço, 2010; *Buthacus ahaggar* Lourenço et al., 2017; *Buthacus amitaii*, sp. nov.; *Buthacus arava*, sp. nov.; *Buthacus arenicola* Simon, 1885; *Buthacus a. maroccanus* Lourenço, 2006; *Buthacus armasi* Lourenço, 2013, stat. rev.; *Buthacus birulai* Lourenço, 2006; *Buthacus clevai* Lourenço, 2001; *Buthacus elmenia* Lourenço et al., 2017; *Buthacus foleyi* Vachon, 1948; *Buthacus frontalis* Werner, 1936; *Buthacus fuscata* Pallary, 1929, stat. nov. et stat. rev.; *Buthacus golovatchi* Lourenço et al., 2012; *Buthacus leptochelys* Ehrenberg, 1829; *Buthacus levyi*, sp. nov.; *Buthacus nigerianus* Lourenço and Qi, 2006; *Buthacus nigroaculeatus* Levy et al., 1973; *Buthacus nitzani* Levy et al., 1973, stat. nov.; *Buthacus occidentalis* Vachon, 1953; *Buthacus pakistanensis* Lourenço and Qi, 2006; *Buthacus samiae* Lourenço and Sadine, 2015; *Buthacus spatzi* (Birula, 1911), stat. rev.; *Buthacus spinatus* Lourenço et al., 2016; *Buthacus stockmanni* Kovařík et al., 2016; *Buthacus striffleri* Lourenço, 2004; *Buthacus tadmorensis* Simon, 1892, stat. rev.; *Buthacus villiersi* Vachon, 1949; *Buthacus williamsi* Lourenço and Leguin, 2009; *Buthacus yotvatensis* Levy et al., 1973, stat. rev.; *Buthacus ziegleri* Lourenço, 2000.

**REMARKS:** The original description of *Buthacus frontalis* Werner, 1936, was based on a dry specimen that has never been reexamined. According to Kovařík (2003: 152) the “holotype (a female from Asmara, Eritrea) was destroyed during the air raid on Hamburg in 1943... [the] original description does not contain diagnostic characters, and no additional specimens are known [therefore] this name has to be regarded as dubious.” Levy et al. (1973) and Levy and Amitai (1980) also doubted the assignment of this species to the genus *Buthacus*.

Four species originally described in the genus *Buthacus* were subsequently transferred to other genera (Vachon, 1979; Kovářík et al., 2013; Kovářík, 2018; Lowe et al., 2019). *Buthacus minipectenibus* Levy et al., 1973, was transferred by Vachon (1979) to the genus *Vachoniolus* Levy et al., 1973, becoming *Vachoniolus minipectenibus* (Levy et al., 1973), and later synonymized with *Vachoniolus globimanus* Levy et al., 1973, by Hendrixson (2006). *Buthacus calviceps*, from Somaliland (Pocock, 1900), was transferred to the genus *Gint* Kovářík et al., 2013, becoming *Gint calviceps* (Pocock, 1900). *Buthacus buettikeri*, from Saudi Arabia (Hendrixson, 2006), was transferred to the genus *Trypanothacus* Lowe et al., 2019, becoming *Trypanothacus buettikeri* (Hendrixson, 2006). *Buthacus maliensis* Lourenço and Qi, 2007, from Mali, was synonymized with *Androctonus aleksandrplotkini* Lourenço and Qi, 2007 by Kovářík (2018).

Additionally, three other species, *B. argarwali* from India (Zambre and Lourenço, 2010), *B. pakistanensis* from Pakistan (Lourenço and Qi, 2006a), and *B. williamsi* from the United Arab Emirates (Lourenço and Leguin, 2009), appear to have been erroneously assigned to *Buthacus* based on the carapacial carinae, pedipalp shape, and counts of median denticle subrows on the pedipalp chela fingers, among other characters (see, e.g., Kovářík et al., 2016).

#### Key to the Species of *Buthacus* Occurring in the Levant

1. Metasomal segments IV, V and telson, intercarinal surfaces granular and matte (figs. 27A–C, 29C, E, G).....2
- Metasomal segments IV, V and telson, intercarinal surfaces smooth and glabrous (figs. 27D, 28, 29A, B, D, F, H).....4
2. Pectinal tooth count >22 (♂, ♀; fig. 19C–F); metasomal segments, dorsosubmedian and dorsolateral carinae, and telson, ventral surface densely setose (figs. 23B, C, 25B, C, 29E, G); legs I and II, telotarsal unguis equal in length (fig. 22E, G).....3
- Pectinal tooth count ≤22 (♂, 18–22; ♀, 12–14; fig. 19A, B); metasomal segments, dorsosubmedian and dorsolateral carinae, and telson, ventral surface sparsely setose (figs. 23A, 25A, 29C); legs I and II, telotarsal unguis unequal in length (fig. 22C).....*B. arava*, sp. nov.
3. Metasomal segments II and III, ventrosubmedian and ventrolateral carinae, and V, ventrolateral carinae well developed, posterior processes greatly enlarged, lobate (figs. 25B, 27B).....*B. tadmorensis*, stat. rev.
- Metasomal segments II and III, ventrosubmedian and ventrolateral carinae, and V, ventrolateral carinae weakly developed, posterior processes slightly enlarged, spiniform (figs. 25C, 27C).....*B. yotvatensis*, stat. rev.
4. Pedipalp chela of adult ♂ narrow (fig. 44A, B), manus width:chela length, 19.4% (17.1%–21.3%), resembling chela of adult ♀ (fig. 44C, D), 17% (15.6%–19.6%); chela movable finger, retrolateral accessory denticles usually absent (fig. 21E, F); metasomal segment V ventrolateral carinae, posterior spiniform granules uniformly small (fig. 26A).....*B. levyi*, sp. nov.
- Pedipalp chela of adult ♂ broad (figs. 32A, B, 41A, B, 47A, B), manus width:chela length, 27.1% (25.1%–28.9%) in *B. amitaii*, sp. nov., 24.2% in *B. leptochelys*, and 26.3% (22.3%–29.5%) in *B. nitzani*, stat. nov., unlike chela of adult ♀ (figs. 32C, D, 41C, D, 47C, D), 19.3% (18–20.8), 16.7% (15.9%–17.3%), 19.9% (18%–24.1%), respectively; chela movable finger, retrolateral accessory denticles usually present (fig. 21A, D, G); metasomal segment V ventrolateral carinae, posterior spiniform granules variable, some large (fig. 26B–D).....5
5. Total length >59 mm; pedipalp chela of adult ♂ long (fig. 41A, B), e.g., manus length:movable finger length, 70.7%; pectinal tooth count >35 (32–39) in ♂, >27 (27–31) in ♀.....*B. leptochelys*
- Total length < 59 mm; pedipalp chela of adult ♂ short (figs. 32A, B, 47A, B), manus

- length:movable finger length, 81.8% (72.7%–88.3%) in *B. amitaii*, sp. nov., and 84.4% (76.8%–92.4%) in *B. nitzani*, stat. nov.; pectinal tooth count  $\leq$  35 (26–35) in ♂,  $\leq$  27 (20–27) in ♀ (fig. 20A–D). . . . . 6
6. Metasomal segments II and III, ventrosubmedian and ventrolateral carinae well developed, posterior granules slightly enlarged, spiniform; segment V ventrolateral carinae, posterior granules enlarged, lobate (figs. 28D, 26D). . . . .  
..... *B. amitaii*, sp. nov.
- Metasomal segments II and III, ventrosubmedian and ventrolateral carinae weakly developed, posterior granules similar to preceding granules; segment V ventrolateral carinae, posterior granules slightly enlarged, spiniform (figs. 28C, 26C). . . . .  
..... *B. nitzani*, stat. nov.

***Buthacus amitaii*, sp. nov.**

Figures 1A, 2A, B, 7, 15, 17E, F, 20C, D, 21A, 22H, 24D, 26D, 28D, 29H, 30, 31, 32;  
tables 1, 2, 3

*Buthacus leptochelys leptochelys*: Levy and Amitai, 1980: 76, 77, 79–83, figs. 70–74, map 6; Kabakibi et al., 1999: 82, 88 (misidentification); Fet and Lowe, 2000: 84; Lourenço, 2006: 62.

*Buthacus leptochelys*: El-Hennawy, 1992: 101, 112, 113 (misidentification); Lourenço, 2006: 59–69, figs. 1, 4, table 1.

**TYPE MATERIAL: ISRAEL:** *Mehoz HaDarom (Southern District)*: Holotype ♂ (HUJ INVSC 3480 ex AMNH), Mamshit [Kurnub], road to Negev Camel Ranch 31°01'59.9"N 35°04'25"E, 477 m, 28.viii.2011, L. Prendini and T.L. Bird. Paratypes: Mamshit [Kurnub, 31°01'N 35°03'E], 475 m, 14–20.vi.1971, P. Amitai, 3 ♂ (HUJ INVSC 2283–2284, 2294), 2 ♀ (HUJ INVSC 2278, 2292); Mamshit, road to Negev Camel Ranch 31°01'59.9"N 35°04'25"E, 477 m, 28. viii.2011, L. Prendini and T.L. Bird, 65 ♂, 44 ♀

(AMNH), 2 juv. ♂, 2 juv. ♀ (AMCC [LP 11176]); Mamshit, Negev Camel Ranch, wadi behind camp, 31°01'46.5"N 35°04'39.2"E, 471 m, 28. viii.2011, L. Prendini and T.L. Bird, 1 ♂, 11 ♀ (AMNH), 2 juv. ♂ (AMCC [LP 11173]), 29. viii.2013, L. Prendini, I. Tesler and A. Novikova, 13 ♂, 23 ♀ (AMNH); Mamshit, W of Negev Camel Ranch car park, 31°01'50.7"N 35°04'35.2"E, 475 m, 5.viii.2016, E. Gefen and S. Cain, 3 ♂ (AMCC [LP 15046] ex HUJ INVSC 3202, HUJ INVSC 3203–3204), 2 ♀ (AMNH ex HUJ INVSC 3200, HUJ INVSC 3201); Nahal HaTira, Kholot Tsivoniym campsites, 30°57'07.9"N 35°01'34.9"E, 304 m, 16.iv.2018, Y. Zvik and S. Cain, 1 ♂ (HUJ INVSC 3463), 3 ♀ (HUJ INVSC 3462, 3464 – 3465), 3 juv. ♂ (HUJ INVSC 3466, 3468, 3470), 2 juv. ♀ (HUJ INVSC 3467, 3469); Na al Yamin, SW of Dimona factory, 30°57'01.8"N 35°04'51.7"E, 330 m, 16. iv.2017, Y. Zvik, 2 ♀ (AMCC [LP 15047] ex HUJ INVSC 3207, HUJ INVSC 3205), 1 subad. ♀ (HUJ INVSC 3206), 16.iv.2018, Y. Zvik and S. Cain, 1 ♀ (HUJ INVSC 3471), 1 subad. ♀ (HUJ INVSC 3472).

**DIAGNOSIS:** *Buthacus amitaii* is most closely related to *B. nitzani*, also occurring in Israel, and *B. leptochelys*, occurring in Egypt. *Buthacus amitaii* differs from *B. nitzani* as follows. The metasomal segments of the female are shorter and broader in *B. amitaii* (fig. 28D), with segment IV width:length, 42.8% (40.2%–44.9%,  $n = 5$ ; table 3), than in *B. nitzani* (fig. 28C), with segment IV width:length, 38.4% (34%–43.7%,  $n = 10$ ; table 13). The ventrosubmedian and ventrolateral carinae are more developed on the metasomal segments, especially on segments II and III, in *B. amitaii* than *B. nitzani* (figs. 26C, D, 28C, D). The posterior processes of the ventrolateral carinae of metasomal segment V are broad and lobate in *B. amitaii*, but narrow and spiniform in *B. nitzani*. The median lateral carinae are distinct on metasomal segments I–III in *B. amitaii*, but obsolete in *B. nitzani*. The ventral intercarinal surfaces of metasomal segment V are more coarsely and densely granular in *B. amitaii* than *B. nitzani*. The retrolateral accessory denticles on the mov-

TABLE I  
African and Asian countries with records of sand scorpions (Buthidae: *Buthacus* Birula, 1908)

able finger of the pedipalp chela are often absent, with variable, usually lower counts (sinistral/dextral: 0–9/2–10;  $n = 9$ ; table 2; fig. 21A) in *B. amitaii*, compared to *B. nitzani*, in which the retrolateral accessory denticles are always present, with constant, usually higher counts (6–9/6–9;  $n = 16$ ; table 2; fig. 21G).

*Buthacus amitaii* differs from *B. leptochelys* as follows. *Buthacus amitaii* is smaller, measuring 51.7 mm (48–58.8 mm,  $n = 10$ ; table 3) in total length, than *B. leptochelys*, measuring 65.8 mm (63.1–68 mm,  $n = 5$ ; table 4). The pedipalp chela of the adult male is shorter and broader (fig. 32A, B), with chela manus width:chela length, 27.1% (25.1%–28.9%,  $n = 5$ ; table 3) and chela manus height:length, 69.7% (58.9%–75.5%,  $n = 5$ ), in *B. amitaii* than in *B. leptochelys* (fig. 41A, B), with chela manus width:chela length, 24.2% (table 4), and chela manus height:length, 58.9%. The proximal dentate margins of the pedipalp chela fixed and movable fingers are more deeply emarginate, such that a more pronounced gap is evident proximally when the fingers are closed, in *B. amitaii* (fig. 32B) than in *B. leptochelys* (fig. 41B). The pectinal tooth counts are lower in *B. amitaii*, i.e., 30/31 (28–32/28–33,  $n = 5$ ; table 2) (♂) and 23/23 (21–26/21–26,  $n = 9$ ) (♀), than in *B. leptochelys*, i.e., 35/34 (32–39/32–38,  $n = 6$ ; table 5) (♂) and 29/29 (27–31/28–31,  $n = 10$ ) (♀). The telson vesicle dorsal surface is concave and the ventral surface convex and angular in lateral profile, in *B. amitaii* (fig. 29H), whereas the dorsal surface is flat and the ventral surface convex and rounded in lateral profile, in *B. leptochelys* (fig. 29D).

*Buthacus amitaii* differs from *B. levyi*, another species occurring in Israel with which it may be confused, as follows. The pedipalp chela of the adult male is shorter and broader in *B. amitaii* (fig. 32A, B), with chela manus length:movable finger length, 81.8% (72.7%–88.3%,  $n = 5$ ; table 3) and chela manus width:chela length, 27.1% (25.1%–28.9%,  $n = 5$ ), than in *B. levyi* (fig. 44A, B), with chela manus length:movable finger length, 62.8% (57.4%–67.3%,  $n = 8$ ; table 10) and chela manus

width:chela length, 19.4% (17.1%–21.3%,  $n = 8$ ). The proximal dentate margins of the pedipalp chela fixed and movable fingers are emarginate, such that a gap is evident proximally when the fingers are closed, in *B. amitaii* (fig. 32B), but sublinear, such that no gap is evident proximally when the fingers are closed, in *B. levyi* (fig. 44B). The counts of retrolateral accessory denticles on the movable finger of the pedipalp chela are usually higher in *B. amitaii* (sinistral/dextral: 0–9/2–10;  $n = 9$ ; table 2; fig. 21A) than in *B. levyi* (0–5/0–3;  $n = 13$ ; table 5; fig. 21E, F). The posterior processes on the ventrolateral carinae of segment V are larger and more variable in size in *B. amitaii* (figs. 26D, 28D) than in *B. levyi* (figs. 26A, 28A). The telson dorsal surface is concave and the ventral surface convex and angular in lateral profile, in *B. amitaii* (fig. 29H), whereas the dorsal surface is flat and the ventral surface convex in lateral profile, in *B. levyi* (fig. 29B).

**ETYMOLOGY:** The species name is a patronym, honoring Pinchas Amitai, one of the pioneers of arachnology in Israel, whose publications, some coauthored with Gershon Levy (e.g., Levy and Amitai, 1980), constitute a milestone in understanding the scorpions and other arachnids of the Levant.

**DESCRIPTION:** The following description is based on the type material (see table 2 for counts and table 3 for measurements).

**Total length:** Medium-sized scorpions, 53.9 mm (48–58.8 mm,  $n = 5$ ) (♂) or 49.5 mm (48.5–50.8 mm,  $n = 5$ ) (♀).

**Color:** Uniformly yellowish olive except as follows. Carapace interocular surface, pedipalp femur, and patella, legs, and metasomal segments orange. Pectines pale yellow. Legs articulation points brown.

**Carapace:** Carapace shape trapezoidal (fig. 17E, F), anterior width:posterior width, 52.1% (45.8%–54%,  $n = 10$ ), length:posterior width, 88.7% (83.6%–94.6%,  $n = 10$ ). Five, rarely four, pairs of lateral ocelli; each lateral ocular tubercle with two or, usually, three major ocelli (ALMa, MLMa, PLMa), similar in size, situated anterolat-

TABLE 2

**Meristic data for material of *Buthacus amitaii*, sp. nov., and *Buthacus nitzani* Levy et al., 1973, stat. nov., deposited in the American Museum of Natural History (AMNH), New York, and the National Natural History Collections, Hebrew University of Jerusalem (HUJ), Israel**  
Counts (left/right) follow Tahir et al. (2014); pedipalp chela fix. subrows (fixed finger median denticle subrows); pedipalp chela mov. subrows (movable finger median denticle subrows); pedipalp chela fix. PAD (fixed finger prolateral accessory denticle count); pedipalp chela mov. PAD (movable finger prolateral accessory denticle count); pedipalp chela fix. RAD (fixed finger retrolateral accessory denticle count); pedipalp chela mov. finger RAD (movable finger retrolateral accessory denticle count); pectinal tooth count.

Species	type	Specimen		accession no.	Pedipalp chela				mov. RAD	pectines
		sex	collection		fix. subrows	mov. subrows	fix. PAD	mov. PAD		
<i>B. amitaii</i>										
Holotype	♂	HUJ	3480	9/9	9/9	10/9	10/10	10/10	4/5	4/6
Paratype	♂	AMNH		9/8		9/10	10/10	10/9	8/6	9/7
Paratype	♂	HUJ	3202	9/9	9/10	9/9	10/10	10/10	7/6	7/7
Paratype	♂	HUJ	3203	8/8	10/8	7/9	9/10	9/10	3/2	0/2
Paratype	♂	HUJ	3204	8/9	9/9	10/10	11/10	11/10	6/7	8/6
Paratype	♀	AMNH		10/8	10/10	10/8	9/10	9/10	7/5	7/5
Paratype	♀	HUJ	3205	9/9	9/9	10/10	10/10	10/10	7/7	9/10
Paratype	♀	HUJ	3200	10/9	9/-	9/9	9/-	9/-	3/2	3/-
Paratype	♀	HUJ	3201	8/8	-7/9	8/9	-10/	7/7	-6/	26/26
Paratype	♀	HUJ	3207	9/9	9/10	9/9	8/10	8/10	4/5	5/6
<i>B. nitzani</i>										
♂	HUJ	3210	9/9	9/10	10/10	11/11	8/8	8/8	9/9	32/32
♂	HUJ	3220	9/9	9/9	10/10	11/11	8/8	8/8	8/9	-3/2
♂	HUJ	3222	9/8	10/10	10/10	11/10	8/8	8/8	9/9	-3/0
♂	HUJ	3224	8/9	9/9	10/10	10/11	8/8	8/8	9/9	31/31
♂	HUJ	3232	9/10	8/8	9/9	9/10	6/7	6/7	7/7	34/35
♂	HUJ	3234	8/9	9/9	9/10	10/10	7/8	7/8	8/8	33/31
♂	HUJ	3238	9/9	9/9	9/9	10/10	7/7	7/7	8/8	28/28
♂	HUJ	3245	8/9	10/9	9/9	10/10	5/5	5/5	6/6	26/27
♀	HUJ	3214	9/9	10/9	10/10	11/11	8/6	7/9	25/23	
♀	HUJ	3218	8/-	9/9	10/-	11/11	7/-	9/9	23/23	
♀	HUJ	3221	9/8	-7/8	9/9	-10/	7/7	-8/	24/24	
♀	HUJ	3225	9/7	10/10	10/6	11/11	8/7	8/9	24/23	
♀	HUJ	3226	8/9	10/10	10/10	11/10	8/7	9/9	25/24	
♀	HUJ	3230	9/7	7/9	10/6	7/11	8/7	4/9	24/23	
♀	HUJ	3240	9/8	9/9	8/7	10/10	7/7	8/8	27/27	
♀	HUJ	3247	9/8	9/9	9/7	10/8	7/4	7/6	24/23	
♀	HUJ	3248	8/8	8/8	9/9	10/11	7/7	7/8	23/23	
♀	HUJ	3249	8/8	9/7	9/9	10/10	7/8	7/7	22/23	

erally, and one or, usually, two minor ocelli (ADM<sub>i</sub>, PDM<sub>i</sub>; PDM<sub>i</sub> may be absent) situated posterodorsal to posterior major ocellus. Median ocelli larger than lateral ocelli, distance between them more than 2× ocellus width. Median ocular tubercle situated anteromedially, distance from anterior carapace margin:carapace length, 42.3% (40.6%–43.5%,  $n = 5$ ) (♂) or 42.7% (40.5%–43.6%,  $n = 5$ ) (♀). Superciliary and central median carinae distinct, costate-granular, strongly to weakly connected (♂) or weakly connected to disconnected (♀). Anteromedian sulcus distinct, shallow; posteromedian sulcus deep, narrow anteriorly, wide posteriorly; posterolateral sulci shallow, wide, curved. Carapace intercarinal surfaces finely and densely granular.

***Chelicerae:*** Cheliceral manus prodorsal margin granular; retrodorsal surfaces smooth or finely granular; prolateral and ventral surfaces densely setose. Fixed finger dorsal and ventral surfaces densely setose; dorsal margin with subdistal, medial, and proximal denticles; ventral margin with proximal and medial denticles. Movable finger dorsal surface smooth and glabrous; ventral surface densely setose; dorsal margin with retrodistal, subdistal, medial, and pair of proximal denticles; ventral margin with prodistal, medial, and proximal denticles.

***Pedipalps:*** Femur dorsal prolateral, dorsal retrolateral and ventral prolateral carinae complete, costate-granular; prolateral ventral and prolateral ventrosubmedian carinae each comprising discontinuous row of spiniform granules; retrolateral dorsosubmedian carina absent, represented by fewer than 10 macrosetae; intercarinal surfaces smooth (fig. 31A, B). Patella prolateral median and ventral prolateral carinae discontinuous, each comprising a few spiniform granules; other carinae absent; intercarinal surfaces smooth (fig. 31C–E). Chela short and broad (♂), manus width:length, 62.6% (53.4%–68.3%,  $n = 5$ ), manus height:length, 69.7% (58.9%–75.5%,  $n = 5$ ), and manus length:movable finger length, 81.8% (72.7%–88.3%,  $n = 5$ ) or short and slender (♀), manus width:length, 54.4% (49.4%–58.9%,  $n = 5$ ), manus height:length, 61.2% (55.1%–64.6%,  $n = 5$ ),

and manus length:movable finger length, 58.1% (54.2%–61.5%,  $n = 5$ ). Chela manus acarinate; intercarinal surfaces smooth and glabrous (fig. 32). Fixed and movable fingers each with 8–10 ( $n = 9$ ) oblique median denticle subrows; movable finger with 0–10 ( $n = 9$ ) retrolateral accessory denticles (fig. 21A); proximal dentate margins of fingers emarginate (fig. 32B), such that gap present proximally when fingers closed.

***Legs:*** Legs I–IV, femoral ventral carinae granular; patellar ventral carinae obsolete; intercarinal surfaces smooth. Legs I–IV, macrosetal counts on retrolateral margins of tibiae, 6:9:11:4; basitarsi, 9:12:15:10; telotarsi, 4:6:5:6 ( $n = 1$ ). Legs I–IV, tibial spurs absent on I and II, present on III and IV; pro- and retroventral basitarsal (pedal) spurs present, more developed on III and IV. Telotarsal ungues long, approximately equal to telotarsus length, unequal on legs I and II, subequal to equal on III and IV (fig. 22H).

***Genital operculum:*** Genital opercula suboval, completely divided longitudinally, with overlapping, rounded margins (♂) or partially fused longitudinally (♀) (fig. 20C, D). Genital papillae present (♂) or absent (♀).

***Pectines:*** Three marginal lamellae; 8–10 ( $n = 2$ ) (♂) or 7–9 ( $n = 3$ ) (♀) median lamellae (fig. 20C, D). Fulcra present. Pectinal teeth along most of length, dentate margin length:pecten length, 98.3% (94.4%–106.7%,  $n = 5$ ) (♂) or 95% (91.3%–98.3%,  $n = 5$ ) (♀). Pectinal teeth curved, similar in size; tooth count (sinistral/dextral), 30/31 (28–32/28–33,  $n = 5$ ) (♂) or 23/23 (21–26/21–26,  $n = 9$ ) (♀).

***Mesosoma:*** Tergites I–VII progressively increasing in length posteriorly, tergite VI length:tergite VII length, 57.6% (55.1%–61.3%,  $n = 5$ ) (♂) or 68.9% (55.2%–106.2%,  $n = 5$ ) (♀); increasing in width posteriorly from I–IV, decreasing in width posteriorly from V–VII. Pretergites smooth; posttergites I–VI, intercarinal surfaces uniformly finely granular, becoming more coarsely and densely granular posteriorly, VII, finely to coarsely and sparsely granular. Tergites I–VI, dorsomedian carinae absent on I, granular, vestigial, restricted to

posterior third of II–IV and posterior half of V and VI; dorsosubmedian carinae granular, vestigial, restricted to posterior fifth of I–IV and posterior third of V and VI. Tergite VII, dorsomedian carina absent to granular, vestigial, restricted to anterior half; dorsosubmedian and dorsolateral carinae distinct, granular. Sternites III–VII smooth and glabrous; III–VI acarinate, VII, ventrolateral carinae vestigial, granular; IV–VI, respiratory spiracles (stigmata) width approximately 3× length.

**Metasoma:** Metasomal segments I–V becoming longer and narrower posteriorly (figs. 24D, 26D, 28D), segment I shortest, length I:II, 87.5% (84.2%–89.5%,  $n = 5$ ) (♂) or 86.7% (80.4%–89.8%,  $n = 5$ ) (♀); segments II–IV similar, length II:III, 96.4% (95.1%–97.1%,  $n = 5$ ) (♂) or 97.3% (95%–100.2%,  $n = 5$ ) (♀), length III:IV, 97.4% (93.2%–103.1%,  $n = 5$ ) (♂) or 99.3% (96.4%–103.9%,  $n = 5$ ) (♀); segment V longest, length IV:V, 82.2% (80.8%–83.4%,  $n = 5$ ) (♂) or 77.5% (73.3%–84.8%,  $n = 5$ ) (♀); width:length segment I, 69.1% (61.8%–72.7%,  $n = 5$ ) (♂) or 69.6% (64%–77.4%,  $n = 5$ ) (♀), II, 58.8% (57.8%–61.2%,  $n = 5$ ) (♂) or 56.6% (52.1%–59.6%,  $n = 5$ ) (♀), III, 53.8% (52.2%–55.1%,  $n = 5$ ) (♂) or 52.5% (49.4%–55.7%,  $n = 5$ ) (♀), IV, 42.8% (37.2%–47.3%,  $n = 5$ ) (♂) or 42.8% (40.2%–44.9%,  $n = 5$ ) (♀), V, 35.8% (33.9%–39.5%,  $n = 5$ ) (♂) or 36.1% (33.2%–38.5%,  $n = 5$ ) (♀). Dorsosubmedian carinae distinct, granular on segments I and II, obsolete on III, absent on IV and V; dorsolateral carinae distinct, granular on segments I and II, obsolete on III and IV, absent on V; dorsosubmedian and dorsolateral carinae sparsely setose, macrosetal counts on segments I–V (sinistral/dextral), dorsosubmedian carinae, 1/0 (0/0–3/1,  $n = 5$ ):2/3 (2/2–3/4):3/3 (2/3–4/4):3/3 (1/2–4/4):0/0 (0/0–1/0); dorsolateral carinae, 2/2 (0/1–3/3,  $n = 5$ ):3/3 (2/1–3/4):4/3 (3/1–5/5):3/2 (1/0–5/4):5/6 (2/4–7/8). Median lateral carinae distinct, granular, extending entire length of segment I, restricted to posterior half of II and posterior quarter of III, absent on IV and V. Ventrolateral carinae

distinct, costate, becoming granular posteriorly on segment I; costate-granular along entire length, with granules becoming progressively larger and spiniform posteriorly, on II and III; costate-granular along entire length of IV; distinct, serrate, comprising spiniform granules and lobate processes posteriorly, on V. Ventrosubmedian carinae distinct, costate on segment I; costate-granular along entire length, with granules becoming progressively larger and spiniform posteriorly, on II and III; costate-granular along entire length of IV; granular, restricted to anterior three-quarters of V. Ventromedian carina granular, distinct along entire length of segment V. Dorsal and lateral intercarinal surfaces smooth on segments I–V; ventral intercarinal surfaces smooth on I and II, finely granular on III and IV, finely and densely granular across entire surface of V.

**Telson:** Telson vesicle width:metasomal segment V width, 80.5% (76.6%–82%,  $n = 5$ ) (♂) or 78.3% (74.3%–80.5%,  $n = 5$ ) (♀). Vesicle globbose, dorsal surface concave, ventral surface convex and angular; vesicle height:length, 69.2% (62.6%–74.5%,  $n = 5$ ) (♂) or 66.2% (61.5%–69.9%,  $n = 5$ ) (♀); dorsal and ventral surfaces smooth and glabrous; lateral and ventral surfaces sparsely setose, with 26 (23–29,  $n = 2$ ) (♂) or 32 (29–39,  $n = 3$ ) (♀) macrosetae. Aculeus long, gently curved; aculeus length:telson length, 52.1% (49.6%–55.5%,  $n = 5$ ) (♂) or 55.2% (52.1%–60.5%,  $n = 5$ ) (♀).

**Sexual dimorphism:** Adult males and females differ as follows. The pedipalp chela manus of the male is markedly broader and deeper with proportionally shorter fingers than that of the female (fig. 32), as indicated by the higher ratios of chela manus width:length, manus height:length, and manus length:movable finger length, respectively 62.6%, 69.7%, and 81.8% in the male compared with 54.4%, 61.2%, and 58.1% in the female. The genital opercula are completely divided longitudinally, with overlapping, rounded margins in the male but partially

fused longitudinally in the female (fig. 20C, D), and genital papillae are present in the male but absent in the female. The pectinal tooth count is higher in the male (28–33) than in the female (22–26). The spiniform granules of the ventrosubmedian and ventrolateral carinae of metasomal segments II and III, and the ventrolateral carinae of segment V are less prominent in the male than in the female.

**DISTRIBUTION:** *Buthacus amitaii* appears to be endemic to the inland sandy soils and loess of the Yamin Plain and Mamshit area in the northern Negev, Israel (fig. 7). The known records are located at elevations ranging from 304 m to 477 m.

*Buthacus amitaii* is allopatric with the closely related *B. leptochelys*, distributed from the western Sinai Peninsula across Egypt, and southward along the coast of the Red Sea to Sudan (fig. 6), and *B. nitzani*, distributed from the Sorek (Rubin) River, throughout the sand dunes of the southern coastal plain of Israel, to the Haluza dunes of the interior and probably the adjacent Sinai Peninsula of Egypt (fig. 7).

**ECOLOGY:** The types of *B. amitaii* were collected at night with UV light detection on flat to gently sloping loess plains, comprising compacted sandy loam with soft hummock dunes in places. The substratum was noticeably more compact compared with the habitats in which the closely related *B. leptochelys* and *B. nitzani* were collected. Most specimens were found walking, but some were sitting on the ground or on bushes. The habitat and habitus, notably the pale coloration, smooth tegument, obsolescence of some pedipalpal and metasomal carinae, elongation of the legs, especially legs III and IV, dorsoventral compression of the basitarsi of legs I–III, comblike rows of elongated macrosetae (“sand combs”) along the retrolateral margins of the tibiae and basitarsi of legs I–III, and elongated telotarsal unguis, are consistent with the psammophilous ecomorphotype (Prendini, 2001).

The types of *B. amitaii* were collected in sympatry with five other buthids, *Androctonus bicolor* Ehrenberg, 1828, *Androctonus amoreuxi* (Aud-

ouin, 1826), *Buthus israelis* Shulov and Amitai, 1959, *Leiurus quinquestriatus* (Ehrenberg, 1828), *Orthochirus scrobiculosus* (Grube, 1873), and the scorpionid, *Scorpio palmatus* (Ehrenberg, 1829). *Leiurus quinquestriatus* usually occurs in rocky habitats, however.

**REMARKS:** According to Levy and Amitai (1980), the population of *B. leptochelys* inhabiting the inland sandy soils near Mamshit, in the northern Negev, belonged to the nominotypical subspecies, otherwise occurring along the southern coast of Israel and in the Sinai Peninsula. Based on evidence gathered during the present investigation, including multivariate analysis of morphometrics (fig. 15) and multilocus molecular phylogenetics (fig. 14), this population represents a distinct species, described here as *Buthacus amitaii*, sp. nov.

#### *Buthacus arava*, sp. nov.

Figures 1E, 3A, 4, 15, 16A, B, 19A, B, 21B, 22C, 23A, 25A, 27A, 29C, 33, 34, 35; tables 1, 8, 9

*Buthacus nigroaculeatus*: Amr et al., 2021: 86, fig. 3B (misidentification).

**TYPE MATERIAL:** Holotype ♂ (HUJ INVSC 3672), **ISRAEL:** Mehoz HaDarom (Southern District): Lotan, SE of Lotan Plantations, 30°00'10.4"N 35°05'44.1"E, 128 m, 13.ix.2018, S. Cain. Paratypes: **ISRAEL:** Mehoz HaDarom (Southern District): near Lotan [29°59'N 35°05'E], 123 m, 29.ix.2003, ♂ (HUJ INVSC 2560), U. Shanas; Lotan, SE of Lotan Plantations, 30°00'10.4"N 35°05'44.1"E, 128 m, 15.ix.2017, Y. Olek and S. Cain, 8 ♂ (HUJ INVSC 3282, 3284–3287, 3289–3291), 1 ♂ (AMCC [LP 15042] ex HUJ INVSC 3283) 1 ♂ (AMCC [LP 15043] ex HUJ INVSC 3288), 1 ♀ (HUJ INVSC3381), 27.iii.2018, Y. Olek and S. Cain; Nahal Sha'alav, 4 km S of Kibbutz Yahel, 30°02'40.6"N 35°06'33.7"E, 153 m, 15.ix.2017, Y. Olek and S. Cain, 1 ♂ (HUJ INVSC 3299); Qetura [29°58'N 35°03'E], 100 m, 8.x.1974, M. Israel, 1 ♂ (HUJ INVSC 2329); S of Yahel, sand dunes, 30°02'N

TABLE 3

**Measurement data for adult male and female *Buthacus amitaii*, sp. nov., deposited in the American Museum of Natural History (AMNH), New York, and the National Natural History Collections, Hebrew University of Jerusalem (HUJ), Israel**

Measurements (mm) follow Tahir et al. (2014): total length (sum of carapace, tergites I–VII, metasomal segments I–V, and telson); carapace median ocelli (distance from carapace anterior margin); carapace anterior width (distance between lateral ocelli); chela total length (distance from base of condyle to tip of fixed finger); chela retroventral carina (length along manus retroventral carina); chela movable finger (movable finger length); pectines total length (length along retrolateral margin); pectines dentate margin (length along dentate margin).

Specimen	type	Holotype						Paratypes					
		sex	♂	♂	♂	♂	♂	♀	♀	♀	♀	♀	
			HUJ	AMNH	HUJ	HUJ	HUJ						
		accession no.	3480		3202	3203	3204		3200	3201	3205	3207	
Total length			56.7	58.9	52.8	48.0	53.0	50.4	49.0	50.8	49.0	48.5	
Carapace	median ocelli		2.3	2.4	2.1	2.1	2.2	2.3	2.2	2.2	2.1	2.0	
	length		5.6	5.5	5.2	4.9	5.0	5.3	5.1	5.3	4.8	4.7	
	anterior width		3.1	3.0	3.0	2.9	3.2	3.1	2.8	3.2	3.1	2.8	
	posterior width		6.2	6.5	5.6	5.4	5.9	5.8	5.4	6.1	5.8	5.4	
Tergite I	length		0.9	1.0	1.0	0.8	0.8	0.8	0.8	0.9	0.8	0.9	
Tergite II	length		1.1	1.5	1.2	1.0	1.1	1.2	1.0	1.2	1.1	1.3	
Tergite III	length		1.6	1.7	1.5	1.2	1.4	1.4	1.5	1.7	1.4	1.6	
Tergite IV	length		1.8	1.9	1.8	1.6	1.8	1.9	1.7	2.0	1.7	1.8	
Tergite V	length		2.1	2.0	1.9	1.7	1.9	2.0	1.9	2.2	2.0	1.9	
Tergite VI	length		2.2	2.5	2.0	1.8	2.1	2.2	1.9	2.3	1.9	3.1	
Tergite VII	length		3.9	4.0	3.6	3.2	3.5	3.3	3.4	3.7	3.4	2.9	
Sternite VII	length		3.6	3.7	3.5	3.2	3.4	3.1	3.0	3.0	3.6	2.9	
	width		5.7	5.6	5.0	4.6	5.2	5.2	5.5	5.5	5.4	5.0	
Metasoma I	length		5.1	5.1	4.7	4.4	4.8	4.4	4.2	4.0	4.3	4.2	
	width		3.6	3.6	2.9	3.2	3.3	3.1	2.8	3.1	2.9	2.7	
	height		2.8	3.1	2.6	2.6	2.9	2.5	2.4	2.7	2.6	2.2	
Metasoma II	length		5.8	6.1	5.2	5.1	5.5	4.9	4.9	4.9	4.7	4.7	
	width		3.6	3.5	3.1	3.0	3.2	2.7	2.8	2.9	2.8	2.4	
	height		3.0	3.1	2.7	2.6	2.8	2.6	2.7	2.6	2.5	2.2	
Metasoma III	length		6.0	6.3	5.5	5.3	5.6	5.1	5.1	4.9	5.0	4.8	
	width		3.3	3.4	2.9	2.8	3.1	2.8	2.6	2.7	2.6	2.4	
	height		2.9	2.9	2.5	2.6	2.7	2.6	2.4	2.5	2.5	2.3	
Metasoma IV	length		6.2	6.3	5.9	5.1	5.9	5.1	5.3	5.1	5.0	4.6	
	width		2.8	2.7	2.2	2.4	2.5	2.3	2.1	2.3	2.1	1.9	
	height		2.5	2.5	2.1	2.2	2.3	2.1	2.1	2.2	2.2	1.7	
Metasoma V	length		7.5	7.8	7.2	6.2	7.1	6.7	6.2	6.7	6.9	5.9	
	width		2.6	2.7	2.5	2.4	2.5	2.4	2.3	2.6	2.3	2.2	
	height		2.3	2.5	2.0	2.1	2.2	2.1	2.0	2.2	2.0	1.6	
Telson	vesicle length		3.1	3.5	2.9	2.8	3.1	2.8	2.7	2.9	2.8	2.5	
	vesicle width		2.2	2.2	2.0	1.9	2.1	1.9	1.8	1.9	1.8	1.7	
	vesicle height		2.2	2.2	1.9	2.0	2.3	2.0	1.7	1.9	1.7	1.7	
	aculeus length		3.9	3.7	3.2	2.8	3.3	3.4	3.2	3.1	3.3	3.8	

TABLE 3 *continued*

Specimen	type	Holotype	Paratypes								
			♂	♂	♂	♂	♀	♀	♀	♀	♀
	sex	♂	♂	♂	♂	♂	♀	♀	♀	♀	♀
	collection	HUJ	AMNH	HUJ	HUJ	HUJ	AMNH	HUJ	HUJ	HUJ	HUJ
	accession no.	3480		3202	3203	3204		3200	3201	3205	3207
Femur	length	4.8	4.7	4.4	4.2	4.8	3.7	3.6	3.5	3.7	3.7
	width	1.6	1.6	1.1	1.3	1.2	1.4	1.2	1.7	1.4	1.2
	height	1.2	1.5	1.0	1.0	1.5	1.1	1.2	1.1	1.2	1.0
Patella	length	5.6	5.7	5.1	4.7	5.6	4.7	4.7	5.1	5.3	5.0
	width	2.2	2.3	2.0	1.9	2.2	1.8	1.9	1.9	1.8	1.6
	height	1.8	1.9	1.4	1.5	1.8	1.8	1.4	1.5	1.5	1.1
Chela	total length	9.1	9.1	8.1	7.5	8.4	7.4	7.1	7.5	7.0	6.4
	manus width	2.5	2.5	2.0	2.0	2.4	1.5	1.4	1.4	1.3	1.3
	manus height	2.6	2.7	2.2	2.5	2.7	1.6	1.6	1.6	1.4	1.5
	retroventral carina	3.9	3.7	3.8	3.3	3.6	2.5	2.6	2.6	2.6	2.3
	movable finger	4.8	5.0	4.3	3.9	4.5	4.5	4.2	4.4	4.4	4.1
Pectines	total length	6.8	6.9	5.5	5.3	6.4	4.9	4.4	4.9	4.3	4.1
	dentate margin	6.5	6.7	5.9	5.0	6.3	4.5	4.3	4.6	4.2	3.8

35°06'E, 149 m, 14.x.2004, U. Shanas, 1 ♂ (HUJ INVSC 2587); Yotvata, E side of circle field, 29°53'21.1"N 35°04'34.8"E, 72 m, 14.ix.2017, Y. Olek and S. Cain, 1 ♂ (AMCC [LP 15045] ex HUJ INVSC 3292), 1 ♂ (HUJ INVSC 3293), 29°53'36.1"N 35°04'40.6"E, 72 m, 14.ix.2017, Y. Olek and S. Cain, 3 ♂ (HUJ INVSC 3294–3296), 29°53'45.1"N 35°04'37.5"E, 72 m, 14.ix.2017, Y. Olek and S. Cain, 1 ♂ (AMCC [LP 15044] ex HUJ INVSC 3297), 1 ♂ (HUJ INVSC 3298). **JORDAN:** Aqaba Governorate: E of Qetura, 29°57'N 35°05'E, 98 m, 11.x.2004, U. Shanas, 2 ♂ (HUJ INVSC 2594–2595); Rahma, 29°56'N 35°06'E, 95 m, 27.x.2003, U. Shanas, 1 ♂ (HUJ INVSC 2569); Wadi Aheimir [Hemer], 30°02'N 35°10'E, 212 m, 16.x.2003, U. Shanas, 2 ♂ (HUJ INVSC 2559, 2562); Wadi Quseib, NE of Yahel, 30°06'N 35°10'E, 189 m, 23.x.2003, U. Shanas, 1 ♂ (HUJ INVSC 2563); E of Yotvata, 29°46'N 35°04'E, 156 m, 24.x.2003, U. Shanas, 1 subad. ♀ (HUJ INVSC 2561); NE of Yotvata, sand dunes, 29°54'N 35°04'E, 76 m, 12.x.2004, U. Shanas, 1 ♂ (HUJ INVSC 2597). Karak Governorate: Wadi Khanzeerah (Khanzairh), 30°53'39.9"N 35°25'38.2"E, -294 m, 9.ix.2013, L. Prendini, Z. Amr and L. Al Azam, 1 ♂ (AMNH), 1 ♂ (JUST), 1 juv. ♂, 2 juv. ♀ (AMCC [LP 12198]).

**DIAGNOSIS:** *Buthacus arava* differs from the closely related *B. tadmorensis* and *B. yotvatensis*, occurring in Israel and neighboring states, as follows. The pedipalp chela of *B. arava* is shorter and broader, especially in the adult male (fig. 35A, B), with chela manus width:chela length, 29.8% (27.2%–32.8%, n = 7; table 8) (♂), chela manus length:movable finger length, 90.4% (83.5%–95%, n = 7) or 60.8% (♀), and chela manus width:length, 63.3% (57.3%–74.5%, n = 7) or 61.6% (♀), than that of *B. tadmorensis* (fig. 50A, B), with chela manus width:chela length, 22.3% (♂) (table 4), chela manus length:movable finger length, 64.2% (♂) or 55% (51.9%–59.8%, n = 4) (♀), and chela manus width:length, 58.7% (♂) or 59.1% (53.8%–65.1%, n = 4) (♀), and *B. yotvatensis* (fig. 53A, B), with chela manus width:chela length, 17.4% (16.5%–18.8%, n = 8; tables 6, 7) (♂), chela manus length:movable finger length, 55.2% (51.7%–58.3%, n = 8) (♂) or 47.1% (45.5%–48%, n = 6) (♀), and chela manus width:length, 50.5% (48.1%–54.8%, n = 8) (♂) or 56.9% (51.3%–61.5%, n = 6) (♀). The ungues of the leg telotarsi are longer (approximately equal to the length of the telotarsus) and unequal on legs I and II in *B. arava* (fig. 22C) but shorter

TABLE 4

**Measurement data for adult male and female *Buthacus leptochelys* (Ehrenberg, 1829), and *Buthacus tadmorensis* (Simon, 1892), stat. rev., i.e., types of *Buthus pietschmanni* Penther, 1912, deposited in the American Museum of Natural History (AMNH), New York, the National Natural History Collections, Hebrew University of Jerusalem (HUJ), Israel, the Naturhistorisches Museum Wien (NHMW), Austria, and the Steinhardt Museum of Natural History (SMNH), Tel Aviv University, Israel**

Measurements (mm) follow Tahir et al. (2014): total length (sum of carapace, tergites I–VII, metasomal segments I–V, and telson); carapace median ocelli (distance from carapace anterior margin); carapace anterior width (distance between lateral ocelli); chela total length (distance from base of condyle to tip of fixed finger); chela retroventral (length along manus retroventral carina); chela movable finger (movable finger length); pectines total length (length along retrolateral margin); pectines dentate margin (length along dentate margin).

Specimen	type	<i>B. leptochelys</i>					<i>B. tadmorensis</i>				
		sex	♂	♀	♀	♀	♂	♀	♀	♀	♀
			HUJ	AMNH	HUJ	HUJ	SMNH	NHMW	NHMW	NHMW	NHMW
		accession no.	859		1807	2233	50805	2453	2452	2452	2453
Total length			63.7	67.7	63.2	66.7	68.0	66.8	72.8	75.2	66.6
Carapace	median ocelli		2.4	3.2	2.8	2.7	3.0	3.1	3.5	3.6	3.1
	length		6.1	6.9	6.4	6.5	6.6	6.5	7.2	7.9	6.7
	anterior width		3.4	3.6	4.0	4.3	3.7	3.7	3.9	4.2	3.7
	posterior width		7.1	7.8	7.4	7.6	8.5	7.0	8.7	9.4	7.6
Tergite I	length		0.8	0.8	1.0	0.9	1.0	0.9	1.2	1.0	1.0
Tergite II	length		1.2	1.1	1.1	1.5	1.5	1.3	1.6	1.4	1.4
Tergite III	length		1.6	1.9	2.0	1.8	2.0	1.6	2.3	2.0	2.0
Tergite IV	length		2.1	2.4	2.1	2.3	2.3	2.1	2.6	2.7	2.4
Tergite V	length		2.6	2.6	2.5	2.5	2.5	2.4	3.0	2.9	2.7
Tergite VI	length		2.4	2.9	2.7	2.8	2.7	2.6	3.3	3.0	2.9
Tergite VII	length		4.0	5.1	4.5	4.9	4.9	4.6	5.0	5.3	4.8
Sternite VII	length		4.0	4.1	3.8	4.3	4.8	4.3	4.8	4.9	4.3
	width		6.1	7.4	7.3	6.8	8.0	7.0	8.0	8.3	6.9
Metasoma I	length		5.8	6.2	5.5	5.9	6.1	6.6	6.7	6.9	6.0
	width		3.9	4.2	3.9	3.9	4.3	4.6	4.7	5.3	4.3
	height		3.1	3.4	3.1	3.3	3.4	4.0	4.3	4.7	3.8
Metasoma II	length		6.7	6.9	6.3	6.7	7.1	7.3	7.5	7.6	6.5
	width		3.5	3.9	3.7	3.6	4.0	4.4	4.5	4.9	4.1
	height		3.2	3.3	3.2	3.3	3.6	3.9	4.3	4.4	3.8
Metasoma III	length		7.0	6.9	6.5	7.0	7.2	7.2	7.6	7.8	6.7
	width		3.5	3.6	3.4	3.4	3.8	4.2	4.2	4.9	3.9
	height		2.9	3.2	3.1	3.0	3.5	3.9	4.1	4.5	3.8
Metasoma IV	length		7.4	7.3	6.5	6.9	7.4	7.8	7.9	8.3	7.1
	width		2.8	2.9	2.9	2.8	3.1	3.8	3.9	4.1	3.5
	height		2.5	2.7	2.8	2.7	3.0	3.5	3.6	4.2	3.3
Metasoma V	length		8.5	8.0	8.3	8.7	8.2	8.2	8.8	9.3	8.2
	width		2.8	3.1	3.0	3.1	3.2	3.5	3.8	4.0	3.3
	height		2.5	2.7	2.5	2.6	2.9	2.9	3.1	3.8	3.1
Telson	vesicle length		3.9	3.8	3.2	3.7	3.7	4.1	4.0	4.5	3.9
	vesicle width		2.3	2.4	2.4	2.4	2.5	2.6	3.2	3.5	2.9
	vesicle height		2.3	2.2	2.2	2.3	2.4	2.7	3.2	3.3	2.8
	aculeus length		3.8	4.9	4.5	4.7	4.8	3.7	4.2	4.8	4.5

TABLE 4 *continued*

Specimen	type	<i>B. leptochelys</i>					<i>B. tadmorensis</i>				
		Lectotype		Paralectotypes							
		♂	♀	♂	♀	♀	♂	♀	♀	♀	♀
collection		HUJ	AMNH	HUJ	HUJ	SMNH	NHMW	NHMW	NHMW	NHMW	NHMW
accession no.		859		1807	2233	50805	2453	2452	2452	2453	2453
Femur	length	6.2	5.8	5.1	5.5	5.9	5.5	5.7	5.6	5.2	5.0
	width	1.8	1.7	1.7	1.7	1.8	2.0	2.3	2.5	2.1	2.4
	height	1.3	1.3	1.3	1.5	1.2	1.6	1.7	1.9	1.5	1.6
Patella	length	6.9	7.0	6.5	6.9	6.8	6.6	7.0	6.8	6.0	6.0
	width	2.4	2.2	2.3	2.2	2.4	2.5	2.6	3.1	2.4	2.3
	height	1.8	1.9	1.8	1.8	1.9	2.1	2.2	2.5	2.1	2.0
Chela	total length	10.6	10.4	9.6	10.1	10.6	10.2	10.9	10.6	9.4	9.4
	manus width	2.6	1.8	1.7	1.6	1.8	2.3	2.1	2.4	1.9	1.9
	manus height	2.6	2.0	2.0	1.9	2.1	2.6	2.5	2.6	2.3	2.1
	retroventral carina	4.3	3.4	3.2	3.1	3.5	3.9	3.6	3.7	3.2	3.5
	mov. finger	6.1	6.5	6.0	6.4	6.5	6.1	6.9	6.6	6.1	5.9
Pectines	total length	8.3	7.8	7.6	7.5	7.8	8.4	9.0	7.8	7.2	6.6
	dentate margin	7.5	7.2	6.9	6.8	7.3	7.6	7.4	6.5	6.3	5.6

(approximately two-thirds the length of the telotarsus) and equal on legs I and II in *B. tadmorensis* and *B. yotvatensis* (fig. 22E, G). The pectinal tooth counts are lower in *B. arava*, i.e., 20/20 (18–21/18–22,  $n = 7$ ; table 9) (♂) and 12/13 (♀), than in *B. tadmorensis*, i.e., 30/32 (♂) (table 9) and 24/25 (23–26/23–26,  $n = 3$ ) (♀), and *B. yotvatensis*, i.e., 34/35 (32–37/32–37,  $n = 8$ ; table 9) (♂) and 26/26 (25–28/26–28,  $n = 6$ ) (♀). The metasomal segments and telson are sparsely setose in *B. arava* (figs. 23A, 25A, 29C), with macrosetal counts on segments I–V (sinistral/dextral), dorsosubmedian carinae, 0/0 (0–1/0–1,  $n = 4$ ):2/3 (2–3/2–5):4/3 (2–5/2–6):3/3 (2–3/1–5):0/0 (0–0/0–0), dorsolateral carinae, 1/1 (0–2/0–2):2/2 (1–3/0–3):3/2 (2–4/1–3):3/3 (2–4/2–5):5/6 (3–8/5–7), and telson, 28 (27–29,  $n = 4$ ), but densely setose in *B. tadmorensis* (figs. 23B, 25B, 29E), with macrosetal counts on segments I–V (sinistral/dextral), dorsosubmedian carinae, 10/11 (8–12/10–12,  $n = 2$ ):19/23 (18–19/21–24):23/23 (23–23/21–25):19/20 (17–20/19–21):9/9 (7–11/7–11), dorsolateral carinae, 6/6 (4–8/5–6):11/13 (8–13/11–15):9/11 (8–9/10–11):9/9 (8–9/6–12):9/9 (8–10/8–10), and telson, 100 (80–120,  $n$

= 2), and *B. yotvatensis* (figs. 23C, 25C, 29G), with macrosetal counts on segments I–V (sinistral/dextral), dorsosubmedian carinae, 16/15 (14–20/11–21,  $n = 5$ ):25/26 (20–29/18–30):26/25 (23–31/19–29):30/27 (24–38/23–31):12/11 (6–18/7–15), dorsolateral carinae, 9/8 (7–13/5–13):20/20 (19–23/16–21):22/21 (16–28/18–24):15/14 (11–20/12–17):11/13 (10–13/11–14), and telson, 102 (88–127,  $n = 5$ ). Additionally, the ventrosubmedian and ventrolateral carinae of metasomal segments II and III, and ventrolateral carinae of segment V are less developed in *B. arava* than in *B. tadmorensis* (fig. 25A, B), with narrow, spiniform processes posteriorly in *B. arava* but broad, lobate processes posteriorly in *B. tadmorensis*.

**ETYMOLOGY:** The specific epithet is a noun in apposition, taken from the Arava Valley, to which the species appears to be endemic.

**DESCRIPTION:** The following description is based on the type material (see table 8 for measurements and table 9 for counts).

**Total length:** Large scorpions, 70.4 mm (61.7–75 mm,  $n = 6$ ) (♂) or 62.3 mm (♀).

**Color:** Uniformly pale yellow to yellowish-olive, except as follows. Mesosomal tergites, ster-

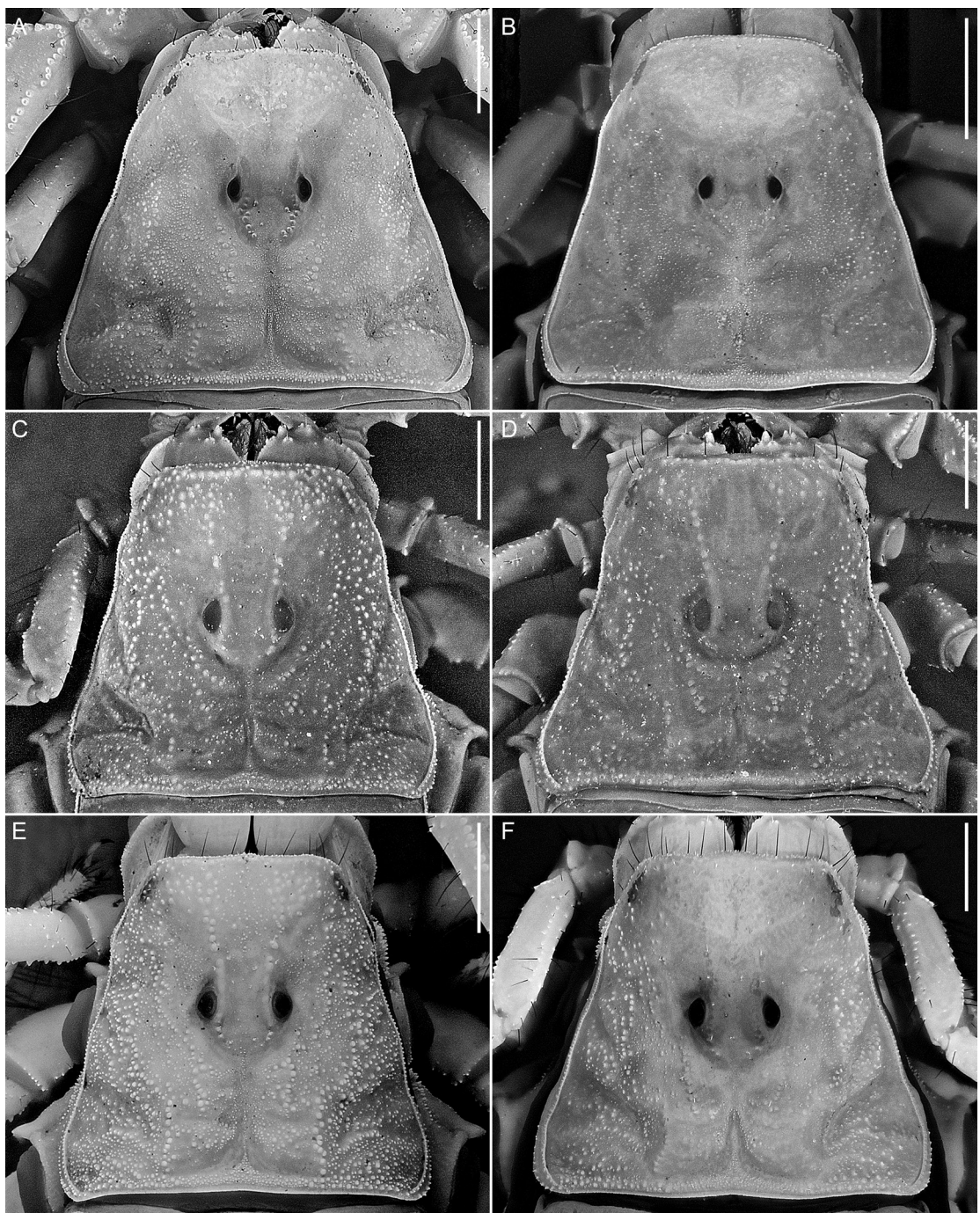


FIGURE 16. *Buthacus* Birula, 1908, carapace, dorsal aspect. A, B. *Buthacus arava*, sp. nov., A. Paratype ♂ (HUJ INVSC 3287), B. Paratype ♀ (HUJ INVSC 2561). C, D. *Buthacus tadmorensis* (Simon, 1892), stat. rev., C. Lectotype ♂ (NHMW 2453) of *Buthus pietschmanni* Penther, 1912, D. Paralectotype ♀ (NHMW 2452). E, F. *Buthacus yotvatensis* Levy et al., 1973, stat. rev., E. ♂ (HUJ INVSC 3344), F. ♀ (HUJ INVSC 3318). Scale bars = 2 mm.

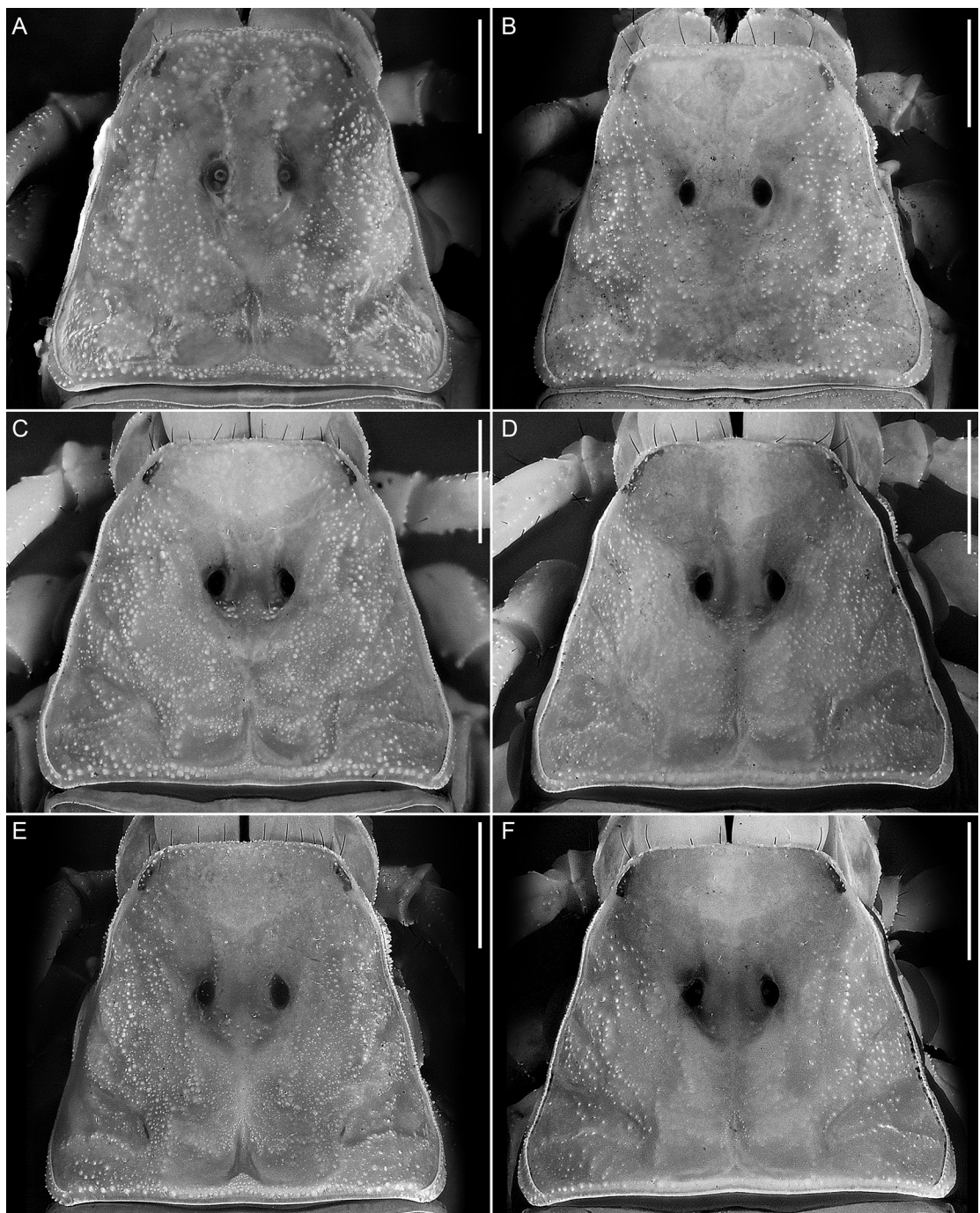


FIGURE 17. *Buthacus* Birula, 1908, carapace, dorsal aspect. A, B. *Buthacus leptochelys* (Ehrenberg, 1829), A. ♂ (HUJ INVSC 859), B. ♀ (HUJ INVSC 1807). C, D. *Buthacus nitzani* Levy et al., 1973, stat. nov., C. ♂ (HUJ INVSC 3227), D. ♀ (HUJ INVSC 3226). E, F. *Buthacus amitaii*, sp. nov., E. Holotype ♂ (HUJ INVSC 3480), F. Paratype ♀ (HUJ INVSC 3205). Scale bars = 2 mm.

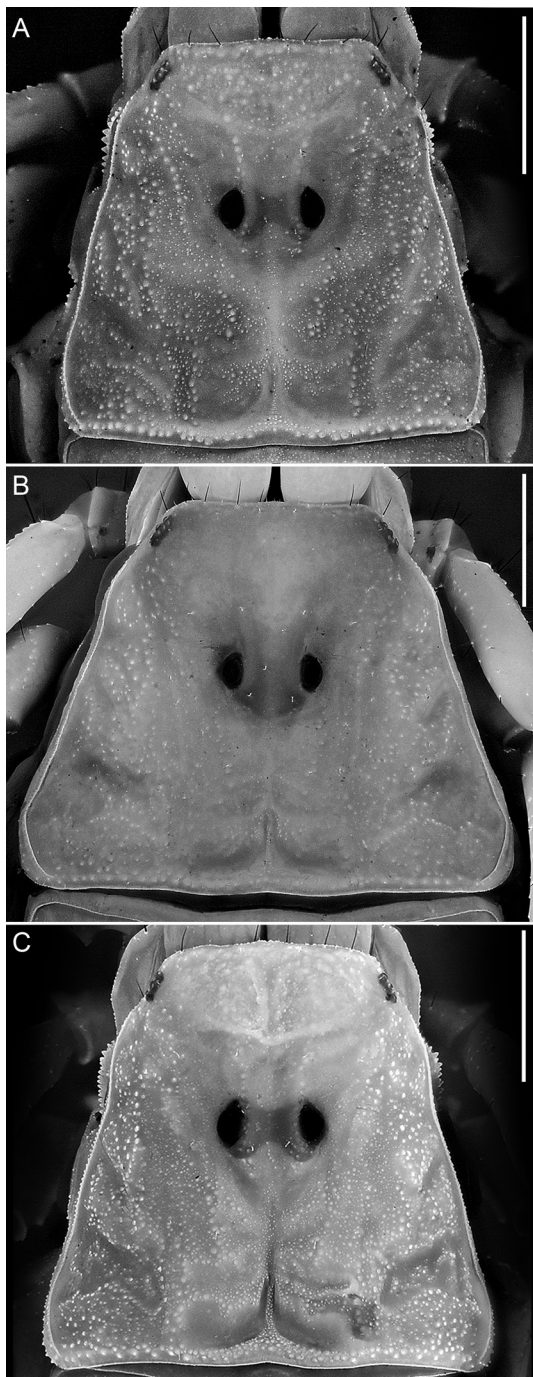


FIGURE 18. *Butthacus* Birula, 1908, carapace, dorsal aspect. A, B. *Butthacus levyi*, sp. nov., A. Holotype ♂ (HUU INVSC 2082), B. Paratype ♀ (HUU INVSC 3274). C. *Butthacus arenicola* (Simon, 1885), ♂ (AMNH). Scale bars = 2 mm.

nite VII and metasomal segments I–V, each with narrow brown stripe posteriorly. Pectines pale yellow. Leg articulation points brown.

**Carapace:** Carapace shape trapezoidal (fig. 16A, B), anterior width:posterior width, 50.6% (44.3%–59.4%,  $n = 8$ ), length:posterior width, 90.6% (84.6%–96.7%,  $n = 8$ ). Five, rarely four, pairs of lateral ocelli; each lateral ocular tubercle with two or, usually, three major ocelli (ALMa, MLMa, PLMa), similar in size, situated anterolaterally, and one or, usually, two minor ocelli (ADMi, PDMi; PDMi may be absent) situated posterodorsal to posterior major ocellus. Median ocelli larger than lateral ocelli, distance between them more than  $2 \times$  ocellus width. Median ocular tubercle situated anteromedially, distance from anterior carapace margin:carapace length, 43.1% (41%–44.7%,  $n = 7$ ) ( $\delta$ ) or 45.2% ( $\varphi$ ). Superciliary and central median carinae distinct, costate-granular, weakly connected to disconnected ( $\delta$ ) or smooth and obsolete ( $\varphi$ ). Anteromedian sulcus absent or shallow; postero-median sulcus shallow, narrow anteriorly, wide posteriorly; posterolateral sulci shallow, wide, curved. Carapace intercarinal surfaces finely and densely granular.

**Chelicerae:** Cheliceral manus prodorsal margin finely granular; retrodorsal surfaces smooth or finely granular; prolateral and ventral surfaces densely setose. Fixed finger dorsal and ventral surfaces densely setose; dorsal margin with subdistal, medial, and proximal denticles; ventral margin with proximal and medial denticles. Movable finger dorsal surface smooth and glabrous; ventral surface densely setose; dorsal margin with retrodistal, subdistal, medial, and pair of proximal denticles; ventral margin with prodistal, medial, and proximal denticles.

**Pedipalps:** Femur dorsal prolateral, dorsal retro-lateral and ventral prolateral carinae complete, costate-granular; prolateral ventral and prolateral ventrosubmedian carinae vestigial, each comprising a few spiniform granules; retro-lateral dorsosubmedian carina absent, represented by fewer than 10 macrosetae; dorsal and ventral intercarinal surfaces finely granular; lateral intercarinal surfaces smooth (fig. 34A, B). Patella dor-

sal prolateral carina obsolete; prolateral median carina partial, costate-granular; ventral prolateral carinae complete, costate-granular; other carinae absent; dorsal, ventral and retrolateral intercarinal surfaces smooth; prolateral intercarinal surfaces finely granular (fig. 34C–E). Chela globose, short and broad (♂), manus width:length, 63.3% (57.3%–74.5%,  $n = 7$ ), manus height:length, 69.1% (60%–84%,  $n = 7$ ), and manus length:movable finger length, 90.4% (83.5%–95%,  $n = 7$ ) or short and narrow (♀), manus width:length, 61.6%, manus height:length, 69.2%, and manus length:movable finger length, 60.8%. Chela manus acarinate; intercarinal surfaces smooth and glabrous (fig. 35). Fixed and movable fingers respectively with 8 or 9 ( $n = 8$ ) and 6–10 ( $n = 8$ ) oblique median denticle subrows; movable finger with 6–9 ( $n = 8$ ) retrolateral accessory denticles (fig. 21B); proximal dentate margins of fingers sublinear (fig. 35B), such that no gap evident proximally when fingers closed.

**Legs:** Legs I–IV, femoral ventral carinae granular; patellar ventral carinae obsolete; intercarinal surfaces smooth. Legs I–IV, macrosetal counts on retrolateral margins of tibiae, 8:9:11:4; basitarsi, 10:13:20:7; telotarsi, 4:5:6:6 ( $n = 1$ ). Legs I–IV, tibial spurs absent on I and II, present on III and IV; pro- and retroventral basitarsal (pedal) spurs present, more developed on legs III and IV. Telotarsal unguis long, approximately equal to telotarsus length, unequal on legs I and II, subequal to equal on III and IV (fig. 22C).

**Genital operculum:** Genital opercula suboval, completely divided longitudinally, with overlapping, rounded margins (♂) or partially fused longitudinally (♀) (fig. 19A, B). Genital papillae present (♂) or absent (♀).

**Pectines:** Three marginal lamellae; 7–8 ( $n = 3$ ) (♂) or 6 (♀) median lamellae (fig. 19A, B). Fulcra present. Pectinal teeth along part of length, dentate margin length:pecten length, 88.1% (85.2%–95%,  $n = 7$ ) (♂) or 67.1% (♀). Pectinal teeth curved, similar in size; tooth count (sinistral/dextral), 20/20 (18–21/18–22,  $n = 7$ ) (♂) or 12/13 (♀).

**Mesosoma:** Tergites I–VII progressively increasing in length posteriorly, tergite VI

length:tergite VII length, 56.4% (52.6%–59%,  $n = 7$ ) (♂) or 47.2% (♀); increasing in width posteriorly from I–IV, decreasing in width posteriorly from V–VII. Pretergites smooth; posttergites I–VI, intercarinal surfaces uniformly finely granular, becoming more coarsely and densely granular posteriorly, VII more coarsely and sparsely granular. Tergites I–VI, dorsomedian carinae absent on I and II, granular, vestigial, restricted to posterior third of III–VI; dorsosubmedian carinae granular, vestigial, restricted to posterior fifth of I–VI. Tergite VII, dorsomedian carina absent; dorsosubmedian and dorsolateral carinae distinct, granular. Sternites III–VII acarinate, smooth and glabrous; IV–VI, respiratory spiracles (stigmata) width approximately 3× length.

**Metasoma:** Metasomal segments I–V becoming longer and narrower posteriorly (figs. 23A, 25A, 27A), segment I shortest, length I:II, 88.5% (86.3%–89.9%,  $n = 7$ ) (♂) or 90.3% (♀); segments II–IV similar, length II:III, 95.8% (93.7%–98.6%,  $n = 7$ ) (♂) or 100.1% (♀), length III:IV, 95.4% (94.7%–96.7%,  $n = 7$ ) (♂) or 92.3% (♀); segment V longest, length IV:V, 86.4 (82.4%–92.8%,  $n = 7$ ) (♂) or 80.5% (♀); width:length segment I, 64.5% (62%–66.4%,  $n = 7$ ) (♂) or 61% (♀), II, 56.3% (52.3%–66.4%,  $n = 7$ ) (♂) or 55.4% (♀), III, 50.5% (47.1%–52.7%,  $n = 7$ ) (♂) or 54.7% (♀), IV, 43.8% (40.6%–46.4%,  $n = 7$ ) (♂) or 46.9% (♀), V, 35% (31.9%–38.3%,  $n = 7$ ) (♂) or 37.1% (♀). Dorsosubmedian and dorsolateral carinae distinct, granular on segments I and III, obsolete on IV, absent on V; dorsosubmedian and dorsolateral carinae sparsely setose, macrosetal counts on segments I–V (sinistral/dextral), dorsosubmedian carinae, 0/0 (0/0–1/1,  $n = 4$ ):2/3 (2/2–3/5):4/3 (2/2–5/6):3/3 (2/1–3/5):0/0 (0/0–0/0), dorsolateral carinae, 1/1 (0/0–2/2):2/2 (1/0–3/3):3/2 (2/1–4/3):3/3 (2/2–4/5):5/6 (3/5–8/7). Median lateral carinae distinct, granular, restricted to posterior two-thirds of segment I, posterior half of II and posterior third of III, absent on IV and V. Ventrolateral carinae distinct, costate-granular on segment I; costate-granular, with granules becoming progressively larger and subspiniform posteriorly,

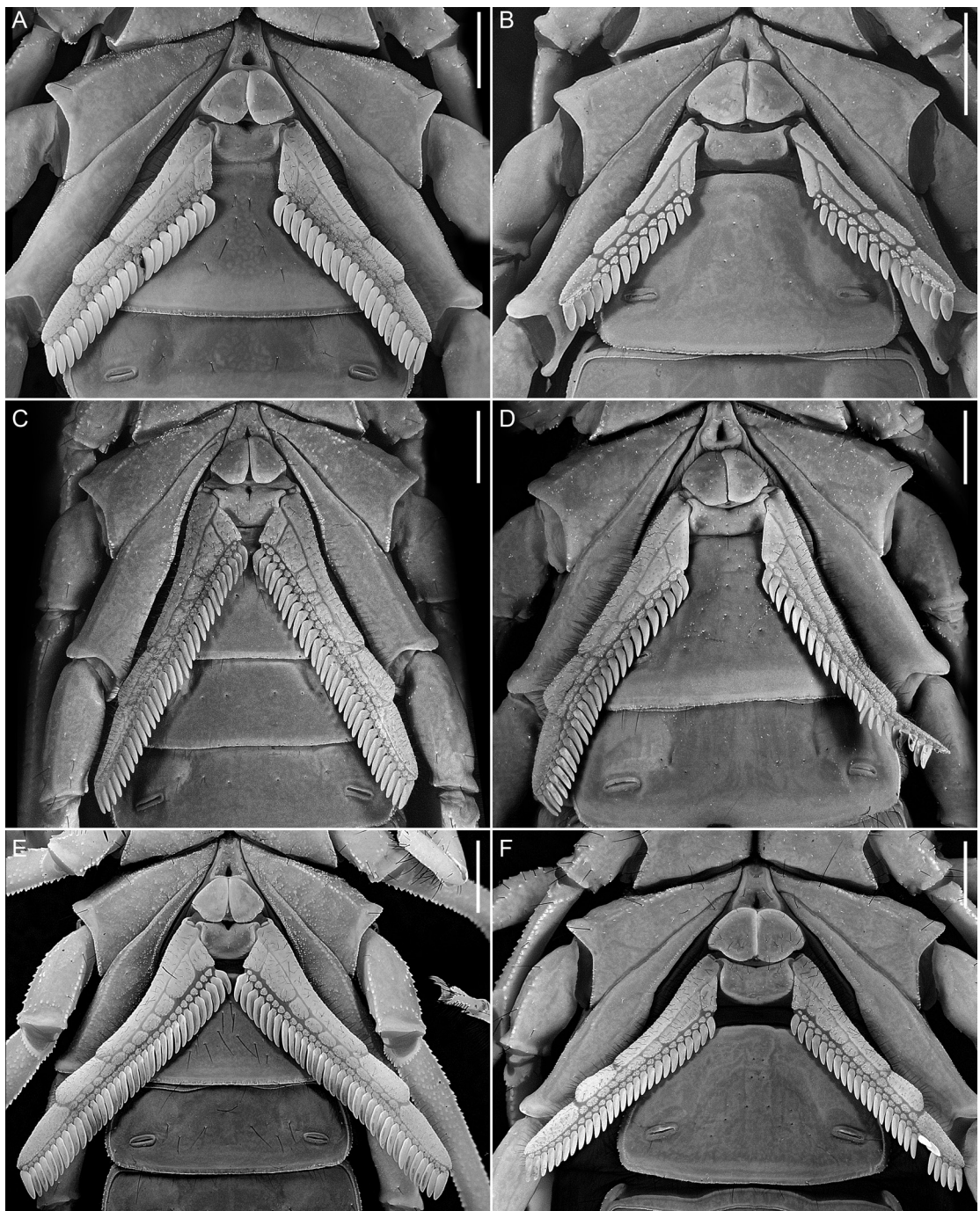


FIGURE 19. *Buthacus* Birula, 1908, sternum, genital opercula and pectines, ventral aspect. A, B. *Buthacus arava*, sp. nov., A. Paratype ♂ (HUJ INVSC 3287), B. Paratype ♀ (HUJ INVSC 2561). C, D. *Buthacus tadmorensis* (Simon, 1892), stat. rev., C. Lectotype ♂ (NHMW 2453) of *Buthus pietschmanni* Penther, 1912, D. Paralectotype ♀ (NHMW 2452). E, F. *Buthacus yotvatensis* Levy et al., 1973, stat. rev., E. ♂ (HUJ INVSC 3344), F. ♀ (HUJ INVSC 3318). Scale bars = 2 mm.

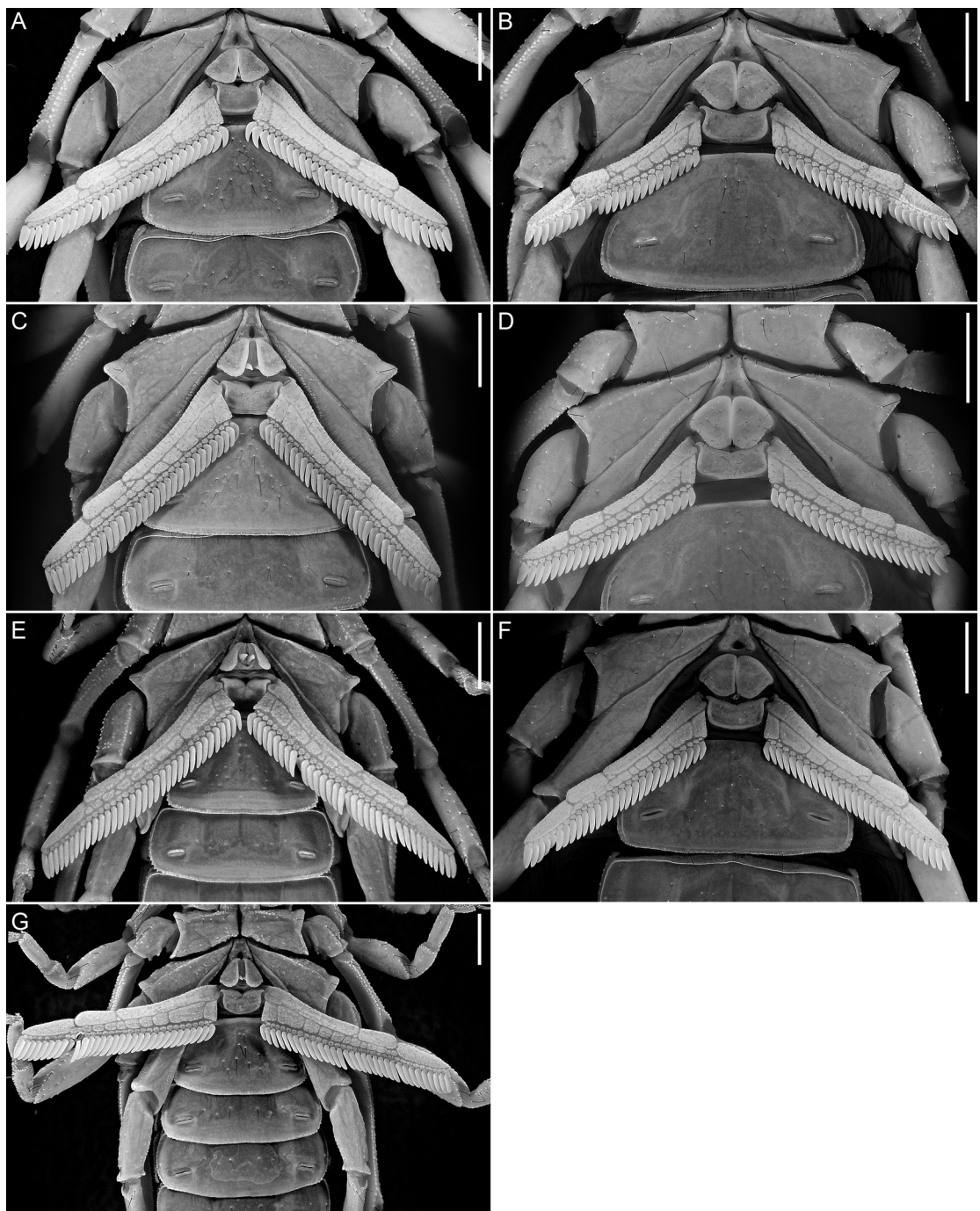


FIGURE 20. *Buthacus* Birula, 1908, sternum, genital opercula and pectines, ventral aspect. A, B. *Buthacus nitzani* Levy et al., 1973, stat. nov., A. ♂ (HUJ INVSC 3227), B. ♀ (HUJ INVSC 3226). C, D. *Buthacus amitaii*, sp. nov., C. Holotype ♂ (HUJ INVSC 3480), D. Paratype ♀ (HUJ INVSC 3205). E, F. *Buthacus levyi*, sp. nov., E. Holotype ♂ (HUJ INVSC 2082), F. Paratype ♀ (HUJ INVSC 3274). G. *Buthacus arenicola* (Simon, 1885), ♂ (AMNH). Scale bars = 2 mm.

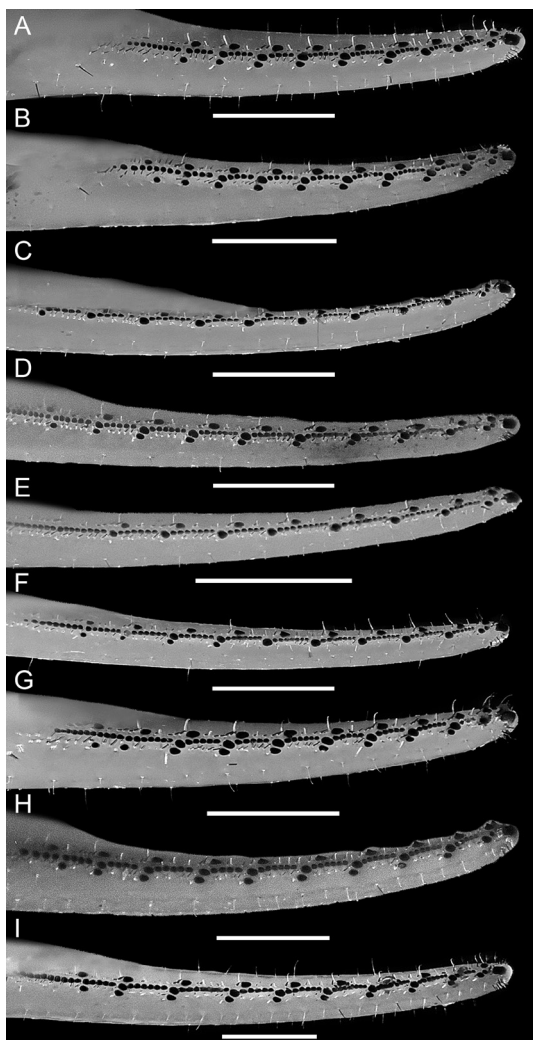


FIGURE 21. *Buthacus* Birula, 1908, dextral pedipalp chela movable finger, dorsal aspect, illustrating dentition. **A.** *Buthacus amitaii*, sp. nov., holotype ♂ (HUJ INVSC 3480). **B.** *Buthacus arava*, sp. nov., paratype ♂ (HUJ INVSC 3290). **C.** *Buthacus arenicola* (Simon, 1885), ♂ (AMNH). **D.** *Buthacus leptochelys* (Ehrenberg, 1829), ♂ (HUJ INVSC 859). **E.** **F.** *Buthacus levyi*, sp. nov., E. Holotype ♂ (HUJ INVSC 2082), F. Paratype ♀ (HUJ INVSC 3252). **G.** *Buthacus nitzani* Levy et al., 1973, stat. nov., ♂ (HUJ INVSC 3227). **H.** *Buthacus tadmorensis* (Simon, 1892), stat. rev., lectotype ♂ (NHMW 2453) of *Buthus pietschmanni* Penther, 1912. **I.** *Buthacus yotvatensis* Levy et al., 1973, stat. rev., ♂ (HUJ INVSC 3302). Scale bars = 1 mm.

on II and III; costate-granular on IV; serrate, comprising spiniform granules of variable size, becoming more prominent posteriorly, on V. Ventrosubmedian carinae distinct, costate-granular on segment I; costate-granular, with granules becoming progressively larger and subspiniform posteriorly, on II and III; costate-granular on IV; granular, restricted to anterior two-thirds of V. Ventromedian carina granular, distinct along entire length of segment V. Dorsal intercarinal surfaces smooth on I–V; lateral intercarinal surfaces smooth on I–III, smooth or very finely granular on segment IV, finely granular on V; ventral intercarinal surfaces finely granular on I–IV, coarsely granular in anterior two-thirds of V.

**Telson:** Telson vesicle width:metasomal segment V width, 69.4% (67.7%–71.5%,  $n = 7$ ) (♂) or 69.7% (♀). Vesicle globose, dorsal surface flat, ventral surface convex and rounded; vesicle height:length, 63.2% (56%–68.2%,  $n = 7$ ) (♂) or 59.9% (♀); dorsal surface smooth, ventral surface granular anteriorly; lateral and ventral surfaces sparsely setose, with 27 (27–29,  $n = 4$ ) macrosetae. Aculeus long, gently curved; aculeus length:telson length, 50.5% (44.9%–55%,  $n = 7$ ) (♂) or 53% (♀).

**Sexual dimorphism:** Adult males and females differ as follows. The carapacial supraciliary and central median carinae are distinct and costate-granular in the male, but obsolete and smooth in the female. The carinae of the pedipalp femur and patella are more coarsely granular in the male than in the female. The pedipalp chela manus of the male is markedly broader and deeper with proportionally shorter fingers than that of the female (fig. 35), as indicated by the higher ratios of chela manus width:length and chela manus length:movable finger length, respectively 63.3% and 90.4% in the male compared with 61.6% and 60.8%, in the female. The genital opercula are completely divided longitudinally, with overlapping, rounded margins in the male but partially fused longitudinally in the female (fig. 19A, B), and genital papillae are present in the male but absent in the female. The pectinal tooth count is higher in

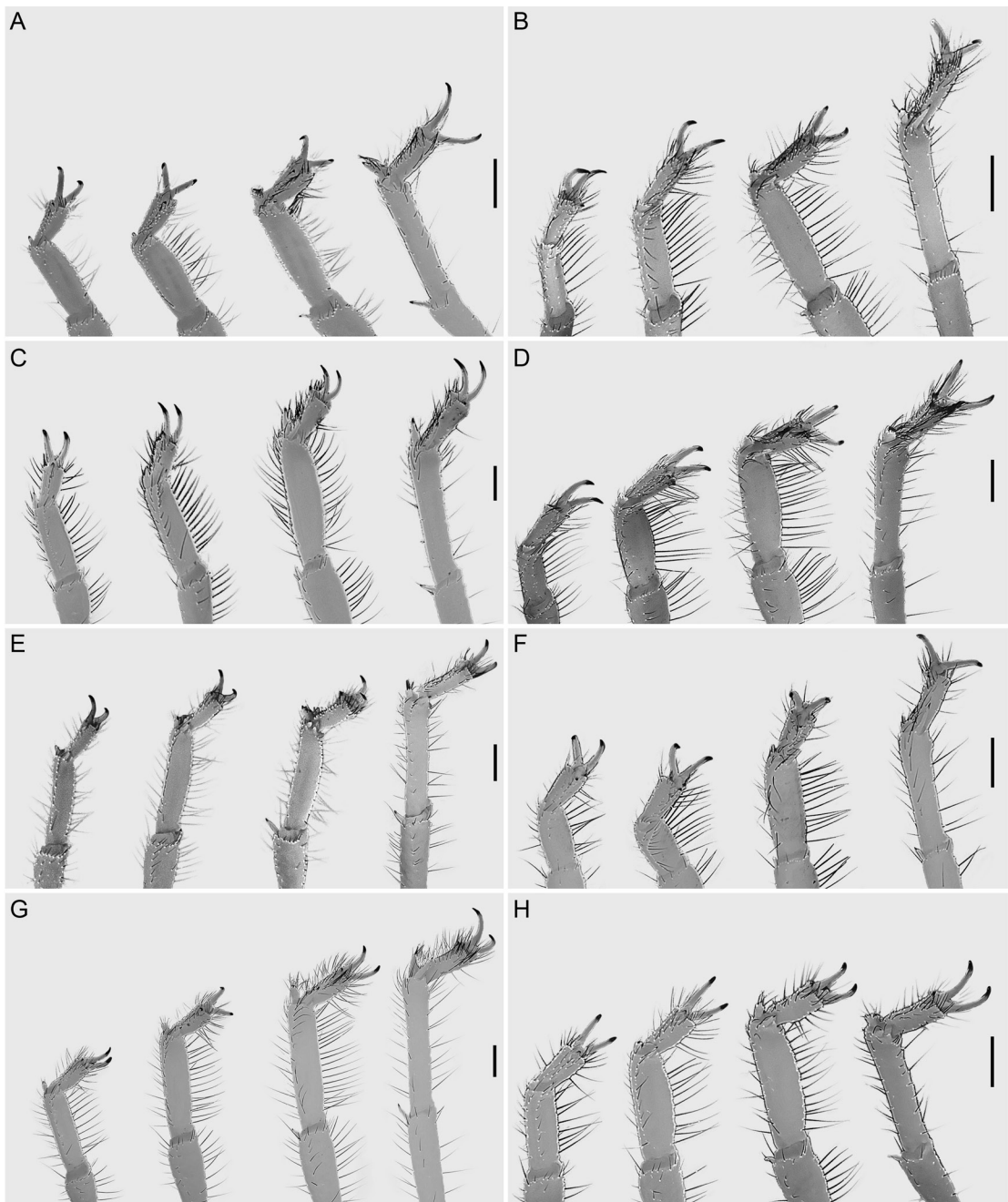


FIGURE 22. *Buthacus* Birula, 1908, dextral legs I–IV, basitarsus and telotarsus, ventral aspect. **A.** *Buthacus arenicola* (Simon, 1885), ♂ (AMNH). **B.** *Buthacus levyi*, sp. nov., holotype ♂ (HUJ INVSC 2082). **C.** *Buthacus arava*, sp. nov., paratype ♂ (HUJ INVSC 3295). **D.** *Buthacus leptochelys* (Ehrenberg, 1829), ♀ (HUJ INVSC 1807). **E.** *Buthacus tadmorensis* (Simon, 1892), stat. rev., lectotype ♂ (NHMW 2453) of *Buthus pietschmanni* Penther, 1912. **F.** *Buthacus nitzani* Levy et al., 1973, stat. nov., ♀ (HUJ INVSC 3226). **G.** *Buthacus yotvatensis* Levy et al., 1973, stat. rev., ♂ (HUJ INVSC 3302). **H.** *Buthacus amitaii*, sp. nov., holotype ♂ (HUJ INVSC 3480). Scale bars = 1 mm.

TABLE 5

Meristic data for material of *Buthacus arenicola* (Simon, 1885), *Buthacus leptochelys* (Ehrenberg, 1829), and *Buthacus levyi*, sp. nov. deposited in the American Museum of Natural History (AMNH), New York, the National Natural History Collections, Hebrew University of Jerusalem (HU), Israel, and the Steinhardt Museum of Natural History (SMMNH), Tel Aviv University, Israel.

Counts (left/right) follow Tahir et al. (2014): pedipalp chela fix. subrows (fixed finger median denticle subrows); pedipalp chela mov. subrows (movable finger median denticle subrows); pedipalp chela fix. PAD (fixed finger prolateral accessory denticle count); pedipalp chela mov. PAD (movable finger prolateral accessory denticle count); pedipalp chela fix. RAD (fixed finger retrolateral accessory denticle count); pedipalp chela mov. finger RAD (movable finger retrolateral accessory denticle count); retinial tooth count

Species	Specimen				Pedipalp chela				Pectines tooth count
	type	sex	collection	accession no.	fix. subrows	mov. subrows	fix. PAD	mov. PAD	
<i>B. arenicola</i>	♂	♂	AMNH AMNH	10/10	11/11	10/9	10/10	0/1	1/1
<i>B. leptochelys</i>	♂	HUJ	859	9/10	10/10	10/11	11/11	—	—
	♀	AMNH	1807	10/10	10/10	11/11	11/11	9/7	8/8
	♀	HUJ	2233	7/10	10/11	5/10	9/11	5/8	30/30
	♀	HUJ	50805	9/9	10/10	8/10	11/11	8/7	27/28
	♀	SMNH	11/10	10/11	11/11	10/11	8/8	7/8	27/28
<i>B. levyyi</i>	♂	HUJ	2082	9/9	10/10	10/9	10/9	0/0	1/0
	♂	AMNH	919	11/9	9/10	10/10	10/10	1/1	4/3
	♂	AMNH	919	9/10	9/10	10/10	10/10	0/0	0/1
	♂	HUJ	1772	9/9	—	10/10	—	0/0	—
	♂	HUJ	2077	10/9	9/9	10/10	10/11	1/1	1/2
	♂	HUJ	2079	8/9	10/10	10/9	11/10	0/0	1/0
	♂	HUJ	2083	10/10	9/8	10/10	11/11	0/0	0/0
	♂	HUJ	3253	—	—	—	—	—	—
	♀	AMNH	919	10/10	10/9	11/11	0/1	1/2	25/26
	♀	AMNH	7/10	7/10	5/9	1/0	0/0	0/0	25/25
	Paratype	HUJ	9/9	8/10	9/9	8/10	0/0	0/1	27/27
	Paratype	HUJ	10/9	10/9	10/10	11/11	0/0	2/1	27/28
	Paratype	HUJ	10/10	10/10	10/10	11/10	1/1	3/2	25/26
	Paratype	HUJ	9/8	9/1-	10/9	10/-	1/0	1/-	29/28
	Paratype	HUJ	9/9	10/8	10/8	11/10	1/0	5/3	11/9

the male (18–22) than in the female (12–14). The mesosoma of the male is relatively narrower than that of the female, as indicated by the higher sternite VII length:width ratio in the male (71.1%) compared to the female (67.8%). The spiniform granules of the ventrosubmedian and ventrolateral carinae of metasomal segments II and III, and the ventrolateral carinae of segment V are less prominent in the male than in the female.

**DISTRIBUTION:** *Buthacus arava* appears to be endemic to the Arava Valley, straddling the southern border between Israel and Jordan (fig. 4). The species is presently known from only two rather restricted areas in the valley. Most specimens were collected in the central sand dunes in the southern part of the valley, extending from northeast of Yahel in the north to east of Yotvata in the south, on both sides of the border. A few were collected in the northeastern corner of the valley, in Jordan. The known records are located at elevations ranging from -290 m to 212 m.

*Buthacus arava* is sympatric with the closely related *B. yotvatensis*, in the Arava Valley (fig. 5), but allopatric with *B. tadmorensis*, distributed from central Jordan, through Syria, southeastern Turkey and Iraq, to the northern shore of the Persian Gulf, in southern Iran (fig. 10).

**ECOLOGY:** The types of *B. arava* were collected from pitfall traps or at night with UV light detection on sparsely vegetated, stable to vegetationless, shifting inland sand dunes. Specimens collected at night were uncommon, sitting still or walking on the surface. The habitat and habitus of *B. arava*, notably the pale coloration, smooth tegument, loss or obsolescence of pedipalpal and metasomal carinae, reduced pectinal tooth count, elongation of the legs, especially legs III and IV, dorsoventral compression of the basitarsi of legs I–III, comblike rows of elongated macrosetae (“sand combs”) along the retrolateral margins of the tibae and the pro- and retrolateral margins of the basitarsi of legs I–III, elongated macrosetae on the lateral and ventral surfaces of the telotarsi, and elongated, unequal length telotarsal unguis, are consistent with the ultrasamomophilous ecomorphotype (Prendini, 2001).

The types of *B. arava* were collected in sympatry with *B. yotvatensis*. Two other buthids, *Androctonus crassicauda* (Olivier, 1807) and *Orthochirus scrobiculosus*, also inhabit the same area, but occur on harder substrata.

#### *Buthacus arenicola* (Simon, 1885)

Figures 1B, 8, 15, 18C, 20G, 21C, 22A, 23D, 25D, 27D, 29A, 36, 37, 38; tables 1, 5, 10

*Butthus arenicola* Simon, 1885: 51, 52; Pocock, 1889: 116; Simon, 1892: 84; Kraepelin, 1895: 82; Birula, 1896: 244; 1905: 138.

*Buthacus leptochelys* (nec *Androctonus leptochelys* Ehrenberg, 1829): Pocock, 1895: 299.

*Butthus* (*Buthacus*) *leptochelys arenicola*: Birula, 1914: 636.

*Buthacus arenicola*: Pallary, 1929: 135, 137, 140, fig. 2C; 1934: 91, 95, 98, fig. 4C; 1938: 280, 281; Vachon, 1949a: 71–79, figs. 247, 253, 256–258, 260, 266; 1950a: 197; 1950b: 400, 407, fig. 586; 1951, 422, 424, 425, 428, 429, 431, 441, 446, 450, 452, 454, 464, figs. 642, 656, 685; 1952: 180, 185, 191, 194–196, 199, 201–202 figs. 256, 266; 1958: 184, 185; Bücherl, 1964: 57; Larrouy et al., 1972: 393; Levy et al., 1973: 125, 128; Pérez, 1974: 19; Levy and Amitai, 1980: 89; Kinzelbach, 1985: map III; Vachon and Kinzelbach, 1987: 102; El-Hennawy, 1992: 97, 112 (part); Kovařík, 1998: 105; Fet and Lowe, 2000: 81, 82; Lourenço, 2001: 255; Crucitti and Vignoli, 2002: 440; Kovařík, 2002: 5; Lourenço, 2004a: 205; 2004b: 225; Kovařík and Whitman, 2004: 106 (misidentification); Kovařík, 2005: 1, 2, 6, 9, 10, fig. 1; Lourenço, 2006: 59, 60, 62–69, figs. 21–27; Lourenço and Qi, 2006a: 161; Kaltsas et al., 2008: 213; Zourgui et al., 2008: 81, 84, 85, 88, 89, table 2, plate 7, fig. 4 (misidentification); Lourenço and Leguin, 2009: 103; Lourenço, 2013: 89, 91; Lourenço and Sadine, 2015: 55; Lourenço et al., 2016: 3; 2017a: 33, fig. 1; 2017b: 20, 22, 24, fig. 1, table 1; Sadine et

TABLE 6

**Measurement data for adult male *Buthacus yotvatensis* Levy et al., 1973, stat. rev., deposited in the National Natural History Collections, Hebrew University of Jerusalem (HUJ), Israel, and Steinhardt Museum of Natural History (SMNH), Tel Aviv University, Israel**

Measurements (mm) follow Tahir et al. (2014): total length (sum of carapace, tergites I–VII, metasomal segments I–V, and telson); carapace median ocelli (distance from carapace anterior margin); carapace anterior width (distance between lateral ocelli); chela total length (distance from base of condyle to tip of fixed finger); chela retroventral carina (length along manus retroventral carina); chela movable finger (movable finger length); pectines total length (length along retrolateral margin); pectines dentate margin (length along dentate margin).

Specimen	type	Holotype								
		sex	♂	♂	♂	♂	♂	♂	♂	
		collection	SMNH	HUJ	HUJ	HUJ	HUJ	HUJ	HUJ	
		accession no.	5223	3376	3333	3316	3336	3351	3344	3355
Total length			66.4	67.8	61.9	67.8	70.5	71.9	64.8	68.0
Carapace	median ocelli		2.9	2.7	2.8	2.6	2.7	3.1	2.8	3.0
	length		6.3	6.1	5.9	6.1	6.1	6.8	6.1	6.3
	anterior width		3.2	3.6	3.5	3.8	3.7	3.9	3.5	3.9
	posterior width		7.0	6.6	6.5	6.8	6.3	7.7	6.7	7.1
Tergite I	length		1.0	1.4	1.1	1.0	1.1	1.2	1.1	1.0
Tergite II	length		1.1	1.5	1.2	1.3	1.2	1.4	1.3	1.4
Tergite III	length		1.7	1.9	1.7	1.8	1.7	1.8	1.7	1.7
Tergite IV	length		1.9	2.2	1.9	1.9	1.9	2.2	1.7	2.0
Tergite V	length		2.1	2.5	2.2	2.3	2.1	2.4	2.0	2.3
Tergite VI	length		2.6	2.7	2.3	2.5	2.4	2.5	2.4	2.6
Tergite VII	length		4.8	4.7	3.9	4.8	4.5	5.1	4.5	4.8
Sternite VII	length		3.9	4.7	3.8	4.1	4.0	4.9	4.0	4.5
	width		6.2	6.1	5.8	5.7	5.8	6.2	5.8	6.3
Metasoma I	length		6.4	6.3	5.4	6.5	6.0	7.0	6.1	6.4
	width		3.7	3.7	3.5	3.9	3.8	4.1	3.8	4.1
	height		3.5	3.3	3.2	3.5	3.3	3.8	3.4	3.6
Metasoma II	length		7.2	7.0	6.4	7.3	6.9	7.8	7.0	7.3
	width		3.7	3.3	3.3	3.7	3.6	4.0	3.6	3.9
	height		3.5	3.3	3.3	3.6	3.3	3.7	3.5	3.6
Metasoma III	length		7.5	7.5	6.8	7.5	7.1	7.9	7.1	7.6
	width		3.4	3.3	3.1	3.7	3.4	4.1	3.5	3.7
	height		3.4	3.1	3.1	3.4	3.2	3.6	3.3	3.6
Metasoma IV	length		7.7	7.8	7.2	7.8	7.3	8.3	7.4	7.8
	width		3.1	2.8	2.9	3.2	2.9	3.3	3.1	3.3
	height		3.0	2.6	2.7	3.0	2.8	3.1	2.8	3.1
Metasoma V	length		8.3	8.9	8.3	9.2	8.6	9.3	8.8	9.4
	width		3.0	2.8	2.8	2.9	2.8	3.1	2.9	3.1
	height		2.6	2.4	2.6	2.6	2.4	2.8	2.4	2.7
Telson	vesicle length		3.7	4.1	4.3	3.4	3.4	4.5	3.6	3.7
	vesicle width		2.3	2.3	2.3	2.2	2.2	2.6	2.4	2.5
	vesicle height		2.4	2.2	2.2	2.3	2.4	2.4	2.4	2.4
	aculeus length		4.1	3.1	3.3	4.3	3.8	3.8	4.0	3.8

TABLE 6 *continued*

Specimen	type	Holotype								
		♂	♂	♂	♂	♂	♂	♂	♂	♂
		sex	♂	HUJ						
		collection	SMNH	HUJ						
		accession no.	5223	3376	3333	3316	3336	3351	3344	3355
Femur	length	6.0	5.5	5.4	5.4	5.5	5.6	5.3	5.7	
	width	1.7	1.6	1.7	1.7	1.7	1.8	1.8	1.9	
	height	1.4	1.3	1.3	1.1	1.3	1.5	1.4	1.4	
Patella	length	6.8	6.6	6.8	6.8	6.6	7.5	6.6	6.9	
	width	2.2	1.9	2.0	2.2	2.0	2.5	2.2	2.2	
	height	1.8	1.8	1.8	1.8	1.7	1.9	1.9	1.9	
Chela	total length	10.0	9.5	9.1	9.3	9.5	10.3	9.6	10.0	
	manus width	1.8	1.6	1.7	1.8	1.6	1.7	1.7	1.7	
	manus height	2.0	1.9	1.8	1.9	1.7	2.0	1.8	2.0	
	retroventral carina	3.3	3.2	3.4	3.2	3.2	3.6	3.3	3.4	
	movable finger	6.4	6.1	5.9	5.5	5.9	6.4	5.7	6.4	
Pectines	total length	8.7	8.0	8.2	8.7	7.8	9.0	8.8	9.0	
	dentate margin	8.0	8.0	7.9	7.8	7.4	8.2	8.2	8.4	

al., 2018: 51, 53–57, figs. 3C, 4, table 1; Bousmaha et al., 2019: 141–145, figs. 2, 3, table 1; Amr et al., 2021: 95, table 17.

*Buthacus leptochelys arenicola*: Pallary, 1929: 134, fig. 1A; Pallary, 1934: 91, 92, fig. 3A.

*Buthacus leptochelys* var. *arenicola*: Pallary, 1929: 135.

*Buthacus arenicola arenicola*: Vachon, 1949a: 76; 1950a: 197; 1952: 193, 196, figs. 253, 256–258, 260, 266; Bouisset and Larrouy, 1963: 295–297, figs. 1, 2; Pérez, 1974: 19; Kovařík, 1997b: 179; Lourenço, 2006: 65, 67, 69, fig. 42, table 1; 2013: 97, fig. 14; Lourenço and Sadine, 2015: 56, 57, fig. 1; Lourenço et al., 2016: 4, fig. 1.

**TYPE MATERIAL:** *Butthus arenicola*: Lectotype ♂ (MNHN RS 1672), TUNISIA: Tozzer [Tozeur, 33°54'N 08°06'E], V. May [examined]; paratype ♀ (MNHN), ALGERIA: Biskra [34°52'N 05°47'E]; paratype (MNHN), TUNISIA: Gabès [Quabis], Séd [33°53'N 10°05'E].

**DIAGNOSIS:** *Buthacus arenicola* differs from the closely related species, *B. levyi*, occurring in Egypt and Israel, as follows. The pedipalp chela movable finger of the adult male is proportionally longer than the manus in *B. arenicola* (fig.

38A, B), with chela manus length:movable finger length, 54% (52.4%–55.6%, n = 2; table 10), than in *B. levyi*, with chela manus length:movable finger length, 62.8% (57.4%–67.3%, n = 8; table 10). The metasomal segments of the male are broader in *B. arenicola* (fig. 27D), with segment width:length, I–V, 72.2% (70.8%–73.6%, n = 2; table 10), 63.8% (60.9%–66.8%), 58.9% (58.9%–59%), 44.8% (43.1%–46.5%), and 34.5% (34%–35.1%), than in *B. levyi* (fig. 28A), with segment width:length, I–V, 65.1% (60.2%–70.8%, n = 8; table 10), 56.9% (53.9%–64.4%), 50.5% (47.6%–57.8%), 40.1% (35.9%–45%), and 33.8% (30.7%–38.9%). The dorsolateral carinae of metasomal segment IV are well developed in *B. arenicola* (figs. 23D, 25D), but obsolete to absent in *B. levyi* (figs. 24A, 26A).

*Buthacus arenicola* differs from *B. amitaii*, *B. leptochelys* and *B. nitzani*, as follows. The pedipalp chela of the adult male is longer and narrower in *B. arenicola* (fig. 38A, B), with chela manus length:movable finger length, 54% (52.4%–55.6%, n = 2; table 10) and chela manus width:chela length, 17.6% (17.1%–18.1%, n = 2), than in *B. amitaii*, *B. leptochelys*, and *B. nitzani* (figs. 32A, B, 41A, B, 47A, B), with chela manus length:movable finger length, 81.8% (72.7%–

TABLE 7

**Measurement data for adult female *Buthacus yotvatensis* Levy et al., 1973, stat. rev., deposited in the National Natural History Collections, Hebrew University of Jerusalem (HUJ), Israel**

Measurements (mm) follow Tahir et al. (2014): total length (sum of carapace, tergites I–VII, metasomal segments I–V, and telson); carapace median ocelli (distance from carapace anterior margin); carapace anterior width (distance between lateral ocelli); chela total length (distance from base of condyle to tip of fixed finger); chela retroventral carina (length along manus retroventral carina); chela movable finger (movable finger length); pectines total length (length along retrolateral margin); pectines dentate margin (length along dentate margin).

Specimen	sex	♀	♀	♀	♀	♀	♀
	collection	HUJ	HUJ	HUJ	HUJ	HUJ	HUJ
	accession no.	3323	3345	3348	3353	3356	3378
Total length		74.0	73.5	85.1	80.3	75.4	71.7
Carapace	median ocelli	3.2	3.2	3.7	3.4	3.5	3.1
	length	7.1	7.1	8.0	7.7	7.6	6.9
	anterior width	4.4	4.5	5.1	4.6	4.7	4.0
	posterior width	7.9	8.2	9.7	9.4	8.9	7.0
Tergite I	length	1.3	1.4	1.2	1.4	1.1	1.2
Tergite II	length	1.8	1.6	1.6	1.7	1.6	1.4
Tergite III	length	2.2	2.2	2.1	2.1	2.2	1.7
Tergite IV	length	2.2	2.4	2.5	2.6	2.6	2.2
Tergite V	length	2.6	2.6	2.7	2.9	2.7	2.8
Tergite VI	length	3.0	2.9	3.1	3.1	3.1	2.9
Tergite VII	length	5.1	5.2	6.0	5.7	5.6	4.8
Sternite VII	length	4.6	4.8	4.9	5.3	5.1	4.9
	width	7.2	7.7	8.7	8.3	8.4	6.7
Metasoma I	length	6.8	6.7	8.1	7.4	7.1	6.6
	width	4.2	4.1	5.0	4.6	4.7	4.0
	height	3.8	3.7	4.6	4.2	4.1	3.5
Metasoma II	length	7.9	7.3	9.0	8.2	8.0	7.4
	width	4.2	3.8	4.9	4.5	4.5	3.8
	height	3.9	3.7	4.5	4.2	4.1	3.6
Metasoma III	length	7.8	7.9	9.2	8.5	8.2	7.6
	width	3.9	3.8	4.6	4.2	4.4	3.8
	height	3.8	3.7	4.4	4.0	3.9	3.6
Metasoma IV	length	7.9	8.1	9.6	9.1	8.6	7.9
	width	3.4	3.2	4.0	3.7	3.9	3.2
	height	3.4	3.2	3.9	3.7	3.5	3.2
Metasoma V	length	9.7	9.7	11.7	10.6	10.5	10.0
	width	3.4	3.2	3.8	3.6	3.7	3.3
	height	3.0	2.9	3.5	3.1	3.2	2.9
Telson	vesicle length	4.5	4.0	4.8	4.6	4.4	4.3
	vesicle width	2.8	2.7	3.4	3.1	2.9	2.6
	vesicle height	2.7	2.7	3.1	2.8	2.8	2.5
	aculeus length	4.5	4.5	5.5	4.8	5.5	3.9
Femur	length	6.2	5.7	6.5	5.8	6.1	5.7
	width	2.1	1.9	2.5	2.3	2.3	1.9
	height	1.5	1.5	2.0	2.0	1.9	1.4

TABLE 7 *continued*

Specimen	sex	♀	♀	♀	♀	♀	♀
	collection	HUJ	HUJ	HUJ	HUJ	HUJ	HUJ
	accession no.	3323	3345	3348	3353	3356	3378
Patella	length	7.0	7.2	8.3	7.4	7.5	6.9
	width	2.5	2.3	2.7	2.6	2.8	2.2
	height	1.8	1.9	2.4	2.1	2.4	1.9
Chela	total length	10.5	10.7	11.9	11.4	11.4	10.3
	manus width	2.0	1.7	2.2	2.1	2.0	1.7
	manus height	2.1	2.0	2.3	2.2	2.3	2.0
	retroventral carina	3.2	3.3	3.8	3.3	3.5	3.2
	movable finger	6.7	7.0	7.9	7.3	7.4	6.7
Pectines	total length	7.0	7.6	9.4	8.2	8.2	7.2
	dentate margin	5.8	6.8	8.0	7.4	6.6	6.4

88.3%,  $n = 5$ ; table 3), 70.7% (table 4), and 84.4% (76.8%–92.4%,  $n = 8$ ; table 12), and chela manus width:chela length, 27.1% (25.1%–28.9%,  $n = 5$ ), 24.2%, and 26.3% (22.3%–29.5%,  $n = 8$ ), respectively. The count of retrolateral accessory denticles on the movable finger of the pedipalp chela is usually lower in *B. arenicola* (fig. 21C), with 1/1 (table 5), than in *B. amitaii*, *B. leptochelys*, and *B. nitzani* (fig. 21A, D, G), with 0–9/2–10 ( $n = 9$ ; table 2), 7–9/7–9 ( $n = 5$ ; table 5) and 6–9/6–9 ( $n = 16$ ; table 2), respectively.

**DESCRIPTION:** The following redescription is based on two adult males collected from the vicinity of type locality (see table 5 for counts and table 10 for measurements).

**Total length:** Medium-sized scorpions, 54.3 mm (54.2–54.4 mm,  $n = 2$ ) (♂).

**Color:** Uniformly pale yellow with legs slightly paler. Pectines whitish.

**Carapace:** Carapace shape trapezoidal (fig. 18C), anterior width:posterior width, 57.1% (55.6%–58.6%,  $n = 2$ ), length:posterior width, 96.1% (94.3%–98%,  $n = 2$ ). Five, rarely four, pairs of lateral ocelli; each lateral ocular tubercle with three major ocelli (ALMa, MLMa, PLMa), similar in size, situated anterolaterally, and one or, usually, two minor ocelli (ADMi, PDMi; PDMi may be absent) situated posterodorsal to posterior major ocellus. Median ocelli larger than lateral ocelli, distance between them approximately 2× ocellus width.

Median ocular tubercle situated anteromedially, distance from anterior carapace margin:carapace length, 42.8% (42.3%–43.3%,  $n = 2$ ) (♂). Superciliary and central median carinae distinct, weakly granular, and disconnected (♂). Anteromedian sulcus distinct, shallow; posteromedian sulcus deep, narrow anteriorly, wide posteriorly; posterolateral sulci deep, wide, curved. Carapace intercarinal surfaces finely and densely granular.

**Chelicerae:** Cheliceral manus prodorsal margin and retrodorsal surfaces smooth, prolateral and ventral surfaces setose. Fixed finger dorsal and ventral surfaces densely setose; dorsal margin with subdistal, medial, and proximal denticles; ventral margin with proximal and medial denticles. Movable finger dorsal surface smooth and glabrous; ventral surface setose; dorsal margin with retrodistal, subdistal, medial, and pair of proximal denticles; ventral margin with prodistal, medial, and proximal denticles.

**Pedipalps:** Femur dorsal prolateral, dorsal retro-lateral and ventral prolateral carinae complete, costate-granular; prolateral ventral and prolateral ventrosubmedian carinae each comprising discontinuous row of spiniform granules; retro-lateral dorsosubmedian carina comprising discontinuous row of spiniform granules and fewer than 15 macrosetae; dorsal, retro-lateral, and intercarinal surfaces smooth; prolateral intercarinal surfaces finely granular (fig. 37A, B). Patella dorsal prolat-



FIGURE 23. *Buthacus* Birula, 1908, metasomal segments I–V and telson, dorsal aspect. A. *Buthacus arava*, sp. nov., paratype ♀ (HUJ INVSC 2561). B. *Buthacus tadmorensis* (Simon, 1892), stat. rev., paralectotype ♀ (NHMW 2452) of *Buthus pietschmanni* Penther, 1912. C. *Buthacus yotvatensis* Levy et al., 1973, stat. rev., ♀ (HUJ INVSC 3318). D. *Buthacus arenicola* (Simon, 1885), ♂ (AMNH). Scale bars = 5 mm.

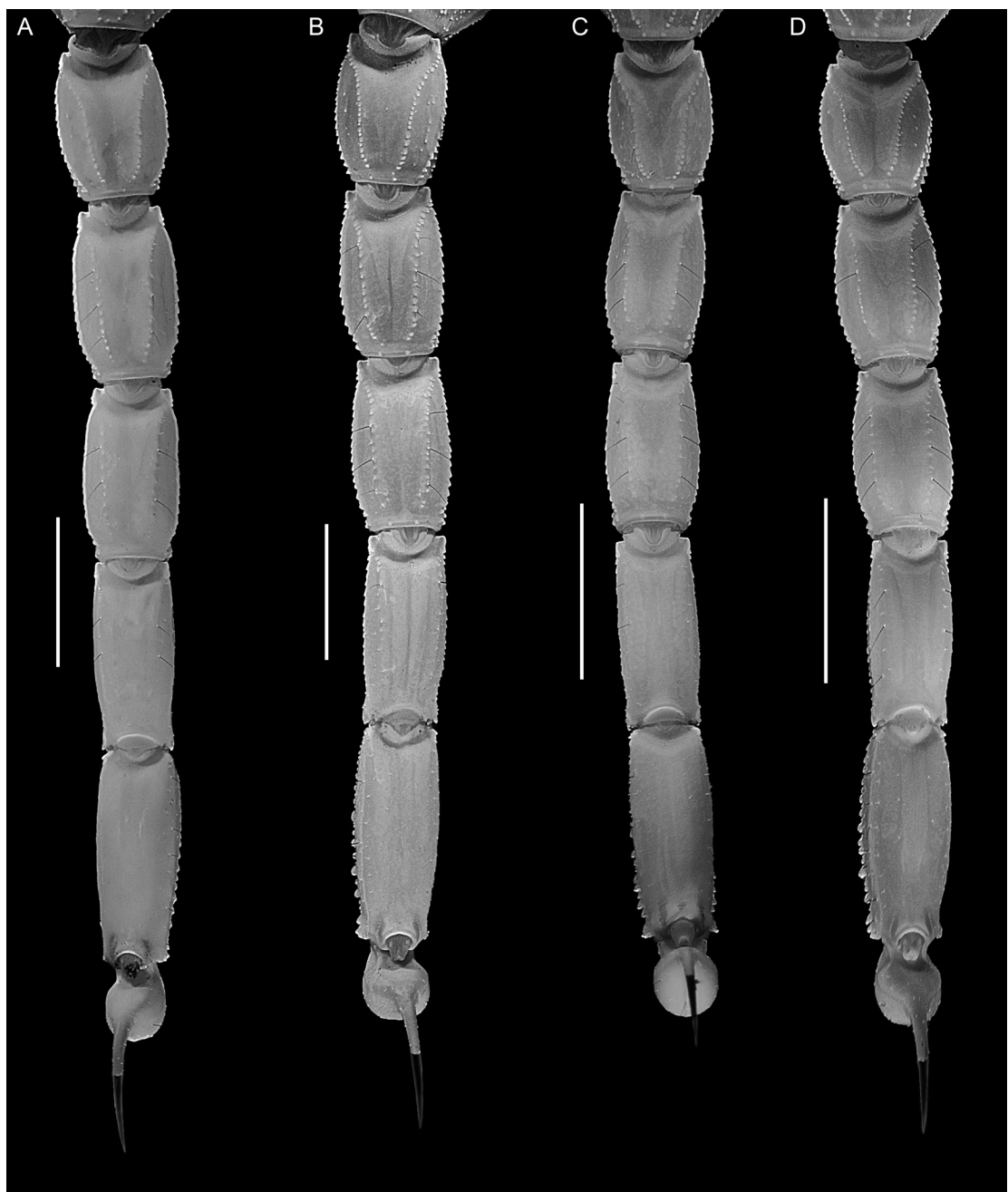


FIGURE 24. *Buthacus* Birula, 1908, metasomal segments I–V and telson, dorsal aspect. **A.** *Buthacus levyi*, sp. nov., paratype ♀ (HUJ INVSC 3274). **B.** *Buthacus leptochelys* (Ehrenberg, 1829), ♀ (HUJ INVSC 1807). **C.** *Buthacus nitzani* Levy et al., 1973, stat. nov., ♀ (HUJ INVSC 3226). **D.** *Buthacus amitaii*, sp. nov., paratype ♀ (HUJ INVSC 3205). Scale bars = 5 mm.



FIGURE 25. *Buthacus* Birula, 1908, metasomal segments I–V and telson, lateral aspect. A. *Buthacus arava*, sp. nov., paratype ♀ (HUJ INVSC 2561). B. *Buthacus tadmorensis* (Simon, 1892), stat. rev., paralectotype ♀ (NHMW 2452) of *Buthus pietschmanni* Penther, 1912. C. *Buthacus yotvatensis* Levy et al., 1973, stat. rev., ♀ (HUJ INVSC 3318). D. *Buthacus arenicola* (Simon, 1885), ♂ (AMNH). Scale bars = 5 mm.

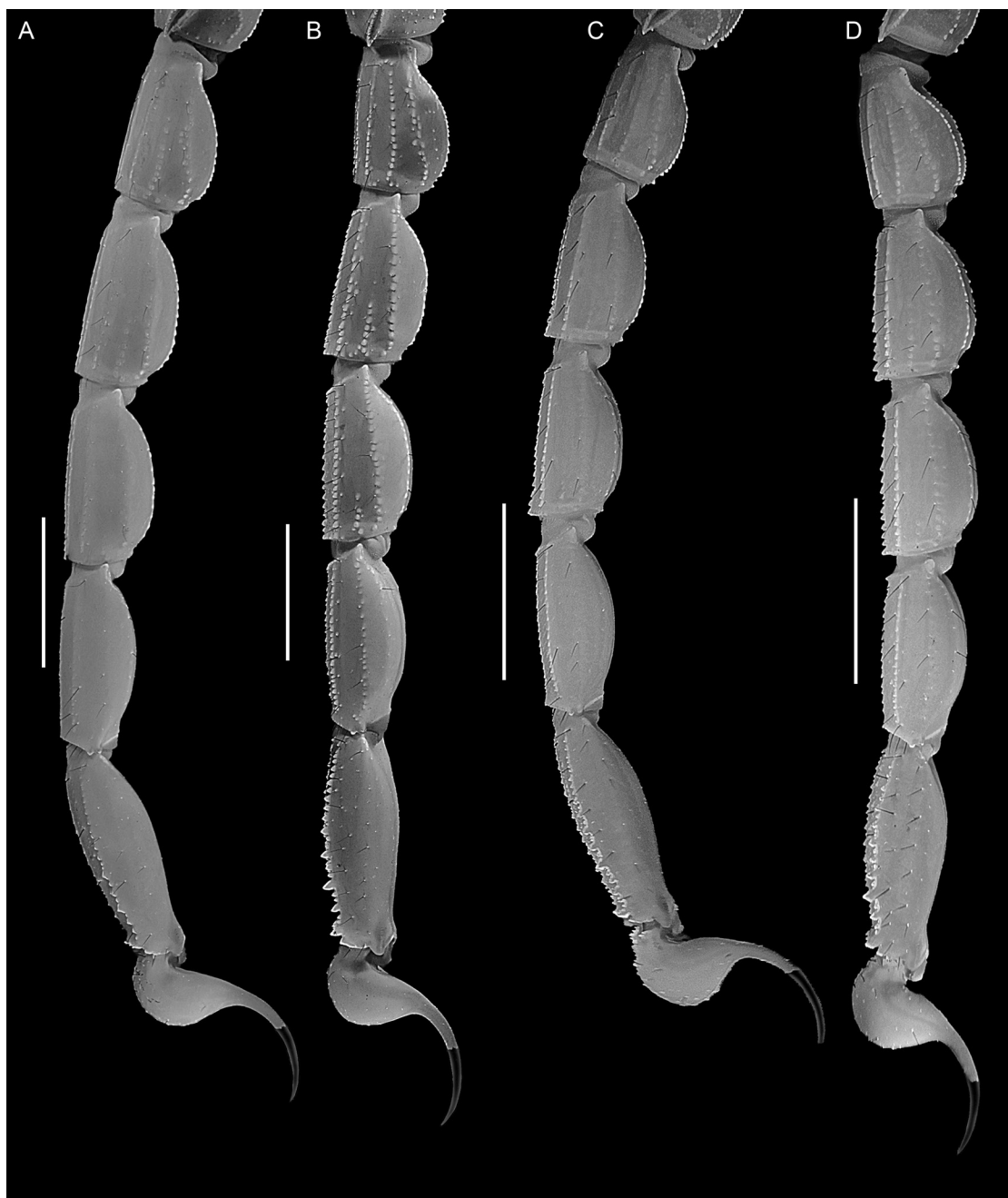


FIGURE 26. *Buthacus* Birula, 1908, metasomal segments I–V and telson, lateral aspect. **A.** *Buthacus levyi*, sp. nov., paratype ♀ (HUJ INVSC 3274). **B.** *Buthacus leptochelys* (Ehrenberg, 1829), ♀ (HUJ INVSC 1807). **C.** *Buthacus nitzani* Levy et al., 1973, stat. nov., ♀ (HUJ INVSC 3226). **D.** *Buthacus amitaii*, sp. nov., paratype ♀ (HUJ INVSC 3205). Scale bars = 5 mm.

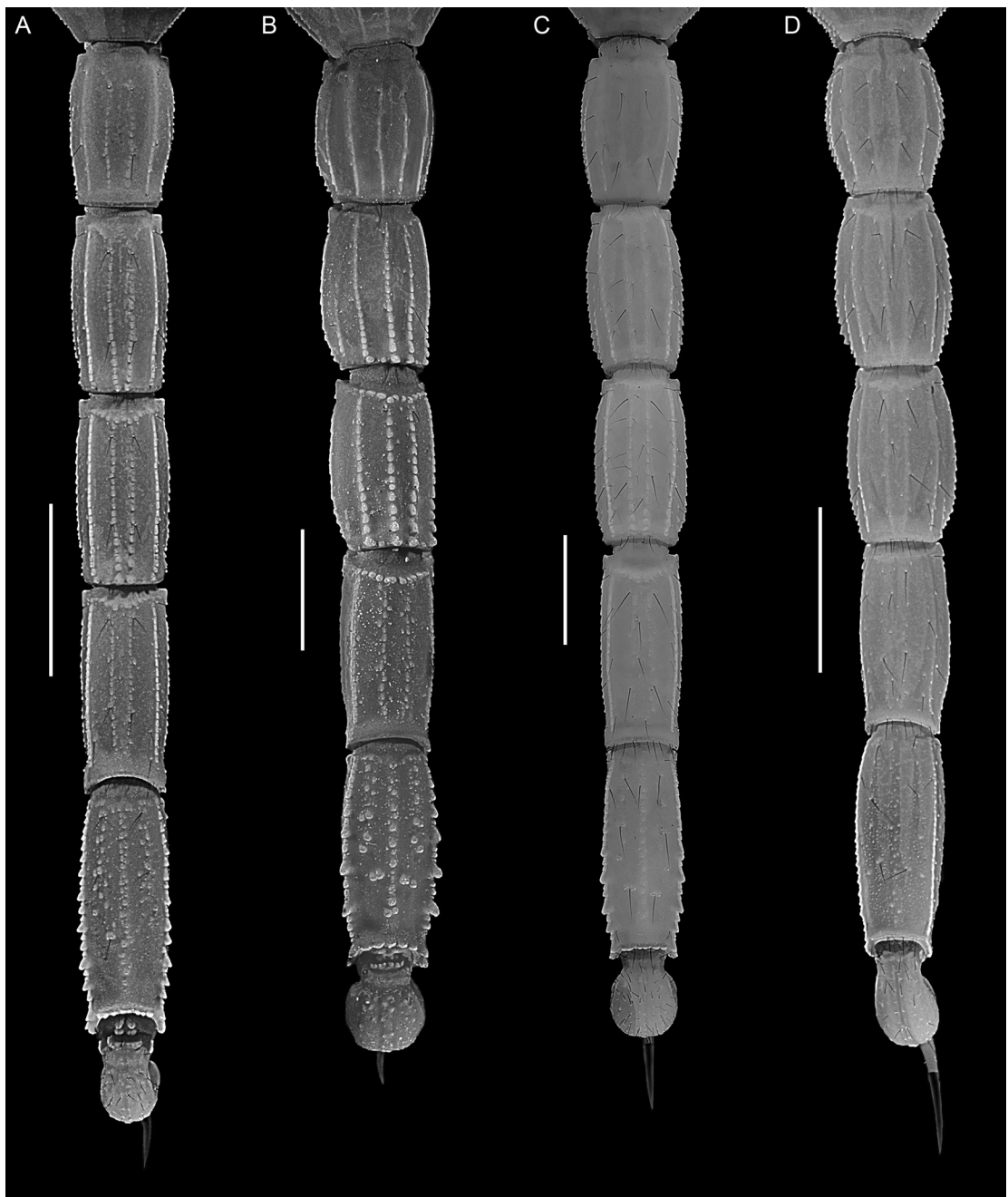


FIGURE 27. *Buthacus* Birula, 1908, metasomal segments I–V and telson, ventral aspect. A. *Buthacus arava*, sp. nov., paratype ♀ (HUJ INVSC 2561). B. *Buthacus tadmorensis* (Simon, 1892), stat. rev., paralectotype ♀ (NHMW 2452) of *Buthus pietschmanni* Penther, 1912. C. *Buthacus yotvatensis* Levy et al., 1973, stat. rev., ♀ (HUJ INVSC 3318). D. *Buthacus arenicola* (Simon, 1885), ♂ (AMNH). Scale bars = 5 mm.

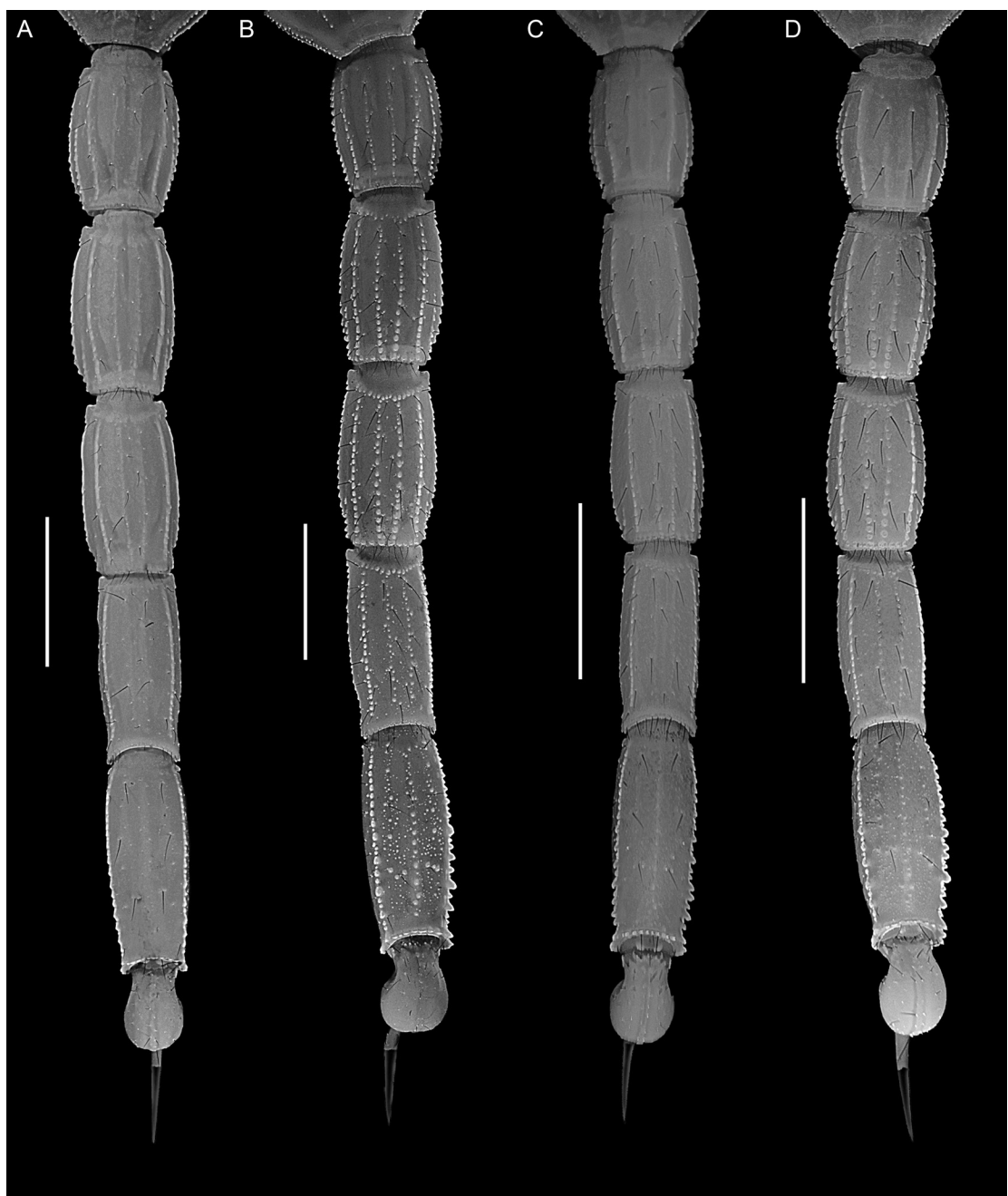


FIGURE 28. *Buthacus* Birula, 1908, metasomal segments I–V and telson, ventral aspect. A. *Buthacus levyi*, sp. nov., paratype ♀ (HUJ INVSC 3274). B. *Buthacus leptochelys* (Ehrenberg, 1829), ♀ (HUJ INVSC 1807). C. *Buthacus nitzani* Levy et al., 1973, stat. nov., ♀ (HUJ INVSC 3226). D. *Buthacus amitaii*, sp. nov., paratype ♀ (HUJ INVSC 3205). Scale bars = 5 mm.

TABLE 8

**Measurement data for adult male and female *Buthacus arava*, sp. nov., deposited in the National Natural History Collections, Hebrew University of Jerusalem (HUJ), Israel**

Measurements (mm) follow Tahir et al. (2014): total length (sum of carapace, tergites I–VII, metasomal segments I–V, and telson); carapace median ocelli (distance from carapace anterior margin); carapace anterior width (distance between lateral ocelli); chela total length (distance from base of condyle to tip of fixed finger); chela retroventral carina (length along manus retroventral carina); chela movable finger (movable finger length); pectines total length (length along retrolateral margin); pectines dentate margin (length along dentate margin).

Specimen	type	Holotype	Paratypes							
			♂	♂	♂	♂	♂	♂	♀	
			collection	HUJ	HUJ	HUJ	HUJ	HUJ	HUJ	
		accession no.	3672	2559	2569	3286	3292	3293	3299	3381
Total length		73.4	67.3	71.5	72.0	71.9	75.0	61.8	64.9	
Carapace	median ocelli	3.1	2.6	2.8	2.8	2.9	3.0	2.5	3.1	
	length	7.0	6.0	6.5	6.7	6.6	7.1	5.7	6.9	
	anterior width	3.4	3.5	3.9	3.8	3.6	3.7	3.7	3.7	
	posterior width	7.7	7.0	7.2	7.0	7.7	7.3	6.2	7.7	
Tergite I	length	1.1	1.2	1.1	1.2	1.2	1.1	1.0	1.1	
Tergite II	length	1.6	1.4	1.2	1.7	1.5	1.5	1.1	1.4	
Tergite III	length	1.8	1.8	1.5	1.9	1.8	2.0	1.7	1.8	
Tergite IV	length	2.3	2.2	2.0	2.3	2.3	2.6	2.0	1.9	
Tergite V	length	2.5	2.4	2.4	2.6	3.0	2.9	2.2	2.2	
Tergite VI	length	2.7	2.6	2.7	3.0	3.1	3.1	2.5	2.5	
Tergite VII	length	5.1	5.0	4.9	5.1	5.3	5.2	4.4	5.3	
Sternite VII	length	5.0	4.3	4.4	4.8	5.3	5.1	3.9	5.0	
	width	7.3	6.1	6.5	6.8	7.0	7.1	5.5	7.3	
Metasoma I	length	7.2	6.3	6.8	6.8	6.6	7.0	5.6	5.9	
	width	4.6	4.1	4.2	4.3	4.4	4.4	3.7	3.6	
	height	4.1	3.4	3.6	3.5	3.5	4.0	3.2	3.4	
Metasoma II	length	8.0	7.1	7.5	7.7	7.6	8.1	6.3	6.5	
	width	4.4	4.0	3.9	5.1	4.1	4.3	3.5	3.6	
	height	4.0	3.5	3.6	4.1	3.7	4.0	3.3	3.3	
Metasoma III	length	8.3	7.4	8.0	8.0	8.0	8.2	6.7	6.5	
	width	4.4	3.8	3.8	3.9	4.0	4.3	3.4	3.6	
	height	4.0	3.4	3.5	3.6	3.7	3.8	3.2	3.6	
Metasoma IV	length	8.6	7.8	8.4	8.5	8.2	8.6	7.0	7.0	
	width	4.0	3.4	3.6	3.4	3.6	4.0	3.1	3.3	
	height	3.5	3.0	3.1	3.2	3.2	3.4	2.9	3.0	
Metasoma V	length	9.3	9.3	10.2	9.3	9.3	10.3	8.4	8.7	
	width	3.6	3.2	3.3	3.2	3.4	3.6	3.0	3.2	
	height	3.3	2.6	2.7	2.7	3.0	3.0	2.5	2.9	
Telson	vesicle length	3.8	3.3	3.7	3.9	3.9	4.0	3.3	3.4	
	vesicle width	2.5	2.2	2.2	2.2	2.3	2.6	2.1	2.3	
	vesicle height	2.4	2.3	2.3	2.2	2.5	2.7	2.0	2.0	
	aculeus length	4.2	3.5	4.5	3.2	3.7	3.4	3.9	3.8	

TABLE 8 *continued*

Specimen	type	Holotype	Paratypes						
			♂	♂	♂	♂	♂	♂	
	sex	♂	HUJ	HUJ	HUJ	HUJ	HUJ	HUJ	
	collection								
	accession no.	3672	2559	2569	3286	3292	3293	3299	3381
Femur	length	6.1	5.8	5.5	5.6	5.8	6.2	4.7	4.8
	width	1.9	1.7	1.9	1.8	2.0	2.2	1.5	1.9
	height	1.8	1.6	1.7	1.7	1.8	2.0	1.5	1.4
Patella	length	6.6	6.2	6.7	6.7	6.8	7.4	5.7	5.8
	width	2.8	2.6	2.6	2.7	2.9	3.0	2.5	2.5
	height	2.4	2.3	2.2	2.1	2.3	2.7	2.0	2.1
Chela	total length	10.2	9.8	10.6	9.9	10.1	10.6	8.7	9.0
	manus width	3.1	2.8	3.0	2.7	3.0	3.4	2.9	2.1
	manus height	3.7	3.0	3.1	3.0	3.4	3.8	2.8	2.4
	retroventral carina	4.9	4.9	5.1	4.6	4.8	4.5	4.1	3.4
	movable finger	5.4	5.2	5.5	5.4	5.2	5.4	4.5	5.6
Pectines	total length	7.2	6.2	6.7	6.6	6.3	6.8	5.6	4.7
	dentate margin	6.2	5.9	5.7	5.7	5.6	6.0	4.9	3.2

eral carinae obsolete; prolateral median and ventral prolateral carinae each comprising discontinuous row of spiniform granules; other carinae absent; intercarinal surfaces smooth (fig. 37C–E). Chela of male long and slender, manus width:length, 52.6% (50.8%–54.3%,  $n = 2$ ) (♂), manus height:length, 62% (56.2%–67.7%,  $n = 2$ ) (♂), and manus length:movable finger length, 54% (52.4%–55.6%,  $n = 2$ ) (♂). Chela manus acarinate; intercarinal surfaces smooth and setose (fig. 38). Fixed and movable fingers respectively with 10 and 11 oblique median denticle subrows; movable finger with one retrolateral accessory denticle (fig. 21C); proximal dentate margins of fingers sublinear (fig. 37B), such that small gap present proximally when fingers closed.

**Legs:** Legs I–IV, femoral ventral carinae granular; patellar ventral carinae absent; intercarinal surfaces smooth. Legs I–IV, macrosetal counts on retrolateral margins of tibiae, 7:12:13: 3; basitarsi, 12:18:19:10; telotarsi, 5:6:8:6 ( $n = 1$ ). Legs I–IV, tibial spurs absent on I and II, present on III and IV; pro- and retroventral basitarsal (pedal) spurs present, more developed on III and IV. Telotarsal unguis long, approximately equal to telotarsus length, unequal on legs I and II, subequal to equal on III and IV (fig. 22A).

**Genital operculum:** Genital opercula suboval, completely divided longitudinally, with overlapping, rounded margins (♂) (fig. 20G) or partially fused longitudinally (♀). Genital papillae present (♂) or absent (♀).

**Pectines:** Three marginal lamellae; 10–12 ( $n = 2$ ) (♂) median lamellae (fig. 20G). Fulcra present. Pectinal teeth along most of length, dentate margin length:pecten length, 96.8% (96.1%–97.5%,  $n = 2$ ) (♂). Pectinal teeth curved, similar in size; tooth count (sinistral/dextral), 31–32/31–32 ( $n = 2$ ) (♂).

**Mesosoma:** Tergites I–VII progressively increasing in length posteriorly, tergite VI length:tergite VII length, 56.5% (53.6%–59.4%,  $n = 2$ ) (♂); increasing in width posteriorly from I–IV, decreasing in width posteriorly from V–VII. Pretergites smooth; posttergites I–VI, intercarinal surfaces uniformly granular, becoming more coarsely and densely granular posteriorly, VII, finely to coarsely and sparsely granular. Tergites I–VI, dorsomedian carinae granular, vestigial, restricted to posterior fifth of I–IV and posterior third of V and VI; dorsosubmedian carinae obsolete to absent on I and II, granular, vestigial, restricted to posterior quarter of III and IV and posterior third of V and VI. Tergite VII, dorsomedian carina obsolete to

TABLE 9

Meristic data for material of *Buthacus arava*, sp. nov., *Buthacus tadmorensis* (Simon, 1892), stat. rev., i.e., types of *Buthus pietschmanni* Penther, 1912, and *Buthacus yotvatensis* Levy et al., 1973, stat. rev., deposited in the Naturhistorisches Museum Wien (NHMW), Austria, the National Natural History Collections, Hebrew University of Jerusalem (HUJ), Israel, and the Steinhardt Museum of Natural History (SMMNH), Tel Aviv University, Israel. Counts (left/right) follow Tahir et al. (2014): pedipalp chela fix. subrows (fixed finger median denticle subrows); pedipalp chela mov. subrows (movable finger median denticle subrows); pedipalp chela fix. PAD (fixed finger prolateral accessory denticle count); pedipalp chela mov. PAD (movable finger prolateral accessory denticle count); pedipalp chela fix. RAD (fixed finger retrolateral accessory denticle count); pedipalp chela mov. finger RAD (movable finger retrolateral accessory denticle count); pectinal tooth count.

Species	type	Specimen			Pedipalp chela						Pectines			
		sex	collection	accession no.	fix.	subrows	mov.	subrows	fix.	PAD	mov.	RAD	mov.	RAD
<i>B. arava</i>	Holotype	♂	HUJ	3672	9/9	9/10	9/10	10/11	7/7	8/7	8/7	21/22		
	Paratype	♂	HUJ	2559	9/9	10/8	9/10	10/10	8/8	9/7	9/7	20/19		
	Paratype	♂	HUJ	2569	9/8	9/9	10/9	10/11	7/7	9/8	9/8	19/19		
	Paratype	♂	HUJ	3286	9/9	9/8	10/9	10/10	7/7	9/9	9/9	19/20		
	Paratype	♂	HUJ	3292	9/9	9/9	10/10	10/10	8/8	9/9	9/9	21/21		
	Paratype	♂	HUJ	3293	9/9	8/8	10/10	11/11	8/6	8/9	8/9	18/19		
	Paratype	♂	HUJ	3299	8/9	8/10	8/10	8/9	5/7	7/9	7/9	19/18		
	Paratype	♀	HUJ	3381	9/9	6/7	9/9	7/7	7/7	6/8	6/8	12/13		
	<i>B. tadmorensis</i>	Lectotype	♂	NHMW	2453	10/10	11/10	10/10	10/11	9/8	9/10	9/10	30/32	
		Paralectotype	♀	NHMW	2452	9/9	11/9	10/10	11/11	7/8	8/8	8/8	-126	
		Paralectotype	♀	NHMW	2453	9/8	9/9	9/10	11/11	8/7	9/9	9/9	23/23	
		Paralectotype	♀	NHMW	2453	9/10	9/9	10/9	11/11	9/8	9/9	9/9	24/25	
		Paralectotype	♀	NHMW	10/10	10/9	10/10	11/11	8/8	8/9	8/9	26/26		
<i>B. yotvatensis</i>	Holotype	♂	SMMNH	5223	10/10	11/10	10/10	10/10	1/3	6/7	6/7	33/34		
	♂	HUJ	3316	10/11	12/11	10/10	11/11	9/9	10/10	10/10	34/35			
	♂	HUJ	3333	11/12	12/11	10/11	11/9	8/9	10/10	10/10	37/37			
	♂	HUJ	3336	10/10	11/11	10/10	11/11	9/9	10/9	10/9	32/32			
	♂	HUJ	3344	9/10	11/11	9/10	11/11	4/5	7/7	7/7	34/35			
	♂	HUJ	3351	10/10	10/10	10/10	11/11	5/5	10/10	10/10	34/35			
	♂	HUJ	3355	11/10	-/12	11/11	-/12	8/8	-/10	-/10	33/34			
	♂	HUJ	3376	10/10	11/11	11/9	11/11	7/7	10/10	10/10	33/36			
	♀	HUJ	3323	10/10	10/10	10/10	11/11	9/9	11/11	11/11	25/26			
	♀	HUJ	3345	10/10	11/11	10/10	11/11	7/8	9/9	9/9	27/26			
	♀	HUJ	3348	10/10	11/11	10/11	11/11	7/8	8/9	8/9	26/27			
	♀	HUJ	3353	10/10	10/9	10/10	11/11	7/7	8/8	8/8	26/26			
	♀	HUJ	3356	10/10	-/11	10/10	-/11	9/9	-/10	-/10	28/28			
	♀	HUJ	3378	10/10	10/10	10/11	11/11	9/8	10/9	10/9	25/26			

absent; dorsosubmedian and dorsolateral carinae distinct, granular. Sternites III–VII smooth and glabrous; III–VI acarinate, VII, ventrolateral carinae vestigial, granular; IV–VI, respiratory spiracles (stigmata) width approximately 3× length.

**Metasoma:** Metasomal segments I–V becoming longer and narrower posteriorly (figs. 23D, 25D, 27D), segment I shortest, length I:II, 89.9% (89.6%–90.2%,  $n = 2$ ) (♂); segments II and III similar, length II:III, 97.9% (95.1%–100.7%,  $n = 2$ ) (♂); segment III shorter than IV, length III:IV, 93.1% (90.8%–95.3%,  $n = 2$ ) (♂); segment V longest, length IV:V, 82.9% (81.3%–84.6%,  $n = 2$ ) (♂); width:length segment I, 72.2% (70.8%–73.6%,  $n = 2$ ) (♂), II, 63.8% (60.9%–66.8%,  $n = 2$ ) (♂), III, 58.9% (58.9%–59%,  $n = 2$ ) (♂), IV, 44.8% (43.1%–46.5%,  $n = 2$ ) (♂), V, 34.5% (34%–35.1%,  $n = 2$ ); dorsosubmedian and dorsolateral carinae distinct, granular on segment I–III, obsolete on IV, absent on V; dorsosubmedian and dorsolateral carinae sparsely setose, macrosetal counts on segments I–V (sinistral/dextral), dorsosubmedian carinae, 0/1 (0/1–0/1,  $n = 2$ ):4/4 (3/3–4/4):4/3 (3/3–4/3):3/4 (3/3–3/4):0/0 (0/0–0/0), dorsolateral carinae, 2/3 (2/2–2/3,  $n = 2$ ):3/3 (3/2–3/4):3/3 (3/2–3/3):3/2 (2/2–3/2):4/3 (3/2–4/3). Median lateral carinae distinct, granular, extending entire length of segment I, restricted to posterior half of II and posterior quarter of III, absent on IV and V. Ventrolateral carinae distinct, costate, becoming granular posteriorly on segments I–IV; serrate, comprising spiniform granules, becoming more prominent posteriorly, on V. Ventrosubmedian carinae distinct, costate on segment I; costate, becoming costate-granular posteriorly, on II–IV; granular on V. Ventromedian carina obsolete, granular on segment V. Dorsal and lateral intercarinal surfaces smooth on segments I–V; ventral intercarinal surfaces smooth on I, finely and sparsely granular on II–IV, finely and densely granular across entire surface of V.

**Telson:** Telson vesicle width:metasomal segment V width, 74.3% (72.2%–76.3%,  $n = 2$ ) (♂).

Vesicle globose, dorsal surface flat, ventral surface convex and rounded; vesicle height:length, 59.1% (58.7%–59.5%,  $n = 2$ ) (♂); dorsal and ventral surfaces smooth and glabrous; lateral and ventral surfaces sparsely setose, with 39 (38–40,  $n = 2$ ) (♂) macrosetae. Aculeus long, gently curved; aculeus length:telson length, 54.5% (54.3%–54.7%,  $n = 2$ ) (♂).

**Sexual dimorphism:** The pedipalp chela manus of the male is slightly broader, with proportionally shorter fingers than that of the female. The genital opercula are completely divided longitudinally, with overlapping, rounded margins in the male but partially fused longitudinally in the female, and genital papillae are present in the male but absent in the female. Additionally, the pectinal tooth count is higher and the mesosoma relatively narrower in the male than in the female.

**DISTRIBUTION:** *Buthacus arenicola* appears to be endemic to central Tunisia and northeastern Algeria, south of the Tell Atlas mountain range and north of the Chott Melhrir and Chott el Djerid salt lakes (fig. 8), from approximately sea level (5 m) to 126 m elevation (Lourenço et al., 2017b; L.P., personal obs.). It is doubtful whether populations from elsewhere, including those formerly assigned to *Buthacus spatzi* (Birula, 1911), stat. rev., are conspecific based on DNA sequence data and morphology (L.P., unpublished data). *Buthacus arenicola* is allopatric with the closely related *B. spatzi*, occurring south of the Chott Melhrir and Chott el Djerid salt lakes, in southern Tunisia and western Libya, and *B. levyi*, endemic to Egypt and Israel.

**ECOLOGY:** Specimens of *B. arenicola* were collected at night with UV light detection on low, stable vegetated white sand dunes with scattered gypsum outcrops and small shrub-coppice dunes around grass tussocks. Specimens were resting or walking on ground and bushes, mostly on shrub-coppice dunes. The habitat and habitus, notably the pale coloration, smooth tegument, loss or obsolescence of pedipalpal and metasomal carinae, elongation of the legs, especially legs III and IV, dorsoventral compression of the basitarsi of

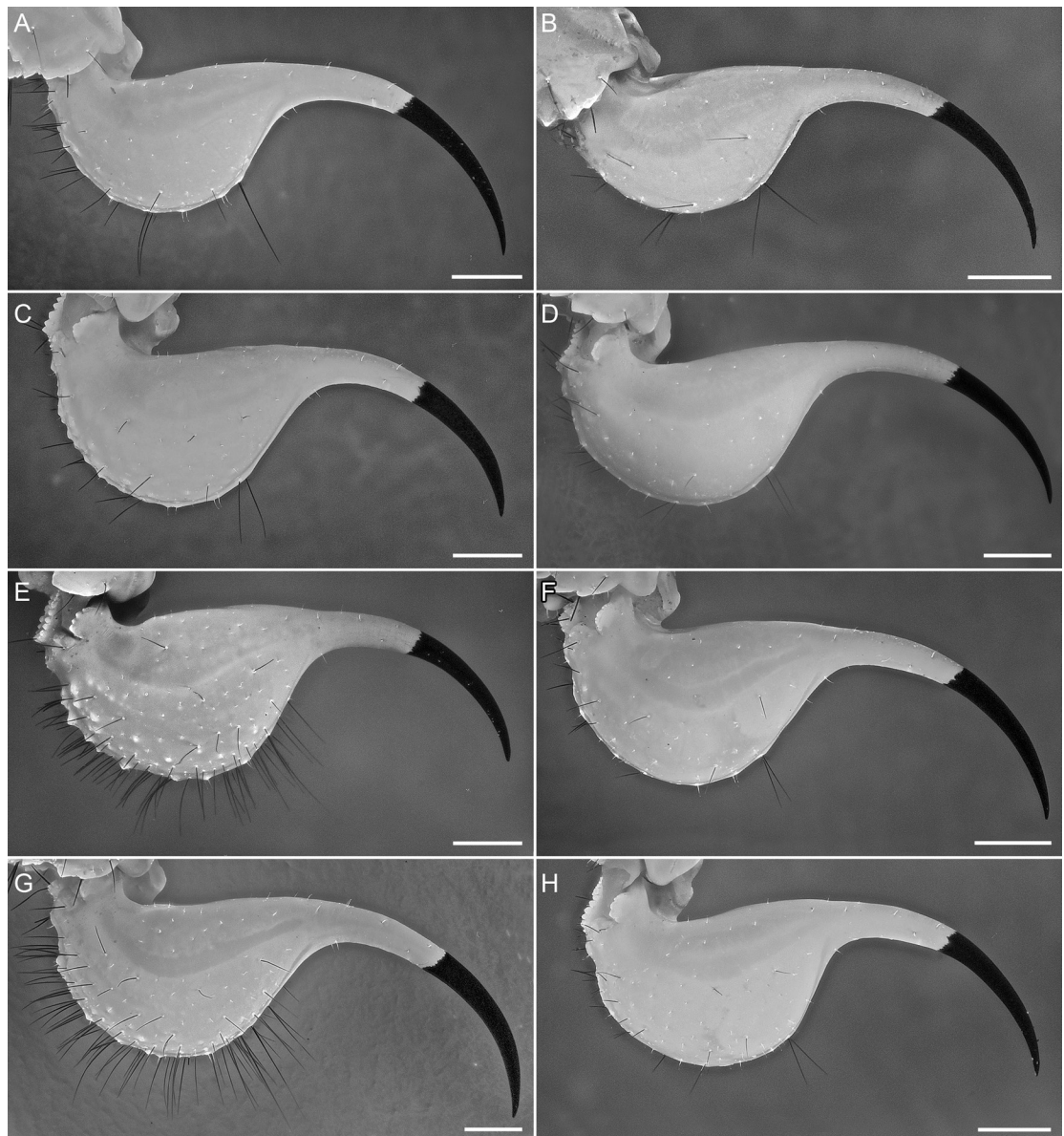


FIGURE 29. *Buthacus* Birula, 1908, telson, lateral aspect. **A.** *Buthacus arenicola* (Simon, 1885), ♂ (AMNH). **B.** *Buthacus levyi*, sp. nov., holotype ♂ (HUI INVSC 2082). **C.** *Buthacus arava*, sp. nov., paratype ♂ (HUI INVSC 2559). **D.** *Buthacus leptochelys* (Ehrenberg, 1829), ♂ (HUI INVSC 859). **E.** *Buthacus tadmorensis* (Simon, 1892), stat. rev., lectotype ♂ (NHMW 2453) of *Buthus pietschmanni* Penther, 1912. **F.** *Buthacus nitzani* Levy et al., 1973, stat. nov., ♂ (HUI INVSC 3227). **G.** *Buthacus yotvatensis* Levy et al., 1973, stat. rev., ♂ (HUI INVSC 3302). **H.** *Buthacus amitaii*, sp. nov., holotype ♂ (HUI INVSC 3480). Scale bars = 1 mm.

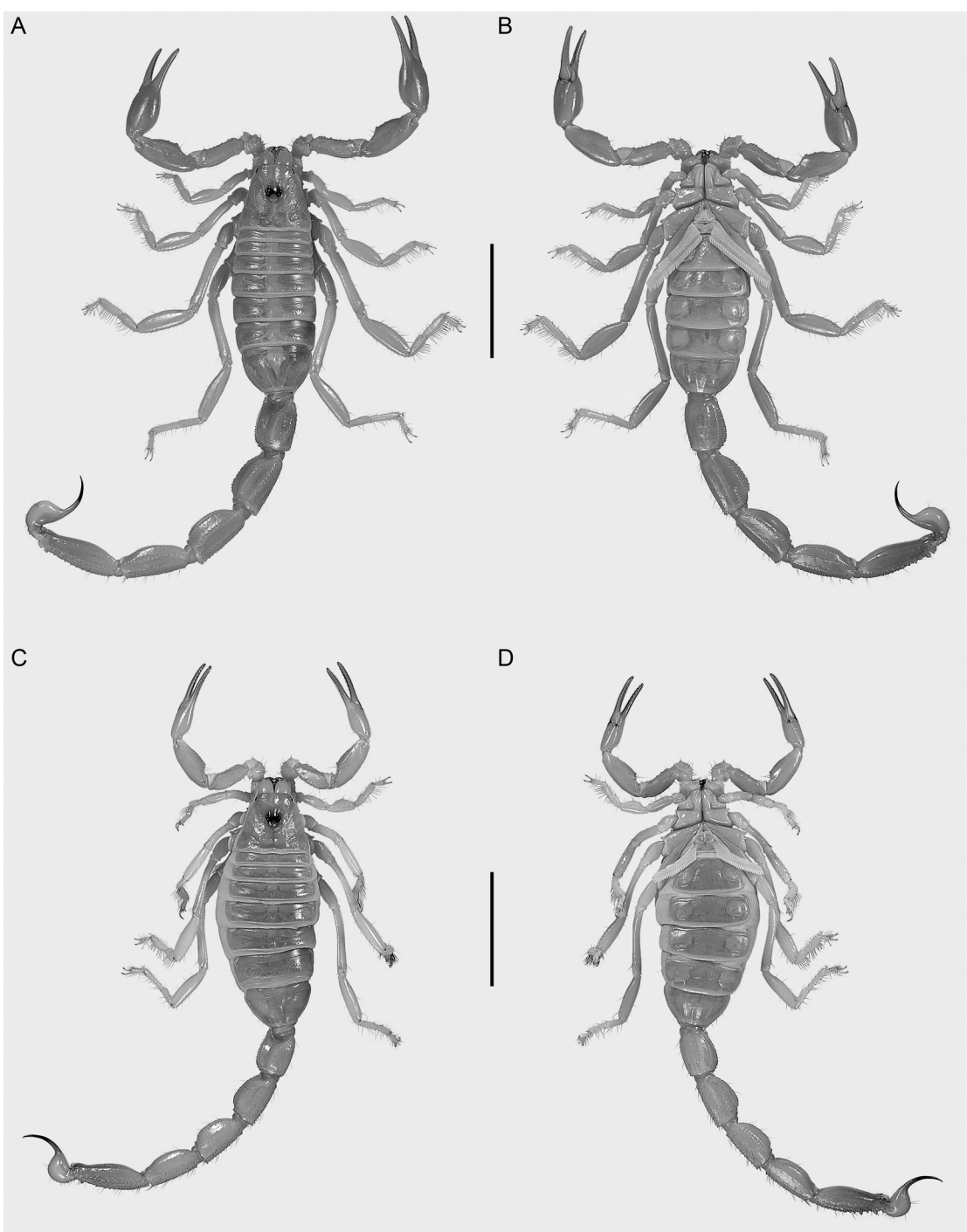


FIGURE 30. *Buthacus amitaii*, sp. nov., habitus, dorsal (A, C) and ventral (B, D) aspects. A, B. Holotype ♂ (HUJ INVSC 3480). C, D. Paratype ♀ (HUJ INVSC 3205). Scale bars = 1 cm.

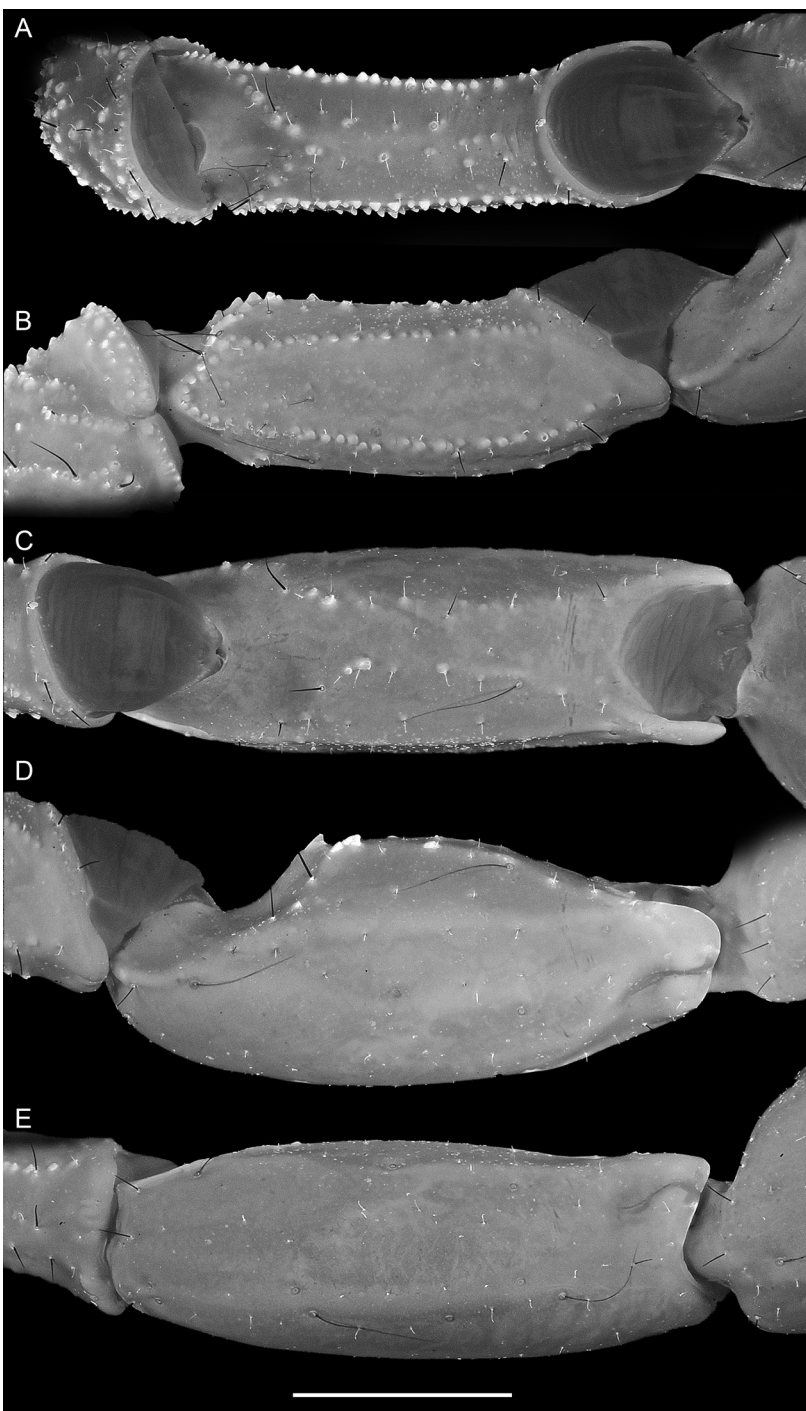


FIGURE 31. *Buthacus amitaii* sp. nov., holotype ♂ (HUJ INVSC 3480), dextral pedipalp femur (A, B) and patella (C, E), prolateral (A, C), dorsal (B, D), and retrolateral (E) aspects. Scale bar = 2 mm.



FIGURE 32. *Buthacus amitaii* sp. nov., dextral pedipalp chela, dorsal (A, C) and retrolateral (B, D) aspects. A, B. Holotype ♂ (HJU INVSC 3480). C, D. Paratype ♀ (HJU INVSC 3205). Scale bar = 2 mm.

legs I–III, with comblike rows of elongated macrosetae (“sand combs”) along the retrolateral margins, elongated macrosetae on the lateral and ventral surfaces of the telotarsi, and elongated telotarsal unguis, are consistent with the psammophilous ecomorphotype (Prendini, 2001). *Buthacus arenicola* was collected in sympatry with another buthid, *Androctonus amoreuxi*, near Naftah, Tunisia.

**REMARKS:** Simon (1885) described *B. arenicola* from Gabès (Séd) and Tozzer [Tozeur] in central Tunisia, noting that the species can also be found in Algeria (Biskra, Bou-Sadaa, and Debila) and Egypt (Port-Saïd and Ramleh). Pocock (1895) subsequently synonymized *B. arenicola* with *B. leptochelys*, a decision accepted by Kraepelin (1899) and Simon (1910). Birula (1908) only considered specimens cited by Simon (1885) from Egypt conspecific with *B. leptochelys*, however. Pallary (1938) revalidated *B. arenicola* and Vachon (1949a) distinguished *B. arenicola* and *B. leptochelys* based on the absence or presence of retrolateral accessory denticles on the movable finger of the pedipalp chela. Following Vachon’s (1952) suggestion that *B. arenicola* and *B. leptochelys* represent species complexes and not single species, Levy and Amitai (1980) recognized the *B. arenicola* and *B. leptochelys* species groups. Levy and Amitai (1980) noted that the distributions of *B. arenicola* and *B. leptochelys* overlap in parts of Egypt and that the population of *B. arenicola* in the Sinai Peninsula differs morphologically from the population in Algeria and Tunisia, suggesting it may represent a distinct subspecies, an opinion shared by Lourenço (2006).

During the present investigation, the types of *B. arenicola* and *B. leptochelys* were examined, in addition to material from the vicinity of the type locality of *B. arenicola*, in Tunisia, and from Egypt, including the Sinai Peninsula, and Israel. These comparisons reinforced the distinction between *B. arenicola* and *B. leptochelys*, and confirmed previous suggestions that the population of *B. arenicola* in Egypt and Israel is distinct from the typical population in Algeria and Tunisia (Levy

and Amitai, 1980; Lourenço, 2006). Based on evidence gathered during the present investigation, including multivariate analysis of morphometrics (fig. 15) and multilocus molecular phylogenetics (fig. 14), *B. arenicola* is restricted to central Tunisia and northeastern Algeria and the population occurring in Egypt and Israel represents a distinct species, described below.

*Buthacus spatzii*, described from the Sahara of southern Tunisia (Birula, 1911), was synonymized with *B. arenicola* by Lourenço (2006), based on an assessment of the original description and an unpublished opinion of M. Vachon (in litt.). The types of *B. spatzii* could not be located at the time of Lourenço’s (2006) study, nor during the present investigation, and appear to be lost. However, material collected from Jebil and elsewhere in southern Tunisia, matching the descriptions of *B. spatzii* in Birula (1911) and Lourenço (2006), was found to be morphologically and genetically distinct from material collected near Naftah, in the vicinity of the type locality of *B. arenicola* (L.P., unpublished data), questioning the decision to synonymize. *Buthacus spatzii* (Birula, 1911), stat. rev., is therefore revalidated. The limits of *B. arenicola* and *B. spatzii*, beyond the scope of the present investigation, will be redefined more precisely, elsewhere. *Buthacus birulai* Lourenço, 2006, described from El Oued, Algeria, will probably prove conspecific with either *B. arenicola* or *B. spatzii*.

*Buthacus arenicola fuscata* Pallary, 1929, described from In Ameri [23°17'N 05°30'E] in the Hoggar Mountains of southern Algeria, and synonymized with *B. arenicola* by El-Hennawy (1992), is unlikely to be conspecific with the latter, and is hereby revalidated and elevated to the rank of species. *Buthacus fuscata* Pallary, 1929, stat. nov. et stat. rev., is probably a senior synonym of one or more of the other species of *Buthacus* described from the vicinity of the Hoggar and Tassili n’Ajjer mountain ranges, e.g., *Buthacus ahaggar* Lourenço, 2017, *Buthacus armasi* Lourenço, 2013, or *Buthacus foleyi* Vachon, 1948, none of which were compared with it in the original descriptions. Which of

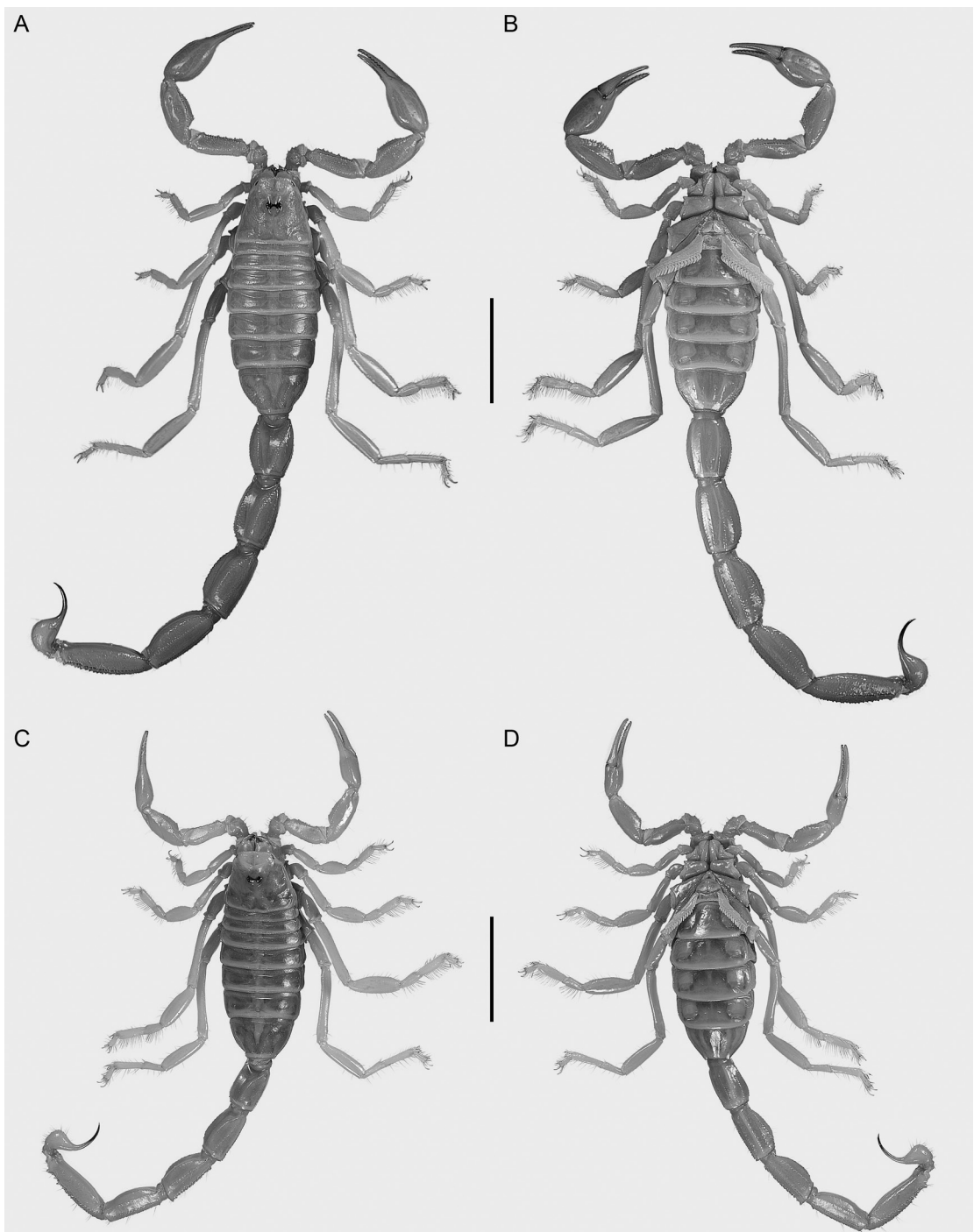


FIGURE 33. *Buthacus arava*, sp. nov., habitus, dorsal (A, C) and ventral (B, D) aspects. A, B. Paratype ♂ (HUJ INVSC 2559). C, D. Paratype ♀ (HUJ INVSC 2561). Scale bars = 1 cm.

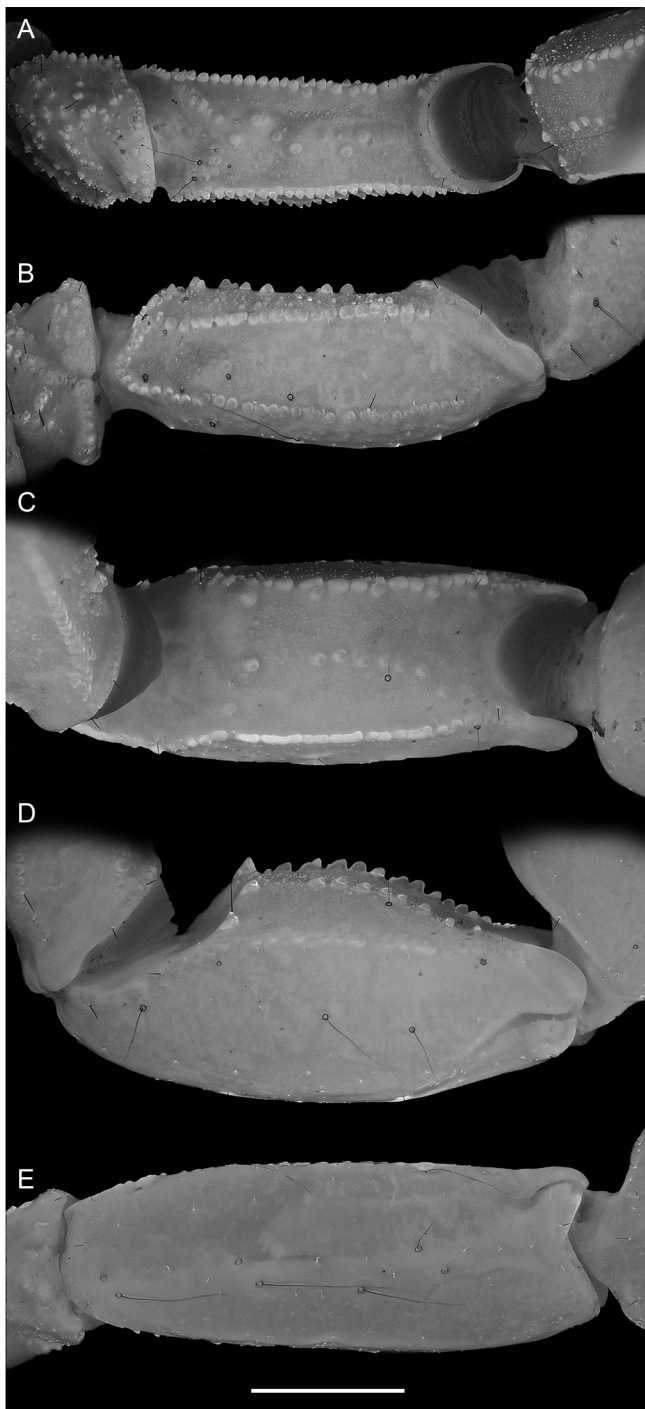


FIGURE 34. *Buthacus arava*, sp. nov., ♂♂ paratypes (HUJ INVSC 2559, 3295), dextral pedipalp femur (A, B) and patella (C, E), prolateral (A, C), dorsal (B, D), and retrolateral (E) aspects. Scale bar = 2 mm.



FIGURE 35. *Buthacus arava*, sp. nov., dextral pedipalp chela, dorsal (A, C) and retrolateral (B, D) aspects. A, B. Paratype ♂ (HUJ INVSC 3295). C, D. Paratype ♀ (HUJ INVSC 2561). Scale bar = 2 mm.

these species are junior synonyms requires further investigation.

MATERIAL EXAMINED: TUNISIA: Tozeur Governorate: Entrée Nefta, 24.v.1994, S. Nouira, dunes de sable, barkhanes, chasse nocturne, UV, 1 ♀, 1 juv. ♂, 3 juv. ♀ (UTM 153); Naftah, ca. 15 km W on P3 to Hazoua, 33°51.209'N 07°44.011'E, 6 m, 24.x.2017, L. Prendini, J. Babay, M. Khammasi and R. Ouni, 1 subad. ♂,

1 juv. ♀ (AMCC [LP 14859]); Naftah, ca. 7 km N on road to Ong Jmal, 33°56.366'N 07°50.321'E, 17 m, 23.x.2017, L. Prendini and J. Babay, 1 ♂, 11 ♀, 5 subad. ♂, 12 subad. ♀, 2 juv. ♂, 4 juv. ♀ (AMNH), 7 juv. ♂, 4 juv. ♀ (AMCC [LP 14858]); Naftah, ca. 8 km N on road to Ong Jmal, 33°56.588'N 07°50.228'E, 5 m, 23.x.2017, L. Prendini, J. Babay and R. Ouni, 1 juv. ♂ (AMCC [LP 14857]).

- Buthacus leptochelys* (Ehrenberg, 1829)
- Figures 1C, 6, 15, 17A, B, 21D, 22D, 24B, 26B, 28B, 29D, 39, 40, 41; tables 1, 4, 5
- Androctonus (Leiurus) leptochelys* Ehrenberg in Hemprich and Ehrenberg, 1829: 355.
- Androctonus (Leiurus) thebanus* Ehrenberg in Hemprich and Ehrenberg, 1828: pl. 1, fig. 4; Ehrenberg in Hemprich and Ehrenberg, 1829: 355, 356; Braunwalder and Fet, 1998: 30, 32 fig. 2.
- Androctonus (Leiurus) macrocentrus* Ehrenberg in Hemprich and Ehrenberg, 1828: pl. 1, fig. 6 (synonymized by Kraepelin, 1891: 60); Ehrenberg in Hemprich and Ehrenberg, 1829: 355; Vachon, 1952: 199, 201; Braunwalder and Fet, 1998: 30, 32 fig. 2; syn. nov.
- Androctonus (Liurus) leptochelys*: Hemprich and Ehrenberg, 1831; Moritz and Fischer, 1980: 317.
- Androctonus (Liurus) macrocentrus*: Hemprich and Ehrenberg, 1831; Moritz and Fischer, 1980: 317.
- Androctonus (Liurus) thebanus*: Hemprich and Ehrenberg, 1831; Moritz and Fischer, 1980: 324.
- Scorpio (Androctonus) leptochelis*: Gervais, 1844: 44.
- Scorpio (Androctonus) macrocentrus*: Gervais, 1844: 44.
- Scorpio (Androctonus) thebanus*: Gervais, 1844: 44.
- Androctonus leptochelys*: C.L. Koch, 1845: 7–9, pl. CCCXCIX, fig. 964.
- Androctonus leptochelis*: C.L. Koch, 1850: 90.
- Buthus leptochelis*: Simon, 1872: 250, 251; Lucas, 1873: 172; Simon, 1879: 99; 1880: 29; 1892: 83; Birula, 1905: 138.
- Buthus macrocentrus*: Simon, 1879: 99.
- Leiurus macrocentrus*: Karsch, 1881a: 8.
- Leiurus thebanus*: Karsch, 1881a: 8.
- Buthus leptochelys*: Karsch, 1881a: 8; 1881b: 89; Kraepelin, 1891: 60–62, pl. I, fig. 8; Pocock, 1895: 299, 300; Kraepelin, 1899: 17; 1901: 266; King, 1925: 81; Gough and Hirst, 1927: 3, fig. 3; Schenkel, 1932: 379.
- Butthus (Buthacus) leptochelys*: Birula, 1908: 140; 1910: 155–157, 170; 1917: 21, 23, 214, 224, 229; Giltay, 1929: 196; Werner, 1929: 30; Whittick, 1947: 122; 1955: [unpaginated] (part).
- Buthacus leptochelys*: Simon, 1910: 75, 76, fig. 11; Borelli, 1914: 158, 159; 1927: 352; Pallary, 1929: 133–135; Caporiacco, 1932: 396; Borelli, 1934: 172; Pallary, 1934: 90–92, 99 (misidentification); Werner, 1934: 269, fig. 332; Caporiacco, 1936: 94, 98; Werner, 1936a: 176; Bodenheimer, 1937: 235; Caporiacco, 1937: 347; Sergent, 1941: 355, fig. 2.9, pl. 35, fig. 9; Vachon, 1949a: 79–83, figs. 262–266; 1950a: 197; 1950b: 406 (part); 1951: 432–434, 436, 437, 441, 446, 447, 450, 453, 456, 458, 460, 462, 465, figs. 661, 677, 697 (misidentification); 1952: 180, 185, 191, 194, 198–203, figs. 262–266 (part); 1954: 188 (misidentification); 1958: 184; Pringle, 1960: 76, fig. 2 (misidentification); L. Khalaf, 1962: 1, 2 (misidentification); K.I. Khalaf, 1963: 59 (misidentification); Vachon, 1966: 210; Habibi, 1971: 43 (misidentification); Larrouy et al., 1972: 393; Levy et al., 1973: 126, 128, 134; Pérez, 1974: 19; Lamoral and Reynders, 1975: 499; Vachon, 1979: 31, 36–39, 41, 47, 49, 63, 65, figs. 7, 8, 26, 29, 61–63 (part); Levy and Amitai, 1980: 77, 78; Kettel, 1982: 6; Kinzelbach, 1984: 99; 1985: map III; Vachon and Kinzelbach, 1987: 101; Amr et al., 1988: 374; El-Hennawy, 1987: 17; Farzanpay, 1988: 36 (misidentification); El-Hennawy, 1991: 86, 87; 1992: 97, 101, 112, 113 (part); Amr and El-Oran, 1994: 187, 188 (misidentification); Kovařík, 1998: 105; Braunwalder and Fet, 1998: 32–34; Fet and Lowe, 2000: 82–84; ICZN, 2000: 7; Kovařík, 2001: 80; Lourenço, 2001: 255; Stathi and Mylonas, 2001: 288; Crucitti and Vignoli, 2002: 440, 441; Kovařík, 2002: 5; 2003: 135, 155, table 1 (misidentification); Lourenço,

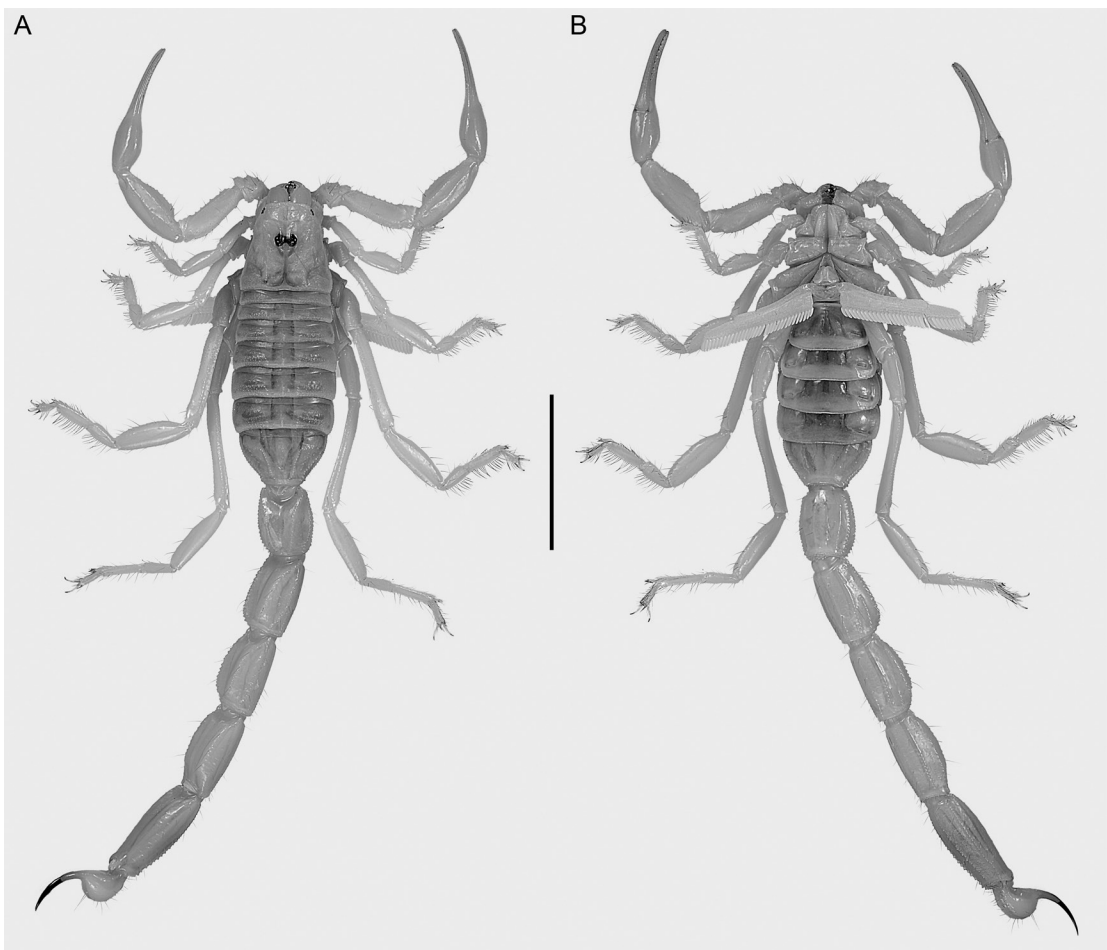


FIGURE 36. *Buthacus arenicola* (Simon, 1885), ♂ (AMNH), dorsal (A) and (B) ventral aspects. Scale bar = 1 cm.

2003: 877, 880, fig. 10 (misidentification); 2004a: 205; 2004b: 225, 226, 229; Kovařík, 2005: 1–3, 6, 8, 9, 10, figs. 2, 5, 7; Lourenço, 2006: 59–69, figs. 1, 4, table 1; Lourenço and Qi, 2006a: 161; Kaltsas et al., 2008: 214; Kamenz and Prendini, 2008: 8, 40, table 2 (misidentification); Navidpour et al., 2008: 8; Zourgui et al., 2008: 81, 84, 85, 88, 89, table 2, plate 5, fig. 4 (misidentification); Al-Asmari et al., 2009a: 612, 613, 617–619, 621, 622, 624, 626, figs. 9, 12G, tables 1, 2 (misidentification); 2009b: 96, 100, 102, 104, 106, fig. 6K, L, tables 5–7

(misidentification); Lourenço and Leguín, 2009: 103; Zarei et al., 2009: 46–49, 51, fig. 2, table 1 (misidentification); Lourenço et al., 2012: 315; Al-Asmari et al., 2013: 2, 5–7, 10–12, 15, figs. 6, 7, 9, 10, 12A, table 1 (misidentification); Kovařík et al., 2013: 3; Lourenço, 2013: 89, 91, 93; Amr, 2015: 183–185, 192, 197, figs. 1, 2, table 3 (misidentification); Amr et al., 2015: 32; Lourenço and Sadine, 2015: 55; Kovařík et al., 2016: 1, 2; Lourenço et al., 2016: 3; Badry et al., 2018: 77, 83; Kovařík, 2018: 1, 9, 10; Saleh et al., 2017: 7–9, fig. 3, table 2; Francke,

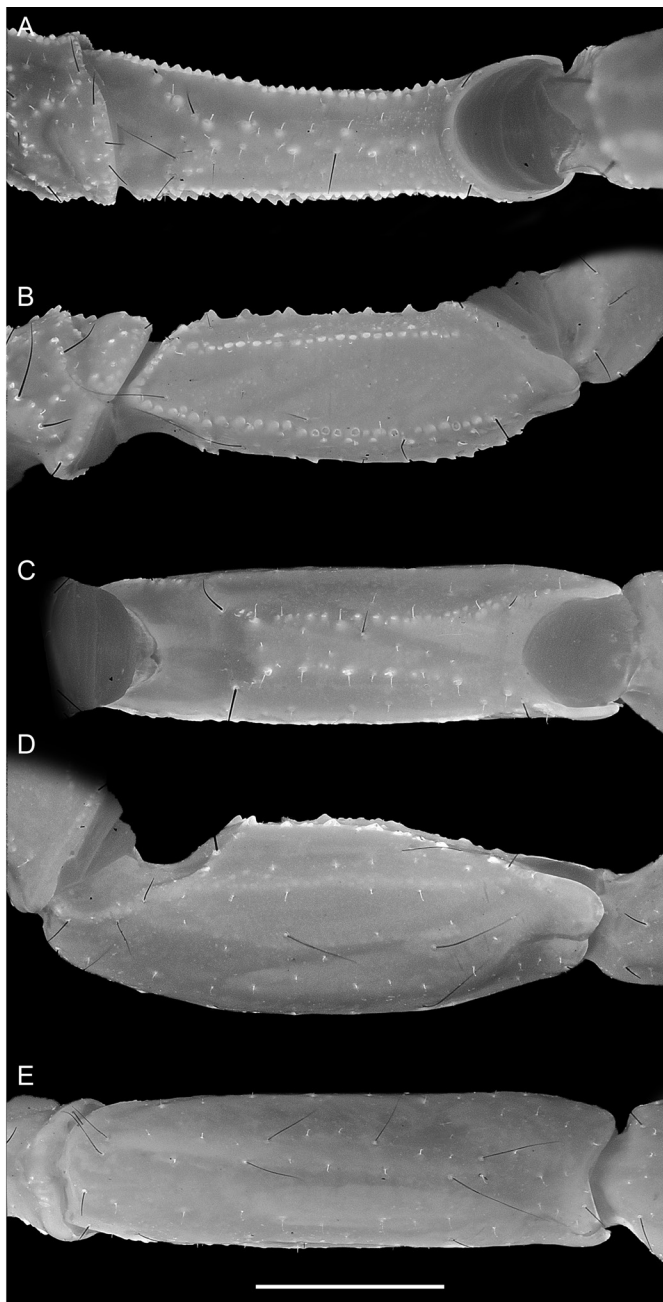


FIGURE 37. *Buthacus arenicola* (Simon, 1885), ♂ (AMNH), dextral pedipalp femur (A, B) and patella (C, E), prolateral (A, C), dorsal (B, D), and retrolateral (E) aspects. Scale bar = 2 mm.

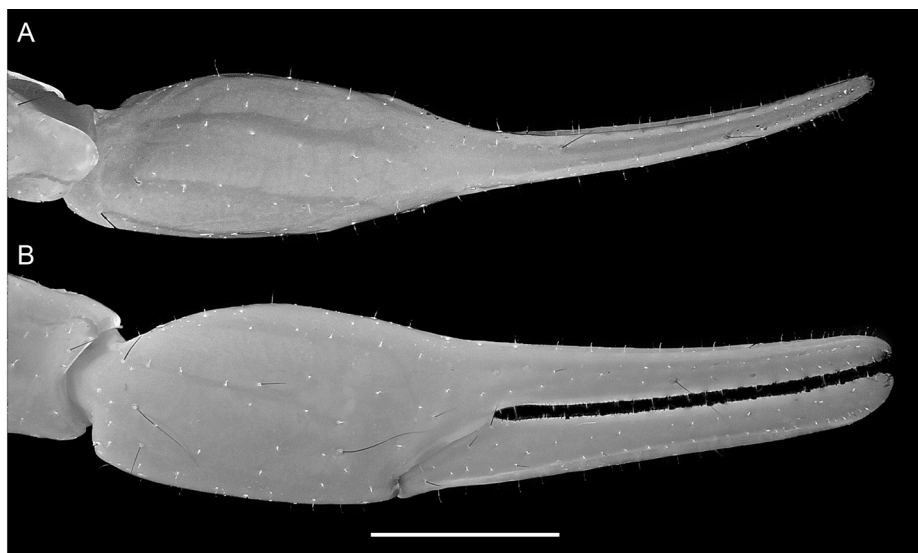


FIGURE 38. *Buthacus arenicola* (Simon, 1885), ♂ (AMNH), dextral pedipalp chela, dorsal (A) and retrolateral (B) aspects. Scale bar = 2 mm.

2019: 20; Lowe et al., 2019: 22; Alqahtani and Badry, 2020: 178–183, figs. 1–3, tables 1, 2; Hussen and Ahmed, 2020: 6722; Obuid-Allah et al., 2020: 227, 229–237, figs. 2G, H, 3D, tables 1, 3–6; Amr et al., 2021: 85, 88–90, tables 4, 5, 9, 10 (misidentification); Said et al., 2021: 17, 18, 20, 21, 25, 26, fig. 4, table 1. *Buthacus granosus* Borelli, 1929: 297–299, pl. VI, figs. 1–3; Probst, 1973: 329; Lamoral and Reynders, 1975: 499; syn. nov.

*Buthus granosus*: Vachon, 1949b: 162; 1952: 248. *Buthacus leptochelys*: Le Coroller, 1967: 63.

*Buthacus macrocentrus*: Kovařík, 2005: 1, 7, 9, 10, fig. 8 (part); Lourenço, 2006: 63, 64, figs. 15, 16; Lourenço and Qi, 2006a: 161; Kovařík et al., 2016: 1; Kovařík, 2018: 10.

*Buthacus thebanus*: Vachon, 1952: 180; Pérez, 1974: 19; Lourenço, 2006: 62.

*Buthacus leptochelys leptochelys*: Levy et al., 1973: 125; Levy and Amitai, 1980: 76, 77, 79–83, figs. 70–74, map 6; Kinzelbach, 1984: 99, 101 (misidentification); Kovařík, 1995: 19 (misidentification); Kovařík, 1997a: 49 (misidentification); Kabakibi et al., 1999: 82, 88 (misidentification); Fet and Lowe, 2000:

84; Hendrixson, 2006: 50; Lourenço, 2006: 62, 69, fig. 42.

*Buthacus leptochelys granosus*: Levy et al., 1973: 125; Vachon, 1979: 38; Levy and Amitai, 1980: 76; El-Hennawy, 1992: 97, 113; Kovařík, 1998: 105; Fet and Lowe, 2000: 84.

**TYPE MATERIAL:** *Androctonus (Leiurus) leptochelys*: Lectotype ♀, paralectotype ♀ (No. 1) (ZMB 152), Sinai [examined]. *Androctonus (Leiurus) macrocentrus*: Lectotype ♀, paralectotype ♀ (ZMB 153), EGYPT: Sinai [examined]. *Androctonus (Leiurus) thebanus*: Lectotype ♂, paralectotype ♂ (ZMB 154), EGYPT: Luxor Governorate: Thebae [Thebes, Luxor, 25°43'N 32°37'E]. *Buthacus granosus*: Holotype ♂ (MIZT), SUDAN: Red Sea State: Port Sudan [19°33'N 37°11'E], 24.iv.1926, H.B. Johnston.

**DIAGNOSIS:** *Buthacus leptochelys* differs from the closely related species *B. amitaii* and *B. nitzani*, occurring in Israel, as follows. *Buthacus leptochelys* is larger, measuring 65.8 mm (63.1–68 mm,  $n = 5$ ; table 4) in total length, than *B. amitaii*, measuring 51.7 mm (48–58.8 mm,  $n = 10$ ; table 3) and *B. nitzani*, measuring 50.6 mm (44.4–58.5 mm,  $n = 18$ ; tables 12, 13). The

pedipalp chela of the adult male is longer and narrower (fig. 41A, B), with chela manus width:chela length, 24.2% (table 4) and chela manus height:length, 58.9%, in *B. leptochelys* than in *B. amitaii* (fig. 32A, B), with chela manus width:chela length, 27.1% (25.1%–28.9%,  $n = 5$ ; table 3) and chela manus height:length, 69.7% (58.9%–75.5%,  $n = 5$ ), and *B. nitzani* (fig. 47A, B), with chela manus width:chela length, 26.3% (22.3%–29.5%,  $n = 8$ ; table 12) and chela manus height:length, 62.5% (57.7%–66.6%,  $n = 8$ ). The proximal dentate margins of the pedipalp chela fixed and movable fingers are shallowly emarginate to sublinear, such that a less pronounced gap is evident proximally when the fingers are closed in *B. leptochelys* (fig. 41B) than in *B. amitaii* and *B. nitzani* (figs. 32B, 47B). The pectinal tooth counts are higher in *B. leptochelys*, i.e., 35/34 (32–39/32–38,  $n = 6$ ; table 5) ( $\delta$ ) and 29/29 (27–31/28–31,  $n = 10$ ) ( $\varphi$ ), than in *B. amitaii*, i.e., 30/31 (28–32/28–33,  $n = 5$ ; table 2) ( $\delta$ ) and 23/23 (21–26/21–26,  $n = 9$ ) ( $\varphi$ ), and *B. nitzani*, i.e., 31/31 (26–34/27–35,  $n = 6$ ; table 2) ( $\delta$ ) and 23/23 (20–27/21–27,  $n = 17$ ) ( $\varphi$ ). The metasomal segments of the female are longer and narrower in *B. leptochelys* (fig. 28B), with the segment IV width:length, 42.1% (40.3%–44.6%,  $n = 4$ ; table 4), than in *B. nitzani* (fig. 28C), 38.4% (34%–43.7%,  $n = 10$ ; table 13). The median lateral carinae of metasomal segments I–III are distinct in *B. leptochelys*, but obsolete in *B. nitzani*. The telson dorsal surface is flat and the ventral surface convex and rounded in lateral profile in *B. leptochelys* (fig. 29D), whereas the dorsal surface is concave and the ventral surface convex and angular in lateral profile in *B. amitaii* and *B. nitzani* (fig. 29F, H).

*Buthacus leptochelys* differs from *B. levyi*, occurring in sympatry in Egypt, including the Sinai Peninsula, as follows. The pedipalp chela of the adult male is broader and deeper in *B. leptochelys* (fig. 41A, B), with chela manus width:length, 59.1% and chela manus height:length, 58.9% (table 4), than in *B. levyi* (fig. 44A, B), with chela manus width:chela

length, 19.4% (17.1%–21.3%,  $n = 8$ ; table 10) and chela manus height:length, 59.7% (55.8%–64%,  $n = 8$ ). The proximal dentate margins of the pedipalp chela fixed and movable fingers are shallowly emarginate, such that a small gap is evident proximally when the fingers are closed, in *B. leptochelys* (fig. 41B), but sublinear, such that no gap is evident proximally when the fingers are closed, in *B. levyi* (fig. 44B). The retro-lateral accessory denticles on the movable finger of the pedipalp chela are present, with higher counts, in *B. leptochelys* (sinistral/dextral: 7–9/7–9;  $n = 5$ ; table 5; fig. 21D), than in *B. levyi*, in which the denticles are often absent (0–5/0–3;  $n = 13$ ; table 5; fig. 21E, F).

**DESCRIPTION:** The following description is based on specimens collected in Egypt, including Sinai (see table 4 for measurements and table 5 for counts).

**Total length:** Large scorpions, 63.7 mm ( $\delta$ ) or 66.3 mm (63.1–68 mm,  $n = 4$ ) ( $\varphi$ ).

**Color:** Uniformly yellow. Legs paler with articulation points brown. Pectines whitish.

**Carapace:** Shape trapezoidal (fig. 17A, B), anterior width:posterior width, 49.7% (43.7%–56.5%,  $n = 5$ ), length:posterior width, 84.8% (77.4%–88.7%,  $n = 5$ ). Five, rarely four, pairs of lateral ocelli; each lateral ocular tubercle with three major ocelli (ALMa, MLMa, PLMa), similar in size, situated anterolaterally, and one or, usually, two minor ocelli (ADMi, PDMi; PDMi may be absent) situated posterodorsal to posterior major ocellus. Median ocelli larger than lateral ocelli, distance between them more than 2× ocellus width. Median ocular tubercle situated anteromedially, distance from anterior carapace margin:carapace length, 40.1% ( $\delta$ ) or 44% (41%–45.9%,  $n = 4$ ) ( $\varphi$ ). Superciliary and central median carinae distinct, costate-granular, strongly to weakly connected. Anteromedian sulcus distinct; posteromedian sulcus deep, narrow anteriorly, wide posteriorly; posterolateral sulcus deep, wide, curved. Carapace intercarinal surfaces coarsely granular.

**Chelicerae:** Cheliceral manus prodorsal margin granular; retrodorsal surfaces smooth or

finely granular; prolateral and ventral surfaces densely setose. Fixed finger dorsal and ventral surfaces densely setose; dorsal margin with subdistal, medial, and proximal denticles; ventral margin with proximal and medial denticles. Movable finger dorsal surface smooth and glabrous; ventral surface densely setose; dorsal margin with retrodistal, subdistal, medial, and pair of proximal denticles; ventral margin with prodistal, medial, and proximal denticles.

**Pedipalps:** Femur dorsal prolateral, dorsal retrolateral, and ventral prolateral carinae complete, costate-granular; prolateral ventral and prolateral ventrosubmedian carinae each comprising discontinuous row of spiniform granules; retrolateral dorsosubmedian carina comprising discontinuous row of spiniform granules and fewer than 10 macrosetae; intercarinal surfaces smooth (fig. 40A, B). Patella prolateral median and ventral prolateral carinae each comprising discontinuous row of spiniform granules; dorsal prolateral carinae obsolete; other carinae absent; intercarinal surfaces smooth (fig. 40C–E). Chela long and broad (♂), manus width:length, 59.1%, manus height:length, 58.9%, and manus length:movable finger length, 70.7% or long and slender (♀), manus width:length, 51.7% (50.4%–52.4%, n = 4), manus height:length, 60.5% (58.4%–63.2%, n = 4), and manus length:movable finger length, 51.9% (48.2%–54.1%, n = 4). Chela manus acarinate; intercarinal surfaces smooth and glabrous (fig. 41). Fixed and movable fingers respectively with 7–11 (n = 5) and 10–11 (n = 5) oblique median denticle subrows; movable finger with 7–9 (n = 5) retrolateral accessory denticles (fig. 21D); proximal dentate margins of fingers sublinear (fig. 41B), such that small gap weakly present when fingers closed.

**Legs:** Legs I–IV, femoral ventral carinae granular; patellar ventral carinae obsolete; intercarinal surfaces smooth. Legs I–IV, tibial spurs absent on I and II, present on III and IV; pro- and retroventral basitarsal (pedal) spurs present, more developed on III and IV. Legs I–IV, macrosetal counts on retrolateral margins of tibiae, 10:11:11:3; basitarsi, 9:13:21:9; telotarsi, 6:8:9:7

(n = 1). Telotarsal unguis long, approximately equal to telotarsus length, unequal on legs I and II, subequal to equal on III and IV (fig. 22D).

**Genital operculum:** Genital opercula suboval, completely divided longitudinally, with overlapping, rounded margins (♂) or partially fused longitudinally (♀). Genital papillae present (♂) or absent (♀).

**Pectines:** Three marginal lamellae; 11–13 (n = 3) (♂) or 11–14 (n = 2) (♀) median lamellae. Fulcra present. Pectinal teeth along most of length, dentate margin length:pecten length, 90.8% (♂) or 91.8% (90.7%–92.9%, n = 4) (♀). Pectinal teeth curved, similar in size; tooth count (sinistral/dextral), 35/34 (32–39/32–38, n = 6) (♂) or 29/29 (27–31/28–31, n = 10) (♀).

**Mesosoma:** Tergites I–VII progressively increasing in length posteriorly, tergite VI length:tergite VII length, 58.4% (♂) or 57.2% (55%–59.5%, n = 4) (♀); increasing in width posteriorly from I–IV, decreasing in width posteriorly from V–VII. Pretergites smooth; posttergites I–VI, intercarinal surfaces uniformly granular, becoming more coarsely and densely granular posteriorly, VII, finely to coarsely and sparsely granular. Tergites I–VI, dorsomedian carinae granular, vestigial, restricted to posterior fifth of I–III and posterior two-thirds of IV–VI; dorsosubmedian carinae granular, vestigial, restricted to posterior fifth of I–III, and posterior two-thirds of IV–VI. Tergite VII, dorsomedian carina granular, vestigial, restricted to anterior half; dorsosubmedian and dorsolateral carinae distinct, granular. Sternites III–VII acarinate; III sparsely granular, IV–VII smooth and glabrous; IV–VI, respiratory spiracles (stigmata) width approximately 3× length.

**Metasoma:** Metasomal segments I–V becoming longer and narrower posteriorly (figs. 24B, 26B, 28B), segment I shortest, length I:II, 87.5% (♂) or 87.5% (86.6%–89%, n = 4) (♀); segments II–IV similar, length II:III, 95.1% (♂) or 97.7% (95.7%–99.7%, n = 4) (♀), length III:IV, 94.6% (♂) or 98.7% (95.4%–101.7%, n = 4) (♀); segment V longest, length IV:V, 87% (♂) or 84.5% (78.8%–

79.7%,  $n = 4$ ) ( $\varphi$ ); width:length segment I, 66.9% ( $\delta$ ) or 68.4% (66.2%–70%,  $n = 4$ ) ( $\varphi$ ), II, 52.8% ( $\delta$ ) or 55.7% (53.3%–57.6%,  $n = 4$ ) ( $\varphi$ ), III, 49.4% ( $\delta$ ) or 51.3% (48.4%–52.6%,  $n = 4$ ) ( $\varphi$ ), IV, 37.9% ( $\delta$ ) or 42.1% (40.3%–44.6%,  $n = 4$ ) ( $\varphi$ ), V, 33.4% ( $\delta$ ) or 37.5% (35.2%–39.3%,  $n = 4$ ) ( $\varphi$ ); dorsosubmedian and dorsolateral carinae distinct, granular on segments I–III, dorsosubmedian carinae obsolete, dorsolateral carinae granular on IV; dorsosubmedian and dorsolateral carinae absent on V; dorsosubmedian and dorsolateral carinae sparsely setose, macrosetal counts on segments I–V (sinistral/dextral), dorsosubmedian carinae, 1/0 (0/0–1/0,  $n = 2$ ):2/3 (2/3–2/3):3/3 (3/3–3/3):2/2 (1/1–2/2):0/0 (0/0–0/0), dorsolateral carinae, 2/3 (2/2–2/3,  $n = 2$ ):2/3 (1/2–3/3):4/3 (3/2–4/3):5/4 (4/3–6/4):4/5 (4/5–4/5). Median lateral carinae distinct, granular, extending entire length of segment I, restricted to posterior half of II and posterior third of III, absent on IV and V. Ventrolateral carinae distinct, costate-granular on segments I–IV; serrate, comprising spiniform granules of variable size, becoming more prominent posteriorly on V. Ventrosubmedian carinae distinct, costate-granular on segment I; granular, with granules becoming progressively larger and subspiniform posteriorly on II and III; costate-granular on IV; granular, restricted to anterior three-quarters of V. Ventromedian carina granular, distinct along entire length of segment V. Dorsal and lateral intercarinal surfaces smooth to finely and sparsely granular on segment I, smooth on II–V; ventral intercarinal surfaces smooth on I and II, finely and sparsely granular on III, finely granular across entire surface on IV and V.

**Telson:** Telson vesicle width:metasomal segment V width, 81.3% ( $\delta$ ) or 77.2% (76.2%–77.8%,  $n = 4$ ) ( $\varphi$ ). Vesicle globose, dorsal surface flat, ventral surface convex and rounded; vesicle height:length, 58.4% ( $\delta$ ) or 63.3% (57.2%–67.8%,  $n = 4$ ) ( $\varphi$ ); dorsal and ventral surfaces smooth and glabrous; lateral and ventral surfaces sparsely setose, with 20 ( $\delta$ ) or 25 ( $\varphi$ ) macrosetae. Aculeus long, gently curved; aculeus length:telson length, 49.4% ( $\delta$ ) or 56.7% (56%–58.4%,  $n = 4$ ) ( $\varphi$ ).

**Sexual dimorphism:** Adult males and females differ as follows. The pedipalp chela manus of the male is slightly broader than that of the female (fig. 41), as indicated by the higher chela manus width:length ratio in the male (59.1%) compared with the female (58.9%). The pedipalp chela manus of the male is markedly broader and deeper with proportionally shorter fingers than that of the female (fig. 41), as indicated by the higher ratios of chela manus width:length and chela manus length:movable finger length, respectively 59.1% and 70.7% in the male compared with 58.9% and 51.9% in the female. The genital opercula are completely divided longitudinally, with overlapping, rounded margins in the male but partially fused longitudinally in the female, and genital papillae are present in the male but absent in the female. The pectinal tooth count is higher in the male (32–33) than in the female (27–30). The mesosoma of the male is relatively narrower than that of the female, as indicated by the higher sternite VII length:width ratio in the male (66.5%) compared with the female (57.5%). The spiniform granules of the ventrosubmedian and ventrolateral carinae of metasomal segments II and III, and the ventrolateral carinae of segment V are less prominent in the male than in the female.

**DISTRIBUTION:** *Buthacus leptochelys* appears to be distributed from the western Sinai Peninsula across Egypt, and southward along the coast of the Red Sea to Sudan (fig. 6). It probably also occurs in Libya. The known records range from -28 m to 1155 m in elevation.

*Buthacus leptochelys* is allopatric with the closely related *B. amitaii*, endemic to the inland sandy soils and loess of the Yamin Plain and Mamshit area in the northern Negev, Israel (fig. 7), and *B. nitzani*, distributed from the Sorek (Rubin) River, throughout the sand dunes of the southern coastal plain of Israel, to the Haluza dunes of the interior and probably the adjacent Sinai Peninsula of Egypt (fig. 7).

**ECOLOGY:** Specimens of *B. leptochelys* were collected at night with UV light detection in arid to hyperarid sandy habitats, including gravel

plains and soft sandy plains, inland and coastal sand dunes, with variable vegetation cover (Badry et al., 2018; L.P., personal obs.). The habitat and habitus, notably the pale coloration, smooth tegument, loss or obsolescence of pedipalpal and metasomal carinae, elongation of the legs, especially legs III and IV, dorsoventral compression of the basitarsi of legs I–III, comblike rows of elongated macrosetae (“sand combs”) along the retrolateral margins of the tibiae and the pro- and retrolateral margins of the basitarsi of legs I–III, elongated macrosetae on the lateral and ventral surfaces of the telotarsi, and elongated, unequal-length telotarsal unguis, are consistent with the ultrapsammophilous ecomorphotype (Prendini, 2001).

*Buthacus leptochelys* has been collected in sympatry with the following buthids: *Androctonus australis* (Linnaeus, 1758), *Buthus intumescens* (Ehrenberg, 1829), *Compsobuthus egyptiensis* Lourenço et al., 2009, *Leiurus quinquestriatus*, *Orthochirus aristidis* (Simon, 1882), *Orthochirus innesi* Simon, 1910, and *Parabuthus abyssinicus* Pocock, 1910 (Badry et al., 2018; L.P., personal obs.).

**REMARKS:** Ehrenberg (1829) described *B. leptochelys* and *B. macrocentrus* from the same region, the Sinai Peninsula, one year after describing *B. thebanus* from Thebes, near Luxor, in southern Egypt. Kraepelin (1891) regarded the three species from Egypt and the Sinai Peninsula as a single species, *B. leptochelys*. Pocock (1895) subsequently synonymized *B. arenicola* with *B. leptochelys*, an opinion accepted by Kraepelin (1899), who also synonymized *B. tadmorensis* with *B. leptochelys*. Birula (1908) revalidated *B. arenicola* and *B. tadmorensis*, but the limits and validity of *B. arenicola*, *B. macrocentrus*, and *B. tadmorensis* continued to be debated thereafter (Levy et al., 1973; Levy and Amitai, 1980; Kinzelbach, 1985; Fet and Lowe, 2000; Kovářík, 2005, 2018; Lourenço, 2006; Lourenço and Qi, 2006a; Lourenço and Leguin, 2009; Kovářík et al., 2016).

Levy et al. (1973) downgraded *Buthacus granosus* Borelli, 1929, described from Port Sudan on the coast of the Red Sea, to a subspecies of *B. leptochelys*, without justification. Com-

parison of Borelli’s (1929) description of *B. granosus* with the redescription of *B. leptochelys* presented here revealed few differences that might merit their recognition as different taxa, justifying the following synonymy: *Buthacus granosus* Borelli, 1929 = *Buthacus leptochelys* (Ehrenberg, 1829), syn. nov.

Kovářík (2018) recently synonymized *Buthacus armasi* Lourenço, 2013, from the Tassili n’Ajjer of southern Algeria, with *B. leptochelys*. Setting aside the vast geographical distance between the type locality of *B. armasi* and the known locality records of *B. leptochelys*, most of which occur in Egypt, comparison of Lourenço’s (2013) description and illustrations with specimens of *B. leptochelys* from Egypt including the Sinai Peninsula examined during the present investigation casts doubt on Kovářík’s (2018) decision. For example, differences are evident in the dentition of the pedipalp chela fingers of *B. armasi* and *B. leptochelys*, specifically the curvature of the median denticle subrows and the deviations of the retrolateral accessory denticles from the subrows, cf. Lourenço’s (2013: 94, 96) description and figure 9 with figure 21D of the present contribution. The two species also differ in pectinal tooth counts, with 27–28 (♂) or 21–23 (♀) in *B. armasi* and 35/34 (32–39/32–38,  $n = 6$ ) (♂) or 29/29 (27–31/28–31,  $n = 10$ ) (♀) in *B. leptochelys*. The ventral carinae of the metasoma of *B. armasi* were described as “vestigial on segment I, weak on II, moderate on III–IV” (Lourenço, 2013: 96), whereas in *B. leptochelys* these carinae are distinct on segments I–IV. Unpublished DNA sequence data from samples originating in the vicinity of the type locality of *B. armasi* are also inconsistent with the hypothesis that the two taxa are conspecific. Insofar as the evidence refutes the hypothesis that it is conspecific with *B. leptochelys*, *Buthacus armasi* Lourenço, 2013, stat. rev., is hereby revalidated, although it may prove to be a junior synonym of *B. fuscata* and/or *B. foleyi*, two other species described from the vicinity of the Hoggar and Tassili n’Ajjer mountain ranges, neither of which were compared with it in the original description.

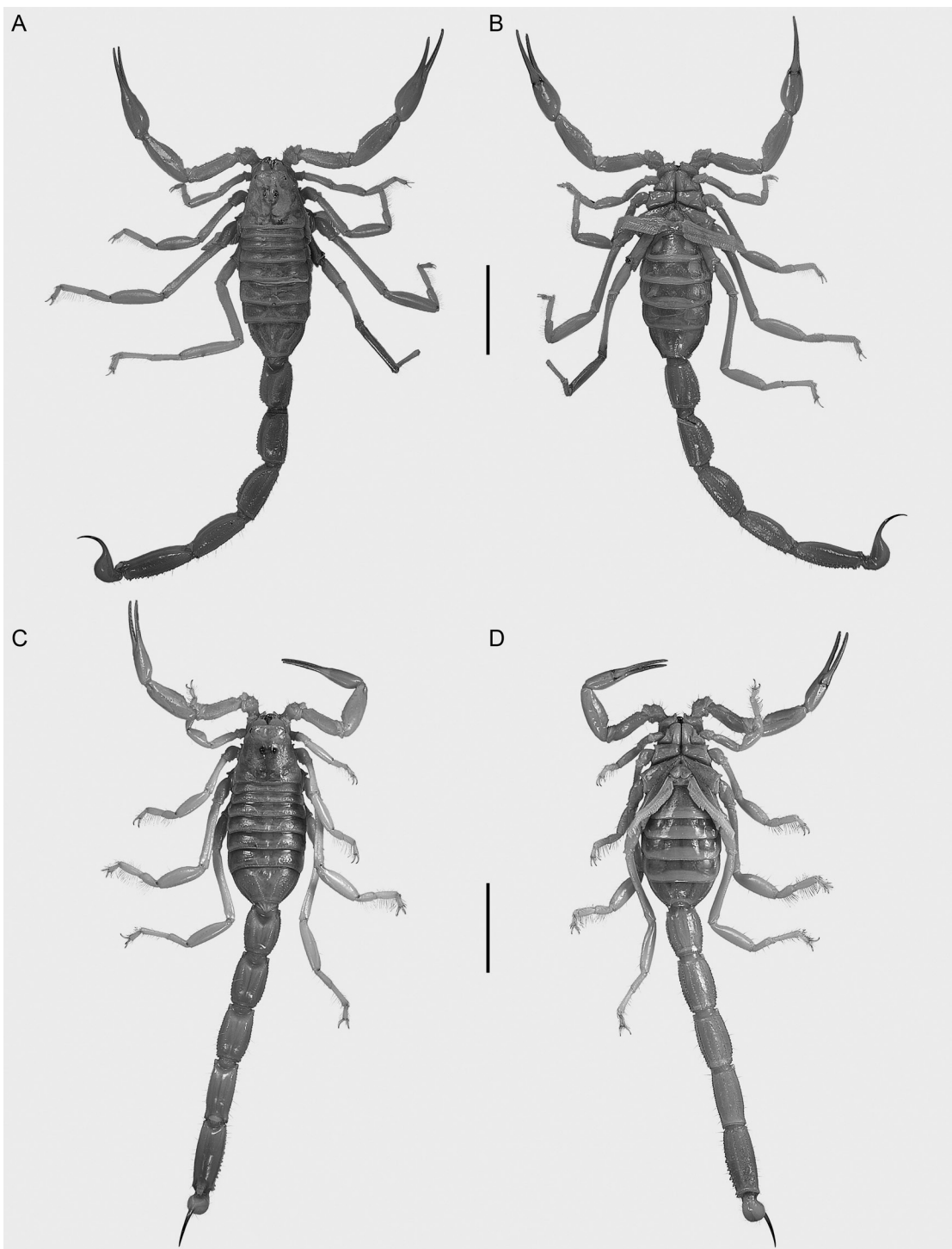


FIGURE 39. *Buthacus leptochelys* (Ehrenberg, 1829), habitus, dorsal (A, C), and ventral (B, D) aspects. A, B. ♂ (HUJ INVSC 859). C, D. ♀ (HUJ INVSC 1807). Scale bars = 1 cm.

During the present investigation, the types of *B. arenicola*, *B. leptochelys*, and *B. macrocentrus* were examined in addition to material from the vicinity of the type locality of *B. arenicola* in Tunisia and from Egypt and Israel. These comparisons, including multivariate analysis of morphometrics (fig. 15) and multilocus molecular phylogenetics (fig. 14), confirmed the validity of *B. arenicola* and *B. leptochelys*. Kraepelin's (1891) synonymy of *A. (L.) thebanus* with *B. leptochelys* was also confirmed, the lectotype male of *A. (L.) thebanus* closely matching a male *B. leptochelys* from Wadi Sidri (HJU INVSC 859).

As concluded by Kovařík (2005), the type series of *B. leptochelys* comprises more than one species: paralectotype 2 is heterospecific with the lectotype and paralectotype 1, instead representing a species of the *B. arenicola* group. However, Kovařík (2005) misidentified paralectotype 2 as the Tunisian species, *B. spatzii*; it is conspecific with *B. levyi*, the distribution of which overlaps that of *B. leptochelys* in the Sinai Peninsula (fig. 9).

Also contrary to Kovařík (2005) and others (e.g., Lourenço, 2006), the types *B. macrocentrus* were found to be conspecific with one another and with the types of *B. leptochelys*, as originally deduced by Kraepelin (1891) and confirmed by Vachon (1952) and Levy and Amitai (1980). No evidence was found to support Kovařík's (2005) contention that the types of *B. macrocentrus* are heterospecific, with only the paralectotype conspecific with *B. leptochelys*. The lectotype of *B. macrocentrus* closely resembles the paralectotype of *B. macrocentrus*, the lectotype and paralectotype 1 of *B. leptochelys*, and other material of *B. leptochelys* from southwestern Sinai (e.g., HJU INVSC 1807, 2233, 2278) in the armature of the leg tarsi and the shape and ventral carination of the metasomal segments, notably II and III, and differs markedly in these characters from *B. tadmorensis* and *B. yotvatensis*, two species erroneously synonymized with *B. macrocentrus* by Kovařík (2005) and revalidated below. Similarly, Kovařík's (2005: 9) assertion that the "Type locality 'Sinai' (Ehrenberg in Hemprich and Ehrenberg, 1829: 355 and label) must be regarded as

"erroneous" is unfounded. The type locality of *B. macrocentrus* is consistent with the type locality of *B. leptochelys* as well as the known distribution of that species (fig. 6). In view of the evidence, *B. macrocentrus* is returned to synonymy: *Androctonus (Leiurus) macrocentrus* Ehrenberg, 1829 = *Buthacus leptochelys* (Ehrenberg, 1829), syn. nov.

**MATERIAL EXAMINED: EGYPT:** 1994, ex. M. Scharmach, 1 ♀ (AMNH [LP 324]). Sinai, 1890, Ehrenberg, 1 ♀ (ZMH ex Mus. Berol.). Cairo Governorate: Cairo, vi.1913, 1 ♂ (ZMH ex Mus. Basel). Faiyum Governorate: Faiyum Oasis, N side, 29°32'11"N 30°48'08.8"E, -28 m, 24.ii.2019, L. Prendini, E. Attia, T. Saïd, F. Sayed, and N. Abdelrazik, 1 ♀, 4 subad. ♂, 6 subad. ♀, 23 juv. ♂, 23 juv. ♀ (AMNH), 5 juv. ♂, 2 juv. ♀ (AMCC [LP 16600]). North Sinai Governorate: Gebel Iqme [28°38'N 33°18'E], 1 ♀ (SMNH TAU AR 50805); Mitla Pass [Ma'avar Ha Mithleh], 30°00'N 32°55'E, 414 m, xi.1970, J. Gershoni, 1 ♀ (HJU INVSC 1807), 15.xii.1970, A. Bara'am, 1 ♀ (HJU INVSC 2233). Red Sea Governorate: Zafarana, ca. 22 km SW on al Kurimat-al Zafrana Road, 23.ii.2019, L. Prendini, E. Attia, M. Omran, and T. Saïd, 29°04'36.3"N 32°27'07.9"E, 109 m, 4 juv. ♀ (AMNH), 1 juv. ♂, 2 juv. ♀ (AMCC [LP 16598]), 29°04'22"N 32°26'48.9"E, 129 m, 2 subad. ♂, 1 juv. ♂, 2 juv. ♀ (AMNH), 1 juv. ♂, 3 juv. ♀ (AMCC [LP 16599]). South Sinai Governorate: Ramlet Himayir (Sinai), sands SE of Abu Zanima, 29°04'N 33°27'E, 509 m, 25.xi.1969, A. Haim, 1 juv. ♀ (HJU INVSC 1545); on way to Sarabit-el-Hadem, 29°03'N 33°25'E, 485 m, 4.iii.1970, A. Haim, 1 juv. ♂ (HJU INVSC 1750); Shech-el Ka'rai, 29°05'N 33°20'E, 523 m, 8.iv.1968, Oranim Seminar, 1 subad. ♀ (HJU INVSC 857); Wadi Sidri, Abu Rudies area, 28°51'N 33°15'E, 113 m, 3.vii.1968, N. Tademor and A. Haim, 1 ♂ (HJU INVSC 859); Wadi Zalka, 28°52'N 34°00'E, 1155 m, 1.iii.1970, A. Haim, 1 juv. ♂ (HJU INVSC 1749), 1 juv. ♀ (HJU INVSC 1748). Suez Governorate: E of Suez City, 29°55'N 32°37'E, 16 m, v.1971, D. Simon, 1 ♂ (HJU INVSC 2274), 1 juv. ♀ (HJU INVSC 2275).

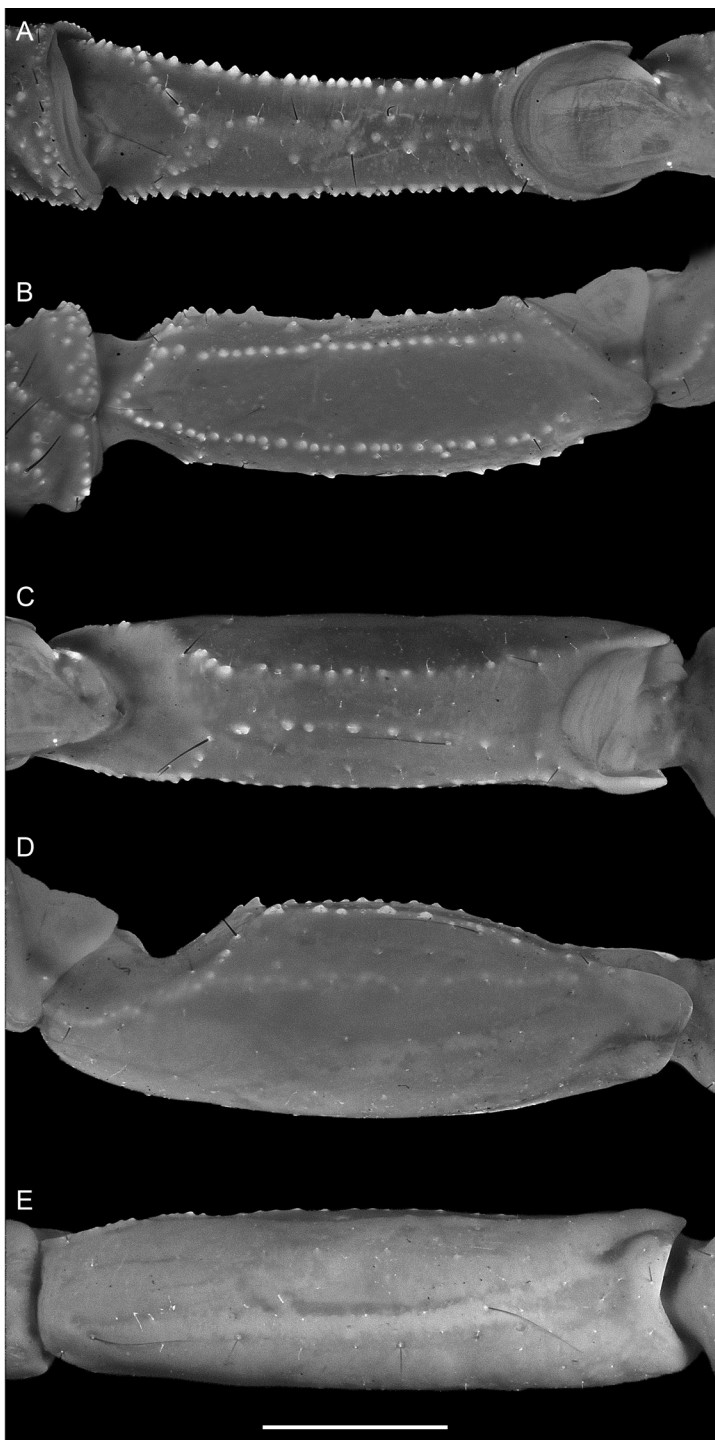


FIGURE 40. *Buthacus leptochelys* (Ehrenberg, 1829), ♂ (HUJ INVSC 859), dextral pedipalp femur (A, B) and patella (C, E), prolateral (A, C), dorsal (B, D), and retrolateral (E) aspects. Scale bar = 2 mm.



FIGURE 41. *Buthacus leptochelys* (Ehrenberg, 1829), dextral pedipalp chela, dorsal (A, C) and retrolateral (B, D) aspects. A, B. ♂ (HUJ INVSC 859). C, D. ♀ (HUJ INVSC 1807). Scale bar = 2 mm.

*Buthacus levyi*, sp. nov.

Figures 1F, 2E, F, 9, 15, 18A, B, 20E, F, 21E, F, 22B, 24A, 26A, 28A, 29B, 42, 43, 44;  
tables 1, 5, 10, 11

*Buthus arenicola*: Simon, 1885: 50–52.

*Buthus leptochelys*: Pocock, 1895: 299, 300.

*Buthacus leptochelys*: Birula, 1908: 140  
(misidentification).

*Buthacus arenicola*: Vachon, 1949a: 71; Levy et al., 1973: 125, 128; Levy and Amitai, 1980: 76, 77, 82, 86–89, figs. 79–81, map 6; El-Hennawy, 1987: 17 (misidentification); El-Hennawy, 1992: 97, 112 (part); Fet and Lowe, 2000: 81, 82; Kovařík and Whitman, 2004: 106 (part); Lourenço, 2006: 59, 65, 62–69; Kovařík et al., 2013: 3, fig. 5; Kaltsas et al., 2008: 213; Kamenz and Prendini, 2008: 8, 40, table 2; Badry et al., 2018: 77, 83; Saleh et al., 2017: 7, 8, fig. 3, table 2; Alqahtani and Badry, 2020: 178–183, figs. 1–3, tables 1, 2.

*Buthacus spatzi*: misidentification: *Androctonus (Leiurus) leptochelys* paralectotype ♀ (No. 2): Kovařík, 2005: 3, 6, 7, fig. 6; Kovařík et al., 2016: 1.

**TYPE MATERIAL:** Holotype ♂ (HUJ INVSC 2082), **EGYPT:** *North Sinai Governorate*: Quseima, 7.5 km SW, 30°37'N 34°18'E, 236 m, 12.ix.1970, I. Israeli. Paratypes: **EGYPT:** *North Sinai Governorate*: Quseima, 7.5 km SW, 30°37'N 34°18'E, 236 m, 12.ix.1970, I. Israeli, 4 ♂ (HJUJ INVSC 2077–2079, 2083), 3 ♀ (HJUJ INVSC 2076, 2080, 2081), 2 juv. ♂ (HJUJ INVSC 2085, 2086), 2 juv. ♀ (HJUJ INVSC 2084). *Giza Governorate*: Abou Rawash, Imbaba, 30°02'32.3"N 31°05'10.2"E, 34 m, 16.xii.2018, T. Adly, 1 ♀ (AMCC [LP 16587]). *Ismailia Governorate*: Qantara, 10 km E, 30°55'N 32°26'E, 4 m, 5.iv.1975, A. Dahlman, 1 ♀ (HJUJ INVSC 2371); Timsach Lake [30°35'N 32°18'E], 10 m, 1.iii.1971, Yehezkel, 1 subad. ♂ (HJUJ INVSC 2265), 1 juv. ♂ (HJUJ INVSC 2264), 1 juv. ♀ (HJUJ INVSC 2266). *Matrouh Governorate*: Qesm Ad Dabaah, N of El

Dabaa, 31°02'34.7"N 28°26'37.2"E, 23 m, 7.ii.2019, M. Mehana, 3 subad. ♂ (AMCC [LP 16586]); Qesm Ad Dabaah, SW of El Dabaa, 30°58'40.1"N 28°28'33.6"E, 43 m, 25.ii.2019, L. Prendini, E. Attia, T. Saïd and F. Sayed, 2 juv. ♂ (AMCC [LP 16601]), 1 juv. ♂, 2 juv. ♀ (AMNH). *North Sinai Governorate*: Bir Gifgafa, 30°26'N 33°07'E, 313 m, 1968, A. Shulov, 1 juv. ♀ (HJUJ INVSC 856), 8.iv.1968, A. Shulov, 2 ♀ (HJUJ INVSC 1245, 1251), 15.ii.1973, D. Simon, 1 ♂ (HJUJ INVSC 2529); Gebel Libri, near road, 30°40'N 33°44'E, 129 m, 15.xi.1967, P. Amitai, 1 juv. ♂ (HJUJ INVSC 661); sands between Gebel Ya'laq and Gebel Me'rara [30°33'N 33°26'E], 268 m, 2.ii.1970, J. Gershoni, 1 ♂ (HJUJ INVSC 1772), 1 ♀ (HJUJ INVSC 1771), 1 juv. ♂ (HJUJ INVSC 1773); Qesm Remanah, Om Okba, 30°59'39.1"N 32°46'17.9"E, 17 m, 5.xii.2018, T. Ragab, 1 ♀ (AMCC [LP 16585]); Wadi Masagid, 30°45'N 33°27'E, 274 m, 2.iv.1968, O. Seminar, 1 ♀ (HJUJ INVSC 858), 2 juv. ♀ (HJUJ INVSC 854, 855). *South Sinai Governorate*: Wadi Tal, 29°08'N 33°04'E, 131 m, 14.i.1970, M. Broza, 1 juv. ♀ (HJUJ INVSC 1684); *Suez Governorate*: E of Suez City, 29°55'N 32°37'E, 16 m, v.1971, D. Simon, 1 ♂ (HJUJ INVSC 2273), 1 ♀ (HJUJ INVSC 2276), 1 juv. ♂ (HJUJ INVSC 2277). **ISRAEL:** *Mehoz HaDarom (Southern District)*: Holot Haluza sand dunes, E of Be'er Milka, 30°55'42.57"N 34°24'41.95"E, 213 m, 19.ix.2016, B. Shacham, 1 ♀ (HJUJ INVSC 3260), 28.ix.2016, S. Talal and S. Cain, 1 ♂ (HJUJ INVSC 3253), 2 ♀ (AMCC [LP 15063, 15064] ex HJUJ INVSC 3251, 3252), 6 juv. ♂ (AMCC [LP 15065–15067] ex HJUJ INVSC 3257–3259, HJUJ INVSC 3254–3256), 23.iv.2017, S. Talal and Oranim students, 1 ♀ (AMNH ex HJUJ INVSC 3261), 20.iv.2017, Y. Zvik, 1 ♀ (AMNH ex HJUJ INVSC 3112), 2 subad. ♂ (AMNH ex HJUJ INVSC 3110, 3111), 25.v.2017, Y. Zvik and S. Cain, 2 subad. ♂ (AMNH ex HJUJ INVSC 3268, 3270), 2 juv. ♂ (AMNH ex HJUJ INVSC 3265, 3266), 5 juv. ♀ (AMNH ex HJUJ INVSC 3263, 3267, 3271, HJUJ INVSC 3264, 3269), 31.vii.2017, S. Cain, 2 ♀ (HJUJ INVSC 3272, 3274), 4 subad. ♂ (AMNH ex HJUJ INVSC 3276, 3278, HJUJ INVSC 3275, 3279), 2 subad. ♀

(HUJ INVSC 3273, 3281), 1 juv. ♂ (HUJ INVSC 3277), 15.iv.2018, Y. Zvik and S. Cain, 1 ♂ (HUJ INVSC 3382), 2 ♀ (HUJ INVSC 3383, 3386), 2 subad. ♂ (HUJ INVSC 3384, 3385), 1 juv. ♀ (HUJ INVSC 3387), 14.vi.2019, D. Kotter, R. Agmon, A. Rinot and S. Cain, 1 ♂ (HUJ INVSC 3669), 1 ♀ (HUJ INVSC 3670), 1 subad. ♂ (HUJ INVSC 3671).

**DIAGNOSIS:** *Buthacus levyi* differs from the closely related species, *B. arenicola*, occurring in Algeria and Tunisia, as follows. The pedipalp chela movable finger of the adult male is proportionally shorter than the manus in *B. levyi* (fig. 44A, B), with chela manus length:movable finger length, 62.8% (57.4%–67.3%,  $n = 8$ ; table 10), than in *B. arenicola* (fig. 38A, B), with chela manus length:movable finger length, 54% (52.4%–55.6%,  $n = 2$ ; table 10). The metasomal segments of the male are narrower in *B. levyi* (fig. 28A), with segment width:length, I–V, 65.1% (60.2%–70.8%,  $n = 8$ ; table 10), 56.9% (53.9%–64.4%), 50.5% (47.6%–57.8%), 40.1% (35.9%–45%), and 33.8% (30.7%–38.9%), than in *B. arenicola* (fig. 27D), with segment width:length, I–V, 72.2% (70.8%–73.6%,  $n = 2$ ; table 10), 63.8% (60.9%–66.8%), 58.9% (58.9%–59%), 44.8% (43.1%–46.5%), and 34.5% (34%–35.1%). The dorsolateral carinae of metasomal segment IV are obsolete to absent in *B. levyi* (figs. 24A, 26A), but well developed in *B. arenicola* (figs. 23D, 25D).

*Buthacus levyi* differs from *B. amitaii*, *B. leptochelys* and *B. nitzani*, occurring in Egypt and Israel, as follows. The pedipalp chela of the adult male is longer and narrower in *B. levyi* (fig. 44A, B), with chela manus length:movable finger length, 62.8% (57.4%–67.3%,  $n = 8$ ; table 10) and chela manus width:chela length, 19.4% (17.1%–21.3%,  $n = 8$ ), than in *B. amitaii*, *B. leptochelys*, and *B. nitzani* (figs. 32A, B, 41A, B, 47A, B), with chela manus length:movable finger length, 81.8% (72.7%–88.3%,  $n = 5$ ; table 3), 70.7% (table 4), and 84.4% (76.8%–92.4%,  $n = 8$ ; table 10), and chela manus width:chela length, 27.1% (25.1%–28.9%,  $n = 5$ ), 24.2%, and 26.3% (22.3%–29.5%,  $n = 8$ ), respectively. The count of retrolateral accessory denticles on the

movable finger of the pedipalp chela is usually lower in *B. levyi* (fig. 21E), with 0–5/0–3 ( $n = 13$ ; table 5), than in *B. amitaii*, *B. leptochelys*, and *B. nitzani* (fig. 21A, D, G), with 0–9/2–10 ( $n = 9$ ; table 2), 7–9/7–9 ( $n = 5$ ; table 5) and 6–9/6–9 ( $n = 16$ ; table 2), respectively.

*Buthacus levyi* differs further from *B. amitaii* and *B. nitzani*, as follows. The proximal dentate margins of the pedipalp chela fixed and movable fingers are sublinear, such that no gap is evident proximally when the fingers are closed, in *B. levyi* (fig. 44B), but emarginate, such that a gap is evident proximally when the fingers are closed, in the other species (figs. 32B, 47B). The posterior processes on the ventrolateral carinae of segment V are smaller and more uniform in size in *B. levyi* (figs. 26A, 28A) than in the other species (figs. 26C, D, 28C, D). The telson dorsal surface is flat and the ventral surface convex and rounded in lateral profile in *B. levyi* (fig. 29B), whereas the dorsal surface is concave and the ventral surface convex and angular in lateral profile in the other species (fig. 29F, H).

**ETYMOLOGY:** The species name is a patronym, honoring Gershon Levy, former Curator of the Arachnida Collection at the National Natural History Collections, Hebrew University of Jerusalem, Israel. Levy promoted the study of arachnids in Israel in particular, and in the Middle East in general; his publications (e.g., Levy and Amitai, 1980) constitute a milestone in understanding the scorpions and other arachnids of the region.

**DESCRIPTION:** The following description is based on the type material (see table 5 for counts and tables 10 and 11 for measurements).

**Total length:** Medium-sized scorpions, 49.2 mm (45.4–52.5 mm,  $n = 8$ ) (♂) or 57.2 mm (53.6–62 mm,  $n = 7$ ; 1 ♀ with tip of aculeus broken, 67.2 mm) (♀).

**Color:** Uniformly yellowish olive, except as follows. Carapace interocular surface orange. Mesosomal tergite VII and metasomal segments I–V, each with narrow brown stripe posteriorly. Pectines whitish. Leg articulation points brown. Immature more orange in color than adults.

**Carapace:** Carapace shape trapezoidal (fig. 18A, B), anterior width:posterior width, 51.5% (43.9%–60.5%,  $n = 17$ ), length:posterior width, 90.1% (80.2%–99.8%,  $n = 17$ ). Five, rarely four, pairs of lateral ocelli; each lateral ocular tubercle with two or, usually, three major ocelli (ALMa, MLMa, PLMa), similar in size, situated anterolaterally, and one or, usually, two minor ocelli (ADMi, PDMi; PDMi may be absent) situated posterodorsal to posterior major ocellus. Median ocelli larger than lateral ocelli, distance between them more than  $2 \times$  ocellus width. Median ocular tubercle situated anteromedially, distance from anterior carapace margin:carapace length, 42.5% (40.2%–45.5%,  $n = 8$ ) ( $\delta$ ) or 43.2% (41.3%–45.3%,  $n = 9$ ) ( $\varphi$ ). Superciliary and central median carinae distinct, costate-granular, and weakly connected to disconnected ( $\delta$ ) or smooth and obsolete ( $\varphi$ ). Anteromedian sulcus distinct, shallow; postero-median sulcus deep, narrow anteriorly, wide posteriorly; posterolateral sulci shallow, wide, curved. Carapace intercarinal surfaces finely and densely granular.

**Chelicerae:** Cheliceral manus prodorsal margin finely granular; retrodorsal surfaces smooth or finely granular; prolateral and ventral surfaces setose. Fixed finger dorsal and ventral surfaces densely setose; dorsal margin with subdistal, medial, and proximal denticles; ventral margin with proximal and medial denticles. Movable finger dorsal surface smooth and glabrous; ventral surface setose; dorsal margin with retrodistal, subdistal, medial, and pair of proximal denticles; ventral margin with prodistal, medial, and proximal denticles.

**Pedipalps:** Femur dorsal prolateral, dorsal retrolateral, and ventral prolateral carinae complete, costate-granular; prolateral ventral and prolateral ventrosubmedian carinae each comprising discontinuous row of spiniform granules; retrolateral dorsosubmedian carina comprising discontinuous row of spiniform granules and fewer than 10 macrosetae; dorsal, ventral, and retrolateral intercarinal surfaces smooth; prolateral intercarinal surfaces finely granular (fig. 43A,

B). Patella prolateral median and ventral prolateral carinae each comprising discontinuous row of spiniform granules; other carinae absent; intercarinal surfaces smooth (fig. 43C–E). Chela long and slender in both sexes, manus width:length, 52.3% (47.2%–55.9%,  $n = 8$ ) ( $\delta$ ) or 56% (52.3%–60.3%,  $n = 9$ ) ( $\varphi$ ), manus height:length, 59.7% (55.8%–64%,  $n = 8$ ) ( $\delta$ ) or 63% (59.5%–66.5%,  $n = 9$ ) ( $\varphi$ ), and manus length:movable finger length, 62.8% (57.4%–67.3%,  $n = 8$ ) ( $\delta$ ) or 46.6% (43%–52%,  $n = 9$ ) ( $\varphi$ ). Chela manus acarinate; intercarinal surfaces smooth and setose (fig. 44). Fixed and movable fingers respectively with 8–10 ( $n = 13$ ) and 7–11 ( $n = 13$ ) ( $\varphi$ ) oblique median denticle subrows; movable finger with 0–5 ( $n = 13$ ) retrolateral accessory denticles (fig. 21E, F); proximal dentate margins of fingers sublinear (fig. 44B), such that small gap present proximally when fingers closed.

**Legs:** Legs I–IV, femoral ventral carinae granular; patellar ventral carinae absent; intercarinal surfaces smooth. Legs I–IV, tibial spurs absent on I and II, present on III and IV; pro- and retroventral basitarsal (pedal) spurs present, more developed on III and IV. Legs I–IV, macrosetal counts on retrolateral margins of tibiae, 8:10:12:3; basitarsi, 12:16:16:10; telotarsi, 6:7:8:8 ( $n = 1$ ). Telotarsal unguis long, approximately equal to telotarsus length, unequal on legs I and II, subequal to equal on III and IV (fig. 22B).

**Genital operculum:** Genital opercula suboval, completely divided longitudinally, with overlapping, rounded margins ( $\delta$ ) or partially fused longitudinally ( $\varphi$ ) (fig. 20E, F). Genital papillae present ( $\delta$ ) or absent ( $\varphi$ ).

**Pectines:** Three marginal lamellae; 11–13 ( $n = 3$ ) ( $\delta$ ) or 10–13 ( $n = 3$ ) ( $\varphi$ ) median lamellae (fig. 20E, F). Fulcra present. Pectinal teeth along most of length, dentate margin length:pecten length, 97.4% (90.5%–101.2%,  $n = 8$ ) ( $\delta$ ) or 91.8% (86.4%–96.3%,  $n = 9$ ) ( $\varphi$ ). Pectinal teeth curved, similar in size; tooth count (sinistral/dextral), 33/32 (31–35/31–34,  $n = 7$ ) ( $\delta$ ) or 27/27 (25–29/25–28,  $n = 9$ ) ( $\varphi$ ).

**Mesosoma:** Tergites I–VII progressively increasing in length posteriorly, tergite VI

length:tergite VII length, 53.3% (44.6%–60.3%,  $n = 8$ ) (♂) or 53.8% (47.1%–57.5%,  $n = 9$ ) (♀); increasing in width posteriorly from I–IV, decreasing in width posteriorly from V–VII. Pretergites smooth; posttergites I–VI, intercarinal surfaces uniformly granular, becoming more coarsely and densely granular posteriorly, VII, finely to coarsely and sparsely granular. Tergites I–VI, dorsomedian carinae granular, vestigial, restricted to posterior fifth of I–IV and posterior third of V and VI; dorsosubmedian carinae granular, vestigial, restricted to posterior fifth of I–III and posterior third of IV–VI. Tergite VII, dorsomedian carina granular, vestigial, restricted to anterior half; dorsosubmedian and dorsolateral carinae distinct, granular. Sternites III–VII smooth and glabrous; III–VI acarinate, VII, ventrolateral carinae vestigial, granular; IV–VI, respiratory spiracles (stigmata) width approximately 3× length.

**Metasoma:** Metasomal segments I–V becoming longer and narrower posteriorly (figs. 24A, 26A, 28A), segment I shortest, length I:II, 90.8% (85.9%–95%,  $n = 8$ ) (♂) or 90.4% (82.8%–101%,  $n = 9$ ) (♀); segments II–IV similar, length II:III, 96.8% (95.3%–100.5%,  $n = 8$ ) (♂) or 95.7% (86.6%–98.9%,  $n = 9$ ) (♀), length III:IV, 97.8% (91.2%–108.7%,  $n = 8$ ) (♂) or 97.8% (95%–100.6%,  $n = 9$ ) (♀); segment V longest, length IV:V, 83.6% (73.1%–90.8%,  $n = 8$ ) (♂) or 84.5% (78.2%–91.8%,  $n = 9$ ) (♀); width:length segment I, 65.1% (60.2%–70.8%,  $n = 8$ ) (♂) or 66.9% (62.5%–71%,  $n = 9$ ) (♀), II, 56.9% (53.9%–64.4%,  $n = 8$ ) (♂) or 56.4% (51.1%–61.6%,  $n = 9$ ) (♀), III, 50.5% (47.6%–57.8%,  $n = 8$ ) (♂) or 51.3% (46.2%–56.4%,  $n = 9$ ) (♀), IV, 40.1% (35.9%–45%,  $n = 8$ ) (♂) or 41.9% (39.9%–44.1%,  $n = 9$ ) (♀), V, 33.8% (30.7%–38.9%,  $n = 8$ ) (♂) or 35.4% (31.8%–40.5%,  $n = 9$ ) (♀); dorsosubmedian carinae distinct, granular on segment I, obsolete on II and III, absent on IV and V; dorsolateral carinae distinct, granular on segments I and II, obsolete on III and IV, absent on V; dorsosubmedian and dorsolateral carinae sparsely setose, macrosetal counts on segments I–V (sinistral/dextral), dorsosubmedian carinae, 1/1

(0/0–2/1,  $n = 5$ ):3/2 (2/2–4/3):3/2 (2/2–3/3):2/2 (0/1–3/2):0/0 (0/0–0/0), dorsolateral carinae, 2/2 (2/1–2/3,  $n = 5$ ):3/3 (2/2–3/3):2/3 (1/2–2/3):3/2 (1/1–3/3):3/4 (1/2–4/5). Median lateral carinae distinct, granular, restricted to posterior half of segment I, posterior third of II, vestigial, reduced to posterior margin on III, absent on IV and V. Ventrolateral carinae distinct, costate, becoming granular posteriorly on segments I–IV; serrate, comprising spiniform granules, becoming more prominent posteriorly, on V. Ventrosubmedian carinae distinct, costate on segment I; costate, becoming costate-granular posteriorly, on II and III; costate on IV; obsolete, granular on V. Ventromedian carina obsolete, granular on segment V. Dorsal and lateral intercarinal surfaces smooth on segments I–V; ventral intercarinal surfaces smooth on segments I–IV, finely and sparsely granular on V.

**Telson:** Telson vesicle width:metasomal segment V width, 72.8% (65.8%–81.9%,  $n = 8$ ) (♂) or 74.8% (71.7%–80.1%,  $n = 9$ ) (♀). Vesicle globbose, dorsal surface flat, ventral surface convex and rounded; vesicle height:length, 56% (51.6%–59.7%,  $n = 8$ ) (♂) or 59.3% (55.4%–65%,  $n = 9$ ) (♀); dorsal and ventral surfaces smooth and glabrous; lateral and ventral surfaces sparsely setose, with 22 (♂: 18–26,  $n = 2$ ; ♀: 22–23,  $n = 3$ ) macrosetae. Aculeus long, gently curved; aculeus length:telson length, 52.5% (49.4%–57.8%,  $n = 8$ ) (♂) or 54.9% (53.1%–58.8%,  $n = 7$ ) (♀).

**Sexual dimorphism:** Adult males and females differ as follows. Males are slightly smaller, on average 49.2 mm in total length, than females, on average 57.2 mm. The pedipalp chela of the male has proportionally shorter fingers than that of the female (fig. 44), as indicated by the higher chela manus length:movable finger length ratio in the male (62.8%) compared with the female (46.6%). The mesosoma of the male is relatively narrower than that of the female, as indicated by the higher sternite VII length:width ratio in the male (67.9%) compared with the female (59%). The pectinal tooth count is higher in the male (31–35) than in the female (25–29). The genital opercula are completely divided longitudinally,

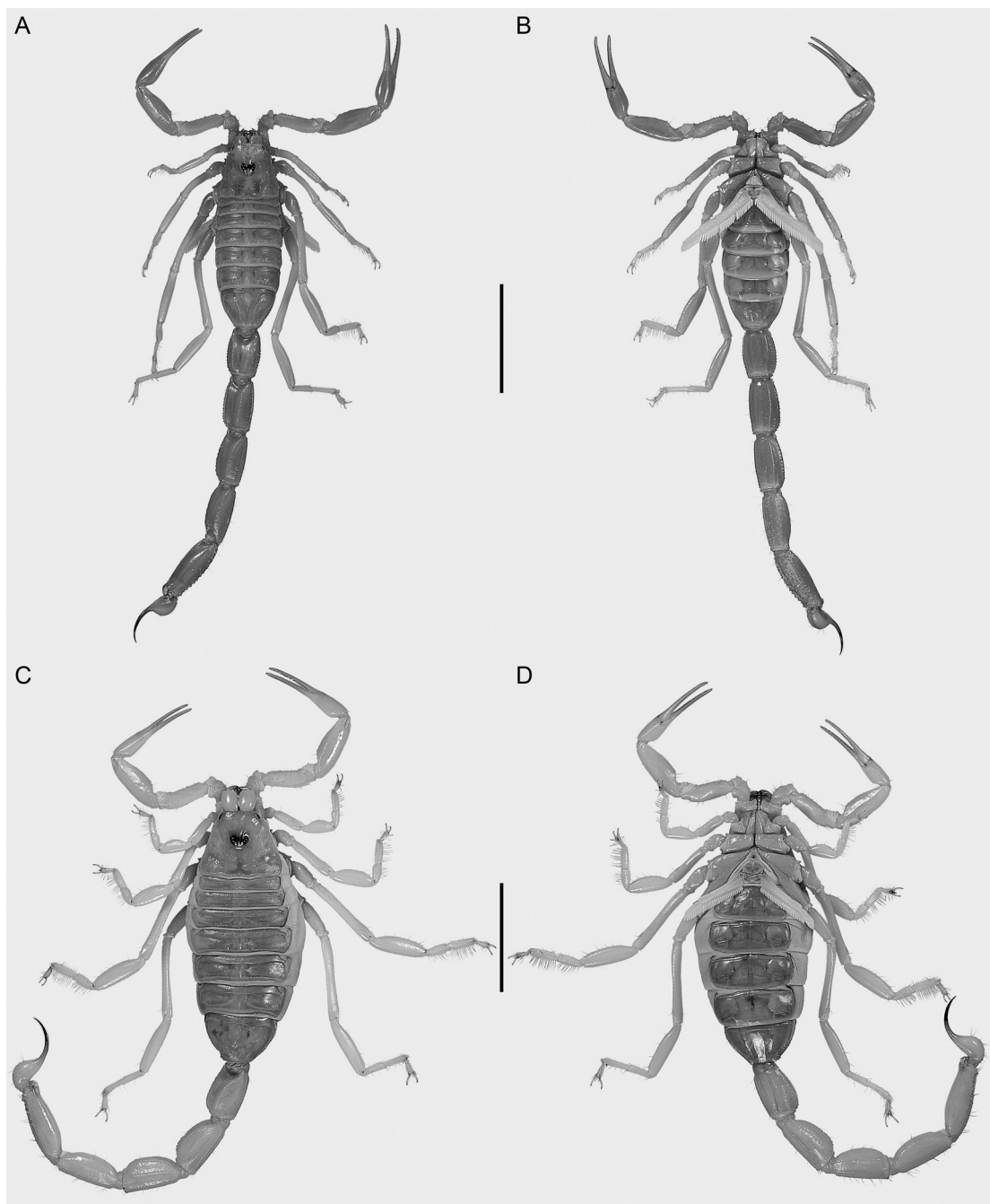


FIGURE 42. *Butthacus levyi*, sp. nov., habitus, dorsal (A, C), and ventral (B, D) aspects. A, B. Holotype ♂ (HUJ INVSC 2082). C, D. Paratype ♀ (HUJ INVSC 3274). Scale bars = 1 cm.

with rounded margins in the male but partially fused longitudinally in the female (fig. 20E, F), and genital papillae are present in the male but absent in the female.

**DISTRIBUTION:** The known locality records suggest *B. levyi* may be endemic to Egypt and Israel, extending from the coast of northern Egypt, across the sand dunes of the northern and western Sinai Peninsula, to the southern part of the Haluza sand dunes, near the Israeli border with Egypt (fig. 9). Records of *B. arenicola* from northeastern Libya (Kovařík and Whitman, 2004) may be referable to *B. levyi*, but this requires confirmation. The known records range from 4 m to 313 m in elevation. *Buthacus levyi* is allopatric with the closely related *B. arenicola*, endemic to central Tunisia and northeastern Algeria.

**ECOLOGY:** The types of *B. levyi* were collected at night with UV light detection on soft, sparsely vegetated to vegetationless inland sand dunes. The habitat and habitus, notably the pale coloration, smooth tegument, loss or obsolescence of pedipalpal and metasomal carinae, elongation of the legs, especially legs III and IV, dorsoventral compression of the basitarsi of legs I–III, comblike rows of elongated macrosetae (“sand combs”) along the retrolateral margins of the tibae and the pro- and retrolateral margins of the basitarsi of legs I–III, elongated macrosetae on the lateral and ventral surfaces of the telotarsi, and elongated, unequal length telotarsal unguis, are consistent with the ultrasamphophilous ecomorphotype (Prendini, 2001). *Buthacus levyi* was collected in sympatry with three other buthids, *Androctonus amoreuxi*, *Buthus israelis*, and *Orthochirus scrobiculosus*, at Be'er Milka, Israel.

**REMARKS:** As noted above, the types of *B. arenicola* and *B. leptochelys* were examined during the present investigation, along with material from the vicinity of the type locality of *B. arenicola*, in Tunisia, and from Egypt, including the Sinai Peninsula, and Israel. These comparisons, multivariate analysis of morphometrics (fig. 15), and multilocus molecular phylogenetics (fig. 14),

confirmed previous suggestions (Levy and Amitai, 1980; Lourenço, 2006) that the population of *B. arenicola* occurring in Egypt and Israel represents a distinct species, described here as *Buthacus levyi*, sp. nov.

Additionally, as noted above, Kovařík’s (2005) conclusion that the type series of *B. leptochelys* comprises more than one species was also confirmed: paralectotype 2 is heterospecific with the lectotype and paralectotype 1, instead representing a species of the *B. arenicola* group. However, Kovařík (2005) misidentified paralectotype 2 as the Tunisian species, *B. spatzi*; it is conspecific with *B. levyi*, the distribution of which overlaps that of *B. leptochelys* in the Sinai Peninsula (fig. 6).

**MATERIAL EXAMINED: EGYPT:** Sinai, *Androctonus (Leiurus) leptochelys* paralectotype ♀ (No. 2) (ZMB 152).

#### *Buthacus nitzani* Levy et al., 1973, stat. nov.

Figures 1D, F, 2C, D, 7, 11, 12A, 13, 15, 17C, D, 20A, B, 21G, 22F, 24C, 26C, 28C, 29F, 45, 46, 47; tables 1, 2, 12, 13

#### *Buthacus leptochelys nitzani* Levy et al., 1973:

126; Vachon, 1979: 38, 39; Levy and Amitai, 1980: 83–86, figs. 70–74, map 6; Kinzelbach, 1984: 101 (misidentification); Fet et al., 1998: 616; Kovařík, 1998: 105; Fet and Lowe, 2000: 84; Hendrixson, 2006: 50; Lourenço, 2006: 64; Al-Asmari et al., 2013: 5, 8, 9, fig. 8, table 1 (misidentification).

*Buthacus leptochelys*: Vachon, 1950b: 406 (part); 1952: 180, 185, 191, 194, 198–203, figs. 262–266 (part); Kinzelbach, 1984: 101; Vachon and Kinzelbach, 1987: 101; El-Hennawy, 1992: 101, 112, 113 (misidentification); Kovařík, 2005: 2, 3; Kaltsas et al., 2008: 214; Lowe et al., 2019: 5.

**TYPE MATERIAL:** Holotype 1 ♀ (HUJ INVSC 280), **ISRAEL:** Mehoz HaDarom (Southern District): Haluza sand dunes, Ze’elim [31°12'N 34°32'E], 20.vi.1961, M. Nizan [examined].

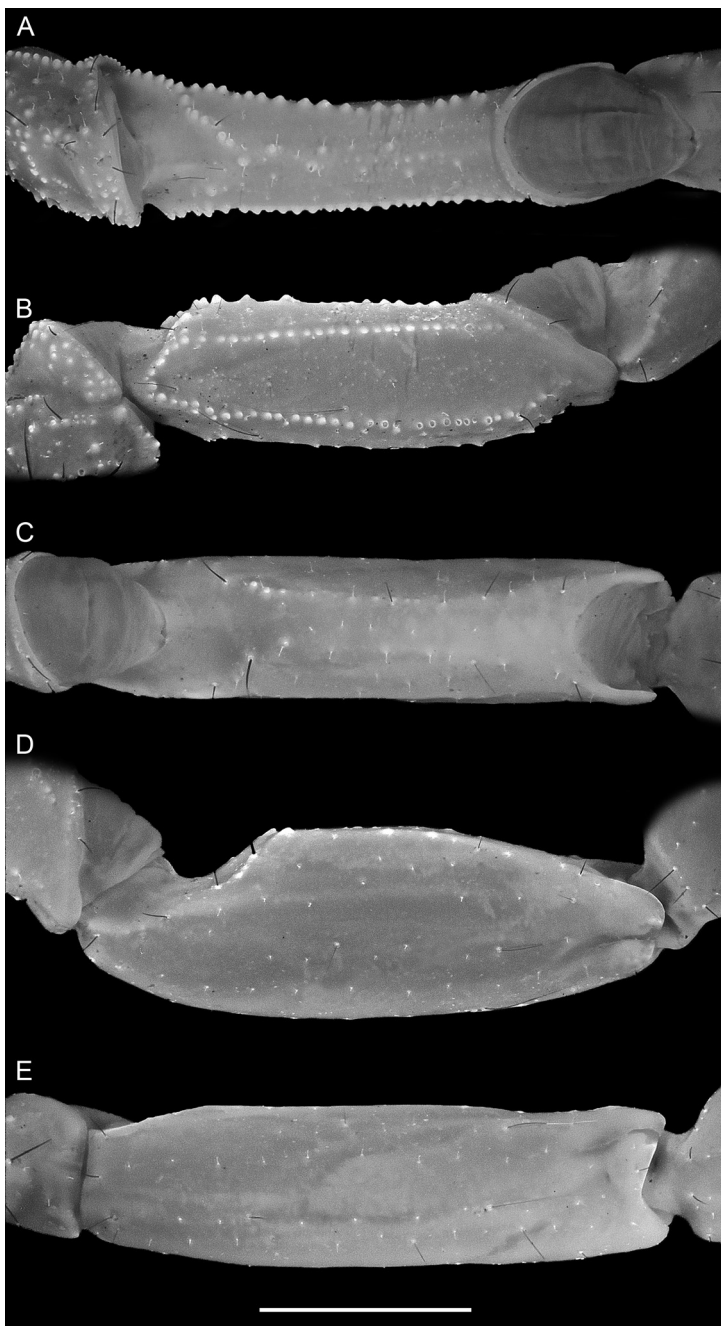


FIGURE 43. *Buthacus levyi*, sp. nov., holotype ♂ (HUA INVSC 2082), dextral pedipalp femur (A, B) and patella (C, E), prolateral (A, C), dorsal (B, D), and retrolateral (E) aspects. Scale bar = 2 mm.

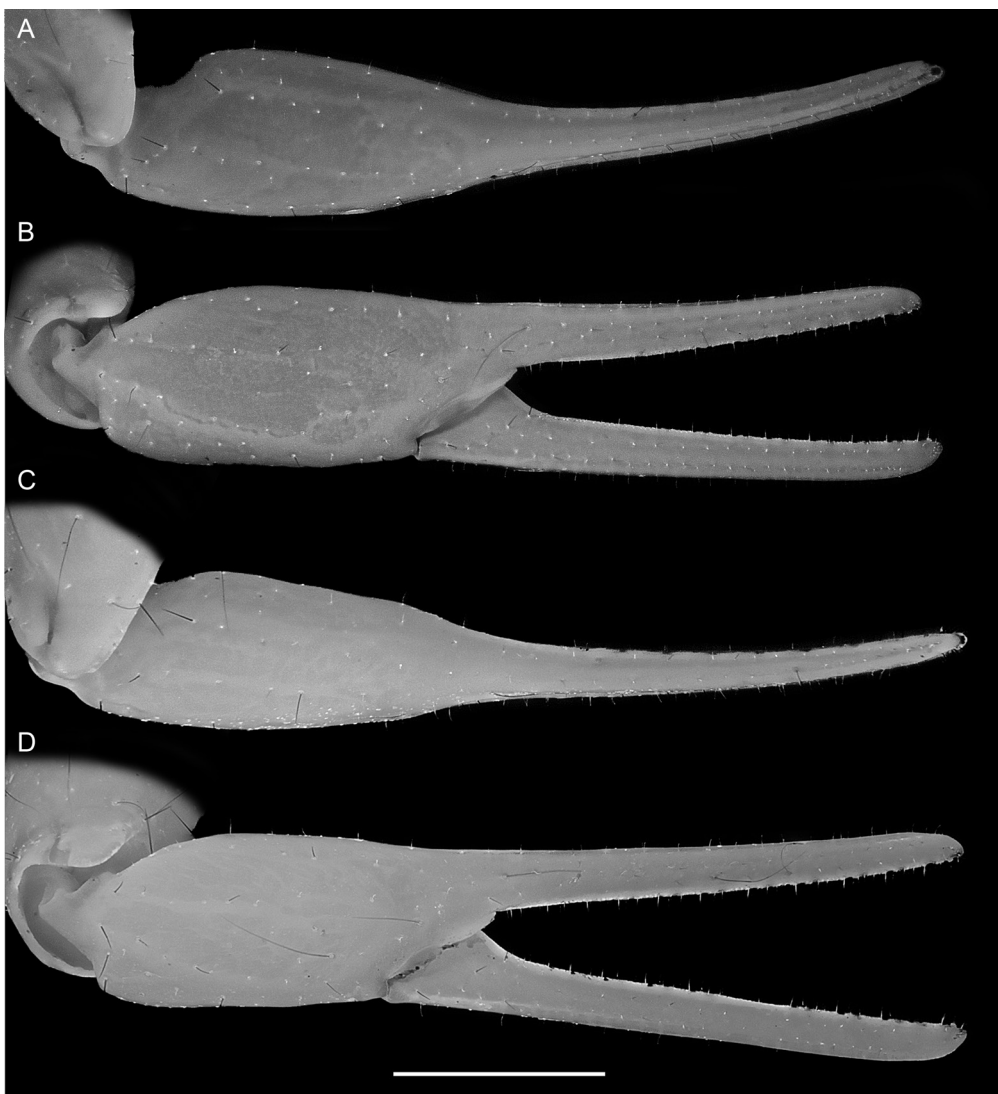


FIGURE 44. *Buthacus levyi*, sp. nov., dextral pedipalp chela, dorsal (A, C) and retrolateral (B, D) aspects. A, B. Holotype ♂ (HUJ INVSC 2082). C, D. Paratype ♀ (HUJ INVSC 3274). Scale bar = 2 mm.

**DIAGNOSIS:** *Buthacus nitzani* is most closely related to *B. amitaii*, also occurring in Israel, and *B. leptochelys*, occurring in Sinai and Egypt. *Buthacus nitzani* differs from *B. amitaii* as follows. The metasomal segments of the female are longer and narrower in *B. nitzani* (fig. 28C), with segment IV width:length, 38.4% (34%–43.7%,  $n = 10$ ; table 13), than in *B. amitaii* (fig. 28D), with segment IV width:length, 42.8% (40.2%–44.9%,  $n = 5$ ; table 3).

The ventrosubmedian and ventrolateral carinae are less developed on the metasomal segments, especially on segments II and III, in *B. nitzani* than in *B. amitaii* (figs. 26C, D, 28C, D). The posterior processes of the ventrolateral carinae of metasomal segment V are narrow and conical in *B. nitzani*, but broad and lobate in *B. amitaii*. The median lateral carinae are obsolete on metasomal segments I–III in *B. nitzani*, but distinct in *B. amitaii*. The ventral

intercarinal surfaces of metasomal segment V are more finely and sparsely granular in *B. nitzani* than in *B. amitaii*. The retrolateral accessory denticles on the movable finger of the pedipalp chela are always present, with constant, usually higher counts (sinistral/dextral: 6–9/6–9;  $n = 16$ ; table 2; fig. 21G) in *B. nitzani*, compared to *B. amitaii*, in which the retro-lateral accessory denticles are often absent, with variable, usually lower counts (0–9/2–10;  $n = 9$ ; table 2; fig. 21A).

*Buthacus nitzani* differs *B. leptochelys* as follows. *Buthacus nitzani* is smaller, measuring 50.6 mm (44.4–58.5 mm,  $n = 18$ ; tables 12, 13) in total length, than *B. leptochelys*, measuring 65.8 mm (63.1–68 mm,  $n = 5$ ; table 4). The pedipalp chela of the adult male is shorter and broader (fig. 47A, B), with chela manus length:movable finger length, 84.4% (76.8%–92.4%,  $n = 8$ ; table 12) and chela manus width:chela length, 26.3% (22.3%–29.5%,  $n = 8$ ), in *B. nitzani* than in *B. leptochelys* (fig. 41A, B), with chela manus length:movable finger length, 70.7% (table 4) and chela manus width:chela length, 24.2%. The proximal dentate margins of the pedipalp chela fixed and movable fingers are more deeply emarginate, such that a more pronounced gap is evident proximally when the fingers are closed, in *B. nitzani* (fig. 47B), than in *B. leptochelys* (fig. 41B). The pectinal tooth counts are lower in *B. nitzani*, i.e., 31/31 (26–34/27–35,  $n = 6$ ; table 2) ( $\delta$ ) and 23/23 (20–27/21–27,  $n = 17$ ) ( $\varphi$ ), than in *B. leptochelys*, i.e., 35/34 (32–39/32–38,  $n = 6$ ; table 5) ( $\delta$ ) and 29/29 (27–31/28–31,  $n = 10$ ) ( $\varphi$ ). The metasomal segments of the female are shorter and broader in *B. nitzani* (fig. 28C), with segment IV width:length, 38.4% (34%–43.7%,  $n = 10$ ; table 13), than in *B. leptochelys* (fig. 28B), with segment IV width:length, 42.1% (40.3%–44.6%,  $n = 4$ ; table 4). The median lateral carinae of metasomal segments I–III are obsolete in *B. nitzani*, but distinct in *B. leptochelys*. The telson dorsal surface is concave and the ventral surface convex and angular in lateral profile, in *B. nitzani* (fig. 29F), whereas the dorsal surface is flat and the ventral surface convex and rounded in lateral profile, in *B. leptochelys* (fig. 29D).

*Buthacus nitzani* differs from *B. levyi*, with which it is sympatric in Israel and the Sinai Peninsula, as follows. The pedipalp chela of the adult male is shorter and broader in *B. nitzani* (fig. 47A, B), with chela manus length:movable finger length, 84.4% (76.8%–92.4%,  $n = 8$ ; table 12) and chela manus width:chela length, 26.3% (22.3%–29.5%,  $n = 8$ ), than in *B. levyi* (fig. 44A, B), with chela manus length:movable finger length, 62.8% (57.4%–67.3%,  $n = 8$ ; table 10) and chela manus width:chela length, 19.4% (17.1%–21.3%,  $n = 8$ ). The proximal dentate margins of the pedipalp chela fixed and movable fingers are emarginate, such that a gap is evident proximally when the fingers are closed, in *B. nitzani* (fig. 47B), but sub-linear, such that no gap is evident proximally when the fingers are closed, in *B. levyi* (fig. 44B). The retrolateral accessory denticles on the movable finger of the pedipalp chela are present, with higher counts, in *B. nitzani* (sinistral/dextral: 6–9/6–9;  $n = 16$ ; table 2; fig. 21G), than in *B. levyi*, in which the denticles are often absent (0–5/0–3;  $n = 13$ ; table 5; fig. 21E, F). The posterior processes on the ventrolateral carinae of segment V are larger and more variable in size in *B. nitzani* (figs. 26C, 28C) than in *B. levyi* (figs. 26A, 28A). The telson dorsal surface is concave and the ventral surface convex and angular in lateral profile, in *B. nitzani* (fig. 29F), whereas the dorsal surface is flat and the ventral surface convex and rounded in lateral profile, in *B. levyi* (fig. 29B).

**DESCRIPTION:** The following description is based on the type material and specimens from across the distribution of the species in Israel (see table 2 for counts and tables 12 and 13 for measurements).

**Total length:** Medium-sized scorpions, 53 mm (47.4–58.5 mm,  $n = 8$ ) ( $\delta$ ) or 48.6 mm (44.4–54.5 mm,  $n = 10$ ) ( $\varphi$ ).

**Color:** Uniformly yellowish olive except as follows. Carapace interocular surface, pedipalp femur and patella, legs, anterior part of metasomal segments I–IV, and entire segment V orange. Pectines pale yellow. Leg articulation points brown.

**Carapace:** Carapace shape trapezoidal (fig. 17C, D), anterior width:posterior width, 52.8%

(47.7%–57.4%,  $n = 18$ ), length:posterior width, 88.3% (75.2%–98.3%,  $n = 18$ ). Five, rarely four, pairs of lateral ocelli; each lateral ocular tubercle with two or, usually, three major ocelli (ALMa, MLMa, PLMa), similar in size, situated anterolaterally, and one or, usually, two minor ocelli (ADMi, PDMi; PDMi may be absent) situated posterodorsal to posterior major ocellus. Median ocelli larger than lateral ocelli, distance between them more than 2× ocellus width. Median ocular tubercle situated anteromedially, distance from anterior carapace margin:carapace length, 39.7% (35.7%–43.1%,  $n = 8$ ) (♂) or 41.3% (39.2%–44.6%,  $n = 10$ ) (♀). Superciliary and central median carinae distinct, costate-granular, strongly to weakly connected (♂) or weakly connected to disconnected (♀). Anteromedian sulcus distinct, shallow; posteromedian sulcus deep, narrow anteriorly, wide posteriorly; posterolateral sulci shallow, wide, curved. Carapace intercarinal surfaces finely and densely granular.

**Chelicerae:** Cheliceral manus prodorsal margin finely granular; retrodorsal surfaces smooth or finely granular; prolateral and ventral surfaces setose. Fixed finger dorsal and ventral surfaces densely setose; dorsal margin with subdistal, medial, and proximal denticles; ventral margin with proximal and medial denticles. Movable finger dorsal surface smooth and glabrous; ventral surface setose; dorsal margin with retrodistal, subdistal, medial, and pair of proximal denticles; ventral margin with prodistal, medial, and proximal denticles.

**Pedipalps:** Femur dorsal prolateral, dorsal retrolateral, and ventral prolateral carinae complete, costate-granular; prolateral ventral and prolateral ventrosubmedian carinae each comprising discontinuous row of spiniform granules; retrolateral dorsosubmedian carina absent, represented by fewer than 10 macrosetae; intercarinal surfaces smooth (fig. 46A, B). Patella prolateral median and ventral prolateral carinae discontinuous, each comprising a few spiniform granules; other carinae absent; intercarinal surfaces smooth (fig. 46C–E). Chela short and broad (♂), manus width:length,

59% (48.6%–67%,  $n = 8$ ), manus height:length, 62.5% (57.7%–66.6%,  $n = 8$ ), and manus length:movable finger length, 84.4% (76.8%–92.4%,  $n = 8$ ) or short and slender (♀), manus width:length, 54.1% (51.2%–63.1%,  $n = 10$ ), manus height:length, 61.5% (57.3%–68.5%,  $n = 10$ ), and manus length:movable finger length, 63.8% (56.4%–83%,  $n = 10$ ). Chela manus acarinate; intercarinal surfaces smooth and glabrous (fig. 47). Fixed and movable fingers each with 7–10 ( $n = 16$ ) oblique median denticle subrows; movable finger with 6–9 ( $n = 16$ ) retrolateral accessory denticles (fig. 21G); proximal dentate margins of fingers emarginate (fig. 47B), such that gap present proximally when fingers closed.

**Legs:** Legs I–IV, femoral ventral carinae granular; patellar ventral carinae obsolete; intercarinal surfaces smooth. Legs I–IV, tibial spurs absent on I and II, present on III and IV; pro- and retroventral basitarsal (pedal) spurs present, more developed on III and IV. Legs I–IV, macrosetal counts on retrolateral margins of tibiae, 7:9:11:4; basitarsi, 9:14:17:7; telotarsi, 4:6:7:7 ( $n = 1$ ). Telotarsal unguis long, approximately equal to telotarsus length, unequal on legs I and II, subequal to equal on III and IV (fig. 22F).

**Genital operculum:** Genital opercula suboval, completely divided longitudinally, with overlapping, rounded margins (♂) or partially fused longitudinally (♀) (fig. 20A, B). Genital papillae present (♂) or absent (♀).

**Pectines:** Three marginal lamellae; 7–9 (♂) or 8–10 ( $n = 3$ ) (♀) median lamellae (fig. 20A, B). Fulcra present. Pectinal teeth along most of length, dentate margin length:pecten length, 96.9% (93.9%–101.6%,  $n = 8$ ) (♂) or 94.5% (88.7%–99%,  $n = 10$ ) (♀). Pectinal teeth curved, similar in size; tooth count (sinistral/dextral), 31/31 (26–34/27–35,  $n = 6$ ) (♂) or 23/23 (20–27/21–27,  $n = 17$ ) (♀).

**Mesosoma:** Tergites I–VII progressively increasing in length posteriorly, tergite VI length:tergite VII length, 55.9% (51.9%–61.9%,  $n = 8$ ) (♂) or 59.7% (52.2%–70.8%,  $n = 10$ ) (♀); increasing in width posteriorly from I–IV, decreasing in width posteriorly from V–VII.

TABLE 10

**Measurement data for adult male *Buthacus arenicola* (Simon, 1885), and *Buthacus levyi*, sp. nov., deposited in the American Museum of Natural History (AMNH), New York, and the National Natural History Collections, Hebrew University of Jerusalem (HUJ), Israel**

Measurements (mm) follow Tahir et al. (2014): total length (sum of carapace, tergites I–VII, metasomal segments I–V, and telson); carapace median ocelli (distance from carapace anterior margin); carapace anterior width (distance between lateral ocelli); chela total length (distance from base of condyle to tip of fixed finger); chela retroventral carina (length along manus retroventral carina); chela movable finger (movable finger length); pectines total length (length along retrolateral margin); pectines dentate margin (length along dentate margin).

Specimen	type	<i>B. arenicola</i>				<i>B. levyi</i>					
				Holotype						Paratypes	
		♂	♂	♂	♂	♂	♂	♂	♂	♂	♂
		collection	AMNH	AMNH	HUJ	AMNH	AMNH	HUJ	HUJ	HUJ	HUJ
		accession no.		2082			1772	2077	2079	2083	3253
Total length		54.4	54.3	50.9	46.0	45.4	49.0	51.8	49.0	52.6	49.0
Carapace	median ocelli	2.3	2.4	2.0	1.9	1.9	2.1	2.2	2.1	2.2	1.9
	length	5.3	5.6	4.9	4.5	4.5	4.8	4.9	4.5	5.3	4.7
	anterior width	3.2	3.3	2.9	2.2	2.2	2.8	3.1	2.9	3.1	2.6
	posterior width	5.4	5.9	4.9	5.0	4.7	5.1	5.0	5.1	5.6	5.2
Tergite I	length	0.8	1.0	0.5	0.6	0.7	0.7	0.8	0.8	0.8	0.7
Tergite II	length	1.2	1.2	0.9	0.8	0.9	1.0	1.0	0.9	1.0	1.0
Tergite III	length	1.5	1.5	1.4	1.2	1.1	1.2	1.3	1.2	1.3	1.3
Tergite IV	length	1.7	1.8	1.5	1.5	1.3	1.5	1.7	1.5	1.6	1.5
Tergite V	length	1.9	2.0	1.7	1.7	1.5	1.7	1.8	1.7	1.9	1.8
Tergite VI	length	2.1	2.2	2.0	2.2	1.7	1.9	2.1	1.9	1.7	2.0
Tergite VII	length	4.0	3.7	3.8	3.6	3.3	3.6	3.6	3.6	3.7	3.6
Sternite VII	length	3.6	3.1	3.1	3.1	2.9	2.9	3.3	2.9	3.7	3.3
	width	5.0	5.4	4.6	4.4	4.4	4.6	4.7	4.7	4.8	4.8
	height	2.8	3.0	2.3	2.3	2.3	2.4	2.4	2.3	2.6	2.3
Metasoma I	length	4.9	4.8	4.8	4.3	4.3	4.5	4.7	4.7	5.0	4.5
	width	3.5	3.5	2.9	3.0	3.0	3.0	3.2	2.9	3.2	2.9
	height	2.8	3.0	2.3	2.3	2.3	2.4	2.4	2.3	2.6	2.3
Metasoma II	length	5.5	5.3	5.2	4.5	4.8	5.0	5.4	5.0	5.5	5.3
	width	3.3	3.5	2.9	2.9	2.7	2.8	3.0	2.8	3.2	2.8
	height	2.8	2.9	2.4	2.4	2.4	2.3	2.6	2.4	2.7	2.4
Metasoma III	length	5.4	5.6	5.4	4.7	4.9	5.2	5.6	5.2	5.7	5.2
	width	3.2	3.3	2.7	2.7	2.5	2.5	2.8	2.5	2.8	2.6
	height	2.7	2.7	2.3	2.3	2.3	2.2	2.4	2.3	2.5	2.2
Metasoma IV	length	6.0	5.8	5.4	5.0	5.0	5.5	6.2	5.4	5.6	4.8
	width	2.6	2.7	2.0	2.1	2.1	2.2	2.2	2.1	2.3	2.2
	height	2.3	2.4	2.1	2.0	2.0	2.1	2.3	2.1	2.2	2.0
Metasoma V	length	7.1	7.2	6.8	5.6	5.6	6.6	7.0	6.3	7.2	6.6
	width	2.4	2.5	2.1	2.1	2.2	2.1	2.2	2.1	2.4	2.2
	height	2.2	2.0	2.0	1.9	1.9	1.9	2.0	1.8	2.2	2.0
Telson	vesicle length	3.2	3.2	2.8	2.8	2.6	2.8	2.9	2.9	3.2	3.0
	vesicle width	1.8	1.8	1.6	1.5	1.5	1.6	1.8	1.5	1.6	1.6
	vesicle height	1.9	1.9	1.6	1.4	1.5	1.6	1.6	1.7	1.8	1.7
	aculeus length	3.9	3.8	3.8	3.2	3.1	3.0	2.8	3.3	3.2	3.0

TABLE 10 *continued*

Specimen	type	<i>B. arenicola</i>				<i>B. levyi</i>						
				Holotype						Paratypes		
		sex	♂	♂	♂	♂	♂	♂	♂	♂	♂	♂
		collection	AMNH	AMNH	HUJ	AMNH	AMNH	HUJ	HUJ	HUJ	HUJ	HUJ
		accession no.			2082			1772	2077	2079	2083	3253
Femur	length	4.9	4.7	4.6	4.2	4.0	4.3	4.9	4.7	4.8	4.3	
	width	1.3	1.5	1.3	1.3	1.3	1.2	1.4	1.3	1.6	1.2	
	height	1.1	1.2	1.0	1.0	1.0	1.1	1.0	1.1	1.3	1.2	
Patella	length	5.7	5.9	5.5	5.0	5.1	5.5	5.5	5.4	5.7	5.8	
	width	1.8	2.0	1.7	1.7	1.7	1.7	1.9	1.8	1.9	1.8	
	height	1.6	1.5	1.4	1.3	1.3	1.3	1.5	1.4	1.6	1.6	
Chela	total length	8.8	8.9	8.0	7.5	7.4	7.9	8.4	7.9	8.5	7.9	
	manus width	1.5	1.6	1.5	1.5	1.6	1.4	1.6	1.6	1.6	1.6	
	manus height	1.7	2.0	1.6	1.8	1.8	1.8	1.9	1.6	1.8	1.7	
	retroventral carina	3.0	3.0	2.9	3.0	2.9	2.9	3.1	2.8	3.0	3.0	
	movable finger	5.7	5.4	4.4	4.6	4.3	4.8	4.9	4.7	5.1	4.7	
Pectines	total length	8.5	7.8	7.5	6.4	6.4	7.4	7.8	7.8	7.9	7.0	
	dentate margin	8.3	7.5	7.3	6.4	6.3	6.7	7.6	7.4	7.7	6.9	

Pretergites smooth; posttergites I–VI, intercarinal surfaces uniformly granular, becoming more coarsely and densely granular posteriorly, VII, finely to coarsely and sparsely granular. Tergites I–VI, dorsomedian carinae granular, vestigial, restricted to posterior fifth of I–V and posterior third of VI; dorsosubmedian carinae granular, vestigial, restricted to posterior fifth of I–VI. Tergite VII, dorsomedian carina granular, vestigial, restricted to anterior half; dorsosubmedian and dorsolateral carinae distinct, granular. Sternites III–VII smooth and glabrous; III–VI acarinate, VII, ventrolateral carinae vestigial, granular; IV–VI, respiratory spiracles (stigmata) width approximately 3× length.

**Metasoma:** Metasomal segments I–V becoming longer and narrower posteriorly (figs. 24C, 26C, 28C), segment I shortest, length I:II, 87.7% (83.1%–91.8%, n = 8) (♂) or 89.2% (84.4%–97.8%, n = 10) (♀); segments II–IV similar, length II:III, 98.2% (95.7%–100%, n = 8) (♂) or 98.3% (91.1%–103.1%, n = 10) (♀), length III:IV, 95.4% (93.2%–98.6%, n = 8) (♂) or 95% (91.6%–104.8%, n = 10) (♀); segment V longest, length IV:V, 83.4% (77.6%–88.5%, n = 8)

(♂) or 81.7% (77.9%–88.9%, n = 10) (♀); width:length segment I, 64.2% (60.4%–68.8%, n = 8) (♂) or 64.6% (59.1%–67.8%, n = 10) (♀), II, 55.1% (53.3%–58%, n = 8) (♂) or 54.3% (47.9%–61%, n = 10) (♀), III, 51% (49%–54.4%, n = 8) (♂) or 50.8% (46%–56%, n = 10) (♀), IV, 42% (37.9%–50.7%, n = 8) (♂) or 38.4% (33.9%–43.7%, n = 10) (♀), V, 34.1% (30.8%–36.1%, n = 8) (♂) or 34% (31.7%–38.7%, n = 10) (♀); dorsosubmedian carinae distinct, granular on segments I and II, obsolete on III, absent on IV and V; dorsolateral carinae distinct, granular on segment I, granular on II, obsolete on III and IV, absent on V; dorsosubmedian and dorsolateral carinae sparsely setose, macrosetal counts on segments I–V (sinistral/dextral), dorsosubmedian carinae, 1/1 (0/0–1/2, n = 4):2/2 (1/1–4/3):2/3 (2/3–3/3):2/1 (1/0–2/3):0/0 (0/0–0/0), dorsolateral carinae, 2/2 (1/1–3/3, n = 4):3/2 (2/2–4/3):3/3 (1/2–4/3):4/3 (4/1–4/4):4/4 (3/3–6/5). Median lateral carinae obsolete, granular along entire length of segment I, restricted to posterior third of II and posterior quarter of III, absent on IV and V. Ventrolateral carinae distinct, costate-granular,

TABLE 11

**Measurement data for adult female *Buthacus levyi*, sp. nov., deposited in the American Museum of Natural History (AMNH), New York, and the National Natural History Collections, Hebrew University of Jerusalem (HUJ), Israel**

Measurements (mm) follow Tahir et al. (2014): total length (sum of carapace, tergites I–VII, metasomal segments I–V, and telson); carapace median ocelli (distance from carapace anterior margin); carapace anterior width (distance between lateral ocelli); chela total length (distance from base of condyle to tip of fixed finger); chela retroventral carina (length along manus retroventral carina); chela movable finger (movable finger length); pectines total length (length along retrolateral margin); pectines dentate margin (length along dentate margin).

Specimen	type	Paratypes						
		♀	♀	♀	♀	♀	♀	♀
		collection	AMNH	AMNH	HUJ	HUJ	HUJ	HUJ
	accession no.			1251	1771	3251	3260	3274
Total length		54.4	56.0	62.0	53.6	60.3	56.6	58.0
Carapace	median ocelli	2.5	2.6	2.6	2.2	2.5	2.4	2.5
	length	5.6	5.7	6.2	5.4	5.8	5.6	5.9
	anterior width	2.8	3.0	3.8	3.2	3.7	3.4	3.6
	posterior width	6.3	6.4	7.0	6.0	6.9	6.5	7.4
Tergite I	length	0.9	0.8	1.0	0.9	0.9	0.8	1.0
Tergite II	length	1.2	1.2	1.2	1.1	1.3	1.3	1.2
Tergite III	length	1.6	1.7	1.7	1.6	1.7	1.5	1.6
Tergite IV	length	1.8	1.9	2.2	1.9	2.0	2.0	2.0
Tergite V	length	2.1	2.0	2.4	1.9	2.2	2.1	2.1
Tergite VI	length	2.3	2.3	2.6	2.0	2.4	2.2	2.3
Tergite VII	length	4.1	4.1	4.5	4.1	4.3	4.1	4.3
Sternite VII	length	3.8	3.6	4.3	3.0	3.7	3.5	3.7
	width	6.1	6.1	6.3	5.4	6.8	5.6	6.2
Metasoma I	length	5.0	5.0	5.4	4.7	5.5	4.9	5.4
	width	3.4	3.6	3.6	3.0	3.6	3.3	3.5
	height	2.8	3.0	3.1	2.4	2.9	2.7	2.8
Metasoma II	length	4.9	5.6	6.5	5.2	6.1	5.6	5.8
	width	3.0	3.5	3.3	2.8	3.2	3.2	3.2
	height	2.8	2.9	2.9	2.4	2.9	2.7	2.8
Metasoma III	length	5.7	5.7	6.6	5.6	6.3	5.8	6.1
	width	3.0	3.2	3.2	2.6	3.2	3.0	3.0
	height	2.7	3.0	2.8	2.4	2.8	2.6	2.8
Metasoma IV	length	5.9	6.0	6.7	5.6	6.5	6.0	6.1
	width	2.5	2.6	2.7	2.2	2.8	2.5	2.6
	height	2.3	2.5	2.6	2.1	2.4	2.2	2.5
Metasoma V	length	6.5	6.6	7.8	7.2	7.9	7.6	7.6
	width	2.5	2.7	2.7	2.4	2.5	2.4	2.6
	height	2.1	2.6	2.4	2.1	2.3	2.2	2.3
Telson	vesicle length	3.1	3.4	3.4	3.0	3.1	3.2	3.1
	vesicle width	1.9	2.0	1.9	1.8	2.0	1.9	1.9
	vesicle height	1.9	2.0	1.9	1.8	2.0	1.8	2.0
	aculeus length	3.8	3.8	4.0	3.4	4.4	4.0	3.7
Femur	length	4.6	4.7	5.3	4.7	5.0	4.6	4.7
	width	1.5	1.5	1.7	1.3	1.5	1.4	1.6
	height	1.2	1.1	1.4	1.1	1.1	1.0	1.2

TABLE 11 *continued*

Specimen	type	Paratypes						
		sex		♀		♀		
		collection		AMNH	AMNH	HUJ	HUJ	HUJ
		accession no.			1251	1771	3251	3260
Patella	length	5.5	5.8	6.8	6.1	6.4	6.2	6.2
	width	1.9	2.1	2.1	1.8	2.1	1.9	2.1
	height	1.4	1.6	1.7	1.4	1.5	1.5	1.6
Chela	total length	8.3	8.4	9.1	8.2	8.7	8.3	8.4
	manus width	1.3	1.6	1.6	1.3	1.4	1.4	1.4
	manus height	1.7	1.7	1.8	1.4	1.7	1.5	1.6
	retroventral carina	2.6	2.7	2.8	2.3	2.5	2.4	2.6
	movable finger	5.5	5.2	6.1	5.3	5.7	5.1	5.4
Pectines	total length	6.3	5.9	7.5	6.2	6.6	5.9	6.3
	dentate margin	5.7	5.5	7.2	5.7	5.7	5.7	5.9

restricted to posterior two-thirds of segment I; costate-granular, extending entire length of II–IV; serrate, comprising spiniform granules of variable size, becoming more prominent posteriorly, on V. Ventrosubmedian carinae distinct, costate on segment I; granular, with granules becoming progressively larger and subspiniform posteriorly on II and III; costate-granular along entire length of IV; granular, restricted to anterior three-quarters of V. Ventromedian carina granular, distinct along entire length of segment V. Dorsal and lateral intercarinal surfaces smooth to finely and sparsely granular on segment I, smooth on II–V; ventral intercarinal surfaces smooth on I and III, finely granular on IV, finely and densely granular across entire surface of V.

**Telson:** Telson vesicle width:metasomal segment V width, 77.2% (71.9%–79.9%,  $n = 8$ ) (♂) or 79.5% (73.7%–85.6%,  $n = 10$ ) (♀). Vesicle globose, dorsal surface concave, ventral surface convex and angular; vesicle height:length, 58.5% (44.7%–63.5%,  $n = 8$ ) (♂) or 65.6% (56.4%–76.8%,  $n = 10$ ) (♀); dorsal and ventral surfaces smooth and glabrous; lateral and ventral surfaces sparsely setose, with 19 (♂) or 24 ( $n = 3$ ) (♀) macrosetae. Aculeus long, gently curved; aculeus length:telson length, 50.1% (43.1%–53.6%,  $n = 8$ ) (♂) or 55% (51%–60.4%,  $n = 10$ ) (♀).

**Sexual dimorphism:** Adult males and females differ as follows. The carinae of the pedipalp femur and patella are more coarsely granular in the male than in the female. The pedipalp chela manus of the male is markedly broader and deeper with proportionally shorter fingers, than that of the female (fig. 47), as indicated by the higher ratios of chela manus width:length and manus length:movable finger length, respectively 59% and 84.4% in the male compared with 54.1% and 54.1% in the female. The genital opercula are completely divided longitudinally, with overlapping, rounded margins in the male but partially fused longitudinally in the female (fig. 20A, B) and genital papillae are present in the male but absent in the female. The pectinal tooth count is higher in the male (26–35) than in the female (22–27). The spiniform granules of the ventrosubmedian and ventrolateral carinae of metasomal segments II and III, and the ventrolateral carinae of segment V are less prominent in the male than in the female.

**DISTRIBUTION:** The known distribution of *B. nitzani* extends from the Sorek (Rubin) River, which appears to be the northern limit of the distribution of *Buthacus* on the Mediterranean coast, throughout the sand dunes of the southern coastal plain of Israel, to the Haluza dunes of the interior (fig. 7). The species probably also occurs

in the Gaza Strip and adjacent Sinai Peninsula of Egypt. The known records range from 17 m to 340 m in elevation.

*Buthacus nitzani* is allopatric with the closely related *B. amitaii*, endemic to the inland sandy soils and loess of the Yamin Plain and Mamshit area in the northern Negev, Israel (fig. 7), and *B. leptochelys*, distributed from the western Sinai Peninsula across Egypt, and southward along the coast of the Red Sea to Sudan (fig. 6).

**ECOLOGY:** Specimens of *B. nitzani* were collected at night with UV light detection on semi-consolidated to stable yellowish-white, partially vegetated to vegetationless coastal and inland sand dunes. Specimens were usually fairly common, mostly sitting still in open areas, some walking on the ground or resting on bushes. The habitat and habitus, notably the pale coloration, smooth tegument, loss or obsolescence of pedipalpal and metasomal carinae, elongation of the legs, especially legs III and IV, dorsoventral compression of the basitarsi of legs I–III, comblike rows of elongated macrosetae ("sand combs") along the retrolateral margins of the tibae and the pro- and retrolateral margins of the basitarsi of legs I–III, elongated macrosetae on the lateral and ventral surfaces of the telotarsi, and elongated, unequal length telotarsal unguis, are consistent with the ultrasammophilous ecomorphotype (Prendini, 2001).

*Buthacus nitzani* was collected in sympatry with *B. levyi* and three other buthids, *Androctonus amoreuxi*, *Buthus israelis*, and *Orthochirus scrobiculosus* at Be'er Milka. In addition to these species, it is sympatric with *Androctonus bicolor* and *Androctonus crassicauda* in the Haluza sand dunes and along the coastal plain.

**REMARKS:** According to Levy et al. (1973) and Levy and Amitai (1980), the subspecies *B. leptochelys nitzani* is restricted to the sand dunes of the central Negev in Israel, and no connection was found to the nominotypical population of *B. leptochelys*, extending from the Egyptian mainland, across the Sinai Peninsula to the Gaza Strip and southern coastline of Israel. Several authors have suggested that *B. l.*

*nitzani* is synonymous with other species, however. Kovařík (2005) synonymized *B. l. nitzani* with the nominotypical form of *B. leptochelys*, whereas Lourenço (2006) suggested it could be synonymous with *B. tadmorensis*.

During the present investigation, examination of the types of *B. leptochelys* and *B. l. nitzani*, as well as material from Egypt, including the Sinai Peninsula, and Israel, demonstrated that *B. nitzani* is a valid species, distinct from both *B. leptochelys* and *B. tadmorensis*, the latter revalidated in accordance with previous authors, e.g., Birula (1908), Kinzelbach (1985), and Lourenço (2006) (see below). This finding is also strongly supported, for both sexes, by multivariate analysis of morphometrics (fig. 14). *Buthacus nitzani* Levy et al., 1973, stat. nov., is therefore elevated to the rank of species.

**MATERIAL EXAMINED: ISRAEL: Mezor HaDrorom (Southern District):** Ashdod Nizzanim Nature Reserve, near Nizzan, 31°44'09"N 34°37'11.4"E, 17 m, 29.viii.2011, L. Prendini and T.L. Bird, 5 ♂, 5 ♀ (AMNH), 3 juv. ♂, 3 juv. ♀ (AMCC [LP 11174]); Ashdod Nizzanim Nature Reserve, 750 m W of turnoff to Nizzanim Military Base, 31°44'06.7"N 34°37'02.4"E, 17 m, 6.viii.2016, E. Gefen and S. Cain, 1 ♀ (HUJ INVSC3214), 1 subad. ♀ (AMCC [LP 15049] ex HUJ INVSC 3213); Ashdod Nizzanim Nature Reserve, dunes N of Nizzan, 31°45'16.0"N 34°38'06.8"E, 39 m, 9.viii.2016, A. Allon, M. Lugassi, S. Livne, and S. Cain, 3 ♂ (AMCC [LP 15051, 15052] ex HUJ INVSC 3219, 3220, HUJ INVSC 3215), 3 ♀ (AMCC [LP 15050] ex HUJ INVSC 3218, HUJ INVSC 3216, 3217), 1.vi.2017, S. Cain, 1 ♀ (HUJ INVSC 3208); Ashdod, the Great Dune, N part of Ashdod Nizzanim Nature Reserve, 31°46'18.3"N 34°39'09.7"E, 43 m, 22.viii.2017, I. Ofer and S. Cain, 2 ♂ (AMNH ex HUJ INVSC 3210, 3212), 2 ♀ (AMCC [LP 15048] ex HUJ INVSC 3211, HUJ INVSC 3209); Ashdod, sand dune at corner of Ben Gurion Ave. and Sderot Herzl, 31°48'53.5"N 34°39'11.3"E, 18 m, 22.viii.2017, I. Ofer and S. Cain, 2 ♂ (AMCC [LP 15054] ex HUJ INVSC 3234, HUJ INVSC 3232), 3 ♀ (AMNH ex HUJ INVSC 3231, HUJ INVSC 3230, 3233); Ashqelon, S of Carlsberg Brewery, E of Ha-Tokhen St., 31°37'50.7"N 34°32'46.3"E, 31 m,

23.viii.2017, S. Cain, 3 ♂ (HUJ INVSC 3227–3229), 2 ♀ (AMCC [LP 15056] ex HUJ INVSC 3225, HUJ INVSC 3226); Holot Haluza sand dunes, Gevulot [31°06'N 34°48'E], 329 m, 20.iii.1969, I. Israeli, 1 ♀ (HUJ INVSC 1330); Holot Haluza sand dunes, Revivim, 31°05'N 34°41'E, 252 m, 27.vii.1970, G. Levy, P. Amitai, and A. Shulov, 2 ♂ (HUJ INVSC 1989, 1991), 1 ♀ (HUJ INVSC 1990); Holot Haluza sand dunes, 3.1 km N of turnoff to Retamim on road Revivim–Ze'elim, 31°04'32"N 34°40'33.1"E, 248 m, 27.viii.2011, L. Prendini and T.L. Bird, 15 ♂, 5 ♀ (AMNH), 1 juv. ♂ (AMCC [LP 11175]); Holot Haluza sand dunes, 2.2 km N of turnoff to Retamim on road Revivim–Ze'elim, 31°04'16.5"N 34°41'55.1"E, 259 m, 5.viii.2016, E. Gefen and S. Cain, 5 ♂ (AMCC [LP 15057, 15058] ex HUJ INVSC 3239, 3240, HUJ INVSC 3236–3238), 31.vii.2017, S. Cain, 6 ♂ (AMCC [LP 15059, 15060] ex HUJ INVSC 3241, 3246, AMNH ex HUJ INVSC 3243, HUJ INVSC 3242, 3244, 3245); Holot Haluza sand dunes, 12.5 km N of turnoff to Retamim on road Revivim–Ze'elim, 31°08'10.1"N 34°37'16.0"E, 205 m, 5.viii.2016, E. Gefen and S. Cain, 1 ♂ (AMCC [LP 15053] ex HUJ INVSC 3235); Holot Haluza sand dunes, E of Be'er Milka, 30°55'42.57"N 34°24'41.95"E, 213 m, 23.iv.2017, S. Talal and Oranim students, 2 ♀ (AMCC [LP 15061] ex HUJ INVSC 3247, AMNH ex HUJ INVSC 3262), 25.v.2017, Y. Zvik and S. Cain, 3 ♀ (AMCC [LP 15062] ex HUJ INVSC 3250, HUJ INVSC 3248, 3249), 31.vii.2017, S. Cain, 1 ♀ (HUJ INVSC 3280), 15.iv.2018, Y. Zvik and S. Cain, 6 ♀ (HUJ INVSC 3388–3392, 3395), 4 subad. ♀ (HUJ INVSC 3393, 3394, 3397, 3398), 2 juv. ♀ (HUJ INVSC 3396, 3399); Holot Haluza sand dunes, 4.5 km S of Ramat Hovav factory, W of road 40, 31°05'32.7"N 34°49'01.6"E, 340 m, 16.iv.2018, Y. Zvik and S. Cain, 7 ♀ (HUJ INVSC 3450–3456), 2 subad. ♀ (HUJ INVSC 3457, 3458), 1 juv. ♂ (HUJ INVSC 3461), 2 juv. ♀ (HUJ INVSC 3459, 3460); Mashabbim sand dunes, between Mashabei Sade and Revivim on road 222, 31°05'00.8"N 34°41'11.0"E, 246 m, 27.viii.2013, L. Prendini, Y. Lubin, E. Gavish-Regev, E. Gefenl, and Israel Taxonomy Initiative scorpion course participants, 24 ♂, 1 ♀ (AMNH), 1 juv. ♀ (AMCC [LP 12200]);

Palmahim sand dunes, E of Palmahim air base, 31°54'39.4"N 34°43'31.8"E, 19 m, 22.viii.2017, I. Ofer, N. Braun and S. Cain, 2 ♂ (AMCC [LP 15055] ex HUJ INVSC 3222, HUJ INVSC 3224), 2 ♀ (AMNH ex HUJ INVSC 3221, HUJ INVSC 3223).

*Buthacus tadmorensis* (Simon, 1892), stat. rev.

Figures 10, 15, 16C, D, 19C, D, 21H, 22E, 23B, 25B, 27B, 29E, 48, 49, 50; tables 1, 4, 9

*Buthus tadmorensis* Simon, 1892: 84; Kraepelin, 1895: 82; Birula, 1905: 136–138; Werner, 1936b: 204.

*Buthacus leptochelys*: Kraepelin, 1899: 17; Pringle, 1960: 76, fig. 2; L. Khalaf, 1962: 1, 2; K.I. Khalaf, 1963: 59; Levy et al., 1973: 126; Levy and Amitai, 1980: 77, 82; Fet and Lowe, 2000: 82; Dehghani and Kassiri, 2018: S881.

*Buthus (Buthacus) tadmorensis*: Birula, 1908: 140; 1910: 172, 173; 1917: 23, 214, 229.

*Buthus pietschmanni* Penther, 1912: 112–114, fig.; Vachon, 1966: 211; Kachel et al., 2021: 2, 3; syn. nov.

*Buthus (Buthacus) leptochelys*: Whittick, 1947: 122; 1955: [unpaginated] (part).

*Buthacus tadmorensis*: Vachon, 1948: 475; 1966: 210; Habibi, 1971: 43; Pérez, 1974: 19; Kinzelbach, 1984: 101; 1985: map III; El-Hennawy, 1992: 101, 114 (part); Kovařík, 1997a: 49; 1998: 105; Kovařík and Whitman, 2004: 106 (misidentification, part); Lourenço, 2006: 63, 64, 69, figs. 17, 18, 42; Lourenço and Qi, 2006a: 161, 162; Lourenço and Leguin, 2009: 103, 104; Shehab et al., 2011: 333–340, fig. 2E, tables 1, 2; Dehghani and Kassiri, 2018: S881; Lowe et al., 2019: 5.

*Buthacus yotvatensis*: Levy et al., 1973: 134 (misidentification).

*Buthacus tadmorensis tadmorensis*: Kinzelbach, 1985: map III; Kovařík, 2002: 5.

*Mesobuthus pietschmanni*: El-Hennawy, 1992: 101, 128.

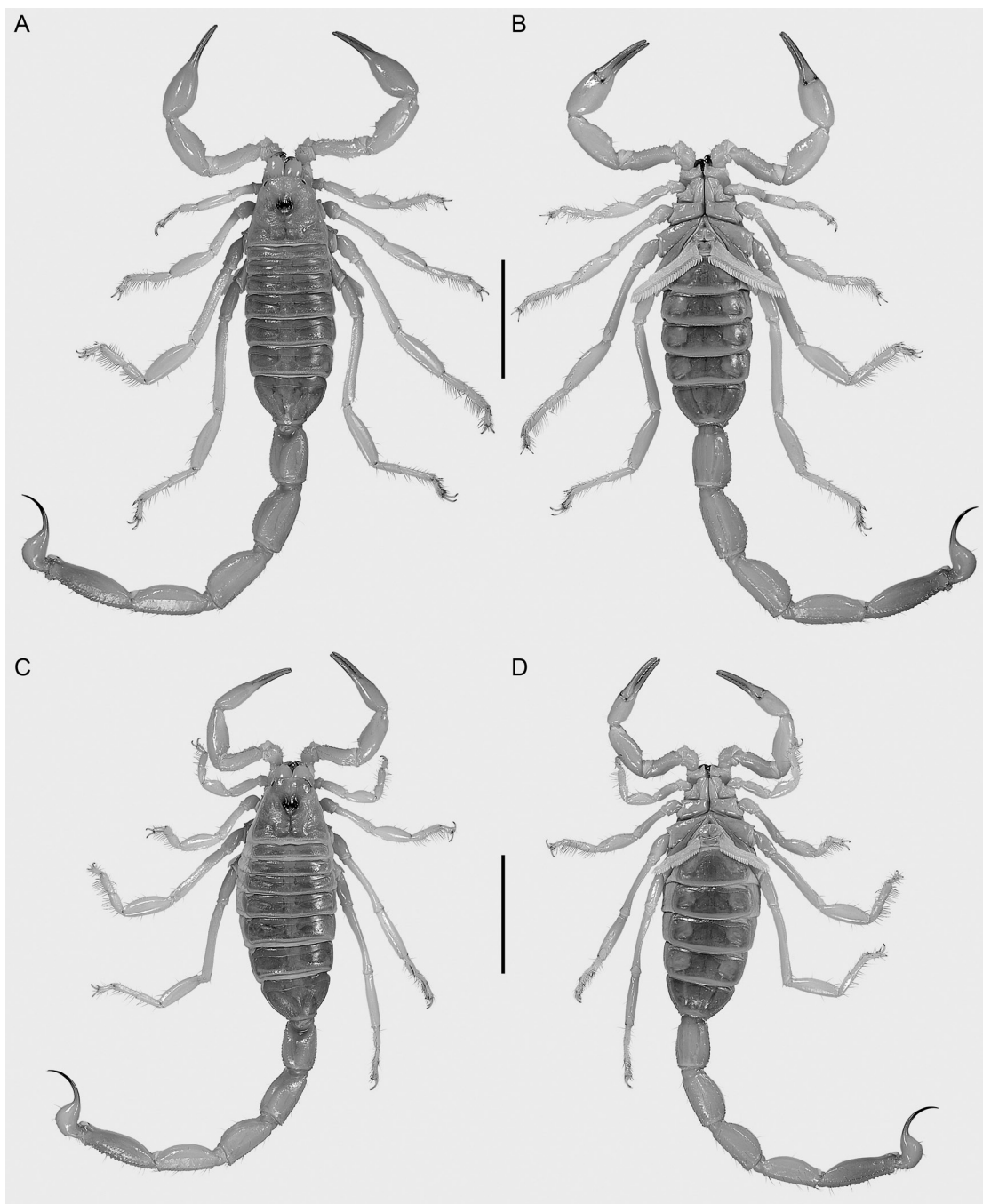


FIGURE 45. *Buthacus nitzani* Levy et al., 1973, stat. nov., habitus, dorsal (A, C), and ventral (B, D) aspects. **A, B.** ♂ (HUJ INVSC 3227). **C, D.** ♀ (HUJ INVSC 3226). Scale bars = 1 cm.

*Buthacus tadmorensis yotvatensis*: El-Hennawy, 1992: 101, 114 (misidentification); Kabakibi et al., 1999: 82, 88 (misidentification).

*Buthacus macrocentrus*: Kovařík, 2005: 1, 7; Lourenço and Qi, 2006a: 161; Kaltsas et al., 2008: 214; Navidpour et al., 2008: 1, 3–8, 28, 30, 35, figs. 3, 6, 12, 56–59; Yağmur et al., 2008: 13–17, figs. 2, 4; Mirshamsi et al., 2011: 17, 24, 26, fig. 1A, table 1; Navidpour et al., 2013: 1, 3–5, 21, figs. 2, 4; Loria and Prendini, 2014: 9, 10, fig. 2C; Caliskan, 2015: 327–332, 336, 337, 343, figs. 1, 3, 5B; Navidpour, 2015: 10, 11; Kovařík et al., 2016: 1; Sharifinia et al., 2017: 232, 233, 235, 236, table 2; Dehghani and Kassiri, 2018: S881; Al-Khzali and Yağmur, 2019: 85–87, fig. 2C (misidentification); Koç et al., 2019: 108–112, figs. 1, 5–7, table 1; Hussen and Ahmed, 2020: 6711–6713, 6715, 6716, 6718, 6719, 6722, 6723, figs. 1, 7, tables 1, 2; Alqahtani and Badry, 2021: 10; Amr et al., 2021: 85, 87, 89, 90, 97, tables 3, 10; Mansouri et al., 2021: 763, 765, 767, table 2; Kachel et al., 2021: 2, 3, 5, 7, table 1.

*Buthacus yotvatensis*: Crucitti and Vignoli, 2002: 438–440, fig. 3 (misidentification).

**TYPE MATERIAL:** *Butthus pietschmanni*: **IRAQ:** Saladin Governorate: Lectotype ♂, 1 ♀, 1 juv. ♂, 2 juv. ♀ paralectotypes (NHMW 2453), Mesopotamien, Kal'at Shergat [Qa'lāt Sherqat, 35°27'N 43°16'E], 11.v.1910, Pietschmann [examined]; 3 ♀, 1 subad. ♀, 3 juv. ♀ paralectotypes (NHMW 2452), Mesopotamien, Assur [Aššur/Ashur, 35°27'N 43°16'E], 19.v.1910, Pietschmann [examined]. *Butthus tadmorensis*: 1 ♂, 1 ♀ syntypes (MNHN). **SYRIA:** Homs Governorate: Palmira [Palmyra/Tadmur/Tadmor, 34°34'N 38°17'E].

**DIAGNOSIS:** *Buthacus tadmorensis* differs from the closely related *B. arava* and *B. yotvatensis*, occurring in Israel and Jordan, as follows. The ventrosubmedian and ventrolateral carinae of metasomal segments II and III, and ventrolateral carinae of segment V are well developed, with

broad, lobate processes posteriorly, in *B. tadmorensis*, but weakly developed, with narrow, spiniform processes posteriorly, in the other species (figs. 25A, B, C, 27A, B, C).

*Buthacus tadmorensis* differs further from *B. arava*, as follows. The pedipalp chela of *B. tadmorensis* is longer and narrower, especially in the adult male (fig. 50A, B), with chela manus width:chela length, 22.3% (♂) (table 4), chela manus length:movable finger length, 64.2% (♂) or 55% (51.9%–59.8%, n = 4) (♀), and chela manus width:length, 58.7% (♂) or 59.1% (53.8%–65.1%, n = 4) (♀), than that of *B. arava* (fig. 35A, B), with chela manus width:chela length, 29.8% (27.2%–32.8%, n = 7; table 8) (♂), chela manus length:movable finger length, 90.4% (83.5%–95%, n = 7) or 60.8% (♀), and chela manus width:length, 63.3% (57.3%–74.5%, n = 7) or 61.6% (♀). Additionally, the unguis of the leg telotarsi are shorter (approximately two-thirds the length of the telotarsus) and equal on legs I and II in *B. tadmorensis* (fig. 22E) but longer (approximately equal to the length of the telotarsus) and unequal on legs I and II in *B. arava* (fig. 22C). The pectinal tooth counts are higher in *B. tadmorensis*, i.e., 30/32 (♂) (table 9) and 24/25 (23–26/23–26, n = 3) (♀), than in *B. arava*, i.e., 20/20 (18–21/18–22, n = 7; table 9) (♂) and 12/13 (♀). The metasomal segments and telson are densely setose in *B. tadmorensis* (figs. 23B, 25B, 29E), with macrosetal counts on segments I–V (sinistral/dextral), dorsosubmedian carinae, 10/11 (8–12/10–12, n = 2):19/23 (18–19/21–24):23/23 (23–23/21–25):19/20 (17–20/19–21):9/9 (7–11/7–11), dorsolateral carinae, 6/6 (4–8/5–6):11/13 (8–13/11–15):9/11 (8–9/10–11):9/9 (8–9/6–12):9/9 (8–10/8–10), and telson, 100 (80–120, n = 2), but sparsely setose in *B. arava* (figs. 23A, 25A, 29C), with macrosetal counts on segments I–V (sinistral/dextral), dorsosubmedian carinae, 0/0 (0–1/0–1, n = 4):2/3 (2–3/2–5):4/3 (2–5/2–6):3/3 (2–3/1–5):0/0 (0–0/0–0), dorsolateral carinae, 1/1 (0–2/0–2):2/2 (1–3/0–3):3/2 (2–4/1–3):3/3 (2–4/2–5):5/6 (3–8/5–7), and telson, 28 (27–29, n = 4).



FIGURE 46. *Buthacus nitzani* Levy et al., 1973, stat. nov., ♂ (HUJ INVSC 3227), dextral pedipalp femur (A, B) and patella (C, E), prolateral (A, C), dorsal (B, D), and retrolateral (E) aspects. Scale bar = 2 mm.

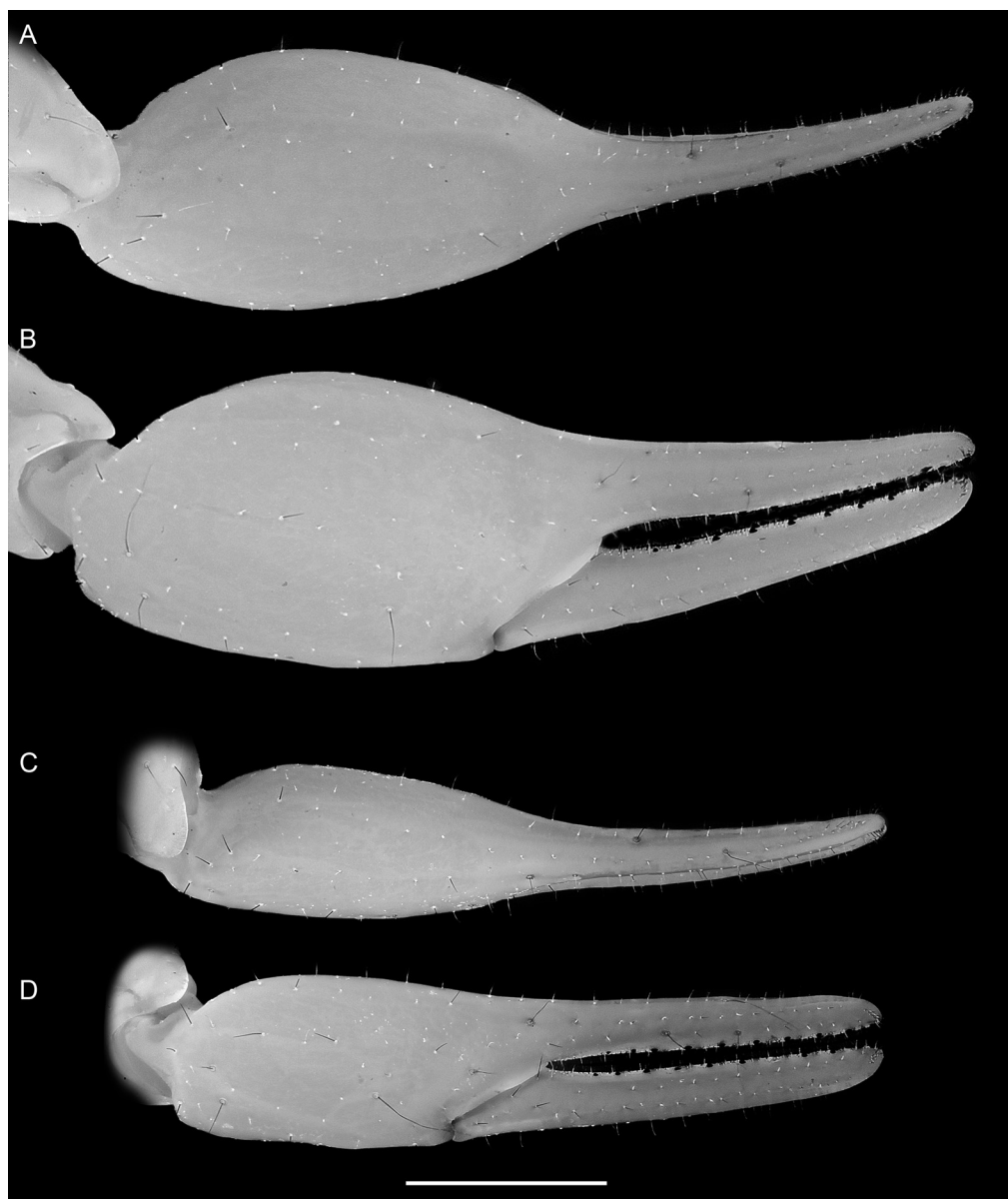


FIGURE 47. *Buthacus nitzani* Levy et al., 1973, stat. nov., dextral pedipalp chela, dorsal (A, C) and retrolateral (B, D) aspects. A, B. ♂ (HUJ INVSC 3227). C, D. ♀ (HUJ INVSC 3226). Scale bar = 2 mm.

*Buthacus tadmorensis* differs further from *B. yotvatensis*, as follows. The pedipalp chela of *B. tadmorensis* is shorter and broader (fig. 50A, B), with chela manus width:chela length, 22.3% ( $\delta$ ) (table 4), chela manus length:movable finger length, 64.2% ( $\delta$ ) or 55% (51.9%–59.8%,  $n = 4$ ) ( $\varphi$ ), and chela manus width:length, 58.7% ( $\delta$ ) or 59.1% (53.8%–65.1%,  $n = 4$ ) ( $\varphi$ ), than that of *B. yotvatensis* (fig. 53A, B), with chela manus width:chela length, 17.4% (16.5%–18.8%,  $n = 8$ ; table 6) ( $\delta$ ), chela manus length:movable finger length, 55.2% (51.7%–58.3%,  $n = 8$ ) ( $\delta$ ) or 47.1% (45.5%–48%,  $n = 6$ ; table 7) ( $\varphi$ ), and chela manus width:length, 50.5% (48.1%–54.8%,  $n = 8$ ) ( $\delta$ ) or 56.9% (51.3%–61.5%,  $n = 6$ ) ( $\varphi$ ). The telson ventral surface is densely granular anteriorly in *B. tadmorensis* but sparsely granular anteriorly in *B. yotvatensis* (fig. 29E, G).

**DESCRIPTION:** The following description is based on the type material of *B. pietschmanni* and additional material examined (see table 4 for measurements and table 9 for counts).

**Total length:** Large scorpions, 66.8 mm ( $\delta$ ) or 70.2 mm (66.3–75.2 mm) ( $\varphi$ ).

**Color:** Uniformly yellowish olive with pale yellow legs and whitish pectines.

**Carapace:** Carapace shape trapezoidal (fig. 16C, D), anterior width:posterior width, 47.8% (44%–53.1%,  $n = 5$ ), length:posterior width, 86.7% (82.2%–92.8%,  $n = 5$ ). Five, rarely four, pairs of lateral ocelli; each lateral ocular tubercle with three major ocelli (ALMa, MLMa, PLMa), similar in size, situated anterolaterally, and one or, usually, two minor ocelli (ADMi, PDMi; PDMi may be absent) situated posterodorsal to posterior major ocellus. Median ocelli larger than lateral ocelli, distance between them more than 2 $\times$  ocellus width. Median ocular tubercle situated anteromedially, distance from anterior carapace margin:carapace length, 48% ( $\delta$ ) or 47.1% (45.2%–49.4%,  $n = 4$ ) ( $\varphi$ ). Superciliary and central median carinae distinct, costate-granular and disconnected to weakly connected. Anteromedian sulcus distinct, deep; posteromedian sulcus deep, narrow anteriorly, wide poste-

riorly; posterolateral sulcus deep, wide, curved. Carapace intercarinal surfaces coarsely and densely granular.

**Chelicerae:** Cheliceral manus prodorsal margin finely granular; retrodorsal surfaces smooth or finely granular; prolateral and ventral surfaces setose. Fixed finger dorsal surface setose; dorsal margin with subdistal, medial, and proximal denticles; ventral margin with proximal and medial denticles. Movable finger smooth and glabrous; dorsal margin with retrodistal, subdistal, medial, and pair of proximal denticles; ventral margin with prodistal, medial, and proximal denticles.

**Pedipalps:** Femur dorsal prolateral, dorsal retrolateral, and ventral prolateral carinae complete, costate-granular; prolateral ventral and prolateral ventrosubmedian carinae each comprising discontinuous row of spiniform granules; retrolateral dorsosubmedian carina obsolete, comprising discontinuous row of spiniform granules and more than 15 macrosetae; dorsal, prolateral, and ventral intercarinal surfaces finely granular; retrolateral intercarinal surfaces smooth (fig. 49A, B). Patella prolateral median and ventral prolateral carinae complete, costate-granular to finely serrate; dorsal prolateral carinae complete, costate-granular; other carinae obsolete; intercarinal surfaces smooth (fig. 49C–E). Chela long and slender in both sexes, manus width:length, 58.7% ( $\delta$ ) or 59.1% (53.8%–65.1%,  $n = 4$ ) ( $\varphi$ ), manus height:length, 67.4% ( $\delta$ ) or 67.7% (59.2%–70.8%,  $n = 4$ ) ( $\varphi$ ), and manus length:movable finger length, 64.2% ( $\delta$ ) or 55% (51.9%–59.8%,  $n = 4$ ) ( $\varphi$ ). Chela manus acarinate; intercarinal surfaces smooth and setose (fig. 50). Fixed and movable fingers respectively with 8–10 ( $n = 5$ ) and 9–11 ( $n = 5$ ) oblique median denticle subrows; movable finger with 8–10 ( $n = 5$ ) retrolateral accessory denticles (fig. 21H); proximal dentate margins of fingers sublinear (fig. 50B), such that no gap evident proximally when fingers closed.

**Legs:** Legs I–IV, femoral ventral carinae granular; patellar ventral carinae obsolete; intercarinal surfaces smooth. Legs I–IV, tibial spurs

absent on I and II, present on III and IV; pro- and retroventral basitarsal (pedal) spurs present, more developed on III and IV. Legs I–IV, macrosetal counts on retrolateral margins of tibiae, 9:13:12:5; basitarsi, 13:18:21:8; telotarsi, 7:7:6:5 ( $n = 1$ ). Telotarsi unguis short, approximately equal to three-quarters of telotarsus length, equal on legs I–IV (fig. 22E).

**Genital operculum:** Genital opercula suboval, completely divided longitudinally, without overlapping, rounded margins ( $\delta$ ) or partially fused longitudinally ( $\varphi$ ) (fig. 19C, D). Genital papillae present ( $\delta$ ) or absent ( $\varphi$ ).

**Pectines:** Three marginal lamellae; 12 ( $\delta$ ) or 9–12 ( $n = 4$ ) ( $\varphi$ ) median lamellae (fig. 19C, D). Fulcra present. Pectinal teeth along part of length, dentate margin length:pecten length, 89.7% ( $\delta$ ) or 84.4% (81.5%–87.7%,  $n = 4$ ) ( $\varphi$ ). Pectinal teeth curved, similar in size; tooth count (sinistral/dextral), 30/32 ( $\delta$ ) or 24/25 (23–26/23–26,  $n = 3$ ) ( $\varphi$ ).

**Mesosoma:** Tergites I–VII progressively increasing in length posteriorly, tergite VI length:tergite VII length, 56.5% ( $\delta$ ) or 60.7% (55.3%–65.1%,  $n = 4$ ) ( $\varphi$ ); increasing in width posteriorly from I–IV, decreasing in width posteriorly from V–VII. Pretergites smooth; posttergites I–VI, intercarinal surfaces uniformly finely granular, becoming more coarsely and densely granular posteriorly, VII, finely to coarsely and sparsely granular. Tergites I–VI, dorsomedian carinae smooth, vestigial, restricted to posterior half of I, granular, complete on II–VI; dorsosubmedian carinae granular, vestigial, restricted to posterior fifth of I–V and posterior half of VI. Tergite VII, dorsomedian carina obsolete, granular, dorsosubmedian and dorsolateral carinae distinct, granular. Sternites III–VII smooth and glabrous; III–VI acarinate, VII, ventrosubmedian and ventrolateral carinae obsolete, smooth; IV–VI, respiratory spiracles (stigmata) width approximately 3× length.

**Metasoma:** Metasomal segments I–V becoming longer and narrower posteriorly (fig. 23B, 25B, 27B), segment I shortest, length I:II, 90.5%

( $\delta$ ) or 92.2% (89.9%–95.3%,  $n = 4$ ) ( $\varphi$ ); segments II and III similar, length II:III, 100.5% ( $\delta$ ) or 97.6% (97.1%–98%,  $n = 4$ ) ( $\varphi$ ); segments IV longer, length III:IV, 92.4% ( $\delta$ ) or 94.4% (92.7%–96.7%,  $n = 4$ ) ( $\varphi$ ); segment V longest, length IV:V, 94.7% ( $\delta$ ) or 88.9% (86.7%–90.2%,  $n = 4$ ) ( $\varphi$ ); width:length segment I, 70.5% ( $\delta$ ) or 71.4% (67.8%–76.2%,  $n = 4$ ) ( $\varphi$ ), II, 60.1% ( $\delta$ ) or 62.1% (60.1%–64.7%,  $n = 4$ ) ( $\varphi$ ), III, 57.9% ( $\delta$ ) or 58.6% (55.2%–63.1%,  $n = 4$ ) ( $\varphi$ ), IV, 48.3% ( $\delta$ ) or 49.2% (48.9%–49.4%,  $n = 4$ ) ( $\varphi$ ), V, 42.1% ( $\delta$ ) or 42.7% (40.9%–43.9%,  $n = 4$ ) ( $\varphi$ ); dorsosubmedian and dorsolateral carinae distinct, granular on segments I–III, obsolete on IV, absent on V; dorsosubmedian and dorsolateral carinae densely setose, macrosetal counts on segments I–V (sinistral/dextral), dorsosubmedian carinae, 10/11 (8/10–12/12,  $n = 2$ ):19/23 (18/21–19/24):23/23 (23/21–23/25):19/20 (17/19–20/21):9/9 (7/7–11/11), dorsolateral carinae, 6/6 (4/5–8/6,  $n = 2$ ):11/13 (8/11–13/15):9/11 (8/10–9/11):9/9 (8/6–9/12):9/9 (8/8–10/10). Median lateral carinae distinct, granular in posterior two-thirds of segment I, posterior half of II and posterior third of III, absent on IV and V. Ventrolateral carinae distinct, weakly granular on segment I; costate-granular to serrate, with granules becoming progressively larger and spiniform posteriorly, on II and III; costate-granular on IV; serrate, comprising spiniform granules of variable size and lobate processes posteriorly, on V. Ventrosubmedian carinae distinct, weakly granular on segment I, costate-granular to serrate, with granules becoming progressively larger and spiniform to lobate posteriorly, on II and III; costate-granular on IV, granular, restricted to anterior three-quarters of V. Ventromedian carina granular, distinct along entire length of segment V. Dorsal and lateral intercarinal surfaces matte and punctate on segments I–V; ventral intercarinal surfaces smooth on I and II, finely granular across entire surface on III–V.

**Telson:** Telson vesicle width:metasomal segment V width, 76.1% ( $\delta$ ) or 86.2% (83.4%–88%,  $n = 4$ ) ( $\varphi$ ). Vesicle globose, dorsal surface flat, ventral surface convex and rounded; vesicle

TABLE 12

**Measurement data for adult male *Buthacus nitzani* Levy et al., 1973, stat. nov. deposited in the National Natural History Collections, Hebrew University of Jerusalem (HUJ), Israel**

Measurements (mm) follow Tahir et al. (2014): total length (sum of carapace, tergites I–VII, metasomal segments I–V, and telson); carapace median ocelli (distance from carapace anterior margin); carapace anterior width (distance between lateral ocelli); chela total length (distance from base of condyle to tip of fixed finger); chela retroventral carina (length along manus retroventral carina); chela movable finger (movable finger length); pectines total length (length along retrolateral margin); pectines dentate margin (length along dentate margin).

Specimen	sex	♂	♂	♂	♂	♂	♂	♂	♂
	collection	HUJ							
	accession no.	3210	3220	3222	3224	3232	3234	3238	3245
Total length		47.5	51.0	56.3	51.8	58.5	54.5	55.2	49.5
Carapace	median ocelli	2.0	1.9	2.1	2.0	2.2	2.1	1.9	2.0
	length	4.6	4.9	5.2	5.0	5.6	5.4	5.2	4.8
	anterior width	2.6	2.9	3.1	2.8	3.6	2.9	3.1	2.9
	posterior width	4.7	5.3	5.9	5.2	6.3	5.8	5.8	5.1
Tergite I	length	0.8	0.7	0.9	0.8	1.0	0.9	1.0	0.8
Tergite II	length	1.0	1.1	1.1	1.2	1.4	1.0	1.2	1.0
Tergite III	length	1.4	1.3	1.4	1.4	1.6	1.5	1.6	1.2
Tergite IV	length	1.6	1.7	1.7	1.7	1.8	1.8	1.9	1.5
Tergite V	length	1.8	1.7	2.0	1.9	2.0	2.1	2.0	1.8
Tergite VI	length	1.9	1.9	2.2	2.0	2.3	2.2	2.1	1.9
Tergite VII	length	3.3	3.6	4.1	3.3	4.1	4.0	3.7	3.7
Sternite VII	length	2.9	2.8	3.4	3.4	3.9	3.6	3.5	3.0
	width	4.4	4.5	5.3	4.7	5.2	5.3	5.0	4.6
Metasoma I	length	4.1	4.7	5.2	4.9	5.2	5.0	5.0	4.3
	width	2.8	2.9	3.2	2.9	3.5	3.5	3.1	2.8
	height	2.3	2.5	2.7	2.7	3.0	2.8	2.7	2.4
Metasoma II	length	4.8	5.2	5.8	5.5	6.0	5.7	5.4	5.2
	width	2.7	2.8	3.1	2.9	3.3	3.3	3.1	2.8
	height	2.4	2.4	2.8	2.6	3.0	2.9	2.7	2.4
Metasoma III	length	4.9	5.5	5.9	5.5	6.2	5.7	5.5	5.2
	width	2.5	2.7	3.0	2.8	3.1	2.9	3.0	2.8
	height	2.3	2.3	2.6	2.6	2.7	2.7	2.5	2.3
Metasoma IV	length	5.3	5.7	6.2	5.9	6.4	5.9	5.9	5.3
	width	2.1	2.2	2.4	2.5	2.7	2.6	3.0	2.1
	height	2.1	2.1	2.3	2.2	2.3	2.4	2.0	1.9
Metasoma V	length	6.3	7.0	7.7	6.6	7.5	7.2	6.8	6.8
	width	2.1	2.2	2.4	2.3	2.7	2.6	2.4	2.3
	height	1.8	1.8	2.1	2.0	2.3	2.3	2.1	1.8
Telson	vesicle length	2.8	2.9	3.4	3.1	3.7	3.0	4.6	3.0
	vesicle width	1.6	1.8	1.9	1.8	2.1	1.9	1.9	1.8
	vesicle height	1.7	1.8	1.9	1.9	2.2	1.9	2.0	1.7
	aculeus length	2.9	3.3	3.6	2.9	3.8	3.1	3.5	3.2
Femur	length	3.9	4.2	4.4	4.3	4.7	4.6	4.4	3.9
	width	1.2	1.3	1.5	1.3	1.5	1.6	1.5	1.4
	height	1.2	1.1	1.0	1.0	1.3	1.2	1.1	1.3

TABLE 12 *continued*

Specimen	sex	♂	♂	♂	♂	♂	♂	♂
	collection	HUJ						
	accession no.	3210	3220	3222	3224	3232	3234	3245
Patella	length	4.7	5.3	5.6	5.3	5.8	5.4	4.5
	width	1.9	1.9	2.1	2.0	2.3	2.1	1.9
	height	1.5	1.4	1.6	1.5	1.9	1.6	1.4
Chela	total length	7.7	8.4	8.6	8.1	8.8	8.4	8.2
	manus width	2.1	2.2	1.9	2.1	2.5	2.2	2.1
	manus height	2.1	2.2	2.3	2.2	2.6	2.4	2.2
	retroventral carina	3.2	3.6	3.9	3.5	4.1	3.8	3.5
	movable finger	4.1	4.4	4.6	4.4	4.5	4.5	4.0
Pectines	total length	5.9	6.6	6.8	6.2	7.5	5.8	5.6
	dentate margin	5.7	6.2	6.7	6.3	7.4	5.7	5.3

height:length, 67.1% (♂) or 72.9% (65.4%–79.2%,  $n = 4$ ) (♀); dorsal surface smooth; entire ventral surface finely granular; lateral and ventral surfaces densely setose, with 80 (♂) or 120 (♀) ( $n = 2$ ) macrosetae. Aculeus long, gently curved; aculeus length:telson length, 47.2% (♂) or 51.7% (50.2%–53.7%,  $n = 4$ ) (♀).

**Sexual dimorphism:** Adult males and females differ as follows. The carinae of the pedipalp femur and patella are more coarsely granular in the male than in the female. The pedipalp chela of the male has proportionally shorter fingers than that of the female (fig. 50), as indicated by the higher chela manus length:movable finger length ratio in the male (64.2%) compared with the female (55%). The genital opercula are completely divided longitudinally, with overlapping, rounded margins in the male but partially fused longitudinally in the female (fig. 19C, D) and genital papillae are present in the male but absent in the female. The pectinal tooth count is higher in the male (30–32) than in the female (23–26). The spiniform granules of the ventrosubmedian and ventrolateral carinae of metasomal segments II and III, and the ventrolateral carinae of segment V are less prominent in the male than in the female.

**DISTRIBUTION:** *Buthacus tadmorensis* is widely distributed across the Fertile Crescent of the Middle East (fig. 10) from central Jordan,

through Syria, southeastern Turkey and Iraq, to the northern shore of the Persian Gulf, in southern Iran (Simon, 1892; Penther, 1912; El-Hennawy, 1992; Kabakibi et al., 1999; Crucitti and Vignoli, 2002; Kovařík and Whitman, 2004; Kovařík, 2005; Yağmur et al., 2008; Navidpour et al., 2008; Shehab et al., 2011; Sharifinia et al., 2017). The known distribution covers most of the drainage of the Tigris and Euphrates rivers. Records are located at elevations ranging from 13 m to 924 m (Navidpour et al., 2008; Shehab et al., 2011; Sharifinia et al., 2017).

*Buthacus tadmorensis* is allopatric with the closely related *B. arava* and *B. yotvatensis*, both endemic to the Arava Valley, straddling the southern border between Israel and Jordan (figs. 4, 5), and, in the case of *B. yotvatensis*, extending west into the Negev.

**ECOLOGY:** *Buthacus tadmorensis* inhabits loose to hard, compacted sandy habitats (Shehab et al., 2011). Specimens have been collected under stones or in pitfall traps on sparsely vegetated plains and wadis with hard soil and few to many stones (Shehab et al., 2011). The habitat and habitus, e.g., the pale coloration, lobate granules and processes posteriorly on the ventrosubmedian and ventrolateral carinae of metasomal segments II, III and V, dorsoventral compression of the basitarsi of legs I–III, with weakly developed comblike

TABLE 13

**Measurement for adult female *Buthacus nitzani* Levy et al., 1973, stat. nov., deposited in the National Natural History Collections, Hebrew University of Jerusalem (HUJ), Israel**

Measurements (mm) follow Tahir et al. (2014): total length (sum of carapace, tergites I–VII, metasomal segments I–V, and telson); carapace median ocelli (distance from carapace anterior margin); carapace anterior width (distance between lateral ocelli); chela total length (distance from base of condyle to tip of fixed finger); chela retroventral carina (length along manus retroventral carina); chela movable finger (movable finger length); pectines total length (length along retrolateral margin); pectines dentate margin (length along dentate margin).

Specimen	sex	♀	♀	♀	♀	♀	♀	♀	♀	♀	♀
	collection	HUJ									
	accession no.	3214	3218	3221	3225	3226	3230	3240	3247	3248	3249
Total length		54.6	49.1	53.9	47.4	51.3	46.6	44.4	48.9	44.4	45.8
Carapace	median ocelli	2.3	2.1	2.2	1.8	2.1	1.9	1.8	2.1	1.8	1.8
	length	5.5	4.8	5.4	4.6	5.0	4.3	4.3	5.0	4.6	4.5
	anterior width	3.4	3.0	3.3	2.8	2.9	2.8	2.5	3.0	2.9	2.7
	posterior width	6.6	5.4	5.9	5.6	6.1	5.7	4.8	5.4	6.0	5.1
Tergite I	length	1.0	0.8	0.9	0.9	0.9	0.9	0.8	0.9	1.1	0.8
Tergite II	length	1.3	1.0	1.4	1.2	1.1	1.0	1.0	1.2	1.2	0.8
Tergite III	length	1.6	1.5	1.4	1.4	1.4	1.3	1.2	1.7	1.4	1.3
Tergite IV	length	1.9	1.8	1.8	1.6	2.0	1.9	1.4	1.9	1.8	1.6
Tergite V	length	2.2	1.9	2.1	1.9	2.0	1.6	1.5	2.0	1.7	1.7
Tergite VI	length	2.4	2.1	2.6	1.7	2.2	1.9	1.6	2.1	2.0	1.9
Tergite VII	length	4.0	3.3	3.9	3.1	3.7	3.4	3.1	3.1	2.8	3.6
Sternite VII	length	3.6	3.2	3.0	2.6	3.4	2.9	2.9	3.0	2.8	3.3
	width	6.4	5.0	5.9	4.3	5.2	5.1	4.5	4.8	5.0	5.1
Metasoma I	length	5.0	4.2	5.0	4.2	4.3	4.2	4.0	4.2	4.0	4.0
	width	3.1	2.8	3.2	2.7	2.9	2.7	2.7	2.8	2.6	2.3
	height	2.5	2.4	2.6	2.2	2.4	2.1	2.2	2.4	2.2	2.1
Metasoma II	length	5.6	4.9	5.3	4.7	5.0	4.6	4.6	4.8	4.1	4.6
	width	3.0	2.5	2.9	2.5	2.8	2.6	2.4	2.7	2.5	2.2
	height	2.6	2.5	2.6	2.3	2.5	2.2	2.2	2.4	2.3	2.0
Metasoma III	length	5.4	4.9	5.3	4.8	5.0	5.0	4.6	4.7	4.5	4.7
	width	2.7	2.6	2.8	2.4	2.6	2.3	2.3	2.4	2.5	2.2
	height	2.6	2.3	2.5	2.1	2.3	2.0	2.2	2.3	2.2	1.8
Metasoma IV	length	5.9	5.2	5.7	5.0	5.5	4.7	4.8	5.1	4.7	4.9
	width	2.3	1.9	2.3	1.8	2.1	1.6	1.9	1.9	2.1	1.9
	height	2.3	2.0	2.2	2.0	2.1	1.9	1.8	1.8	2.0	1.8
Metasoma V	length	6.6	6.5	7.0	6.5	6.6	6.0	6.0	6.3	5.5	6.2
	width	2.4	2.2	2.3	2.1	2.3	2.0	2.0	2.2	2.1	2.0
	height	2.3	2.0	2.1	1.8	1.9	1.8	1.7	2.0	2.0	1.8
Telson	vesicle length	3.1	2.8	3.1	2.6	2.9	2.4	2.6	2.6	2.4	2.1
	vesicle width	2.1	1.7	1.9	1.6	1.7	1.6	1.6	1.7	1.6	1.5
	vesicle height	2.0	1.8	1.8	1.7	1.9	1.9	1.6	1.8	1.5	1.5
	aculeus length	3.3	3.3	3.2	3.2	3.7	3.6	2.8	3.4	2.7	3.2
Femur	length	4.5	3.7	4.4	3.7	3.8	3.6	3.5	3.7	3.8	3.8
	width	1.5	1.4	1.4	1.3	1.4	1.3	1.2	1.2	1.1	1.2
	height	1.3	1.1	1.2	1.0	1.0	1.1	0.7	1.1	1.0	1.0

TABLE 13 *continued*

Specimen	sex	♀	♀	♀	♀	♀	♀	♀	♀	♀	♀
	collection	HUJ									
	accession no.	3214	3218	3221	3225	3226	3230	3240	3247	3248	3249
Patella	length	5.3	4.9	5.4	4.7	5.0	4.5	4.6	4.8	4.8	4.5
	width	2.1	1.8	1.9	1.6	1.7	1.6	1.9	1.6	1.7	1.6
	height	1.7	1.4	1.5	1.2	1.4	1.4	1.3	1.4	1.5	1.2
Chela	total length	7.5	7.0	7.5	6.4	7.3	6.5	6.7	6.7	5.9	6.4
	manus width	1.5	1.3	1.5	1.3	1.3	1.3	1.6	1.3	1.3	1.2
	manus height	1.7	1.4	1.7	1.4	1.6	1.4	2.1	1.5	1.2	1.4
	retroventral carina	2.9	2.5	2.8	2.4	2.4	2.3	3.0	2.4	2.1	2.2
	movable finger	4.4	4.2	4.1	3.8	4.3	3.7	3.6	3.9	3.7	3.8
Pectines	total length	5.0	4.5	4.9	4.4	4.6	4.4	4.7	4.6	4.1	4.3
	dentate margin	5.0	4.4	4.7	3.9	4.3	3.9	4.6	4.2	3.8	4.1

rows of elongated macrosetae (“sand combs”) along the retrolateral margins, are consistent with the semipsammophilous ecomorphotype (Prendini, 2001).

Other scorpion species recorded in sympatry with *B. tadmorensis* include the buthids *Androctonus crassicauda*, *Aristobuthus susanae* Lourenço, 1998, *Compsobuthus jakesi* Kovařík, 2003, *Hottentotta saulcyi* (Simon, 1880), *Leiurus hebraeus* (Birula, 1908), *Mesobuthus phillipsii* (Pocock, 1889), *Odontobuthus bidentatus* Lourenço and Pézier, 2002, *Orthochirus iranicus* Kovařík, 2004, *Orthochirus scrobiculosus*, *Razianus zarudnyi* (Birula, 1903); the hemiscorpiid *Hemiscorpius lepturus* Peters 1861; and the scorpionids *Scorpio kruglovi* Birula, 1910 and *Scorpio townsendi* (Pocock, 1900) (Navidpour et al., 2008; Shehab et al., 2011; Sharifinia et al., 2017).

**REMARKS:** *Buthacus tadmorensis*, originally described from Palmyra, Syria (Simon, 1892), was synonymized with *B. leptochelys* by Kraepelin (1899), but incorrectly attributed to Levy et al. (1973) by Fet and Lowe (2000). Others (e.g., Birula, 1905, 1908, 1910, 1917; Werner, 1936; Vachon, 1948, 1966; Habibi, 1971) continued to recognize *B. tadmorensis*, however. Pérez (1974) subsequently synonymized *Buthus pietschmanni*, described from Qal’at Sherqat [Aššur, Iraq], with *B. tadmorensis*. Kinzelbach (1985) relegated *B. yotvatensis* and *B. yotvatensis nigroaculeatus* Levy

et al., 1973, to subspecies of *B. tadmorensis*, a decision accepted by some (e.g., Vachon and Kinzelbach, 1987; Amr et al., 1988; El-Hennawy, 1992) and rejected by others (e.g., Fet and Lowe, 2000; Lourenço, 2004a).

Kovařík (2005) subsequently revalidated *B. macrocentrus*, originally synonymized with *B. leptochelys* by Kraepelin (1891), and synonymized *B. tadmorensis*, *B. pietschmanni*, and *B. yotvatensis* with it. This decision was accepted uncritically by most subsequent workers (e.g., Kaltsas et al., 2008; Navidpour et al., 2008; 2013; Navidpour, 2015; Sharifinia et al., 2017; Dehghani and Kassiri, 2018; Al-Khazali and Yağmur, 2019; Koç et al., 2019; Hussen and Ahmed, 2020; Amr et al., 2021; Kachel et al., 2021).

After comparing two specimens from Palmyra, the type locality of *B. tadmorensis*, presumed to be part of the original type series, with a paratype of *B. yotvatensis*, deposited at the MNHN, Lourenço (2006) suggested that *B. tadmorensis* is a valid species whereas *B. yotvatensis* could be a junior synonym of *B. macrocentrus*. Lourenço (2006: 64) noted “the very developed ventral carinae of metasomal segments II and III” in *B. tadmorensis*, a character originally described by Simon (1892: 84) as “segmentis caudae 2° et 3° carinis inferioribus apicem versus sensim validioribus et dente apicali reliquis majoribus,” and which is absent in the types of *B. macrocentrus* and *B. yotvatensis*. Nev-

ertheless, Kovařík et al. (2016) and others (Kaltsas et al., 2008; Navidpour et al., 2008; 2013; Navidpour, 2015; Kachel et al., 2021) continued to regard *B. tadmorensis*, *B. pietschmanni*, and *B. yotvatensis* as junior synonyms of *B. macrocentrus*. Moreover, Lowe et al. (2019) recently rejected Lourenço's (2006) assessment of the validity of *B. tadmorensis*, along with the suggestion that *Buthacus buettikeri* could be a junior synonym of the latter. According to Lowe et al. (2019: 5):

Lourenço (2006) incorrectly restored *Buthacus tadmorensis* (Simon, 1892) of Palmyra, Syria, which was synonymized under *Buthacus macrocentrus* (Ehrenberg, 1828) by Kovarik (2005), arguing that the former is distinguished by strongly developed ventromedian carinae on metasoma II–III with enlarged denticles, a character that Simon (1982) cited in his description. However, the Palmyra specimens examined by Lourenço (2006) were characterized only as "... possibly part of the type material of Simon", leaving ambiguity about the identity of this species. The opinion was expressed that *Buthacus leptochelys nitzani* Levy, Amitai & Shulov, 1973, a relatively robust form, could be a junior synonym of *B. tadmorensis*.

Lourenço & Qi (2006) remarked that *B. buettikeri* was similar to, and could be a "regional morph" or synonym of *B. tadmorensis*, because "...the areas of distribution of *B. tadmorensis* and *Buthacus buettikeri* are not very much distinct..." The latter claim is questionable. Palmyra is far from the localities in central Saudi Arabia where we have confirmed [*Trypanothacus*] *buettikeri* resides based on our restudy of the type series. A few other types from a single, disjunct northern site near the Saudi Arabia–Jordan border, closer to Syria, have not been restudied and their taxonomic status remains unclear (see below). The posterior metasoma and telson of a male from Palmyra labeled as "*B. tadmorensis*" was illustrated in lateral view by Lourenço (2006: 63, fig. 18). If this figure is accurate, the enlarged denticles on ventromedian carinae of metasoma III and ventrolateral carinae of metasoma V are consistent with *T. buettikeri*, but the more slender segments (metasoma IV L/D 2.12, V L/D 2.7), denser setation on dorsal metasomal carinae and ventral telson vesicle, and the less bulbous telson with longer aculeus, are not.

Examination of the types of *B. leptochelys* and *B. macrocentrus* for the present investigation demonstrated that they are conspecific, as originally concluded by Kraepelin (1891),

requiring *B. macrocentrus* to be returned to synonymy with *B. leptochelys* (see above). In addition, examination of the types of *B. pietschmanni*, as well as conspecific material from Jordan, Turkey, Iraq, and Iran, closely matching the descriptions of the type specimens from Palmyra by Simon (1892) and the probable type specimens, also from Palmyra, described by Lourenço (2006), demonstrated that *B. tadmorensis* is a valid species and *B. pietschmanni* a junior synonym thereof. This finding is supported by multivariate analysis of morphometrics (fig. 15) as well as multilocus phylogenetic analysis (L.P., unpublished data). *Buthacus tadmorensis* (Simon, 1892), stat. rev., is revalidated accordingly and *B. pietschmanni* returned to synonymy with it: *Buthus pietschmanni* Penther, 1912 = *Buthacus tadmorensis* (Simon, 1892), syn. nov. On the contrary, examination of the holotype of *B. yotvatensis* as well as material from across the distributions of both species, multivariate analysis of morphometrics (fig. 15), and multilocus phylogenetic analysis (fig. 14), confirmed that *B. yotvatensis* is a valid species, as originally indicated by Levy et al. (1973). Furthermore, it would appear, based on the evidence available, that *B. buettikeri* is a valid species, regardless of its generic assignment. Material conspecific with *B. buettikeri*, from al-Mudawwarah, Jordan, slightly north of the border with Saudi Arabia, was collected by the last author and deposited in the AMNH, confirming the validity of the record doubted by Lowe et al. (2019).

**MATERIAL EXAMINED: IRAN:** *Bushehr Province*: Delvar, 28°42'59"N 51°04'52"E, 4 m, xi.2007, Masihipour and Hayader, 1 ♂ (AMCC [LP 11060]); Omidiyah to Genaveh road, 30°13'42"N 50°12'01"E, 128 m, vi.2007, S. Navidpour and B. Masihipour, 1 ♂, 1 juv. ♀ (AMCC [LP 9720]). *Ilam Province*: Dashte Abbas, Ein Saleh village, 32°25'24"N 47°43'86"E, 182 m, x.2007, S. Navidpour, 2 juv. ♂ (AMCC [LP 9721, 11076]). *Khoozestan Province*: Ahvaz–Omidiyah road (40 km to Omidiyah), 30°37'49"N 49°31'47"E, 79 m, v.2007, B. Masihipour and H.

Bahrani, 1 ♂ (AMCC [LP 9719]); Shush (Apadana Palace), 32°10'55"N 48°15'39"E, 75 m, x.2007, S. Navidpour, B. Masihipour and H. Bahrani, 1 ♀, 1 subad. ♂ (AMCC [LP 9722]). **IRAQ: Erbil Governorate:** Bardber, 36°02'50.8"N 44°19'20.5"E, 14.vii.2019, F.S. Hussen, 1 ♀ (AMCC [LP 16876]). **JORDAN: Dieban District:** Wadi Deb'èm [31°31'N 35°49'E], SE of Amman, 709 m, vii.1938, O. Theodor, 2 juv. ♀ (HUJ INVSC 2491). **TURKEY: Şanlıurfa (Urfa) Province:** Birecik, ca. 20 km E, 37°00'38.4"N 38°11'41.1"E, 686 m, 23.v.2007, A.V. Gromov and E.A. Yağmur, 2 ♀, 2 subad. ♂, 1 subad. ♀ (AMNH), 2 juv. (AMCC [LP 7355]); Harran ruins, 36°51'50.5"N 39°01'42.5"E, 358 m, 17.v.2007, A.V. Gromov, H. Koç and E.A. Yağmur, 56 ♀, 52 subad. ♂, 46 subad. ♀, 17 juv. ♂, 79 juv. ♀ (AMNH), 2 juv. (AMCC [LP 7357]).

*Buthacus yotvatensis* Levy et al., 1973, stat. rev.

Figures 1E, 3B, C, 5, 12B, 15, 16E, F, 19E, F, 21I, 22G, 23C, 25C, 27C, 29G, 51, 52, 53; tables 1, 6, 7, 9

*Buthacus yotvatensis* Levy et al., 1973: 130–133, 134 (misidentification, part), figs. 32–37; Levy and Amitai, 1980: 90–93, figs. 82–85, map 6; Kinzelbach, 1984: 99, 101 (misidentification); Fet et al., 1998: 615, 616; Fet and Lowe, 2000: 85; Soleglad and Fet, 2003a: 5 (misidentification); 2003b: 7, 149, 151, 152, 156, fig. B1-2 (misidentification); Fet et al., 2003: 3, 4, table 1 (misidentification); Hendrixson, 2006: 47, 52, 54, 56; Amr et al., 2015: 30–33, fig. 1D; Alqahtani et al., 2019: 19, 22, 24, 25, fig. 2C (misidentification); Alqahtani and Badry, 2021: 4, 10, table 1; Amr et al., 2021: 86, 88, fig. 3A, table 4; Kachel et al., 2021: 2, 3.

*Buthacus yotvatensis yotvatensis*: Vachon, 1979: 36; Fet and Lowe, 2000: 85; Lourenço, 2004a: 206; Hendrixson, 2006: 55.

*Buthacus tadmorensis yotvatensis*: Kinzelbach, 1985: map III; Vachon and Kinzelbach,

1987: 101; Amr et al., 1988: 374; El-Hennawy, 1992: 101, 114 (part).

*Buthacus tadmorensis*: Vachon, 1952: 180 (misidentification); El-Hennawy, 1992: 101, 104 (misidentification); Kovařík, 2001: 80. *Buthacus macrocentrus*: Kovařík, 2005: 1, 8; Lourenço, 2006: 64; Kaltsas et al., 2008: 214.

**TYPE MATERIAL:** Holotype 1 ♂ (SMNH TAU AR 5223 old NS 5223), **ISRAEL:** *Mehoz HaDaram (Southern District)*: Arava Valley, dunes E of Yotvata [29°53'N 35°04'E], 2.v.1965, H. Zinner [examined].

**DIAGNOSIS:** *Buthacus yotvatensis* differs from the closely related *B. arava*, also occurring in Israel and Jordan, as follows. The pedipalp chela of *B. yotvatensis* is longer and narrower, especially in the adult male (fig. 53A, B), with chela manus width:chela length, 17.4% (16.5%–18.8%, n = 8; table 6) (♂), chela manus length:movable finger length, 55.2% (51.7%–58.3%, n = 8) (♂) or 47.1% (45.5%–48%, n = 6, table 7) (♀), and chela manus width:length, 50.5% (48.1%–54.8%, n = 8) (♂) or 56.9% (51.3%–61.5%, n = 6) (♀), than that of *B. arava* (fig. 35A, B), with chela manus width:chela length, 29.8% (27.2%–32.8%, n = 7; table 8) (♂), chela manus length:movable finger length, 90.4% (83.5%–95%, n = 7) or 60.8% (♀), and chela manus width:length, 63.3% (57.3%–74.5%, n = 7) or 61.6% (♀). The unguis of the leg telotarsi are shorter (approximately two-thirds the length of the telotarsus) and equal on legs I and II in *B. yotvatensis* (fig. 22G) but longer (approximately equal to the length of the telotarsus) and unequal on legs I and II in *B. arava* (fig. 22C). The pectinal tooth counts are higher in *B. yotvatensis*, i.e., 34/35 (32–37/32–37, n = 8; table 9) (♂) and 26/26 (25–28/26–28, n = 6) (♀), than in *B. arava*, i.e., 20/20 (18–21/18–22, n = 7; table 9) (♂) and 12/13 (♀). The metasomal segments and telson are densely setose in *B. yotvatensis* (figs. 23C, 25C, 29G), with macrosetal counts on segments I–V (sinistral/dextral), dorsosubmedian carinae, 16/15 (14–20/11–21, n = 5):25/26 (20–29/18–30):26/25 (23–31/19–29):30/27 (24–38/23–31):12/11 (6–18/7–15),

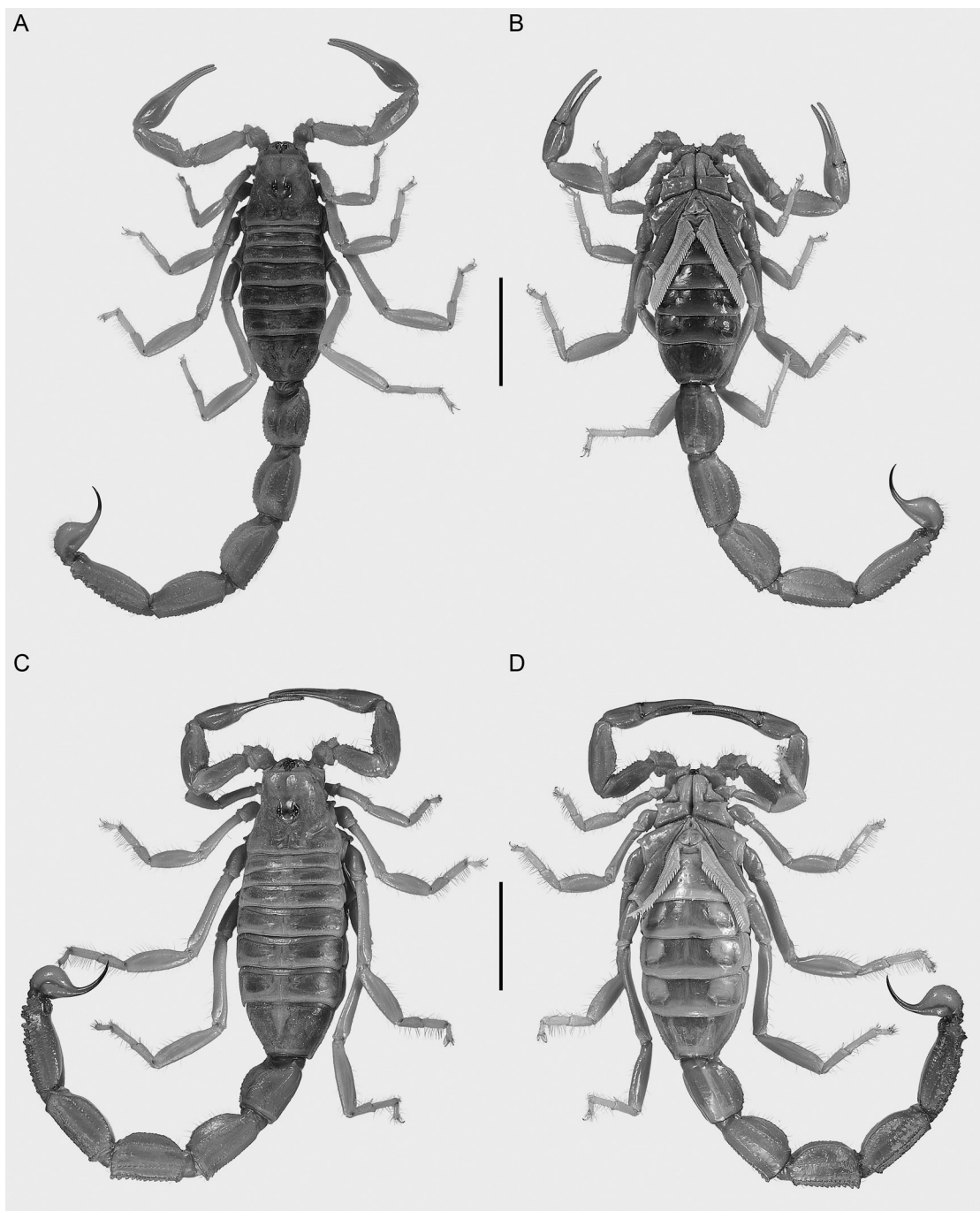


FIGURE 48. *Buthacus tadmorensis* (Simon, 1892), stat. rev., habitus, dorsal (A, C), and ventral (B, D) aspects. A, B. Lectotype ♂ (NHMW 2453) of *Buthus pietschmanni* Penther, 1912. C, D. Paralectotype ♀ (NHMW 2452). Scale bars = 1 cm.

dorsolateral carinae, 9/8 (7–13/5–13):20/20 (19–23/16–21):22/21 (16–28/18–24):15/14 (11–20/12–17):11/13 (10–13/11–14), and telson, 102 (88–127,  $n = 5$ ), but sparsely setose in *B. arava* (figs. 23A, 25A, 29C), with macrosetal counts on segments I–V (sinistral/dextral), dorsosubmedian carinae, 0/0 (0–1/0–1,  $n = 4$ ):2/3 (2–3/2–5):4/3 (2–5/2–6):3/3 (2–3/1–5):0/0 (0–0/0–0), dorsolateral carinae, 1/1 (0–2/0–2):2/2 (1–3/0–3):3/2 (2–4/1–3):3/3 (2–4/2–5):5/6 (3–8/5–7), and telson, 28 (27–29,  $n = 4$ ).

*Buthacus yotvatensis* differs from the closely related *B. tadmorensis*, occurring in neighboring countries, as follows. The pedipalp chela of *B. yotvatensis* is longer and narrower (fig. 53A, B), with chela manus width:chela length, 17.4% (16.5%–18.8%,  $n = 8$ ; table 6) (♂), chela manus length:movable finger length, 55.2% (51.7%–58.3%,  $n = 8$ ) (♂) or 47.1% (45.5%–48%,  $n = 6$ ; table 7) (♀), and chela manus width:length, 50.5% (48.1%–54.8%,  $n = 8$ ) (♂) or 56.9% (51.3%–61.5%,  $n = 6$ ) (♀), than that of *B. tadmorensis* (fig. 50A, B), with chela manus width:chela length, 22.3% (♂) (table 4), chela manus length:movable finger length, 64.2% (♂) or 55% (51.9%–59.8%,  $n = 4$ ) (♀), and chela manus width:length, 58.7% (♂) or 59.1% (53.8%–65.1%,  $n = 4$ ) (♀). The ventrosubmedian and ventrolateral carinae of metasomal segments II and III, and ventrolateral carinae of segment V are less developed in *B. yotvatensis* than in *B. tadmorensis* (fig. 25B, C), with narrow, spiniform processes posteriorly in *B. yotvatensis* but broad, lobate processes posteriorly in *B. tadmorensis*. The telson ventral surface is sparsely granular anteriorly in *B. yotvatensis* but densely granular anteriorly in *B. tadmorensis* (fig. 29E, G).

**DESCRIPTION:** The following description is based on specimens from across the distribution of the species in Israel (see tables 6 and 7 for measurements, and table 9 for counts).

**Total length:** Large scorpions, 67.4 mm (61.9–71.9 mm,  $n = 8$ ) (♂) or 76.6 mm (71.6–85 mm,  $n = 6$ ) (♀).

**Color:** Uniformly pale yellow to yellowish olive, except as follows. Mesosomal tergites, ster-

nite VII and metasomal segments I–V, each with narrow brown stripe posteriorly. Pectines pale yellow. Leg articulation points brown.

**Carapace:** Carapace shape trapezoidal (fig. 16C, D), anterior width:posterior width, 53.3% (46.3%–59.2%,  $n = 14$ ), length:posterior width, 89.4% (81.7%–98.4%,  $n = 14$ ). Five, rarely four, pairs of lateral ocelli; each lateral ocular tubercle with three major ocelli (ALMa, MLMa, PLMa), similar in size, situated anterolaterally, and one or, usually, two minor ocelli (ADMi, PDMi; PDMi may be absent) situated posterodorsal to posterior major ocellus. Median ocelli larger than lateral ocelli, distance between them more than 2× ocellus width. Median ocular tubercle situated anteromedially, distance from anterior carapace margin:carapace length, 45.4% (42.6%–47%,  $n = 8$ ) (♂) or 45.5% (43.9%–46.8%,  $n = 6$ ) (♀). Superciliary and central median carinae distinct, costate-granular and weakly connected to disconnected. Anteromedian sulcus distinct; posteromedian sulcus deep, narrow anteriorly, wide posteriorly; posterolateral sulcus deep, wide, curved. Carapace intercarinal surfaces coarsely and densely granular.

**Chelicerae:** Cheliceral manus prodorsal margin finely granular; retrodorsal surfaces smooth or finely granular; prolateral and ventral surfaces setose. Fixed finger dorsal surface setose; dorsal margin with subdistal, medial, and proximal denticles; ventral margin with proximal and medial denticles. Movable finger smooth and glabrous; dorsal margin with retrodistal, subdistal, medial, and pair of proximal denticles; ventral margin with prodistal, medial, and proximal denticles.

**Pedipalps:** Femur dorsal prolateral, dorsal retrolateral and ventral prolateral carinae complete, costate-granular; prolateral ventral and prolateral ventrosubmedian carinae each comprising discontinuous row of spiniform granules; retrolateral dorsosubmedian carina obsolete, comprising discontinuous row of spiniform granules and more than 15 macrosetae; dorsal, prolateral and ventral intercarinal surfaces finely granular; retrolateral intercarinal surfaces smooth (fig. 52A, B). Patella prolateral median and ventral prolateral carinae

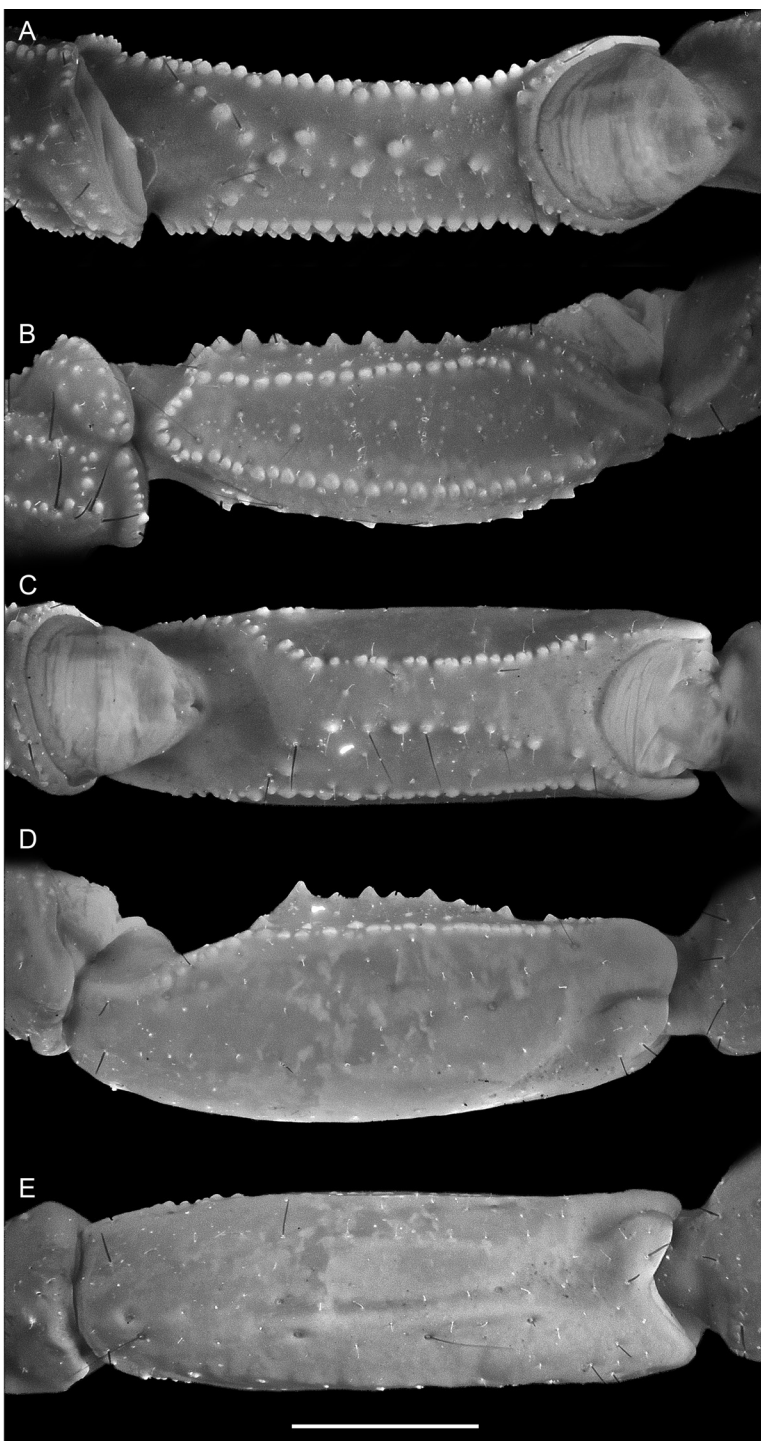


FIGURE 49. *Buthacus tadmorensis* (Simon, 1892), stat. rev., lectotype ♂ (NHMW 2453) of *Buthus pietschmanni* Penther, 1912, dextral pedipalp femur (A, B) and patella (C, E), prolateral (A, C), dorsal (B, D), and retrolateral (E) aspects. Scale bar = 2 mm.



FIGURE 50. *Buthacus tadmorensis* (Simon, 1892), stat. rev., dextral pedipalp chela, dorsal (A, C) and retro-lateral (B, D) aspects. A, B. Lectotype ♂ (NHMW 2453) of *Buthus pietschmanni* Penther, 1912. C, D. Paralectotype ♀ (NHMW 2452). Scale bar = 2 mm.

complete, costate-granular to finely serrate; dorsal prolateral carinae complete, costate-granular; other carinae obsolete; intercarinal surfaces smooth (fig. 52C–E). Chela long and slender in both sexes, manus width:length, 50.5% (48.1%–54.8%,  $n = 8$ ) ( $\delta$ ) or 56.9% (51.3%–61.5%,  $n = 6$ ) ( $\varphi$ ), manus height:length, 56.9% (53.3%–60.7%,  $n = 8$ ) ( $\delta$ ) or 63.5% (60.1%–67.2%,  $n = 6$ ) ( $\varphi$ ), and manus length:movable finger length, 55.2% (51.7%–58.3%,  $n = 8$ ) ( $\delta$ ) or 47.1% (45.5%–48%,  $n = 6$ ) ( $\varphi$ ). Chela manus acarinate; intercarinal surfaces smooth and setose (fig. 53). Fixed and movable fingers each with 9–12 ( $n = 12$ ) oblique median denticle subrows; movable finger with 6–11 ( $n = 12$ ) retrolateral accessory denticles (fig. 21I); proximal dentate margins of fingers straight (fig. 53B), such that no gap evident proximally when fingers closed.

**Legs:** Legs I–IV, femoral ventral carinae granular; patellar ventral carinae obsolete; intercarinal surfaces smooth. Legs I–IV, tibial spurs absent on I and II, present on III and IV; pro- and retroventral basitarsal (pedal) spurs present, more developed on III and IV. Legs I–IV, macrosetal counts on retrolateral margins of tibiae, 11:14:12:9; basitarsi, 13:20:23:10; telotarsi, 7:8:7:6 ( $n = 1$ ). Telotarsi unguis slightly elongated, more than three-quarters of telotarsus length, equal on legs I–IV (fig. 22G).

**Genital operculum:** Genital opercula suboval, completely divided longitudinally, without overlapping, rounded margins ( $\delta$ ) or partially fused longitudinally ( $\varphi$ ) (fig. 19E, F). Genital papillae present ( $\delta$ ) or absent ( $\varphi$ ).

**Pectines:** Three marginal lamellae; 11–12 ( $n = 3$ ) ( $\delta$ ) or 9–12 ( $n = 2$ ) ( $\varphi$ ) median lamellae (fig. 19E, F). Fulcra present. Pectinal teeth along most ( $\delta$ ) or part ( $\varphi$ ) of length, dentate margin length:pecten length, 94.1% (90.4%–99.6%,  $n = 8$ ) ( $\delta$ ) or 86.3% (81.2%–90.2%,  $n = 6$ ) ( $\varphi$ ). Pectinal teeth curved, similar in size; tooth count (sinistral/dextral), 34/35 (32–37/32–37,  $n = 8$ ) ( $\delta$ ) or 26/27 (25–28/26–28,  $n = 6$ ) ( $\varphi$ ).

**Mesosoma:** Tergites I–VII progressively increasing in length posteriorly, tergite VI length:tergite VII length, 53.8% (47.7%–58.3%,  $n$

= 8) ( $\delta$ ) or 55.9% (51.8%–60.5%,  $n = 6$ ) ( $\varphi$ ); increasing in width posteriorly from I–IV, decreasing in width posteriorly from V–VII. Pretergites smooth; posttergites I–VI, intercarinal surfaces uniformly finely granular, becoming more coarsely and densely granular posteriorly, VII, finely to coarsely and sparsely granular. Tergites I–VI, dorsomedian carinae granular, vestigial, restricted to posterior fifth of I–III and posterior third of IV–VI; dorsosubmedian carinae granular, vestigial, restricted to posterior fifth of I–III and posterior third of IV–VI. Tergite VII, dorsomedian carina granular, vestigial, restricted to anterior half, dorsosubmedian and dorsolateral carinae distinct, granular. Sternites III–VII acarinate, smooth, and glabrous; IV–VI, respiratory spiracles (stigmata) width approximately 3 $\times$  length.

**Metasoma:** Metasomal segments I–V becoming longer and narrower posteriorly (figs. 23C, 25C, 27C), segment I shortest, length I:II, 88% (84.3%–89.7%,  $n = 8$ ) ( $\delta$ ) or 89.5% (87.1%–91%,  $n = 6$ ) ( $\varphi$ ); segments II–IV similar, length II:III, 96.3% (93.4%–98.1%,  $n = 8$ ) ( $\delta$ ) or 96.7% (92.8%–100.7%,  $n = 6$ ) ( $\varphi$ ), length III:IV, 96.3% (94.1%–98.2%,  $n = 8$ ) ( $\delta$ ) or 96.3% (93.8%–99.1%,  $n = 6$ ) ( $\varphi$ ); segment V longest, length IV:V, 86.7% (83.6%–91.8%,  $n = 8$ ) ( $\delta$ ) or 82.3% (79.1%–85.9%,  $n = 6$ ) ( $\varphi$ ); width:length segment I, 61.1% (57.8%–64.4%,  $n = 8$ ) ( $\delta$ ) or 62.5% (60.7%–65.2%,  $n = 6$ ) ( $\varphi$ ), II, 51.3% (47.2%–53.7%,  $n = 8$ ) ( $\delta$ ) or 53.5% (51.1%–56.1%,  $n = 6$ ) ( $\varphi$ ), III, 47.7% (43.2%–51%,  $n = 8$ ) ( $\delta$ ) or 50% (48.4%–53%,  $n = 6$ ) ( $\varphi$ ), IV, 40.1% (36.3%–41.8%,  $n = 8$ ) ( $\delta$ ) or 41.7% (39.9%–45.1%,  $n = 6$ ) ( $\varphi$ ), V, 33% (31.2%–36.2%,  $n = 8$ ) ( $\delta$ ) or 33.8% (32.7%–35.5%,  $n = 6$ ) ( $\varphi$ ). Dorsosubmedian and dorsolateral carinae distinct, granular on segments I–III, obsolete on IV, absent on V; dorsosubmedian and dorsolateral carinae densely setose, macrosetal counts on segments I–V (sinistral/dextral), dorsosubmedian carinae, 16/15 (14/11–20/21,  $n = 5$ ):25/26 (20/18–29/30):26/25 (23/19–31/29):30/27 (24/23–38/31):12/11 (6/7–18/15), dorsolateral carinae, 9/8 (7/5–13/13,  $n = 5$ ):20/20 (19/16–23/21):22/21 (16/18–28/24):15/14 (11/12–20/17):11/13 (10/11–

13/14). Median lateral carinae distinct, granular in posterior three-quarters of segment I, posterior half of II and posterior third of III, absent on IV and V. Ventrolateral carinae distinct, granular, restricted to posterior edge of segment I; granular, with granules becoming progressively larger and subspiniform posteriorly, on II and III; costate-granular on IV; serrate, comprising spiniform granules of variable size, becoming more prominent posteriorly, on V. Ventrosubmedian carinae distinct, costate on segment I; granular, with granules becoming progressively larger and subspiniform posteriorly, on II and III; costate-granular on IV; granular, restricted to anterior three-quarters of V. Ventromedian carina granular, distinct along entire length of V. Dorsal and lateral intercarinal surfaces smooth to finely and sparsely granular on segment I, smooth on II–V; ventral intercarinal surfaces smooth on I and III, finely granular across entire surface on IV and V.

**Telson:** Telson vesicle width:metasomal segment V width, 80.7% (74.8%–84.6%,  $n = 8$ ) (♂) or 83% (77.6%–88.5%,  $n = 6$ ) (♀). Vesicle globose, dorsal surface flat, ventral surface convex and rounded; height:length, 61.2% (51.6%–69.4%,  $n = 8$ ) (♂) or 62.9% (59.5%–67.6%,  $n = 6$ ) (♀); dorsal surface smooth; ventral surface finely granular anteriorly, smooth posteriorly; lateral and ventral surfaces densely setose, with 98 (91–102,  $n = 3$ ) (♂) or 107 (88–127,  $n = 2$ ) (♀) macrosetae. Aculeus long, gently curved; aculeus length:telson length, 49.6% (43.3%–55.5%,  $n = 8$ ) (♂) or 51.8% (47.8%–55.5%,  $n = 6$ ) (♀).

**Sexual dimorphism:** Adult males and females differ as follows. Males are slightly smaller, on average 67.4 mm in total length, than females, on average 76.6 mm. The carapace intercarinal surfaces are more densely granular and the carinae of the pedipalp femur and patella more coarsely granular in the male than in the female. The pedipalp chela of the male has proportionally shorter fingers than that of the female (fig. 53), as indicated by the higher chela manus length:movable finger length ratio in the male (55.2%) compared with the female (47.1%). The genital opercula are completely divided longitudi-

nally, with overlapping, rounded margins in the male but partially fused longitudinally in the female (fig. 19E, F) and genital papillae are present in the male but absent in the female. The pectinal tooth count is higher in the male (32–37) than in the female (25–28). The spiniform granules of the ventrosubmedian and ventrolateral carinae of metasomal segments II and III, and the ventrolateral carinae of segment V are less prominent in the male than in the female.

**DISTRIBUTION:** *Buthacus yotvatensis* appears to be endemic to Israel and Jordan. Most of the known records occur in the northern and southern parts of the Arava Valley, straddling the southern border between Israel and Jordan, but the species has also been recorded at one locality in the Negev (fig. 5). Whereas records from the Arava Valley range from -294 m to 127 m in elevation, the Negev locality, Ein Zik, is situated at 345 m.

*Buthacus yotvatensis* is sympatric with the closely related *B. arava*, in the Arava Valley (fig. 4), but allopatric with *B. tadmorensis*, distributed from central Jordan, through Syria, southeastern Turkey and Iraq, to the northern shore of the Persian Gulf, in southern Iran (fig. 10).

**ECOLOGY:** Specimens of *B. yotvatensis* were collected at night with UV light detection on gravel flats and sparsely vegetated, stable to vegetationless, shifting inland sand dunes. Specimens were fairly common at night, mostly sitting still or walking on the ground surface, some sitting on bushes. The habitat and habitus, notably the pale coloration, smooth tegument, obsolescence of some pedipalpal and metasomal carinae, elongation of the legs, especially legs III and IV, slight dorsoventral compression of the basitarsi of legs I–III, with comblike rows of elongated macrosetae (“sand combs”) along the retrolateral margins, elongated macrosetae on the lateral and ventral surfaces of the telotarsi, and slightly elongated telotarsal unguis, are consistent with the psammophilous ecomorphotype (Prendini, 2001).

Specimens of *B. yotvatensis* were collected in sympatry with *B. arava*. Two other buthids,

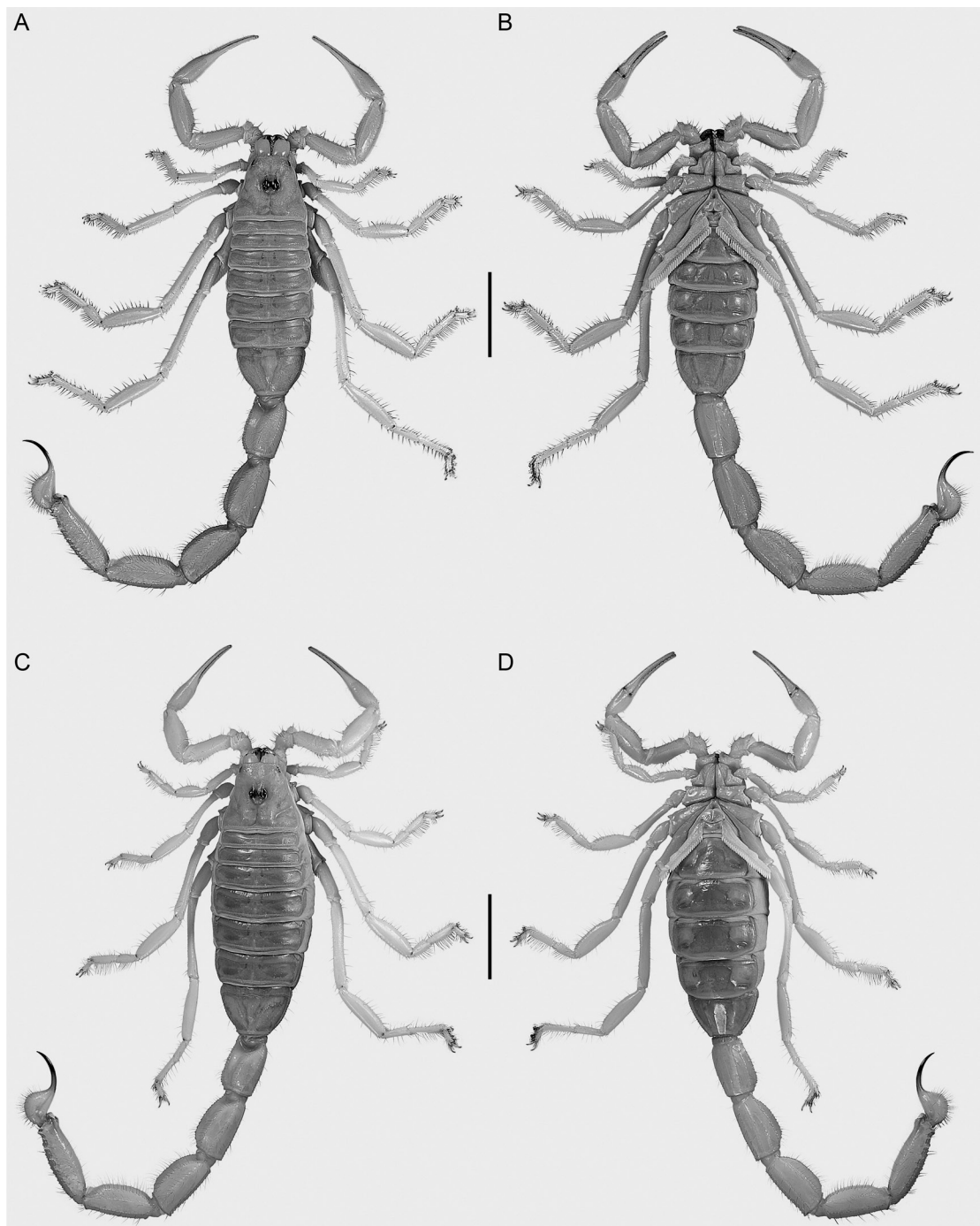


FIGURE 51. *Buthacus yotvatensis* Levy et al., 1973, stat. rev., habitus, dorsal (A, C), and ventral (B, D) aspects. A, B. ♂ (HUI INVSC 3302). C, D. ♀ (HUI INVSC 3318). Scale bars = 1 cm.

*Androctonus crassicauda* and *Orthochirus scrobiculosus*, also inhabit the same area, but occur on harder substrata.

**REMARKS:** In the original description, Levy et al. (1973: 133), stated: “*B. yotvatensis* is completely different from all scorpions so far described [and] for some time it was doubted whether it should not be placed in a genus of its own.” Kinzelbach (1985) relegated *B. yotvatensis* to a subspecies of *B. tadmorensis*, a decision accepted by some authors (e.g., Vachon and Kinzelbach, 1987; Amr et al., 1988; El-Hennawy, 1992) and rejected by others (e.g., Fet and Lowe, 2000; Lourenço, 2004a). Kovařík (2005) subsequently revalidated *B. macrocentrus*, originally synonymized with *B. leptochelys* by Kraepelin (1891), and synonymized *B. tadmorensis* and *B. yotvatensis* with it. After comparing a paratype of *B. yotvatensis*, deposited at the MNHN, with two specimens from Palmyra, the type locality of *B. tadmorensis*, presumed to be part of the original type series, Lourenço (2006) suggested that *B. tadmorensis* is a valid species and *B. yotvatensis* could be a junior synonym of *B. macrocentrus*. Nevertheless, Kovařík et al. (2016) and others (Kaltsas et al., 2008; Navidpour et al., 2008, 2013; Navidpour, 2015) continued to regard *B. tadmorensis*, *B. pietschmanni*, and *B. yotvatensis* as junior synonyms of *B. macrocentrus*. Lowe et al. (2019) recently rejected Lourenço’s (2006) assessment of the validity of *B. tadmorensis*.

During the present investigation, examination of the types of *B. leptochelys* and *B. macrocentrus*, as well as additional material from Sinai and Israel, demonstrated that they are conspecific, as originally concluded by Kraepelin (1891), requiring *B. macrocentrus* to be returned to synonymy with *B. leptochelys* (see above). On the contrary, examination of the holotype of *B. yotvatensis* as well as material from across the distributions of both species, multivariate analysis of morphometrics (fig. 15), and multilocus phylogenetic analysis (fig. 14), confirmed that *B. yotvatensis* is a valid species, as originally indicated by Levy et al. (1973). *Buthacus yotvatensis* Levy et al., 1973, stat. rev., is revalidated accordingly.

**MATERIAL EXAMINED: ISRAEL:** *Mehoz HaDaram (Southern District)*: Arava Valley, Avrona Nature Reserve, 29°41'12.5"N 34°59'46.2"E, 48 m, 14–18.ix.2017, E. Gavish-Regev, N. Segev and S. Cain, 13 ♂ (HUJ INVSC 3360, 3362–3367, 3370, 3371, 3373, 3374, 3376, AMNH ex HUJ INVSC 3379), 1 ♀ (HUJ INVSC 3378), 2 subad. ♂ (AMNH ex HUJ INVSC 3377, HUJ INVSC 3372), 1 subad. ♀ (HUJ INVSC 3368), 3 juv. ♂ (HUJ INVSC 3369, 3375, 3380), 1 juv. ♀ (HUJ INVSC 3361); Ein-Zik campsite, 30°48'22.4"N 34°51'03.1"E, 345 m, 11.ix.2018, Y. Zvik, 2 ♂ (HUJ INVSC 3483, 3485), ♀ (HUJ INVSC 3484), juv. ♀ (HUJ INVSC 3481, 3482); Hai-Bar Yotvata Nature Reserve, 29°50'51.0"N 35°01'42.5"E, 68 m, 26.viii.2011, L. Prendini and T.L. Bird, 32 ♂, 2 ♀, 1 subad. ♀ (AMNH), 1 juv. ♂, 3 juv. ♀ (AMCC [LP 11172]), 4.viii.2016, E. Gefen and S. Cain, 3 ♂ (AMCC [LP 15075] ex HUJ INVSC 3331, HUJ INVSC 3333, 3335), 1 ♀ (AMCC [LP 15076] ex HUJ INVSC 3332), 2 subad. ♀ (HUJ INVSC 3329, 3334), 1 juv. ♂ (HUJ INVSC 3330); Hazeva [30°42'N 35°15'E], -129 m, 7.vii.1983, A. Bouskila, 1 ♀ (HUJ INVSC 2532); Hazeva, Nahal Gidron, 30°46'52.2"N 35°14'33.5"E, -136 m, 16. ix.2017, Y. Olek and S. Cain, 1 ♂ (HUJ INVSC 3352); Hazeva, Nahal Mashaq, 30°47'26.1"N 35°15'26.5"E, -155 m, 16.ix.2017, Y. Olek and S. Cain, 2 ♂ (AMNH ex HUJ INVSC 3354, HUJ INVSC 3355), 3 ♀ (AMNH ex HUJ INVSC 3353, 3357, HUJ INVSC 3356); Hazeva, Nahal Shezaf, 30°44'36.0"N 35°16'03.2"E, -134 m, 16.ix.2017, Y. Olek and S. Cain, 1 ♂ (AMCC [LP 15080] ex HUJ INVSC 3359), 1 subad. ♀ (HUJ INVSC 3358); Iddan, N of (Hamada), 30°50'N 35°16'E, -174 m, 15.ix.1988, B. Shalmon, 1 subad. ♂ (HUJ INVSC 2611); Lotan, SE of Lotan Plantations, 30°00'10.4"E 35°05'44.1"E, 127 m, 15.ix.2017, Y. Olek and S. Cain, 5 ♂ (AMCC [LP 15079] ex HUJ INVSC 3350, HUJ INVSC 3346, 3347, 3349, 3351), 1 ♀ (AMCC [LP 15078] ex HUJ INVSC 3348); Nahal Sha'alav, 4 km S of Kibbutz Yahel, 30°02'40.6"N 35°06'33.7"E, 153 m, 15.ix.2017, Y. Olek and S. Cain, 3 ♂ (AMCC [LP 15077] ex HUJ INVSC 3342, AMNH ex HUJ INVSC 3343, HUJ INVSC 3344), 1 ♀ (HUJ INVSC 3345);

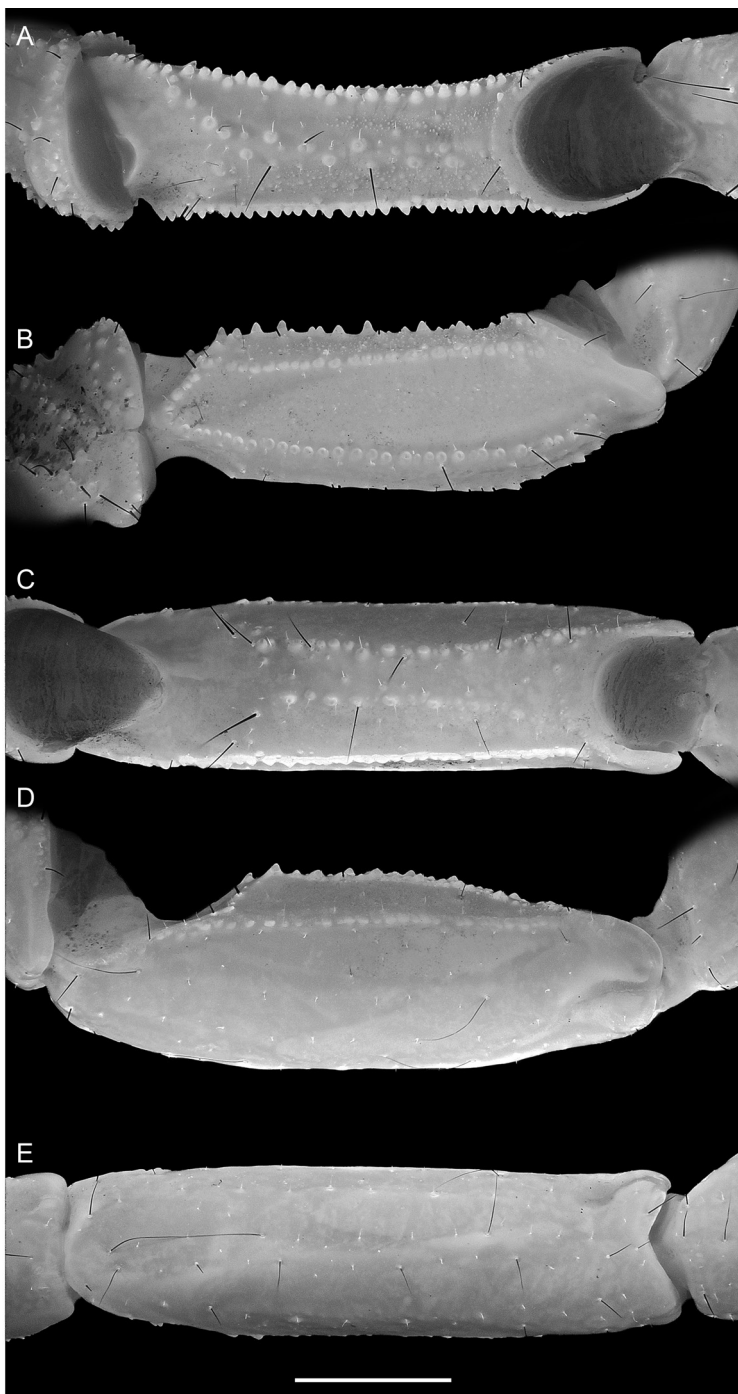


FIGURE 52. *Buthacus yotvatensis* Levy et al., 1973, stat. rev., ♂ (HUJ INVSC 3302), dextral pedipalp femur (A, B) and patella (C, E), prolateral (A, C), dorsal (B, D), and retrolateral (E) aspects. Scale bar = 2 mm.

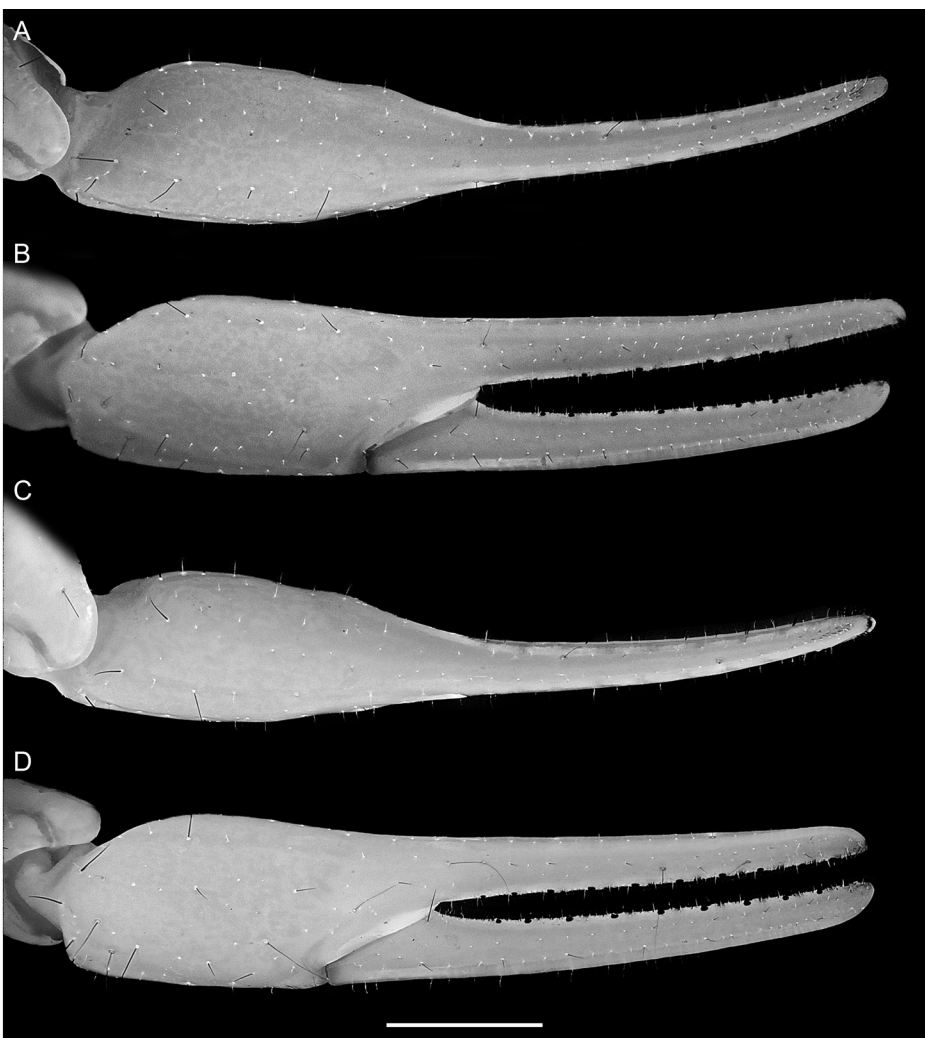


FIGURE 53. *Buthacus yotvatensis* Levy et al., 1973, stat. rev., dextral pedipalp chela, dorsal (A, C) and retro-lateral (B, D) aspects. A, B. ♂ (HUJ INVSC 3302). C, D. ♀ (HUJ INVSC 3318). Scale bar = 2 mm.

Qetura [29°58'N 35°03'E], 100 m, M. Israel, 8.x.1974, 1 ♂ (HUJ INVSC 2330), 20.x.1974, 1 ♀ (HUJ INVSC 2332), 17.iv.1975, 2 ♀ (HUJ INVSC 2336, 2337); Samar [29°50'N 35°01'E], 103 m, 25.ii.1985, U. Mendel, 1 subad. ♀ (HUJ INVSC 2612); Samar sand dunes, E of Eliphaz date plantations, 29°48'06.6"N 35°02'19.2"E, 64 m, 4.viii.2016, E. Gefen and S. Cain, 4 ♂ (AMCC [LP 15073, 15074] ex HUJ INVSC 3311, 3312, HUJ INVSC 3313, 3314), 30.vii.2017, S. Cain, 4 ♂ (AMNH ex HUJ INVSC 3319, 3320, HUJ INVSC

3316, 3317), 1 ♀ (HUJ INVSC 3318), 24.v.2017, S. Cain, 1 subad. ♀ (HUJ INVSC 3315); Samar sand dunes, old quarry, 29°48'25.9"N 35°02'06.6"E, 70 m, 13.ix.2017, Y. Olek and S. Cain, 3 ♂ (AMNH ex HUJ INVSC 3308, HUJ INVSC 3305, 3307), 1 subad. ♀ (HUJ INVSC 3306); Samar sand dunes, E side of Samar date plantations, 29°48'44.2"N 35°02'27.9"E, 67 m, 4.viii.2016, E. Gefen and S. Cain, 1 ♂ (HUJ INVSC 3321), 24.v.2017, S. Cain, 4 ♂ (AMNH ex HUJ INVSC 3324, 3327, HUJ INVSC 3322,

3326), 1 ♀ (AMNH ex HUJ INVSC 3323), 1 subad. ♂ (AMNH ex HUJ INVSC 3328), 1 juv. ♂ (HUJ INVSC 3325); Samar sand dunes, N part of Samar Nature Reserve, 29°49'36.8"N 35°02'35.8"E, 65 m, 13.ix.2017, Y. Olek and S. Cain, 5 ♂ (AMNH ex HUJ INVSC 3303, 3304, HUJ INVSC 3300–3302); Samar sand dunes, Samar Nature Reserve, 29°49'06.9"N 35°02'40.2"E, 64 m, 13.ix.2017, Y. Olek and S. Cain, 2 ♂ (AMNH ex HUJ INVSC 3309, HUJ INVSC 3310); Timna, sand dunes E of, [29°45'N 35°00'E], 109 m, 24.iii.1972, Y. Ayal, 1 ♂ (HUJ INVSC 2303), 1 juv. ♀ (HUJ INVSC 2304), 22.ii.1972, M. Broza, 1 juv. ♀ (HUJ INVSC 2305); Wadi Fukra [Zin Tichon, 30°50'N 34°49"E], 384 m, 20.iii.1944, 1 ♀ (HUJ INVSC 2492); Yotvata, [29°53'N 35°03'E], 64 m, 20.x.1974, M. Israel, 1 ♀ (HUJ INVSC 2333); Yotvata, E side of circle field, 29°53'28.7"N 35°04'40.5"E, 72 m, 14. ix.2017, Y. Olek and S. Cain, 3 ♂ (AMNH ex HUJ INVSC 3340, HUJ INVSC 3339, 3341); Yotvata, NE side of circle field, 29°54'02.6"N 35°04'42.1"E, 77 m, 30.vii.2017, S. Cain, 2 ♂ (AMNH ex HUJ INVSC 3337, HUJ INVSC 3338); Yotvata, SE side of circle field, 29°53'21.8"N 35°04'40.9"E, 71 m, 30.vii.2017, S. Cain, 1 ♂ (AMNH ex HUJ INVSC 3336). **JORDAN:** Karak Governorate: Wadi Khanzeerah (Khanzairh), 30°53'39.9"N 35°25'38.3"E, -294 m, 9.ix.2013, L. Prendini, Z. Amr and L. Al Azam, 1 ♀ (AMNH). Tafilah Governorate: Wadi Al Ghwaibeh (Ghwaqibeh), 30°47'35.6"N 35°23'39.7"E, -119 m, 9. ix.2013, L. Prendini, Z. Amr and L. Al Azam, 2 ♂, 1 ♀ (AMNH), [leg] (AMCC [LP 13561]); Wadi Al Ghwaibeh (Ghwaqibeh), 30°48'13.3"N 35°24'21.6"E, -106 m, 9.ix.2013, L. Prendini, Z. Amr, and L. Al Azam, 2 ♂, 1 ♀ (AMNH).

#### ACKNOWLEDGMENTS

This research was funded by U.S.-Israel Binational Science Foundation award 47441 to E.G. and L.P. The 26th European Congress of Arachnology and Ben-Gurion University of the Negev (BGU), Israel, partially supported L.P.'s visit to

Israel in 2011, and the Israel Taxonomy Initiative and BGU (Jacob Blaustein Center for Scientific Cooperation) supported his visit in 2013. We thank Efrat Gavish-Regev (HUJ), Sergei Zonstein and Ariel-Leib-Leonid Friedman (SMNH), and Christoph Hörweg (NHMW) for lending type and nontype material from collections in their care; Jason Dunlop (ZMB) and Elise-Anne Leguin (MNHN) for images of type material; Rotem Agmon, Ayelet Allon, Nadav Amir, Zuhair Amr, Essam Attia, Jamel Babay, Tharina Bird, Noach Braun, Efrat Gavish-Regev, Gal Geisler, Alexander V. Gromov, Fenik S. Hussen, Colleen Irby, Manel Khammasi, Halil Koç, David Kotter, Reut Less, Snir Livne, Yael Lubin, Mor Lugassi, Shahrokh Navidpour, Asia Novikova, Itamar Ofer, Yael Olek, Ridha Ouina, Avner Rinot, Nitzan Segev, Boaz Shacham, Stav Talal, Itay Tesler, Ersen A. Yağmur, and Yoram Zvik for donating material and/or assisting the authors with fieldwork; the Israel Nature and National Parks Protection Authority for permission to collect and export scorpions from Israel (permits 2011/38157 and 2013/39974 to L.P. 2015/41081 and 2017/41728 to E.G.); Essam Attia and Hisham K. El-Hennawy for hospitality, logistics and permissions in Egypt; Zuhair Amr and the Royal Jordanian Society for the Conservation of Nature for hospitality, logistics, and permissions in Jordan; Saïd Nouira, Jamel Babay, and Ridha Ouina for hospitality and logistics in Tunisia; Diogo Casellato, Deborah Chin, Ofelia Delgado-Hernandez and Tarang Sharma for generating DNA sequence data at the AMNH; Andrew Fatiukha, Rachel Ben-Shlomo, Stav Talal, and Tamar Krugman for assistance with generating sequence data at the Institute of Evolution, University of Haifa; Emile Cain and Myriam Freund for assisting with French text translations; Stephanie Loria (AMNH) for assistance with phylogenetic analysis; Steve Thurston (AMNH) for assistance with photography and preparing the plates; Pio Colmenares and Lou Sorkin (AMNH) for assistance with import/export logistics from the U.S.; and Oscar F. Francke and an anonymous reviewer for constructive comments on a previous draft of the manuscript.

## REFERENCES

- Al-Asmari, A.K., A.A. Al-Saief, N.M. Abdo, and K.R. Al-Moutaery. 2009a. New additions to the scorpion fauna of Riyadh region, Saudi Arabia. *Journal of Venomous Animals and Toxins including Tropical Diseases* 15 (4): 612–632.
- Al-Asmari, A.K., A.A. Al-Saief, N.M. Abdo, and K.R. Al-Moutaery. 2009b. The scorpion fauna of al-Baha and Hail regions, Saudi Arabia. *Journal of Biological Sciences* 9 (2): 96–108.
- Al-Asmari, A.K., A.A. Al-Saief, N.M. Abdo, and K.R. Al-Moutaery. 2013. A review of the scorpion fauna of Saudi Arabia. *Egyptian Journal of Natural History* 6: 1–21.
- Al-Khazali, A.M., and E.A. Yağmur. 2019. First record of *Androctonus bicolor* Ehrenberg, 1828 (Arachnida: Scorpiones) with scorpion records Dhi Qar Province, Iraq. *Biharean Biologist* 13 (2): 85–88.
- Alqahtani, A.R., and A. Badry. 2020. Interspecific phylogenetic relationship among different species of the genus *Buthacus* (Scorpiones: Buthidae) inferred from 16S rRNA in Egypt and Saudi Arabia. *Zoology in the Middle East* 66 (2): 178–185.
- Alqahtani, A.R., and A. Badry. 2021. A contribution to the scorpion fauna of Saudi Arabia, with an identification key (Arachnida: Scorpiones). *Journal of King Saud University – Science* 33: 101396. [doi: 10.1016/j.jksus.2021.101396]
- Alqahtani, A.R.M., B. Elgammal, K.I. Ghaleb, and A. Badry. 2019. The scorpion fauna of the southwestern part of Saudi Arabia. *Egyptian Academic Journal of Biological Sciences* 11 (1): 19–29.
- Amr, Z.S. 2015. Scorpionism and dangerous species of Jordan. In P. Gopalakrishnakone, L.D. Possani, E.F. Schwartz, and R.C.R de la Vega (editors), *Scorpion venoms*: 181–200. Berlin: Springer.
- Amr, Z.S., and R. El-Oran. 1994. Systematics and distribution of scorpions (Arachnida, Scorpionida) in Jordan. *Bulletino di Zoologia* 61 (2): 185–190.
- Amr, Z.S., K.E. Hyland, R. Kinzelbach, S.S. Amr, and D. Defose. 1988. Scorpions et piqûres de scorpions en Jordanie. *Bulletin de la Société de Pathologie Exotique* 81: 369–379.
- Amr, Z., O.A. Abed, T. Al-Share, N. Hamidan, and L. Prendini. 2015. New records of Jordanian scorpions. *Jordan Journal of Natural History* 2: 30–38.
- Amr, Z.S., M.A.A. Baker, M. Al-Saraireh, and D.A. Warrell. 2021. Scorpions and scorpion sting envenoming (scorpionism) in the Arab countries of the Middle East. *Toxicon* 191: 83–103.
- Badry, A., M. Younes, M.M.H. Sarhan, and M. Saleh. 2018. On the scorpion fauna of Egypt, with an identification key (Arachnida: Scorpiones). *Zoology in the Middle East* 64 (1): 75–87.
- Birula, A.A. 1896. *Miscellanea scorpiologica. I. Zur Synonymie der russischen Skorpione. Annuaire du Musée Zoologique de l'Académie Impériale des Sciences de St.-Pétersbourg* 1: 229–245.
- Birula, A.A. 1905. Beiträge zur Kenntniss der Scorpionenfauna Persiens (Dritter Beiträge). *Bulletin de l'Académie Impériale des Sciences de St. Pétersbourg* 23: 119–148.
- Birula, A.A. 1908. Ergebnisse der mit Subvention aus der Erbschaft Treitl unternommenen zoologischen Forschungsreise Dr. F. Werner's nach dem ägyptischen Sudan und Nord-Uganda. XIV. Scorpiones und Solifugae. *Sitzungsberichte der Mathematisch Naturwissenschaftlichen Klasse der Kaiserlichen Akademie der Wissenschaften (Wien)* 117/2 (1): 121–152.
- Birula, A.A. 1910. Ueber *Scorpio maurus* Linné und seine Unterarten. *Horae Societatis Entomologicae Rossicae* 39: 115–192.
- Birula, A.A. 1911. 3. Scorpiologische Beiträge. 9. *Buthus (Buthacus) spatzi*, sp. nov. *Zoologischer Anzeiger* 37 (6–7): 137–142.
- Birula, A.A. 1914. Ergebnisse einer von Prof. Franz Werner im Sommer 1910 mit Unterstützung aus dem Legate Wedl ausgeführten zoologischen Forschungsreise nach Algérien. VI. Skorpione und Solifugen. *Sitzungsberichte der Kaiserlich-königlichen Akademie der Wissenschaften (Wien)* 123 (1): 633–688.
- Birula, A.A. 1917. Arachnoidea Arthrogaster Caucásica. Pars I. Scorpiones. *Zapiski Kavkazskogo Muzeya [Mémoires du Musée du Caucase]*. Tiflis: Imprimerie de la Chancellerie du Comité pour la Transcaucasie A (5): 1–253. [in Russian; English translation: A.A. Byalynitskii-Birulya. 1964. Arthrogastri arachnids of Caucasia. 1. Scorpions. Jerusalem: Israel Program for Scientific Translations, 170 pp.]
- Bodenheimer, F. 1937. *Prodromus faunae Palestinae. Mémoires Présentés à l'Institut d'Égypte* 33: 1–286.
- Borelli, A. 1914. Contributo allo studio della fauna Libica. Materiali raccolti nelle zone di Misurata e Homs (1912–13) dal Dott. Alfredo Andreini, Capitano Medico. Scorpioni. *Annali del Museo Civico di Storia Naturale di Genova* 6 (3): 148–159.
- Borelli, A. 1927. Risultati zoologici della missione inviata dalla R. Società Geografica Italiana per l'esplorazione dell'oasi di Giarabub. Scorpioni e solfughi. *Annali del Museo Civico di Storia Naturale di Genova* 52: 346–355.

- Borelli, A. 1929. Scorpions du Soudan. Annals and Magazine of Natural History 10 (3): 297–300.
- Borelli, A. 1934. Scorpiones. In E. Zavattari, Prodromo della fauna della Libia: 169–173, 920. Pavia: Tipografia già Cooperativa.
- Bouisset, L., and G. Larrouy. 1963. Nouvelle station d'un scorpion peu connu, *Buthacus arenicola arenicola*. Bulletin de la Société d'Histoire Naturelle de Toulouse 98: 295–297.
- Bousmaha, F., et al. 2019. Inventory of scorpion fauna (Arachnida Scorpiones) in Tiaret Region (Algeria). Biodiversity Journal 10 (2): 141–146.
- Braunwalder, M.E., and V. Fet. 1998. On publications about scorpions (Arachnida, Scorpiones) by Hemprich and Ehrenberg (1828–1831). Bulletin of the British Arachnological Society 11 (1): 29–35.
- Bucherl, W. 1964. Distribuição geográfica dos aracnídeos peçonhentos temíveis. Memórias do Instituto de Butantan 31: 55–66.
- Cain, S., S.F. Loria, R. Ben-Shlomo, L. Prendini, and E. Gefen. in press. Dated phylogeny and ancestral range estimation of sand scorpions (Buthidae: *Buthacus*) reveal Early Miocene divergence across land bridges connecting Africa and Asia. Molecular Phylogenetics and Evolution.
- Caliskan, F. 2015. Scorpion venom research around the world: Turkish scorpions. In P. Gopalakrishnakone, L.D. Possani, E.F. Schwartz, and R.C.R. de la Vega (editors), Scorpion venoms: 327–349. Berlin: Springer.
- Caporiacco, L. 1932. Spedizione scientifica all'oasi di Cufra (Marzo-Luglio 1931). Scorpioni e solifugi. Annali del Museo Civico di Storia Naturale di Genova 55: 395–408.
- Caporiacco, L. 1936. Saggio sulla fauna aracnologica del Casentino Val d'Arno Superiore e Alta Val Tiberina. Festschrift zum 60. Geburtstage von Professor Dr. Embrik Strand 1: 326–369. Riga: Izdevnieciba Latvija.
- Caporiacco, L. 1937. Risultati scientifici della missione del Prof. G. Scortecci nel Fezzan e sui Tassili (1936) con aggiunta di esemplari di altre località Libiche. Atti della Società Italiana di Scienze Naturali e del Museo Civico di Storia Naturale in Milano 76 (3): 340–354.
- Crucitti, P., and V. Vignoli. 2002. Gli Scorpioni (Scorpiones) dell'Anatolia sud-orientale (Turchia). Bollettino della Museo Scienze Naturali in Torino 19 (2): 433–474.
- Dehghani, R., and H. Kassiri. 2018. A checklist of scorpions in Iran (by 2017). Asian Journal of Pharmaceuticals 12 (3): S880–S887.
- Dupré, G. 2007. Conspectus genericus scorpionorum 1758–2006 (Arachnida: Scorpiones). Euscorpius 50: 1–31.
- El-Hennawy, H.K. 1987. A simplified key to Egyptian scorpion species (Arachnida: Scorpionida). Serket 1 (1): 15–17.
- El-Hennawy, H.K. 1991. Arachnida of Wadi El-Raiyan (Egypt). Serket 2 (3): 81–90.
- El-Hennawy, H.K. 1992. A catalogue of the scorpions described from the Arab countries (1758–1990) (Arachnida: Scorpionida). Serket 2 (4): 95–153.
- Esposito, L.A., H.Y. Yamaguti, C.A. Souza, R. Pinto-da-Rocha, and L. Prendini. 2016. Systematic revision of the Neotropical club-tailed scorpions, *Physoctonus*, *Rhopalurus*, and *Troglorhopalurus*, revalidation of *Heterocetus*, and description of two new genera and three new species (Buthidae: Rhopalurusinae). Bulletin of the American Museum of Natural History 415: 1–134.
- Farzanpay, R. 1988. A catalogue of the scorpions occurring in Iran, up to January 1986. Revue Arachnologique 8 (2): 33–44.
- Fet, V., and G. Lowe. 2000. Family Buthidae C.L. Koch, 1837. In V. Fet, W.D. Sissom, G. Lowe, and M.E. Braunwalder. Catalog of the scorpions of the world (1758–1998): 54–286. New York: New York Entomological Society.
- Fet, V., G.A. Polis, and W.D. Sissom. 1998. Life in sandy deserts: the scorpion model. Journal of Arid Environments 39 (4): 609–622.
- Fet, V., E.M. Capes, and W.D. Sissom. 2001. A new genus and species of psammophilic scorpion from eastern Iran (Scorpiones: Buthidae). In V. Fet, and P.A. Selden (editors), Scorpions 2001. In memoriam Gary A. Polis: 113–139. Burnham Beeches, U.K.: British Arachnological Society.
- Fet, V., B. Gantenbein, A. Gromov, G. Lowe, and W.R. Lourenço. 2003. The first molecular phylogeny of Buthidae (Scorpiones). Euscorpius 4: 1–10.
- Francke, O.F. 1985. Conspectus genericus scorpionorum 1758–1982 (Arachnida: Scorpiones). Occasional Papers of the Museum, Texas Tech University 98: 1–32.
- Francke, O.F. 2019. Conspectus genericus scorpionorum 1758–1985 (Arachnida: Scorpiones) updated through 2018. Zootaxa 4657 (1): 1–56.
- Gervais, P.M. 1844. Scorpions. In C.A. Walckenaer (editor), Histoire naturelle des insectes. Aptères. Librairie Encyclopédique de Roret, Paris 3(8): 14–74.
- Giltay, L. 1929. Mission Saharienne Augieras-Draper, 1927–1928. Scorpions. Bulletin du Muséum

- National d'Histoire Naturelle (Paris) (Ser. 2) 1 (3): 193–197.
- Goloboff, P.A., J.S. Farris, and K.C. Nixon. 2008. TNT, a free program for phylogenetic analysis. *Cladistics* 24: 774–786.
- González-Santillán, E., and L. Prendini. 2013. Redefinition and generic revision of the North American vaejovid scorpion subfamily *Syntropinae* Kraepelin, 1905, with descriptions of six new genera. *Bulletin of the American Museum of Natural History* 382: 1–71.
- Gough, L.H., and S. Hirst. 1927. Key to the identification of Egyptian scorpions. A method of identifying Egyptian scorpions from the fifth caudal segment and stings. *Bulletin of the Ministry of Agriculture of Egypt, Technical Scientific Service* 76: 1–7.
- Habibi, T. 1971. Liste de scorpions de l'Iran. *Bulletin of the Faculty of Science, Tehran University* 2 (4): 42–47.
- Hemprich, F.W., and C.G. Ehrenberg. 1828. *Zoologica II. Arachnoidea. Plate I: Buthus; plate II: Androctonus. In Symbolae physicae seu icones et descriptiones animalium evertebratorum sepositis insectis quae ex itinere per Africam borealem et Asiam occidentalem. Friderici Guilelmi Hemprich et Christiani Godofredi Ehrenberg, medicinae et chirurgiae doctorum, studiorvae aut illustratae redierunt. Decas prima.* Berolini: Officina Academica. [plates only]
- Hemprich [F.W.], and [C.G.] Ehrenberg. 1829. Vorläufige Uebersicht der in Nord-Afrika und West-Asien einheimischen Skorpione und deren geographischen Verbreitung. *Verhandlungen der Gesellschaft Naturforschende Freunde in Berlin* 1 (6): 348–362.
- Hemprich, F.W., and C.G. Ehrenberg. 1831. *Animalia articulata, Arachnoidea. Scorpiones Africani et Asiatici. In Symbolae physicae. Animalia evertebrata exclusis insectis percensuit Dr. C.G. Ehrenberg. Series prima cum tabularum decade prima. Continet Animalia Africana et Asiatica 162.* Berolini: Officina Academica, 12 pp. [unpaginated, separate text intended to be part of the 1828 issue of "Symbolae physicae"]
- Hendrixson B.E. 2006. Buthid scorpions of Saudi Arabia, with notes on other families (Scorpiones: Buthidae, Liochelidae, Scorpionidae). *Fauna of Arabia* 21: 33–120.
- Hussen, F.S., and S.T. Ahmed. 2020. New data of scorpion fauna, include two new records with identification key of scorpion species (Arachnida: Scorpiones) in Iraq. *Plant Archives* 20 (2): 6711–6725.
- ICZN (International Commission on Zoological Nomenclature). 1999. International code of zoological nomenclature, 4th ed. London: International Trust for Zoological Nomenclature c/o the Natural History Museum.
- ICZN (International Commission on Zoological Nomenclature). 2000. Precedence of names in wide use over disused synonyms or homonyms in accordance with Article 23.9 of the Code. *Bulletin of Zoological Nomenclature* 57 (1): 6–10.
- Kabakibi, M.M., N. Khalil, and Z. Amr. 1999. Scorpions of southern Syria. *Zoology in the Middle East* 17: 79–89.
- Kachel, H.S., Al-Khazali, A.M., Hussen, F.S., and Yağmur, E.A. 2021. Checklist and review of the scorpion fauna of Iraq (Arachnida: Scorpiones). *Arachnologische Mitteilungen* 61: 1–10.
- Kaltsas, D., I. Stathi, and V. Fet. 2008. Scorpions of the Eastern Mediterranean. In S.E. Makarov, and R.N. Dimitrijević (editors), *Advances in arachnology and developmental biology. Papers dedicated to Prof. Dr. Božidar Čurčić*. Belgrade: Institute of Zoology, Faculty of Biology, University of Belgrade, Monograph12: 209–246.
- Kamenz, C., and L. Prendini. 2008. An atlas of book lung ultrastructure in the Order Scorpiones (Arachnida). *Bulletin of the American Museum of Natural History* 316: 1–259.
- Karsch, F. 1881a. Verzeichniss der während der Rohlfs'schen afrikanischen Expedition erbeuteten Myriopoden und Arachnidien. *Archiv für Naturgeschichte* 47 (1): 1–14.
- Karsch, F. 1881b. Uebersicht der europäischen Skorpione. *Berliner Entomologische Zeitschrift* 25: 89–91.
- Katoh, K., and D.M. Standley. 2013. MAFFT multiple sequence alignment software version 7: improvements in performance and usability. *Molecular Biology and Evolution* 30: 772–780.
- Kettel, J. 1982. Scorpions of Kuwait. *Newsletter of the Ahmadi Natural History Field Studies Group (Kuwait)* 21: 6–8.
- Khalaf, L. 1962. A small collection of scorpions from Iraq. *Bulletin of the Iraq Natural History Institute* 4 (2): 1–3.
- Khalaf, K.I. 1963. Scorpions reported from Iraq. *Bulletin of Endemic Diseases (Baghdad)* 5 (1–2): 59–70.
- King, H.H. 1925. Notes on Sudan scorpions. *Sudan Notes and Records* 8: 79–84.
- Kinzelbach R. 1984. Die Skorpionssammlung des Naturhistorischen Museums der Stadt Mainz. Teil II: Vorderasien. *Mainzer Naturwissenschaftliches Archiv* 22: 97–106.

- Kinzelbach, R. 1985. Vorderer Orient. Skorpione (Arachnida: Scorpiones). Tübinger Atlas der Vorderer Orients (TAVO), Karte Nr. A VI 14.2.
- Koç, H., E.A. Yağmur, and F. Šáhlavský. 2019. Karyotypes of southeastern Turkish scorpions *Hottentotta saulcyi* and *Buthacus macrocentrus* (Scorpiones: Buthidae). European Journal of Biology 78: 108–113.
- Koch, C.L. 1845. Die Arachniden. Nürnberg: C.H. Zeh'sche Buchhandlung 12: 1–166.
- Koch, C.L. 1850. Scorpionen. In Uebersicht des Arachnidensystems. Nürnberg: C.H. Zeh'sche Buchhandlung 5: 86–92.
- Kovařík, F. 1995. First report of *Orthochirus innesi* (Scorpionida: Buthidae) from Morocco. Klapalekiana 31: 19–21.
- Kovařík, F. 1997a. Results of the Czech Biological Expedition to Iran. Part 2. Arachnida: Scorpiones, with descriptions of *Iranobuthus krali* gen. n. et sp. n. and *Hottentotta zagrosensis* sp. n. (Buthidae). Acta Societatis Zoologicae Bohemicae 61: 39–52.
- Kovařík, F. 1997b. A check-list of scorpions (Arachnida) in the collection of the Hungarian Natural History Museum. Budapest. Annales Historico-Naturales Musei Nationalis Hungarici 89: 177–186.
- Kovařík, F. 1998. Štíři. [Scorpions]. Jihlava, Czech Republic: Madagaskar, 175 pp. [in Czech]
- Kovařík, F. 2001. Catalog of the Scorpions of the World (1758–1998) by V. Fet, W. D. Sissom, G. Lowe, and M. Braunwalder (New York Entomological Society, 2000: pp. 690). Discussion and supplement for 1999 and part of 2000. Serket 7 (3): 78–93.
- Kovařík, F. 2002. A checklist of scorpions (Arachnida) in the collection of the Forschungsinstitut und Naturmuseum Senckenberg, Frankfurt am Main, Germany. Serket 8 (1): 1–23.
- Kovařík, F. 2003. Scorpions of Djibouti, Eritrea, Ethiopia, and Somalia (Arachnida: Scorpiones), with a key and descriptions of three new species. Acta Societatis Zoologicae Bohemicae 67: 133–159.
- Kovařík, F. 2005. Taxonomic position of species of the genus *Buthacus* Birula, 1908 described by Ehrenberg and Lourenço, and description of a new species (Scorpiones: Buthidae). Euscorpius 28: 1–13.
- Kovařík, F. 2018. Notes on the genera *Buthacus*, *Compsothelus*, and *Lanzatus* with several synonymies and corrections of published characters (Scorpiones: Buthidae). Euscorpius 269: 1–12.
- Kovařík, F., and S. Whitman. 2004. Cataloghi del Museo di Storia Naturale dell'Università di Firenze—sezione di zoologia “La Specola” XXII. Arachnida Scorpiones. Tipi. Addenda (1998–2004) e checklist della collezione (Euscorpiinae esclusi). Atti della Società Toscana di Scienze Naturali, Memorie (Serie B) 111: 103–119.
- Kovařík, F., G. Lowe, J. Plíšková, and F. Šáhlavský. 2013. A new scorpion genus, *Gint* gen. n., from the Horn of Africa (Scorpiones: Buthidae). Euscorpius 173: 1–19.
- Kovařík, F., G. Lowe, and F. Šáhlavský. 2016. Review of northwestern African *Buthacus*, with description of *Buthacus stockmanni* sp. n. from Morocco and Western Sahara (Scorpiones, Buthidae). Euscorpius 236: 1–18.
- Kraepelin, K. 1891. Revision der Skorpione. I. Die Familie des Androctonidae. Jahrbuch der Hamburgischen Wissenschaftlichen Anstalten 8: 1–144.
- Kraepelin, K. 1895. Nachtrag zu Theil I der Revision der Scorpione. Beiheft zum Jahrbuch der Hamburgischen Wissenschaftlichen Anstalten 12: 73–96.
- Kraepelin, K. 1899. Scorpiones und Pedipalpi. In F. Dahl (editor), Das Tierreich, 8 (Arachnoidea): 1–265. Herausgegeben von der Deutschen Zoologischen Gesellschaft. Berlin: R. Friedländer und Sohn Verlag.
- Kraepelin, K. 1901. Catalogue des scorpions des collections du Muséum d'Histoire Naturelle de Paris. Bulletin du Muséum National d'Histoire Naturelle, Paris 7: 265–273.
- Lamoral, B.H. and S.C. Reynders. 1975. A catalogue of the scorpions described from the Ethiopian faunal region up to December 1973. Annals of the Natal Museum 22 (2): 489–576.
- Larrouy, G., J.P. Seguela, P. Léfèvre-Witier, J.F. Magnaval, and Y. Cambefort. 1972. Notes sur quelques scorpions Sahariens. Bulletin de la Société d'Histoire Naturelle de Toulouse 108 (3–4): 391–393.
- Le Coroller, Y. 1967. Les scorpions du Maroc. Archives de l'Institut Pasteur d'Algérie 45: 62–71.
- Levy, G., and P. Amitai. 1980. Fauna Palaestina. Arachnida I. Scorpiones. Jerusalem: Israel Academy of Sciences and Humanities, 130 pp.
- Levy, G., P. Amitai, and A. Shulov. 1973. New scorpions from Israel, Jordan and Arabia. Zoological Journal of the Linnean Society 52 (2): 113–140.
- Lewis, P.O. 2001. A likelihood approach to estimating phylogeny from discrete morphological character data. Systematic Biology 50: 913–925.
- Loria, S.F., and L. Prendini. 2014. Homology of the lateral eyes of Scorpiones: a six-ocellus model. PLoS One 9: e112913. [doi: 10.1371/journal.pone.0112913]

- Lourenço, W.R. 2001. Further taxonomic considerations on the northwestern African species of *Buthacus* Birula (Scorpiones, Buthidae), and description of two new species. Entomologische Mitteilungen aus dem Zoologischen Museum Hamburg 12 (158): 309–316.
- Lourenço, W.R. 2003. Compléments à la faune de scorpions (Arachnida) de l'Afrique du Nord, avec des considérations sur le genre *Buthus* Leach, 1815. Revue suisse de Zoologie 110 (4): 875–912.
- Lourenço, W.R. 2004a. Description of a new species of *Buthacus* Birula (Scorpiones, Buthidae) from Afghanistan. Entomologische Mitteilungen aus dem Zoologischen Museum Hamburg 14 (170): 205–210.
- Lourenço, W.R. 2004b. New considerations on the northwestern African species of *Buthacus* Birula (Scorpiones, Buthidae), and description of a new species. Revista Ibérica de Aracnología 10: 225–231.
- Lourenço, W.R. 2006. Further considerations on the genus *Buthacus* Birula, 1908 (Scorpiones: Buthidae), with a description of one new species and two new subspecies. Boletín de la Sociedad Entomológica Aragonesa 38: 59–70.
- Lourenço W.R. 2013. The *Buthacus* Birula, 1908 populations from Tassili n'Ajjer, Algeria (Scorpiones, Buthidae) and description of a new species. Entomologische Mitteilungen aus dem Zoologischen Museum Hamburg 16 (190): 89–99.
- Lourenço, W.R., and E.-A. Leguin. 2009. A new species of the genus *Buthacus* Birula, 1908 from the United Arab Emirates (Scorpiones, Buthidae). Zoology in the Middle East 46: 103–108.
- Lourenço, W.R., and J.-X. Qi. 2006a. A new species of the genus *Buthacus* Birula, 1908 (Scorpiones, Buthidae), from Pakistan. Boletín Sociedad Entomológica Aragonesa 39: 161–164.
- Lourenço W.R., and J.-X. Qi. 2006b. A new species of the genus *Buthacus* Birula, 1908 (Scorpiones, Buthidae) from Nigeria. Entomologische Mitteilungen aus dem Zoologischen Museum Hamburg 14 (174): 301–306.
- Lourenço, W.R., and S.E. Sadine. 2015. A new species of *Buthacus* Birula, 1908 from the region of Ghardaïa, Algeria (Scorpiones, Buthidae). Revista Ibérica de Aracnología 27: 55–59.
- Lourenço, W.R., B. Duhem, and J.L. Cloudsley-Thompson. 2012. Scorpions from Ennedi, Kapka and Tibesti, the mountains of Chad, with descriptions of nine new species (Scorpiones: Buthidae, Scorpionidae). Arthropoda Selecta 2 (4): 307–338.
- Lourenço, W.R., S. Bissati, and S.E. Sadine. 2016. One more new species of *Buthacus* Birula, 1908 from the region of Ghardaïa, Algeria (Scorpiones: Buthidae). Rivista Aracnologica Italiana 2 (8): 2–11.
- Lourenço, W.R., M.L. Kourim, and S.E. Sadine. 2017a. Scorpions from the region of Tamanrasset, Algeria. Part I. A new species of *Buthacus* Birula, 1908 (Scorpiones: Buthidae). Rivista Aracnologica Italiana 3 (13): 31–41.
- Lourenço, W.R., S.E. Sadine, S. Bissati, and A. Houtia. 2017b. The genus *Buthacus* Birula, 1908 in northern and central Algeria; description of a new species and comments on possible microendemic populations (Scorpiones: Buthidae). Rivista Aracnologica Italiana 3 (12): 18–30.
- Lowe, G. 2010. The genus *Vachoniolus* (Scorpiones: Buthidae) in Oman. Euscorpius 100: 1–37.
- Lowe, G., F. Kovařík, M. Stockmann, and F. Šťáhlavský. 2019. *Trypanothacus* gen. n., a new genus of burrowing scorpion from the Arabian Peninsula (Scorpiones: Buthidae). Euscorpius 277: 1–30.
- Lucas, H. 1873. [Note relative à des arachnides rencontrés en Syrie]. Annales de la Société Entomologique de France (Série 5) 3: 172–173.
- Mansouri, N.J.S., K. Akbarzadeh, E. Jahanifard, B. Vazirianzadeh, and J. Rafinejad. 2021. Species diversity and abundance of scorpions in Ahvaz city, southwest Iran. Biodiversitas Journal of Biological Diversity 22 (2): 763–768.
- Miller, M.A., W. Pfeiffer, and T. Schwartz. 2010. Creating the CIPRES Science Gateway for inference of large phylogenetic trees. In Gateway Computing Environments Workshop, New Orleans, LA, 1–8. [doi: 10.1109/GCE.2010.5676129]
- Mirshamsi, O., A. Sari, and S. Hosseini. 2011. History of study and checklist of the scorpion fauna (Arachnida: Scorpiones) of Iran. Progress in Biological Sciences 1 (2): 16–28.
- Moritz, M., and S.-C. Fischer. 1980. Die Typen der Arachniden Sammlung des zoologischen Museums Berlin. III. Scorpiones. Mitteilungen aus dem Zooloogischen Museum in Berlin 56: 309–326.
- Navidpour, S. 2015. An annotated checklist of scorpions in south and southwestern parts of Iran. International Journal of Fauna and Biological Studies 2 (3): 9–15.
- Navidpour, S., F. Kovařík, M.E. Soleglad, and V. Fet. 2008. Scorpions of Iran (Arachnida, Scorpiones). Part I. Khoozestan Province. Euscorpius 65: 1–41.
- Navidpour, S., M.E. Soleglad, V. Fet, and F. Kovařík. 2013. Scorpions of Iran (Arachnida, Scorpiones).

- Part IX. Hormozgan Province, with a description of *Odontobuthus tavighiae* sp. n. (Buthidae). *Euscorpius* 170: 1–29.
- Nenilin, A.B., and V. Fet. 1992. Zoogeographical analysis of the world scorpion fauna (Arachnida: Scorpiones). *Arthropoda Selecta* 1: 3–31. [in Russian; extended English summary]
- Obuid-Allah, A.H., N.A. El-Shimy, M.A. Mahbob, and R.S. Ali. 2020. Survey and morphological studies on scorpions inhabiting New Valley Governorate, Egypt. *Egyptian Academic Journal of Biological Sciences (B, Zoology)* 12 (2): 227–238.
- Oksanen, J., et al. 2007. The vegan package. *Community Ecology Package* 10: 631–637.
- Pallary, P. 1929. Les scorpions du Sahara central. *Bulletin de la Société d'Histoire Naturelle de l'Afrique du Nord* 20 (7): 133–141.
- Pallary, P. 1934. Scorpions du Sahara central. Mission du Hoggar III (février à mai 1928). Mémoires de la Société d'Histoire Naturelle de l'Afrique du Nord 4: 90–100.
- Pallary, P. 1938. Sur les scorpions de la Berbérié, de la Syrie et du Congo. *Archives de l'Institut Pasteur d'Algérie* 16 (3): 279–282.
- Penther, A. 1912. Wissenschaftliche Ergebnisse der Expedition nach Mesopotamien, 1910. Scorpiones. *Annalen des Kaiserlich-Königlichen Naturhistorischen Hofmuseums in Wien* 26 (1/2): 109–116.
- Pérez, S.M. 1974. Un inventario preliminar de los escorpiones de la región Paleártica y claves para la identificación de los géneros de la región Paleártica Occidental. Madrid: Universidad Complutense de Madrid, Facultad de Ciencias, Departamento de Zoología, Cátedra de Artrópodos 7: 1–45.
- Pocock, R.I. 1889. Arachnida, Chilopoda, and Crustacea. In J.E.T. Aitchison. On the zoology of the Afghan Delimitation Commission. *Transactions of the Linnean Society of London (Series 2) Zoology* 5 (3): 110–121.
- Pocock, R.I. 1895. On the Arachnida and Myriopoda obtained by Dr. Anderson's collector during Mr T. Brent's expedition to the Hadramaut, South Arabia, with a supplement upon the scorpions obtained by Dr. Anderson in Egypt and the Eastern Soudan. *Journal of the Linnean Society* 25: 292–316.
- Pocock, R. I. 1900. On a collection of insects and arachnids made in 1895 and 1897, by Mr C. A. V. Peel, F. Z. S., in Somaliland, with descriptions of new species. 9. The Chilopoda and Arachnida. *Proceedings of the Zoological Society of London* 1900: 48–55.
- Prendini, L. 2001. Substratum specialization and speciation in southern African scorpions: the Effect Hypothesis revisited. In V. Fet and P.A. Selden (editors), *Scorpions 2001. In memoriam Gary A. Polis*: 113–139. Burnham Beeches, U.K.: British Arachnological Society.
- Prendini, L., and W.C. Wheeler. 2005. Scorpion higher phylogeny and classification, taxonomic anarchy, and standards for peer review in online publishing. *Cladistics* 21 (5): 446–494.
- Pringle, G. 1960. Notes on the scorpions of Iraq. *Bulletin of Endemic Diseases* 3 (3–4): 73–87.
- Probst, P.J. 1973. A review of the scorpions of East Africa with special regard to Kenya and Tanzania. *Acta Tropica* 30 (4): 312–335.
- R Core Team. 2013. R: a language and environment for statistical computing. Vienna: R Foundation for Statistical Computing.
- Ronquist, F., and J.P. Huelsenbeck. 2003. MrBayes 3: Bayesian phylogenetic inference under mixed models. *Bioinformatics* 19: 1572–1574.
- Sadine, S.E., S. Bissati, and M.A. Idder. 2018. Diversity and structure of scorpion fauna from arid ecosystem in Algerian septentrional Sahara (2005–2018). *Serket* 16 (2): 51–59.
- Said, S.M., A.H. Obuid-Allah, N.A. El-Shimy, M.A. Mahbob, and R.S. Ali. 2021. Ultrastructure study on the exo-morphology of four species of scorpion inhabiting New Valley, Egypt. *Egyptian Academic Journal of Biological Sciences (B, Zoology)* 13 (1): 17–29.
- Saleh, M., M. Younes, A. Badry, and M. Sarhan. 2017. Zoogeographical analysis of the Egyptian scorpion fauna. *Al-Azhar Bulletin of Science* 28: 1–14.
- Schenkel, E. 1932. Notizen über einige Scorpione und Solifugen. *Revue suisse de Zoologie* 39 (15): 375–396.
- Sargent, E. 1941. Sur le postabdomen (queue) de quelques scorpions de l'Afrique du Nord. *Archives de l'Institut Pasteur d'Algérie* 19 (3): 353–357.
- Sharifinia, N., I. Gowhari, M. Hoseiny-Rad, and A.A. Aivazi. 2017. Fauna and geographical distribution of scorpions in Ilam Province, south western Iran. *Journal of Arthropod-Borne Diseases* 11 (2): 232–238.
- Shehab, A.H., Z.S. Amr, and J.A. Lindsell. 2011. Ecology and biology of scorpions in Palmyra, Syria. *Turkish Journal of Zoology* 35 (3): 333–341.
- Simon, E. 1872. Arachnides de Syrie rapportés par M. Charles Pioccard de la Brulerie (Scorpions et Galeodes). *Annales de la Société Entomologique de France (Série 5)* 2: 247–264.
- Simon, E. 1879. 3e Ordre. Scorpiones. In *Les arachnides de France. VII. Contenant les ordres des Chernettes, Scorpiones et Opiliones*: 79–115. Paris: Roret.

- Simon, E. 1880. [Scorpions du Mossoul (ancienne Nineve), sur le Tigre, en Mésopotamie]. Bulletin de la Société Entomologique de France (Série 5) 10: 29.
- Simon, E. 1885. Étude sur les arachnides recueillis en Tunisie en 1883 et 1884 par MM. A. Letourneau, M. Sédillot et Valéry Mayet, membres de la mission de l'exploration scientifique de la Tunisie. In Exploration scientifique de la Tunisie. Paris: Imprimerie Nationale, 59 pp.
- Simon, E. 1892. Liste des arachnides recueillis en Syrie par M. le docteur Théod. Barrois. Revue Biologique du Nord de la France 5: 80–84.
- Simon, E. 1910. Révision des scorpions d'Égypte. Bulletin de la Société Entomologique d'Égypte (Cairo) 1910: 57–87.
- Sissom, W.D. 1990. Systematics, biogeography and paleontology. In G.A. Polis (editor), The biology of scorpions: 64–160. Stanford, CA: Stanford University Press.
- Soleglad, M.E., and V. Fet. 2003a. The scorpion sternum: structure and phylogeny (Scorpiones: Orthosterni). *Euscorpius* 5: 1–34.
- Soleglad, M.E., and V. Fet. 2003b. High-level systematics and phylogeny of the extant scorpions (Scorpiones: Orthosterni). *Euscorpius* 11: 1–175.
- Stahnke, H.L. 1972. U.V. light, a useful field tool. *Bi-Science* 22: 604–607.
- Stamatakis, A. 2006. RAxML-VI-HPC: maximum likelihood-based phylogenetic analyses with thousands of taxa and mixed models. *Bioinformatics* 22: 2688–2690.
- Stamatakis, A. 2014. RAxML version 8: a tool for phylogenetic analysis and post-analysis of large phylogenies. *Bioinformatics* 30: 1312–1313.
- Stathi, I., and M. Mylonas. 2001. New records of scorpions from the central-eastern Mediterranean area: biogeographical comments, with a special reference to the Greek species. In V. Fet and P.A. Selden (editors), *Scorpions 2001. In memoriam Gary A. Polis*: 287–295. Burnham Beeches, U.K.: British Arachnological Society.
- Tahir, H.M., S. Navidpour, and L. Prendini. 2014. First reports of *Razianus* (Scorpiones: Buthidae) from Iraq and Pakistan, descriptions of two new species, and redescription of *Razianus zarudnyi*. *American Museum Novitates* 3806: 1–26.
- Tamura, K., G. Stecher, D. Peterson, A. Filipski, and S. Kumar. 2013. MEGA6: molecular evolutionary genetics analysis, version 6.0. *Molecular Biology and Evolution* 30: 2725–2729.
- Vachon, M. 1948. Études sur les scorpions. III (suite). Description des scorpions du nord de l'Afrique. *Archives de l'Institut Pasteur d'Algérie* 26 (4): 441–481.
- Vachon, M. 1949a. Études sur les scorpions. III (suite). Description des scorpions du nord de l'Afrique. *Archives de l'Institut Pasteur d'Algérie* 27 (1): 66–100.
- Vachon, M. 1949b. Études sur les scorpions. III (suite). Description des scorpions du nord de l'Afrique. *Archives de l'Institut Pasteur d'Algérie* 27 (2): 134–169.
- Vachon, M. 1950a. Études sur les scorpions. III (suite). Description des scorpions du nord de l'Afrique. *Archives de l'Institut Pasteur d'Algérie* 28 (2): 152–216.
- Vachon, M. 1950b. Études sur les scorpions. (suite). Détermination des scorpions du nord-ouest de l'Afrique. *Archives de l'Institut Pasteur d'Algérie* 28 (3): 382–413.
- Vachon, M. 1951. Études sur les scorpions (suite et fin). Détermination des scorpions du nord-ouest de l'Afrique. *Archives de l'Institut Pasteur d'Algérie* 29: 46–104.
- Vachon, M. 1952. Études sur les scorpions. Alger: Institut Pasteur d'Algérie, 482 pp.
- Vachon, M. 1953. Contribution à l'étude du peuplement de la Mauritanie. Scorpions. *Bulletin d'Institut Français d'Afrique Noire* 55 (3): 1012–1028.
- Vachon, M. 1954. Les hamadas sud-Marocaines. Résultats de la mission d'étude 1951 de l'Institut Scientifique Chérifien et du Centre des Recherches Sahariennes. Zoologie. II. Scorpions. *Travaux de l'Institut Scientifique Chérifien* (série générale) 2: 187–188.
- Vachon, M. 1958. Scorpions, mission scientifique au Tassili des Ajjer (1949). *Travaux de l'Institut de Recherches Sahariennes de l'Université d'Alger. Zoologie* 3: 177–193.
- Vachon, M. 1966. Liste des scorpions connus en Égypte, Arabie, Israël, Liban, Syrie, Jordanie, Turquie, Irak, Iran. *Toxicon* 4: 209–218.
- Vachon, M. 1979. Arachnids of Saudi Arabia. Scorpiones. *Fauna of Saudi Arabia* 1: 30–66.
- Vachon, M., and R. Kinzelbach. 1987. On the taxonomy and distribution of the scorpions of the Middle East. In F. Krupp, W. Schneider, and R. Kinzelbach (editors), *Proceedings of the Symposium on the Fauna and Zoogeography of the Middle East*, Mainz, 1985. Beihefte zum Tübinger Atlas des Vorderen Orients (TAVO), Reihe A (Naturwissenschaften) 28: 91–103.
- Werner, F. 1929. Wissenschaftliche Ergebnisse einer zoologischen Forschungsreise nach Westalgérien

- und Marokko. *Sitzungsberichte der Akademie der Wissenschaften, Wien, Mathematisch-Naturwissenschaftliche Klasse, Abt. 1*, 138 (1–2): 1–34.
- Werner, F. 1934. Scorpiones, Pedipalpi. In H.G. Bronn (editor), *Klassen und Ordnungen des Tierreichs*. 5, IV, 8, Lief. 1, 2 (Scorpiones): 1–316. Leipzig: Akademische Verlagsgesellschaft.
- Werner, F. 1936a. Neu-Eingänge von Skorpionen im Zoologischen Museum in Hamburg. *Festschrift zum 60. Geburtstage von Professor Dr. Embrik Strand* 2: 171–193.
- Werner, F. 1936b. Reptilien und Gliedertiere aus Persien. *Festschrift zum 60. Geburtstage von Professor Dr. Embrik Strand* 2: 193–204.
- Whittick, R.J. 1947. Results of the Armstrong Expedition to Siwa Oasis (Lybian desert), 1935. Scorpiones (Arachnida). *Bulletin de la Société Fouad 1<sup>er</sup> d'Entomologie* 31: 121–126.
- Whittick, R.J. 1955. Scorpions from Palestine, Syria, Irak and Iran. In H. Field (editor), Contributions to the fauna and flora of southwestern Asia. *Miscellanea Asiatica Occidentalis XII*, American Documentation Institute Microfiche 4612: 76–81. [privately printed by Henry Field, Coconut Grove, FL]
- Wickham, H. 2009. *Elegant graphics for data analysis - ggplot2*. New York: Springer Verlag.
- Yağmur, E.A., M. Yalçın, and G. Çalışır. 2008. Distribution of *Androctonus crassicauda* (Olivier 1807) and *Buthacus macrocentrus* (Ehrenberg 1828) (Scorpiones: Buthidae) in Turkey. *Serket* 11: 13–18.
- Zambre, A.M., and W.R. Lourenço. 2010. A new species of *Buthacus* Birula, 1908 (Scorpiones, Buthidae) from India. *Boletín de la Sociedad Entomológica Aragonesa* 46: 115–119.
- Zarei, A., J. Rafinejad, K. Shemshad, and R. Khaghani. 2009. Faunistic study and biodiversity of scorpions in Qeshm Island (Persian Gulf). *Iranian Journal of Arthropod-Borne Diseases* 3 (1): 46–52.
- Zourgui, L., M. Maammar, and R. Emetris. 2008. Taxonomical and geographical occurrence of Libyans scorpions. *Archives de l'Institut Pasteur de Tunis* 85 (1–4): 81–89.

## APPENDIX 1

CURRENTLY RECOGNIZED SPECIES, SUBSPECIES, AND SYNONYMS OF SAND SCORPIONS, GENUS *BUTHACUS* BIRULA, 1908 (BUTHIDAE C.L. KOCH, 1837), AND SPECIES PREVIOUSLY ASSIGNED TO *BUTHACUS* CURRENTLY ACCOMMODATED IN OTHER GENERA

***Androctonus* Ehrenberg, 1828**

Type species: *Androctonus australis* (Linnaeus, 1758)

*Androctonus aleksandrplotkini* Lourenço and Qi, 2007

= *Buthacus maliensis* Lourenço and Qi, 2007  
(synonymized by Kovařík, 2018)

***Buthacus* Birula, 1908**

Type species: *Buthacus leptochelys* (Ehrenberg, 1829)

*Buthacus agarwali* Zambre and Lourenço, 2010

*Buthacus ahaggar* Lourenço et al., 2017

*Buthacus amitaii*, sp. nov.

*Buthacus arava*, sp. nov.

*Buthacus arenicola* (Simon, 1885)

*Buthacus a. maroccanus* Lourenço, 2006

*Buthacus armasi* Lourenço, 2013, stat. rev.

*Buthacus birulai* Lourenço, 2006

*Buthacus elevai* Lourenço, 2001

*Buthacus elmenia* Lourenço et al., 2017

*Buthacus foleyi* Vachon, 1948

*Buthacus frontalis* Werner, 1936

*Buthacus fuscata* Pallary, 1929, stat. nov. et stat. rev.

*Buthacus golovatchii* Lourenço et al., 2012

*Buthacus leptochelys* (Ehrenberg, 1829)

= *Androctonus (Leiurus) thebanus* Ehrenberg, 1828  
(synonymized by Kraepelin, 1891)

= *Androctonus (Leiurus) macrocentrus* Ehrenberg, 1829 (originally synonymized by Kraepelin, 1891),  
syn. nov.

= *Buthacus granosus* Borelli, 1929, syn. nov.

*Buthacus levyi*, sp. nov.

*Buthacus nigerianus* Lourenço and Qi, 2006

*Buthacus nigroaculeatus* Levy et al., 1973

*Buthacus nitzani* Levy et al., 1973, stat. nov.

*Buthacus occidentalis* Vachon, 1953

= *Buthacus ehrenbergi* Kovařík, 2005 (synonymized by Lourenço, 2006)

= *Buthacus huberi* Lourenço, 2001 (synonymized by Kovařík et al., 2016)

*Buthacus pakistanensis* Lourenço and Qi, 2006

*Buthacus samiae* Lourenço and Sadine, 2015

*Buthacus spatzi* (Birula, 1911), stat. rev.

*Buthacus spinatus* Lourenço et al., 2016

*Buthacus stockmanni* Kovařík et al., 2016

*Buthacus striffleri* Lourenço, 2004

*Buthacus tadmorensis* (Simon, 1892), stat. rev.

= *Buthus pietschmanni* Penther, 1912 (synonymized by Birula, 1917)

*Buthacus villiersi* Vachon, 1949

*Buthacus williamsi* Lourenço and Leguin, 2009

*Buthacus yotvatensis* Levy et al., 1973, stat. rev.

*Buthacus ziegleri* Lourenço, 2000

= *Buthacus mahraouii* Lourenço, 2004 (synonymized by Kovařík et al., 2016)

= *Buthacus leptochelys algerianus* Lourenço, 2006  
(synonymized by Kovařík et al., 2016)

***Gint* Kovařík et al., 2013**

Type species: *Gint gaitako* Kovařík et al., 2013

*Gint calviceps* (Pocock, 1900)

***Trypanothacus* Lowe et al., 2019**

Type species: *Trypanothacus barnesi* Lowe et al., 2019

*Trypanothacus buettikeri* (Hendrixson, 2006)

***Vachoniolus* Levy et al., 1973**

Type species: *Vachoniolus globimanus* Levy et al., 1973

= *Buthacus minipectenibus* Levy et al., 1973

## APPENDIX 2

## Tissue Samples and GenBank Accession Codes for DNA Sequences Used for Phylogenetic Analysis of Sand Scorpions,

GENUS *BUTHACUS* BIRULA, 1908 (BUTHIDAE C.L. KOCH, 1837)

Sequences of the Internal Transcribed Spacer 2 (ITS2), 28S rDNA (28S), 12S rDNA (12S), 16S rRNA (16S), and cytochrome *c* oxidase subunit I (COI) gene loci. Tissue samples deposited in the National Natural History Collections, the Hebrew University of Jerusalem (HUJ), and the Ambrose Monell Collection for Molecular and Microbial Research (AMCC) at the American Museum of Natural History, New York.

Species	Collection	Collection	Country	Locality	ITS2	28S	12S	16S	COI
<i>Androctonus amoreuxi</i>	HUJ INVSC 3486	Israel	Bé'er Milka	MW556875	MW557083	MW556770	MW556797	MW555666	
<i>Buthacus amitaii</i>	HUJ INVSC 3466		Color Sands	MW556876	MW557084	MW556771	MW556880	MW555667	
	HUJ INVSC 3467			MW556877	MW557085	MW556772	MW556981	MW555668	
	HUJ INVSC 3468			MW556878	MW557086	MW556773	MW556982	MW555669	
	HUJ INVSC 3469			MW556879	MW557087	MW556774	MW556983	MW555670	
	HUJ INVSC 3470			MW556880	MW557088	MW556775	MW556984	MW555671	
	AMCC [LP 11173]			MW556881	MW557089	MW556776	MW556985	MW555672	
	AMCC [LP 11176]			MW556882	MW557090	MW556777	MW556986	MW555673	
	HUJ INVSC 3200			MW556883	MW557091	MW556778	MW556987	MW555674	
	HUJ INVSC 3202			MW556884	MW557092	MW556779	MW556988	MW555675	
	HUJ INVSC 3203			MW556885	MW557093	MW556780	MW556989	MW555676	
	HUJ INVSC 3204			MW556886	MW557094	MW556781	MW556990	MW555677	
	HUJ INVSC 3206		Nahal Yamin	MW556887	MW557095	MW556782	MW556991	MW555678	
	HUJ INVSC 3207			MW556888	MW557096	MW556783	MW556992	MW555679	
	HUJ INVSC 3472			MW556889	MW557097	MW556784	MW556993	MW555680	
	HUJ INVSC 3474			MW556890	MW557098	MW556785	MW556994	MW555681	
	HUJ INVSC 3283		Lotan	MW556891	MW557099	MW556786	MW556995	MW555682	
	HUJ INVSC 3284			MW556892	MW557100	MW556787	MW556996	MW555683	
	HUJ INVSC 3288			MW556893	MW557101	MW556788	MW556997	MW555684	
	HUJ INVSC 3291			MW556894	MW557102	MW556789	MW556998	MW555685	
	HUJ INVSC 3479			MW556895	MW557103	MW556790	MW556999	MW555686	
	HUJ INVSC 3299			MW556896	MW557104	MW556791	MW557000	MW555687	
	HUJ INVSC 3292			MW556897	MW557105	MW556792	MW557001	MW555688	
	HUJ INVSC 3298			MW556898	MW557106	MW556793	MW557002	MW555689	

APPENDIX 2 *continued*

Species	Collection	Country	Locality	ITS2	28S	12S	16S	COI
<i>Buthacus arenicola</i>	AMCC [LP 14857] AMCC [LP 14858]	Tunisia	Tozeur	MW556899	MW557107	MW556794	MW557003	MW555690 MW555691
<i>Buthacus leptochelys</i>	AMCC [LP 14859] AMCC [LP 16600]	Egypt	Faiyum Oasis Zatara	MW556900 MW556901 MW556902 MW556903	MW557108 MW557109 MW557110 MW557111	MW556795 MW556796 MW556797 MW556798	MW557004 MW557005 MW557006 MW557007	MW555692 MW555693 MW555694 MW555695
<i>Buthacus levyi</i>	AMCC [LP 16598] AMCC [LP 16599]		unknown	MW556904 MW556913	MW557112 MW557121	MW556799 MW556808	MW557008 MW557017	MW555704
<i>Buthacus levii</i>	AMCC [LP 17226] AMCC [LP 16587]		Abou Rawash unknown	MW556905 MW556914	MW557113 MW557122	MW556800 MW556809	MW557009 MW557018	MW555696 MW555705
<i>Buthacus levii</i>	AMCC [LP 7006] AMCC [LP 16586]		Qesm Ad Dabaah	MW556915	MW557123	MW556810	MW557019	MW555706
<i>Buthacus levii</i>	AMCC [LP 16601] AMCC [LP 16585]			MW556916 MW556917	MW557124 MW557125	MW556811 MW556812	MW557020 MW557021	MW555707 MW555708
<i>Buthacus levii</i>	HUJ INVSC 3251	Israel	Be'er Milka	MW556906	MW557114	MW556801	MW557010	MW555697
<i>Buthacus levii</i>	HUJ INVSC 3252			MW556907	MW557115	MW556802	MW557011	MW555698
<i>Buthacus levii</i>	HUJ INVSC 3254			MW556908	MW557116	MW556803	MW557012	MW555699
<i>Buthacus levii</i>	HUJ INVSC 3255			MW556909	MW557117	MW556804	MW557013	MW555700
<i>Buthacus levii</i>	HUJ INVSC 3257			MW556910	MW557118	MW556805	MW557014	MW555701
<i>Buthacus levii</i>	HUJ INVSC 3258			MW556911	MW557119	MW556806	MW557015	MW555702
<i>Buthacus levii</i>	HUJ INVSC 3476			MW556912	MW557120	MW556807	MW557016	MW555703
<i>Buthacus levii</i>	HUJ INVSC 3230		Ashdod	MW556918	MW557126	MW556813	MW557022	MW555709
<i>Buthacus nitzani</i>	HUJ INVSC 3234			MW556919	MW557127	MW556814	MW557023	MW555710
<i>Buthacus nitzani</i>	HUJ INVSC 3225		Ashqelon	MW556920	MW557128	MW556815	MW557024	MW555711
<i>Buthacus nitzani</i>	HUJ INVSC 3229			MW556921	MW557129	MW556816	MW557025	MW555712
<i>Buthacus nitzani</i>	HUJ INVSC 3247			MW556922	MW557130	MW556817	MW557026	MW555713
<i>Buthacus nitzani</i>	HUJ INVSC 3249			MW556923	MW557131	MW556818	MW557027	MW555714
<i>Buthacus nitzani</i>	HUJ INVSC 3250			MW556924	MW557132	MW556819	MW557028	MW555715
<i>Buthacus nitzani</i>	HUJ INVSC 3398			MW556925	MW557133	MW556820	MW557029	MW555716
<i>Buthacus nitzani</i>	HUJ INVSC 3473			MW556926	MW557134	MW556821	MW557030	MW555717

APPENDIX 2 *continued*

Species	Collection	Country	Locality	ITS2	28S	12S	16S	COI
<i>Buthacus nitzani</i>	HUJ INVSC 3211	Israel	Great Dune	MW556927	MW557135	MW556822	MW557031	MW555718
	HUJ INVSC 3212			MW556928	MW557136	MW556823	MW557032	MW555719
	HUJ INVSC 3478			MW556929	MW557137	MW556824	MW557033	MW555720
AMCC [LP 12200]	Mashabbim			MW556930	MW557138	MW556825	MW557034	MW555721
AMCC [LP 11174]	Nizzanim			MW556931	MW557139	MW556826	MW557035	MW555722
HUJ INVSC 3213				MW556932	MW557140	MW556827	MW557036	MW555723
HUJ INVSC 3215				MW556933	MW557141	MW556828	MW557037	MW555724
HUJ INVSC 3216				MW556934	MW557142	MW556829	MW557038	MW555725
HUJ INVSC 3217				MW556935	MW557143	MW556830	MW557039	MW555726
HUJ INVSC 3218				MW556936	MW557144	MW556831	MW557040	MW555727
HUJ INVSC 3219				MW556937	MW557145	MW556832	MW557041	MW555728
HUJ INVSC 3222	Palmahim			MW556938	MW557146	MW556833	MW557042	MW555729
HUJ INVSC 3223				MW556939	MW557147	MW556834	MW557043	MW555730
HUJ INVSC 3459	Ramat Hovav			MW556940	MW557148	MW556835	MW557044	MW555731
HUJ INVSC 3460				MW556941	MW557149	MW556836	MW557045	MW555732
HUJ INVSC 3461				MW556942	MW557150	MW556837	MW557046	MW555733
AMCC [LP 11175]	Retamim			MW556943	MW557151	MW556838	MW557047	MW555734
HUJ INVSC 3236				MW556944	MW557152	MW556839	MW557048	MW555735
HUJ INVSC 3237				MW556945	MW557153	MW556840	MW557049	MW555736
HUJ INVSC 3239				MW556946	MW557154	MW556841	MW557050	MW555737
HUJ INVSC 3240				MW556947	MW557155	MW556842	MW557051	MW555738
HUJ INVSC 3242				MW556948	MW557156	MW556843	MW557052	MW555739
HUJ INVSC 3245				MW556949	MW557157	MW556844	MW557053	MW555740
HUJ INVSC 3477				MW556950	MW557158	MW556845	MW557054	MW555741

APPENDIX 2 *continued*

Species	Collection	Country	Locality	ITS2	28S	12S	16S	COI
<i>Buthacus yohvatensis</i>	HUJ INVSC 3360	Israel	Avrona	MW556951	MW557159	MW556846	MW557055	MW555742
	HUJ INVSC 3361			MW556952	MW557160	MW556847	MW557056	MW555743
	HUJ INVSC 3369			MW556953	MW557161	MW556848	MW557057	MW555744
	HUJ INVSC 3375			MW556954	MW557162	MW556849	MW557058	MW555745
	HUJ INVSC 3379			MW556955	MW557163	MW556850	MW557059	MW555746
	HUJ INVSC 3380			MW556956	MW557164	MW556851	MW557060	MW555747
	HUJ INVSC 3481		Ein Zik	MW556957	MW557165	MW556852	MW557061	MW555748
	HUJ INVSC 3482			MW556958	MW557166	MW556853	MW557062	MW555749
	AMCC [LP 11172]		Hay-Bar	MW556959	MW557167	MW556854	MW557063	MW555750
	HUJ INVSC 3329			MW556960	MW557168	MW556855	MW557064	MW555751
	HUJ INVSC 3330			MW556961	MW557169	MW556856	MW557065	MW555752
	HUJ INVSC 3331			MW556962	MW557170	MW556857	MW557066	MW555753
	HUJ INVSC 3332			MW556963	MW557171	MW556858	MW557067	MW555754
	HUJ INVSC 3334			MW556964	MW557172	MW556859	MW557068	MW555755
	HUJ INVSC 3347		Lotan	MW556965	MW557173	MW556860	MW557069	MW555756
	HUJ INVSC 3350			MW556966	MW557174	MW556861	MW557070	MW555757
	HUJ INVSC 3352		Nahal Gidron	MW556967	MW557175	MW556862	MW557071	MW555758
	HUJ INVSC 3356		Nahal Mashaq	MW556968	MW557176	MW556863	MW557072	MW555759
	HUJ INVSC 3342		Nahal Shaalav	MW556969	MW557177	MW556864	MW557073	MW555760
	HUJ INVSC 3343			MW556970	MW557178	MW556865	MW557074	MW555761
	HUJ INVSC 3359		Nahal Shezaf	MW556971	MW557179	MW556866	MW557075	MW555762
	HUJ INVSC 3311		Samar	MW556972	MW557180	MW556867	MW557076	MW555763
	HUJ INVSC 3312			MW556973	MW557181	MW556868	MW557077	MW555764
	HUJ INVSC 3313			MW556974	MW557182	MW556869	MW557078	MW555765
	HUJ INVSC 3314			MW556975	MW557183	MW556870	MW557079	MW555766
	HUJ INVSC 3321			MW556976	MW557184	MW556871	MW557080	MW555767
	HUJ INVSC 3325			MW556977	MW557185	MW556872	MW557081	MW555768
	HUJ INVSC 3475			MW556978	MW557186	MW556873	MW557082	MW555769

## APPENDIX 3

QUALITATIVE MORPHOLOGICAL CHARACTERS AND CHARACTER STATES USED FOR  
PHYLOGENETIC ANALYSIS OF THE SAND SCORPIONS, GENUS *BUTHACUS* BIRULA, 1908  
(*BUTHIDAE* C.L. KOCH, 1837) OF THE LEVANT

Character states scored 0–4, \* = [01]. Character descriptions below.

Characters 1, 3–5 and 12 were deactivated in analyses with quantitative characters.

<i>Androctonus amoreuxi</i>	00000 00000 00000 01000 00
<i>Buthacus amitaii</i>	11000 0*101 10001 10011 20
<i>Buthacus arava</i>	01010 20110 11001 01000 10
<i>Buthacus arenicola</i>	10111 21101 00002 11000 20
<i>Buthacus leptochelys</i>	01010 10101 00001 11000 20
<i>Buthacus levyi</i>	10111 21101 00002 12100 20
<i>Buthacus nitzani</i>	11000 00101 10012 11111 20
<i>Buthacus yotvatensis</i>	00111 20000 00101 01000 11

1. Total length: larger, >60 mm (0); smaller, <60 mm (1).
2. Pedipalp chela, sexual dimorphism: ♂ chela resembles ♀ chela (♂ and ♀ chelae globose or slender) (0); male chela unlike ♀ (♂ chela globose, ♀ chela slender) (1).
3. Pedipalp chela, length (adult ♂): short, manus length:movable finger length >70 % (0); long, manus length:movable finger length <70 % (1).
4. Pedipalp chela, length (adult ♀): short, manus length:movable finger length >55 % (0); long, manus length:movable finger length <55 % (1).
5. Pedipalp chela, width (adult ♂): broad, manus width:chela length >22 % (0); narrow, manus width:chela length <22 % (1).
6. Pedipalp chela fixed and movable fingers, proximal dentate margins, curvature: deeply emarginate, pronounced gap evident proximally when fingers are closed (0); shallowly emarginate to sublinear, small gap evident proximally when fingers closed (1); sublinear, no gap evident proximally when fingers closed (2).
7. Pedipalp chela movable finger, retrolateral accessory denticles: always present, high counts (6–10) (0); often absent, low counts (0–5) (1).
8. Legs I and II, telotarsal unguis, relative length: short, equal (0); long, unequal (1).
9. Pectinal first median lamella (scape) (♂), angle: acute (0); obtuse (1).
10. Pectinal first median lamella (scape) (♀), angle: obtuse (0); acute (1).
11. Pectinal median lamella count: > 10 (♂, ♀) (0); < 10 (♂, ♀) (1).
12. Pectinal tooth count: > 25 (♂), > 20 (♀); < 22 (♂), < 13 (♀) (1).
13. Metasomal segments, dorsosubmedian, and dorsolateral carinae, setation: sparsely setose (0); densely setose (1).
14. Metasomal segments I–III, median lateral carinae, development: distinct (0); obsolete (1).
15. Metasomal segments II and III, ventrosubmedian and ventrolateral carinae development: well developed, posterior granules greatly enlarged into broad, lobate processes posteriorly (0); well developed, posterior granules slightly enlarged, subspiniform to spiniform (1); weakly to moderately developed, posterior granules similar to preceding granules (2).
16. Metasomal segments IV and V, intercarinal surfaces, macrosulpture: granular and matte (0); smooth and glabrous (1).
17. Metasomal segment V, ventrolateral carinae, posterior processes: variable in size, some greatly enlarged, broad and lobate (0); variable in size, some slightly enlarged, narrow and conical or spiniform (1); relatively uniform in size, small (2).
18. Metasomal segment V, ventral intercarinal surfaces, macrosulpture: densely granular (0); sparsely granular (1).
19. Telson vesicle, dorsal surface, lateral profile: flat (0); concave (1).
20. Telson vesicle, ventral surface, lateral profile: rounded (0); angular (1).
21. Telson vesicle, ventral surface, macrosulpture: densely granular anteriorly (0); sparsely granular anteriorly (1); smooth and glabrous (2).
22. Telson vesicle, ventral surface, setation: sparsely setose (0); densely setose (1).

## APPENDIX 4

RATIOS AND COUNTS USED FOR NONMETRIC MULTIDIMENSIONAL SCALING AND AS QUANTITATIVE MORPHOLOGICAL CHARACTERS IN PHYLOGENETIC ANALYSIS OF THE SAND SCORPIONS,  
GENUS *BUTHACUS* BIRULA, 1908 (BUTHIDAE C.L. KOCH, 1837) OF THE LEVANT

Char.	Sex	<i>B. ami.</i>	<i>B. ara.</i>	<i>B. are.</i>	<i>B. lep.</i>	<i>B. lev.</i>	<i>B. nitzani</i>			<i>B. yot.</i>
							coastal	N Haluza	Be'er Milka	
1	♂	53.88	70.40	54.33	63.71	49.22	53.28	52.34	—	67.39
	♀	49.55	62.29	—	66.37	57.26	50.50	44.39	47.37	76.66
2	♂	0.27	0.30	0.18	0.24	0.19	0.26	0.28	—	0.17
	♀	0.19	0.23	—	0.17	0.17	0.19	0.23	0.18	0.17
3	♂	0.51	0.51	0.57	0.48	0.53	0.54	0.55	—	0.53
	♀	0.53	0.48	—	0.50	0.50	0.52	0.50	0.54	0.54
4	♂	0.89	0.91	0.96	0.85	0.94	0.92	0.92	—	0.91
	♀	0.89	0.89	—	0.85	0.87	0.84	0.83	0.9	0.87
5	♂	0.42	0.43	0.43	0.40	0.43	0.40	0.38	—	0.45
	♀	0.43	0.45	—	0.44	0.43	0.42	0.41	0.4	0.46
6	♂	0.63	0.63	0.53	0.59	0.52	0.59	0.59	—	0.51
	♀	0.54	0.62	—	0.52	0.56	0.53	0.59	0.52	0.57
7	♂	0.70	0.69	0.62	0.59	0.60	0.62	0.64	—	0.57
	♀	0.61	0.69	—	0.60	0.63	0.60	0.64	0.64	0.64
8	♂	0.82	0.90	0.54	0.71	0.63	0.83	0.88	—	0.55
	♀	0.58	0.61	—	0.52	0.47	0.63	0.70	0.6	0.47
9	♂	0.98	0.88	0.97	0.91	0.97	0.98	0.95	—	0.94
	♀	0.95	0.67	—	0.92	0.92	0.95	0.95	0.94	0.86
10	♂	0.58	0.56	0.57	0.58	0.53	0.56	0.55	—	0.54
	♀	0.69	0.47	—	0.57	0.54	0.59	0.62	0.60	0.56
11	♂	0.69	0.64	0.72	0.67	0.65	0.64	0.64	—	0.61
	♀	0.70	0.61	—	0.68	0.67	0.65	0.66	0.62	0.62
12	♂	0.59	0.56	0.64	0.53	0.57	0.55	0.56	—	0.51
	♀	0.57	0.55	—	0.56	0.56	0.54	0.57	0.52	0.54
13	♂	0.54	0.50	0.59	0.49	0.51	0.50	0.54	—	0.48
	♀	0.53	0.55	—	0.51	0.51	0.51	0.53	0.48	0.50
14	♂	0.43	0.44	0.45	0.38	0.40	0.41	0.45	—	0.40
	♀	0.43	0.47	—	0.42	0.42	0.37	0.42	0.38	0.42
15	♂	0.36	0.35	0.35	0.33	0.34	0.34	0.35	—	0.33
	♀	0.36	0.37	—	0.38	0.35	0.34	0.36	0.33	0.34
16	♂	0.88	0.89	0.90	0.88	0.91	0.88	0.87	—	0.88
	♀	0.87	0.90	—	0.88	0.90	0.89	0.92	0.87	0.90
17	♂	0.96	0.96	0.98	0.95	0.97	0.98	0.99	—	0.96
	♀	0.97	1.00	—	0.98	0.96	0.99	0.95	0.99	0.97
18	♂	0.97	0.95	0.93	0.95	0.98	0.95	0.96	—	0.96
	♀	0.99	0.92	—	0.99	0.98	0.95	0.96	0.94	0.96
19	♂	0.82	0.86	0.83	0.87	0.84	0.84	0.82	—	0.87
	♀	0.78	0.81	—	0.84	0.85	0.82	0.83	0.80	0.82
20	♂	0.81	0.69	0.74	0.81	0.73	0.78	0.76	—	0.81
	♀	0.78	0.70	—	0.77	0.75	0.81	0.78	0.76	0.83
21	♂	0.69	0.63	0.59	0.58	0.56	0.61	0.51	—	0.61
	♀	0.66	0.60	—	0.63	0.59	0.65	0.63	0.70	0.63
22	♂	0.52	0.51	0.55	0.49	0.53	0.51	0.47	—	0.50
	♀	0.55	0.53	—	0.57	0.55	0.55	0.52	0.59	0.52
23	♂	30.60	19.71	31.50	33.00	32.38	31.83	27.50	—	34.75
	♀	24.00	13.00	—	28.50	26.78	23.33	25.00	23.00	26.50
24	♂	0.67	0.71	0.65	0.67	0.68	0.68	0.67	—	0.71
	♀	0.58	0.68	—	0.58	0.59	0.59	0.61	0.63	0.64

APPENDIX 4 *continued*

- 
1. Total length.
  2. Chela manus width:total body length.
  3. Carapace anterior width:posterior width.
  4. Carapace length:posterior width.
  5. Carapace, median ocelli distance from anterior margin:carapace length.
  6. Chela manus width:length along retroventral carina.
  7. Chela manus height:length along retroventral carina.
  8. Chela manus, length along retroventral carina:movable finger length.
  9. Pectines length along dentate margin:total length along "anterior" margin.
  10. Tergite VI length: tergite VII length.
  11. Metasomal segment I, width:length.
  12. Metasomal segment II, width:length.
  13. Metasomal segment III, width:length.
  14. Metasomal segment IV, width:length.
  15. Metasomal segment V, width:length.
  16. Metasomal segment I length:segment II length.
  17. Metasomal segment II length:segment III length.
  18. Metasomal segment III length:segment IV length.
  19. Metasomal segment IV length:segment V length.
  20. Telson vesicle width:metasomal segment V width.
  21. Telson vesicle height:length.
  22. Telson aculeus length:telson length.
  23. Pectinal tooth count right.
  24. Sternite VII length:width.





**SCIENTIFIC PUBLICATIONS OF THE AMERICAN MUSEUM OF NATURAL HISTORY**

*AMERICAN MUSEUM NOVITATES*

*BULLETIN OF THE AMERICAN MUSEUM OF NATURAL HISTORY*

*ANTHROPOLOGICAL PAPERS OF THE AMERICAN MUSEUM OF NATURAL HISTORY*

**PUBLICATIONS COMMITTEE**

ROBERT S. VOSS, CHAIR

**BOARD OF EDITORS**

JIN MENG, PALEONTOLOGY

LORENZO PRENDINI, INVERTEBRATE ZOOLOGY

ROBERT S. VOSS, VERTEBRATE ZOOLOGY

PETER M. WHITELEY, ANTHROPOLOGY

**MANAGING EDITOR**

MARY KNIGHT

Submission procedures can be found at <http://research.amnh.org/scipubs>

All issues of *Novitates* and *Bulletin* are available on the web (<http://digilibRARY.amnh.org/dspace>). Order printed copies on the web from:

<http://shop.amnh.org/a701/shop-by-category/books/scientific-publications.html>

or via standard mail from:

American Museum of Natural History—Scientific Publications  
Central Park West at 79th Street  
New York, NY 10024

∞ This paper meets the requirements of ANSI/NISO Z39.48-1992 (permanence of paper).

*ON THE COVER: BUTHACUS ARAVA, SP. NOV., ♂, FROM THE TYPE LOCALITY,  
LOTAN, ISRAEL.*